Identification and characterization of functionally critical sites of Mdr1p, a multidrug transporter of *Candida albicans*

Thesis submitted to Jawaharlal Nehru University in the partial fulfillment for award of the degree of

DOCTOR OF PHILOSOPHY

by

KHYATI KAPOOR

SCHOOL OF LIFE SCIENCES
JAWAHARLAL NEHRU UNIVERSITY
NEW DELHI-110067
INDIA

2010

SCHOOL OF LIFE SCIENCES
JAWAHARLAL NEHRU UNIVERSITY
NEW DELHI-110067

CERTIFICATE

This is to certify that this thesis titled **"Identification and characterization of functionally critical sites of Mdr1p, a multidrug transporter of *Candida albicans*"** submitted to Jawaharlal Nehru University, New Delhi, in fulfilment of the requirement for the award of the Degree of Doctor of Philosophy, embodies original research work carried out by Ms. Khyati Kapoor at School of Life Sciences, Jawaharlal Nehru University, New Delhi, under our guidance and has not been submitted in part or full for any degree or diploma of this or any other University.

Khyati Kapoor
(Candidate)

Prof. Rajendra Prasad
(Supervisor)
School of life Sciences
Jawaharlal Nehru University
New Delhi-110067

Prof. R. Madhubala
(Dean)
School of life Sciences
Jawaharlal Nehru University
New Delhi-110067

April 2010

Dedicated to

My Beloved Mummy

My Dad

And

My Cute Little

Brother

ACKNOWLEDGEMENTS

ACKNOWLEDGEMENTS

Real life isn't always going to be perfect or go our way, but the acknowledgement of what is working in our lives can help us not only to survive but surmount our difficulties."

The process of Ph.D is a long journey during which you come across so many people who walk with you or support you to go through this period. By this part of my thesis, it is my turn to show gratitude to all those who have stood by me in the successful completion of this work.

My first, and most earnest, acknowledgment must go to my guide and my mentor Prof. Rajendra Prasad. I would like to thank him, for having led me into a fascinating area of research, for his uncanny ability to tell a good story and for teaching me that anything that does not kill you, makes you stronger. I appreciate all his contributions of time, ideas, and funding to make my Ph.D. experience productive and stimulating. The joy and enthusiasm he has for research was contagious and motivational for me, even during tough times in the Ph.D. I am greatly indebted to him for helping me to overcome obstacles in the process of conducting the research. In every sense, none of this work would have been possible without him. I have been fortunate as I have gained much more out of this association than I had ever anticipated. Thank you Sir for everything...

Vibha Ma'am will always be remembered for all the warmth that she holds and cute Mohit for his brilliant shots in cricket. I will cherish the memories of the parties at sir's home.

With deep sense of gratitude, I owe sincere thanks to Dr. Andrew Lynn who was actively involved in my work. I thank him for providing me guidance and space to work in his lab at School of Information Technology (SIT), JNU. His knowledge in the field of bioinformatics is charismatic and was really helpful for my research work.

I am greatly indebted to the past and present Dean of School of Life Sciences (SLS) for providing me excellent facilities at the school.

Special thanks goes to the Council for Scientific and Industrial Research (CSIR), India for providing fellowship (JRF and SRF) and other monetary assistance in the form of travel grant and contingency, which made it possible for me to carry out this work.

I would like to acknowledge the assistance of Mr. B.A. Khan, Mr. A.C. Alexander, Mr. S.P. Sharma, Mr. S. K. Mishra, Rajendra, Aslam, and Faiz of the Central Instrument Facility, SLS. Meenu Ma'am would always be remembered for all the sweetness and her untiring efforts in handling the administrative affairs at SLS. A special mention must go to Ms. Pratima and Mr. Shankar for their constant help with office affairs at 101; they are simply inseparable from the research that I carried out.

I would also like to mention the names of the past and present technical staff in 101, Tiklal, Gagan, Yadavji, Sharmaji, Vijay, Surendra, Vijendra, Karmvirji and Ramesh who assisted me with their unsung efforts and timely support in carrying out various tasks important for laboratory maintenance and assistance.

Far too many people to mention individually have assisted me in so many ways during my work at JNU. These include my seniors, colleagues and my juniors and my sincere thanks to all of them. Few people would need a special mention. I wish to thank my senior Preeti who taught me basics of everything that I know today. I would like to thank Sudhanshu, DB, Hina and Ashutosh for being my co-workers and more so my buddies. Their support, encouragement, and companionship turned my journey into a pleasure. The memories of nights spent at Ganga Dhaba along with a cup of tea will always be cherished. Many a times their cool attitude helped me to come out of tough situations. Thanks a lot guys for being such good friends.

I will always treasure the great time spent with my batchmates Shiteshu, Shivesh, Anupam, Anita, Rashmi, Tara and many more whom I might have inadvertently forgotten to mention. The trip to Vaishno Devi and all the fun we had will always be remembered. I will also thank my friends in SIT who were always jovial irrespective of the conditions. I was always welcome to their lab. Rehan, my bioinformatics friend deserves a special mention, without whom, my work would not have moved ahead. Thanks for the efforts and ideas.

The track of my Ph.D has been really tough both personally as well as professionally. There are few people who deserve a very special mention and I not only owe my thanks to them, rather, I owe my life to them. Naveen, Shuchin, Deepak, Suhail and Naseem, thanks for always being there, anywhere and everywhere, anytime and everytime. Your strong support has helped me come out of the roughest patches of my life. I will never ever forget all the efforts put in, just to make me smile. I would not have been able to survive without you guys. This section can't be complete

without mentioning my cute and sweet friend Kunal. His happy-go-lucky nature and enthusiasm at the fag end of my Ph.D, when one is low on energy and will-power, he was the one who gave the final booster to finish this work with a positive attitude. Thanks.

I treasure great memories of JNU, its dhabas, nearby movie halls; all the fests in JNU but all these fun-filled moments of JNU are incomplete without the mention of my best pal of all times, Soraya. Whether it was sharing happy moments of research or bitching about people she was the one who lend me all ears. Our trips to all silliest places on ma bike and doing all nonsense made this whole experience a light-hearted one. Hey buddy, you hold a special place in my heart.

A penultimate and most heartfelt thank-you goes to my wonderful parents and my brother Ruchir. For always being there when I needed them most, and never once complaining about how infrequently I visit, they deserve far more credit than I can ever give them. The silliest solutions by my cutie bro were a constant source of inspiration to look for solution to every problem during the course of the journey. Mumma, my pillar of strength, you would have been the happiest person to see this moment. Miss you always...

My final acknowledgment must go to Almighty God who put me to all tests in these years of my Ph.D and gave me mental strength to wade through this period with courage.

ABBREVIATIONS

ABC	ATP Binding Cassette
AIDS	Acquired ImmunoDeficiency Syndrome
ALDP	AdrenoLeukoDystrophy Protein
ATP	Adenosine 5'-Triphosphate
ATPase	Adenosine-5'-Triphosphatase
Ca	*Candida albicans*
CaMdr1p	*Candida albicans* Multidrug resistance 1 protein
CM	Crude Membrane
conc.	Concentration
DMSO	Dimethylsulfoxide
DNA	Deoxyribonucleic acid
EDTA	Ethylenediaminetetraacetic acid
HEPES	N-[2-hydroxy ethyl] piperizine-N'-[2-ethanesulfonic acid]
hrs	Hours
kb	kilobase pair
kDa	kilo Dalton
MDR	Multidrug Resistance
MFI	Mean Fluorescense Intensity
MFS	Major Facilitator Superfamily
MIC	Minimum Inhibitory Concentration
Min	Minutes
MSD	Membrane Spanning Domains
NBD	Nucleotide Binding Domain
ORF	Open Reading Frame
PAGE	Polyacrylamide Gel Electrophoresis
PBS	Phosphate Buffered Saline
PCR	Polymerase Chain Reaction
PDR	Pleiotropic Drug Resistance
Pgp	P-glycoprotein
PM	Plasma Membrane

PMSF	Phenylmethyl Sulphonic Fluoride
R6G	Rhodamine 6G
RNA	Ribonucleic acid
rpm	revolutions per minute
Sc	*Saccharomyces cerevisiae*
SDS	Sodium Dodecyl Sulphate
SD-ura$^-$	Synthetic defined-uracil media
sec	Seconds
TEMED	N, N, N, N,'- tetraethylenediamine
TMD	TransMembrane Domain
TMS	Transmembrane Segments
X g	times 'g' (unit gravitational field)
YEPD	Yeast Extract Peptone Dextrose media

LIST OF FIGURES

INTRODUCTION

Figure 1: Some commonly occurring Fungal Infections

Figure 2: Factors which may contribute to clinical resistance

Figure 3: Predominant drug resistance mechanisms in yeast

Figure 4: Ergosterol biosynthetic pathway showing the sites of inhibition by different antifungals

Figure 5: Schematic representation of the two major classes of multidrug transporters

Figure 6: Predicted topology of the principal ABC proteins

Figure 7: Linear representation of a prototype ABC domain, with assignment of the main functional sites

Figure 8: A diagrammatic representation of an MFS transporter

Figure 9: A Typical MFS-MDR transporter from the 12-spanner DHA1 (light blue) and 14-spanner DHA2 (dark blue) families.

Figure 10: Kinetic mechanism of a typical ABC transporter

Figure 11: Typical 3D structure of an MFS transporter

Figure 12: Schematic diagram of the single binding site, alternating access mechanism with a rocker-switch type of movement for the GlpT-mediated G3P-Pi exchange reaction

Figure 13: Strategies commonly used for structural and functional characterization of membrane proteins

MATERIALS AND METHODS

Figure 14: Antifungal susceptibility testing of yeast

RESULTS AND DISCUSSION-I

Figure 15: Multiple sequence alignment of MFS transporters showing conserved residues

Figure 16: Southern Blot Hybridization confirming integrated mutant variants of conserved residues in CaMdr1p

Figure 17: Drug resistance profile of wild-type and conserved residues mutant CaMDR1 strains as determined by the spot assay.

Figure 18: Predicted topology of CaMdr1p with conserved residues shown in colour

Figure 19: Comparison of protein expression profiles of CaMdr1p-GFP and its mutant variants of conserved residues in *S. cerevisiae*

Figure 20: Surface localization of CaMdr1p-GFP and its mutant variants of conserved residues.

Figure 21: [^{3}H] MTX and [^{3}H] FLU accumulation in wild-type and in different mutant variants of conserved residues

Figure 22: Secondary structure of the CaMdr1p with positions of cysteine residues marked therein

Figure 23: Southern Hybridization showing integration of mutant variants of cysteine residues and cysless-variant of CaMdr1p-GFP

Figure 24: Strategy showing the integration of CLCaMDR1-$(His)_{10}$

Figure 25: Southern Hybridization confirming integration of CLCaMDR1-$(His)_{10}$

Figure 26: Drug resistance profile of wild-type, cysteine mutant variants and cysless variants of CaMDR1 as determined by the spot assay

Figure 27: Protein expression profiles of KKCLCaMDR1-GFP and KKCLCH10 in comparison to CaMDR1-GFP and CaMDR1-His in *S. cerevisiae*

Figure 28: Confocal images and FACS analysis of the all the cysteine mutant variants and KKCLCaMDR1-GFP

Figure 29: Multiple sequence alignment of different CaMDR1 polymorphic alleles

Figure 30: N-terminal portion of a Multiple Sequence Alignment of MFS sequences

Figure 31: Southern Blot Hybridization confirming integrated mutant variants of Serine, Asparagine and Aspartate residues of unique stretch of CaMdr1p

Figure 32: Drug resistance profile of wild-type CaMDR1-GFP and mutant variants of Serine, Asparagine and Aspartate residues in unique stretch of CaMdr1p as determined by the spot assay.

Figure 33: Protein expression profiles of CaMdr1p-GFP and its mutant variants of Serine, Asparagine and Aspartate residues of unique stretch in *S. cerevisiae.*

Figure 34: Surface localization of CaMdr1p-GFP and its mutant variants of residues in unique stretch of its N-terminal

Figure 35: [^{3}H] MTX and [^{3}H] FLU accumulation in the different mutant variants of residues in N-terminal of CaMdr1p-GFP in *S. cerevisiae*

Figure 36: The secondary structure of CaMdr1p highlights the N-terminal region where the deletion constructs are made

Figure 37: Drug resistance profile of CaMdr1p deletion mutant variants of the N-terminal compared to RPCaMDR1-GFP (positive control) and AD1-8u- (negative control)

Figure 38: Protein expression profiles of the wild-type compared to the deletion mutant variants of N-terminal of CaMdr1p-GFP

Figure 39: Confocal images of the deletion constructs of the N-terminal of CaMdr1p

Figure 40: Comparison of Flow cytometry analysis of cells expressing CaMdr1p-GFP and its deleted versions

Figure 41: [^{3}H] MTX and [^{3}H] FLU accumulation in the deletion mutant variants of CaMDR1-GFP.

RESULTS AND DISCUSSION-II

Figure 42: A portion of Multiple Sequence Alignment showing conservation and RE_M for each column

Figure 43: Comparative plot of conservation (red), RE (green) and RE_M (blue) across the entire alignment

Figure 44: Distribution curve of RE_M values of complete MSA

Figure 45: Drug susceptibility assay of mutant variants of high RE_M residues in CaMdr1p-GFP in *S. cerevisiae*

Figure 46: [^{3}H] MTX and [^{3}H] FLU accumulation in the mutant variants of high RE_M residues of CaMdr1p-GFP.

Figure 47: Protein expression profiles of CaMdr1p-GFP and its mutant variants of high RE_M residues in *S. cerevisiae.*

Figure 48: The 3D deduced homology model of CaMdr1p.

Figure 49: The contact map derived from the 3D homology model of CaMdr1p

Figure 50: Pictorial representation of inter-helical interactions via these high RE_M residues

RESULTS AND DISCUSSION-III

Figure 51: Representative alignment of DHA1 and SP families of MFS transporters

Figure 52: Distribution curve of CRE_S values from the complete MSA

Figure 53: Drug susceptibility assay of mutant variants of high CRE_S residues in CaMdr1p-GFP

Figure 54: Expression profiles of CaMdr1p-GFP and its mutant variants of high CRE_S residues

Figure 55: [^{3}H] MTX and NR accumulation in the mutant variants of high CRE_S residues in CaMdr1p-GFP

Figure 56: The deduced 3D homology model of CaMdr1p highlighting the positions of the mutated high CRE_S residues

Figure 57: Comparative plot of Conservation, RE_{NULL} and CRE_S across the entire alignment

LIST OF TABLES

INTRODUCTION

Table 1: List of Human Pathogenic Fungi

Table 2: Species commonly causing Invasive Candidiasis

Table 3: Commonly used antifungals and their mode of action

Table 4: List of cellular factors which contribute to drug resistance

Table 5: List of Molecular factors which contribute to drug resistance

Table 6: Time-line of the search for the location of drug-binding sites on P-gp

RESULTS AND DISCUSSION-I

Table 7: MIC_{80} (μg/ml) values of the mutant variants of conserved residues of CaMdr1p

Table 8: MIC_{80} (μg/ml) values of individual cysteine mutant variants and the cysless variants of CaMdr1p

Table 9: MIC_{80} (μg/ml) values of the mutant variants of the Serine, Asparagine and Aspartate residues in the unique stretch of CaMdr1p

Table 10: MIC_{80} (μg/ml) values of the deletion mutants with truncations in the N-terminal of CaMdr1p

RESULTS AND DISCUSSION-II

Table 11: Summary of inter-helical interactions via high RE_M residues

Table 12: High RE_M alignment positions shown to be critical for function in other MFS members

RESULTS AND DISCUSSION-III

Table 13: MIC_{80} (μg/ml) values of the mutant variants of high CRE_S residues in CaMdr1p

SUPPLEMENTARY DATA

This data is stored on the compact disc attached with this thesis

MATERIALS AND METHODS

Table S1: List of Plasmids and Yeast strains used in this study

Table S2: List of Oligonucleotides used in this study

RESULTS AND DISCUSSION-II

Dataset DS1: The PRALINETM alignment of 342 MFS sequences as described in Materials and Methods

Table S3: RE_M, RE and conservation scores for all the positions of the MSA of 342 MFS sequences

Table S4: Comparison of RE_M and conservation scores

RESULTS AND DISCUSSION-III

Dataset DS2: Multiple sequence alignment (MSA) of 37 members of DHA1 family and 44 members of SP family of MFS transporters, as described in Materials and Methods

Table S5: RE across DHA1 and SP families, CRE and CRE_S scores for the entire MSA

TABLE OF CONTENTS

INTRODUCTION **1-45**

1.1 INTRODUCTION **1**
1.2 CANDIDA AND CANDIDIASIS **1**
1.2.1 Mortality/Morbidity due to Candidiasis 2
1.3 MULTIDRUG RESISTANCE **4**
1.3.1 Primary versus secondary resistance 6
1.3.2 What is antifungal drug resistance? 7
1.4 MECHANISM OF RESISTANCE TO ANTIFUNGALS **8**
1.4.1 Clinical Factors 8
1.4.2 Cellular Factors 9
1.4.3 Molecular Factors 9
1.4.3.1 Mechanism of non-azole mediated resistance 9
1.4.3.1.1 Resistance to 5-Flucytosine 9
1.4.3.1.2 Resistance to Polyenes 11
1.4.3.1.3 Resistance to Allylamines 11
1.4.3.1.4 Resistance to Morpholines 12
1.4.3.1.5 Resistance to 1, 3 β-glucan synthase inhibitors 13
1.4.3.2 Mechanism of azole mediated resistance 13
1.4.3.2.1 Permeability Resistance 13
1.4.3.2.2 Molecular alterations in ergosterol pathway genes 15
1.4.3.2.2.1 Alteration in Erg11p 16
1.4.3.2.2.2 Upregulation of *ERG11* 17
1.4.3.2.3 Molecular alterations in other *ERG* genes 18
1.4.3.2.3.1 $\Delta^{5,6}$-desaturase (*ERG3*) 18
1.4.3.2.3.2 Δ^{22}-desaturase (*ERG5*) 19
1.4.3.2.3.3 Membrane Lipid Composition 19
1.4.3.2.4 Import of drugs 19
1.4.3.2.5 Efflux of drugs 20
1.4.3.2.5.1 ABC Superfamily 21
1.4.3.2.5.2 MFS Transporters 25
1.5 STRATEGIES TO COMBAT MDR **27**
1.6 STRUCTURAL AND FUNCTIONAL STUDIES ON EFFLUX TRANSPORTERS **27**
1.6.1 Functional aspects of ABC Transporters 27
1.6.2 Functional aspects of MFS Transporters 30
1.7 APPROACHES FOR STRUCTURAL AND FUNCTIONAL ANALYSIS OF MULTIDRUG EFFLUX PUMPS **34**
1.7.1 Random and Site-directed mutagenesis 38
1.7.2 Domain Analysis 40
1.7.3 Chimeric Analysis 42
1.8 AIMS, OBJECTIVES AND SCOPE OF THE PRESENT WORK **43**

MATERIALS AND METHODS **46-59**

2.1 MATERIALS **46**
2.2 MEDIA AND STRAINS **46**

2.3 OLIGONUCLEOTIDES **47**
2.4 METHODS **47**
2.4.1 COMPUTATIONAL METHODS 47
2.4.1.1 Multiple Sequence Alignments 47
2.4.1.2 Calculation of Conservation Score and RE_M from Multiple Sequence Alignment of MFS transporters 48
2.4.1.3 Calculation of Scaled Cumulative Relative Entropy (CRE_S) score from a profile-profile alignment of DHA1 and SP families of MFS transporters 48
2.4.1.4 Molecular Modelling of CaMdr1p 50
2.4.1.5 Generating the contact map 50
2.4.2 MOLECULAR BIOLOGY PROTOCOLS 50
2.4.2.1 Site-specific mutagenesis and development of transformants 50
2.4.2.2 Bacterial miniprep DNA isolation 51
2.4.2.3 Integrative and episomal DNA transformation 51
2.4.2.4 Yeast Genomic DNA isolation 52
2.4.2.5 Southern blot analysis of genomic DNA 54
2.4.2.6 Plasma membrane preparation and Immunodetection 54
2.4.2.7 Protein gel electrophoresis (SDS-PAGE) 55
2.4.2.8 Confocal microscopy 55
2.4.2.9 Flow cytometry 55
2.4.3 RESISTOTYPING 56
2.4.3.1 Drug Resistance Assays 56
2.4.3.1.1 Filter Disc Assay 56
2.4.3.1.2 Microtiter / Microdilution assay 56
2.4.3.1.3 Spot Assay 58
2.4.4 BIOCHEMICAL TECHNIQUES 58
2.4.4.1 [^{3}H]-Fluconazole and [^{3}H]-Methotrexate accumulation 58
2.4.4.2 Transport of Nile Red 58
2.4.4.3 Statistical Analysis 59

RESULTS AND DISCUSSION **60-135**

SECTION I **60-98**
3.1 RANDOM MUTATIONAL ANALYSES OF THE MULTIDRUG MFS TRANSPORTER CaMdr1p **60**
3.1.1 INTRODUCTION 60
3.1.2 RESULTS 62
3.1.2.1 SITE-DIRECTED MUTATIONAL ANALYSIS OF CONSERVED RESIDUES OF CaMdr1p 62
3.1.2.1.1 Sequence alignment of fungal MFS transporters with CaMdr1p reveals several conserved residues 62
3.1.2.1.2 Mutant variants of conserved residues display different levels of sensitivity to various drugs tested 65
3.1.2.1.3 All Mutant variants of CaMdr1p showed Cell Surface Expression and localization similar to wild-type 71
3.1.2.1.4 Accumulation of drugs [^{3}H] MTX and [^{3}H] FLU by selected mutant variants is enhanced 71
3.1.2.2 CYSTEINE-SCANNING MUTAGENESIS 73

3.1.2.2.1 Location of cysteines marked on the secondary structure of CaMdr1p 73
3.1.2.2.2 Cloning of cysless-CaMDR1-$(His)_{10}$ in the hyper-expression system 74
3.1.2.2.3 Drug resistance profile of individual cysteine mutant variants and the cysless constructs 77
3.1.2.2.4 All cysteine mutants as well as cysless-CaMdr1p showed Cell Surface Expression and localization similar to the wild-type 79
3.1.2.3 CHARACTERIZATION OF UNIQUE N-TERMINAL OF CaMdr1p 80
3.1.2.3.1 Drug resistance profile of individual mutant variants of Serine, Asparagine and Aspartate residues in the (^{68}SSQSSSSNNTIVDNNNNNNDNDVDGD---DDD^{104}) stretch 83
3.1.2.3.2 Expression and localization of CaMdr1p-GFP in the mutant variants remains unaffected 86
3.1.2.3.3 Accumulation assay of [^{3}H] MTX and [^{3}H] FLU exhibits that the activity of mutant variants is similar to wild-type 86
3.1.2.3.4 Deletion Mutants of the unusually long N-terminal of CaMdr1p 89
3.1.2.3.5 Drug resistance profile of the N-terminal deletion mutants 89
3.1.2.3.6 Reduced expression of CaMdr1p in the deletion mutants due to mislocalization as checked by Western Blot Analysis 89
3.1.2.3.7 The deletion mutants of N-terminal of CaMdr1p-GFP show poor surface localization 92
3.1.2.3.8 Accumulation assay of [^{3}H] MTX and [^{3}H] FLU shows aborted activity of CaMdr1p-GFP in these deletion mutants 96
3.1.3 DISCUSSION 96

SECTION II 99-118
3.2 MEMBRANE ENVIRONMENT BASED RATIONAL COMPUTATIONAL APPROACH FOR IDENTIFICATION OF FAMILY-WIDE-FUNCTION SPECIFIC RESIDUES OF CaMdr1p 99
3.2.1 INTRODUCTION 99
3.2.2 RESULTS 101
3.2.2.1 RE_M considers conservation as well as the background probability of each alignment position of a MSA 101
3.2.2.2 Residues with high RE_M are part of the known motifs of Major Facilitator Superfamily 104
3.2.2.3 Site-specific mutagenesis of residues with high RE_M shows that they are functionally critical 105
3.2.2.4 All these mutant variants are properly surface localized 105
3.2.2.5 Distance plot of CaMdr1p from deduced 3D homology model reveals inter-helical interactions 112
3.2.3 DISCUSSION 112

SECTION III **119-135**
3.3 IDENTIFICATION OF DRUG-PROTON ANTIPORTER FUNCTION SPECIFIC RESIDUES OF CaMdr1p BY EMPLOYING INFORMATION THEORETIC MEASURES **119**
3.3.1 INTRODUCTION 119
3.3.2 RESULTS 121
3.3.2.1 CRE_S scores predict functionally important residues of CaMdr1p 121
3.3.2.2 Site-specific mutagenesis confirms CRE_S based selection of functionally critical residues 124
3.3.2.3 All these mutant variants of CaMdr1p are normally expressed and properly localized 127
3.3.2.4 High CRE_S residues displayed abrogated efflux 127
3.3.3 DISCUSSION 130

SUMMARY **136**

REFERENCES **141**

APPENDICES **160**

PUBLICATIONS **164**

INTRODUCTION

1.1 INTRODUCTION

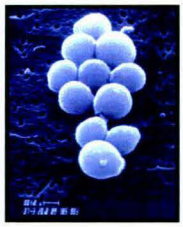

Yeasts are common microorganisms found virtually everywhere. They being ubiquitous in nature are ordinarily non-pathogenic, harmless saprobes but some of them may cause life-threatening infection in seriously ill and / or immuno-compromised patients. Over the past two decades, there has been a sudden increase in the incidence of opportunistic fungal infections, which is probably the result of alteration in immune status associated with the AIDS epidemic, cancer chemotherapy, and organ and bone marrow transplantation.

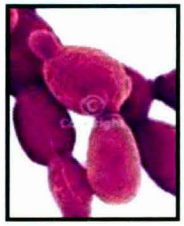

While fungal infections due to *Candida* and *Aspergillus* species are most common, previously rarely encountered opportunistic fungi have emerged recently as significant pathogens [Prasad, 1991]. For instance, *Trichosporon beigelii*, *Fusarium* species, *Pseudallescheria boydii* and moulds of the class Zygomycetes can cause invasive infections. *Candida* spp., *Cryptococcus neoformans*, and *Aspergillus* spp. are among the leading fungi responsible for these invasive infections. The overall mortality rate from candidiaisis exceeds 60% while aspergillosis and fusariosis have a mortality of >90%. Figure 1 shows some commonly occurring fungal infections. Table 1 summarizes a list of human pathogenic fungi. In addition to the opportunistic pathogenic fungi, a limited number of fungi exist with a true pathogenic potential for healthy hosts and cause life threatening infections [Ernst and Schmidt, 2000; Odds, 1988]. These pathogens, e.g., *Histoplasma capsulatum, Paracoccodioides brasiliensis, Pencillium marneffei* and *Coccidioides immitis*, are therefore classified as biohazard class 3 [Marichal, 1999].

1.2 CANDIDA AND CANDIDIASIS

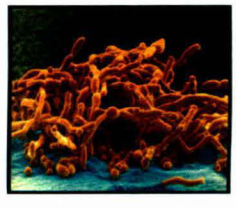

Candida species are classified as oval yeasts of 2-6 µm in diameter with a predominantly unicellular mode of development. The genus *Candida* is composed of heterologous group and includes more than 150 species, whose main common feature is the absence of any sexual form. Members of the genus *Candida* are found in all areas

of the intestinal tract, usually causing no medical problems. However, in patients with a compromised immune system, life threatening diseases may result. The bloodstream infections with *C. albicans* have a more frequent occurrence but also a relative proportion is exhibited due to non-*albicans* species, including species such as *C. glabrata*, *C. krusei, C. parasilopsis*, *C. tropicalis* and *C. lusitaniae* (Table 2).

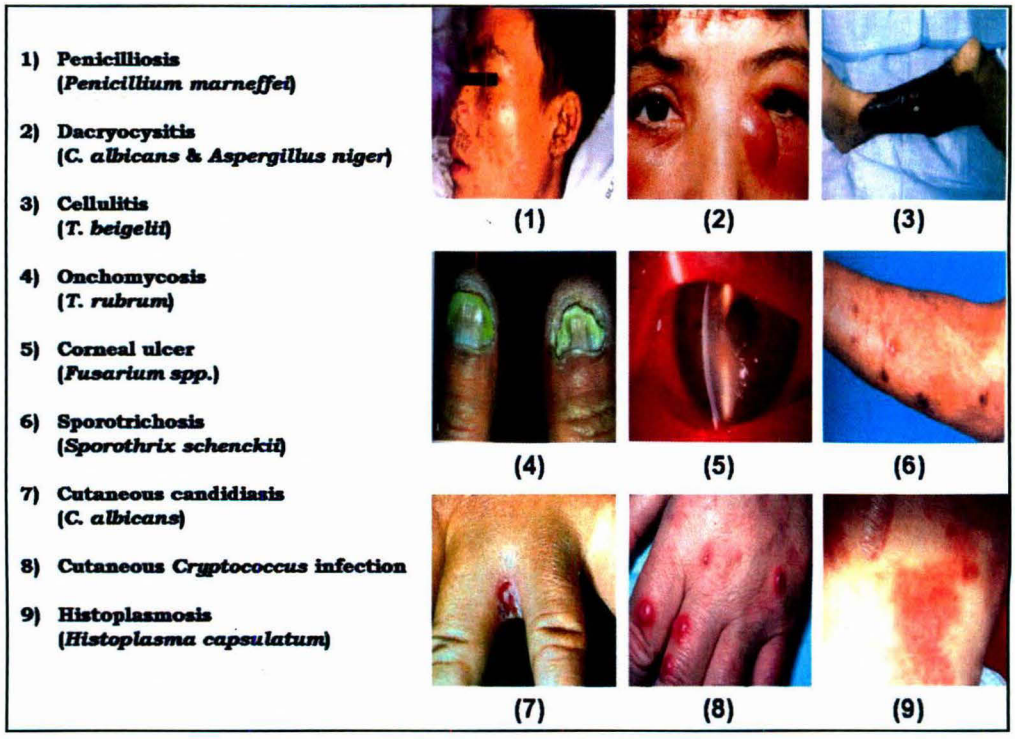

Figure 1: Some commonly occuring Fungal Infections

1.2.1 Mortality/Morbidity due to Candidiasis

Mucocutaneous candidiasis- Most candidal infections are mucocutaneous and, as such, do not cause mortality. However, in patients with advanced immunodeficiency due to HIV infection, these mucosal infections can become refractory to antifungal therapy and may lead to severe oropharyngeal and esophageal candidiasis that initiates a vicious cycle of poor oral intake, malnutrition, wasting, and early death.

Candidemia and disseminated candidiasis- Mortality rates for these infections have not improved markedly over the past few years and remain in the range of 30-40%. Systemic candidiasis is the cause of more case fatalities than any other systemic mycoses. More than a decade ago, investigators reported the enormous economic impact of systemic candidiasis in patients who are hospitalized. Although

mucocutaneous fungal infections, such as oral thrush and *Candida* esophagitis, are extremely common in patients with AIDS, candidemia and disseminated candidiasis are uncommon.

PATHOGENIC SPECIES	ORGANISMS
Common opportunistic fungal pathogens	
Candida	*C. albicans, C. glabrata, C. tropicalis, C. kefyr, C. krusei* and *C. parapsilosis*
Malassezia	*M. furfur, M. ovalis* and *M. pachydermatis*
Cryptococcus	*C. neoformans, C. laurentii* and *C. albidus*
Aspergillus	*A. nidulans* and *A. niger*
Neurospora	*N. crassa*
Rare pathogens	
Fusarium	*F. solani*
Pseudallescheria	*P. boydii*
Rhodotorula	*R. rubra* and *R. pilimanae*
Hansenula	*H. anomala* and *H. polymorpha*
Pichia	*P. farcinosa*
Kluveromyces	*K. marxianus*
Wangiella	*W. dermatitidis*
Blastomyces	*B. dermatitidis*
Trichosporon	*T. capitulum* and *T. beigelii*
Non-opportunistic pathogens	
Histoplasma	*H. capsulatum*
Paracoccidioides	*P. brasiliensis*
Coccidioides	*C. immitis*
Penicillium	*P. marneffei*

Table 1: List of Human Pathogenic Fungi

MEDICALLY SIGNIFICANT *CANDIDA* SPECIES	% ABUNDANCE
Candida albicans (the most common species identified)	50-60 %
Candida glabrata	15-20 %
Candida parapsilosis	10-20 %
Candida tropicalis	6-12 %
Candida gulliermondi	<5 %
Candida kefyr	<5 %
Candida lusitaniae	<5 %
Candida krusei	1-3 %
Candida dubliniensis (primarily recovered from patients who are positive for HIV)	>95%

Table 2: Species commonly causing Invasive Candidiasis
From: http://www.doctorfungus.org/index.htm

1.3 MULTIDRUG RESISTANCE

MDR as a phenomenon is defined as resistance against a spectrum of drugs that share neither a common target nor a common structure. MDR can develop after sequential or simultaneous exposure to all the different drugs to which the cell or microorganism is resistant. However it may also develop surprisingly before exposure to many of the compounds to which the cell or microorganism is found to be resistant. It generally involves a network of membrane-associated transporters acting as multidrug efflux pumps and transcription factors regulating the expression of these pumps. These multidrug efflux systems present a disturbing clinical threat, since the acquisition of a single such system by a cell may decrease its susceptibility to a broad spectrum of chemotherapeutic drugs. The existing antifungal armamentarium contains four classes of drug-polyenes, nucleic acid synthesis inhibitors, ergosterol biosynthesis inhibitors (EBIs), and echinocandins. Clinical resistance has been observed for all classes of antifungal, and no single class of antifungal is effective against all invasive mycoses. Each class of drug has a specific mode of action and a distinct role in the treatment of fungal pathogens (Table 3). The development of drug resistance is a frequent impediment to the effective treatment of infectious and malignant diseases [Kerridge, 1985; Kerridge, 1986]. Mechanisms of

MDR are opportunistic in their manipulation of the normal pathways of cellular homeostasis. Several alterations in the cell take place resulting in drug resistance.

ANTIFUNGAL	SPECTRUM/ COMMENTS	MODE OF ACTION	MECHANISM OF RESISTANCE
Polyenes			
Amphotericin B	Broad activity against *Candida* spp (except *C. lusitaniae*), *Cryptococcus neoformans* and filamentous fungi	Binding to ergosterol and destabilization of cell membrane functions	Alteration in specific steps of ergosterol biosysnthesis
Pyrimidine analogs			
5-Fluorocytosine (5-FC)	Active against *Candida* spp and *Cryptococcus* spp; however rapid emergence of resistance can appear when 5-FC is used as monotherapy	Impairment of nucleic acid biosynthesis by formation of toxic fluorinated pyrimidine antimetabolites	Decreased uptake of 5-FC; decreased formation of toxic antimetabolites
Azoles			
Fluconazole	Active against *Candida* spp and *Cryptococcus* spp, less active against *C. glabrata* and no activity against *C. krusei*; no activity against filamentous fungi	Inhibition of cytochrome P450 14α-lanosterol demethylase	Enhanced efflux by upregulation of multidrug transporter genes. Target alteration by occurrence of mutations. Alteration of specific steps in ergosterol biosynthetic pathway
Itraconazole	Like Fluconazole, but enhanced activity against filamentous fungi		
Voriconazole	Like Fluconazole, but enhanced activity against filamentous fungi, including *Aspergillus* and *Fusarium* spp		
Posaconazole	Closely related to itraconazole, but more potent		
Allylamines			
Terbinafine	Active against most dermatophytes, poor activity against *Candida* spp	Inhibition of squalene epoxidase	Unknown

Morpholines			
Amorolfine	Active against most dermatophytes, poor activity against *Candida* spp	Inhibition of sterol Δ^{14}-reductase and $\Delta^{7,8}$-isomerase	Unknown
Echinocandins			
Caspofungin	Active against *Candida* spp with fungicidal activity, moderately active against *Aspergillus* spp, poor activity against *C. neoformans*	Inhibition of the cell wall synthesis enzyme β-1,3 glucan synthase	Unknown

Table 3: Commonly used antifungals and their mode of action

1.3.1 Primary versus Secondary Resistance

Similar to bacteria, resistance among fungi can be classified as primary or secondary. Primary, or intrinsic, resistance refers to an organism's natural susceptibility to an antimicrobial. This innate level of susceptibility is thought to be a drug-organism characteristic and independent of drug exposure. For example, *C. krusei* can be regarded as intrinsically resistant to fluconazole and *C. parapsilosis* to Amphotericin B [Ernst and Schmidt, 2000]. It is obvious that on a case-by-case basis intrinsic resistance is not a major threat if clinicians are aware of subtle susceptibility differences among *Candida spp*. Primary resistance becomes more problematic when considering the larger picture. If a single agent or class of drugs is widely administered because the fungus most commonly encountered is highly susceptible to it, we run the risk of altering the fungal population dynamics by suppressing or eradicating susceptible species. This creates a niche in the local flora, allowing an organism intrinsically less susceptible to the workhorse antifungal to replicate and spread, and possibly eventually become the predominant pathogen isolated.

Secondary or acquired resistance is much less predictable and potentially more problematic than primary resistance. Under conditions of environmental stress such as exposure to antifungal agents, a population of initially susceptible fungi may begin to display resistance. This may result from expression of newly acquired genetic alterations, translation and expression of previously repressed metabolic pathways, or unmasking of an existing, less susceptible fungal subpopulation [Klepser *et al.*, 1997].

A given population of fungi generally consists of a collection of similar yet heterogeneous strains from the same species. When an MIC is determined for the population, it represents the concentration that inhibits the growth of most of the population. Thus, fractions of the population will be more or less susceptible to the test drug. If the population is repeatedly exposed to a concentration of an agent equal to the observed MIC, the most susceptible members will be quickly eradicated, leaving only the less susceptible subpopulation. Eventually, this more resistant fraction will become the predominant phenotype remaining. Several investigators studying the emergence of drug-resistance verified this concept. *C. albicans* has been found in individuals infected with the human immunodeficiency virus treated with fluconazole, the primary group in whom isolation of drug-resistant *C. albicans* has occurred.

1.3.2 What is antifungal drug resistance?

Antifungal drug resistance was first described more than 20 years ago, when Kessel and co-workers, and Biedler and Riehm, 1970 noted that cell lines made resistant to actinomycin D or Vinca alkaloids displayed cross-resistance to a wide range of other compounds. Ever since then this phenomenon has been observed in various organisms throughout the evolutionary scale. From a clinical perspective, drug resistance may be defined as the persistence or progression of an infection despite appropriate drug therapy and is a multifactorial phenomenon [White, 1997]. The clinical outcome of treatment depends not only on the susceptibility of the pathogen to a given drug but also on many other factors including pharmacokinetics, drug interactions, immune status, and patient compliance, as well as several specific conditions such as the occurrence of biofilms on surfaces of catheters and prosthetic valves [White *et al.,* 1998]. From a mycological viewpoint different classifications of resistance are made. Antifungal drug resistance has been classified as either primary, when a fungus is resistant to a drug prior to any exposure, or secondary, when an initially sensitive fungus becomes resistant after exposure to the drug [Rex *et al.,* 1997; White *et al.,* 1998].

1.4 MECHANISMS OF RESISTANCE TO ANTIFUNGALS

Since the initial studies of antifungal resistance in the early 1980s, tremendous knowledge concerning the clinical, biochemical and genetic aspects of this phenomenon has accumulated which will be discussed in the following sections.

1.4.1 Clinical factors

Over the last several decades, aggressive anticancer chemotherapy has resulted in a population of patients that are increasingly exposed to azole drugs for antifungal treatment and prophylaxis. An increased rate of patient mortality due to candidiasis has been reported in patients suffering from cancer or undergoing organ transplantation [Khan and Gyanchandani, 1998]. Figure 2 summarizes the clinical factors involved in the development of resistance. The role of azoles in treating *Candida* infections in the above patients has been expanding and advances in clinical microbiology have enabled us to detect and define azole resistance.

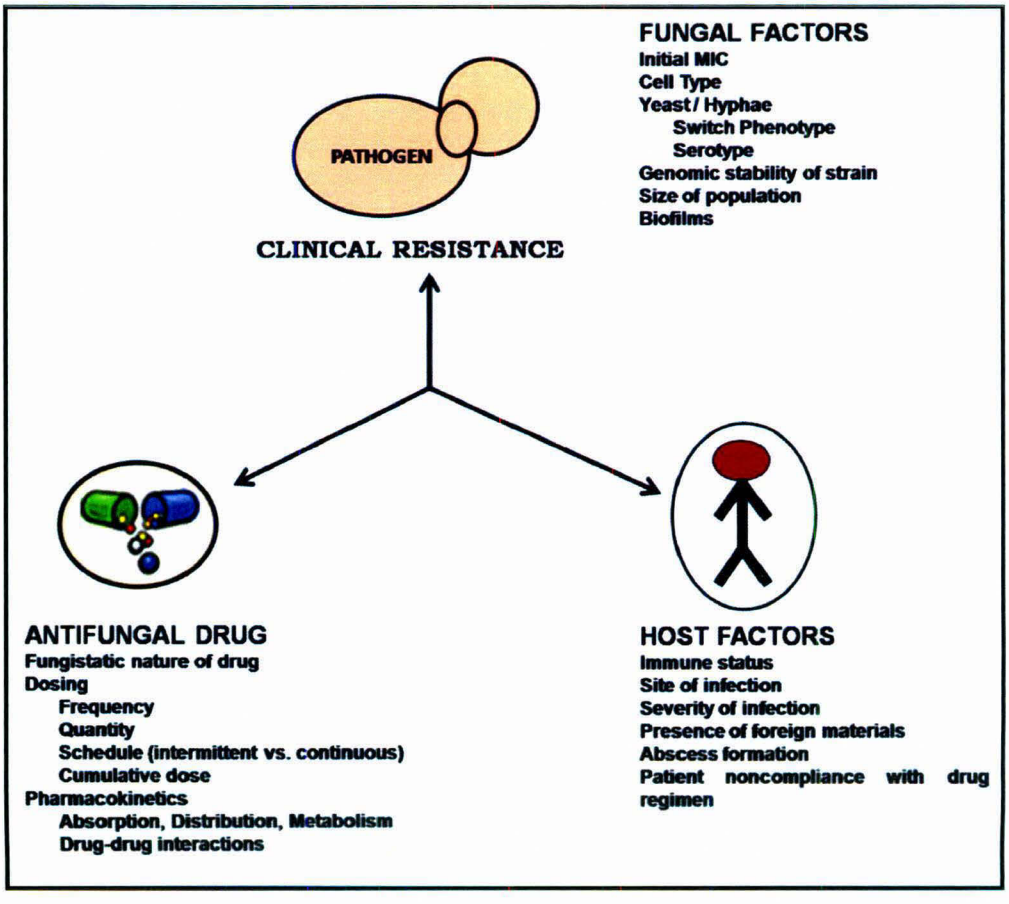

Figure 2: Factors which may contribute to clinical resistance

1.4.2 Cellular factors

A fungal infection, which does not respond to treatment by antifungals, is clinically defined as a drug resistant infection. Thes resistant species may be present by chance in a healthy individual as commensal organism, which can then become a problem when the host becomes immunocompromised and is administered azole therapy. In such patients, the selective pressure of antifungal drugs may allow the replacement of endogenous species with more resistant super-infecting species. Several other factors that can lead to the presence of a resistant strain in a patient are listed as in Table 4 [White *et al.*, 1998].

1.4.3 Molecular factors

Although the molecular basis of drug resistance in *Candida* is not very clear, evidences accumulated so far suggests that MDR is a multi-factorial phenomenon where a combination of mechanisms could contribute to drug resistance. Resistance to antifungals could be visualized as a gradual evolving process wherein different mechanisms may appear during the course of chemotherapy. Some of the well-known mechanisms of drug resistance in pathogenic fungi are discussed below are listed in Table 5. These chiefly include alteration in sterol biosynthesis pathway; reduction in the import of drug into the cell; changes in the interaction of the drug with the target enzyme; and reduced intracellular drug accumulation which is correlated with an increased efflux of the drug from the cell. In contrast, inactivation of the drug once it is inside the cell, a frequent cause of resistance to antibiotics in bacteria, has not been described as a resistance mechanism in *C. albicans*. Some of the well-known mechanisms of resistance in *Candida* are discussed below and these have been broadly divided into non-azole and azole mediated resistance.

1.4.3.1 Mechanisms of non-azole mediated resistance

1.4.3.1.1 Resistance to 5-Flucytosine

5-Flucytosine (5-FC) is a nucleoside analog and constitutes the third class of antifungal agents. It is an antimetabolite type of antifungal drug and is the only available antimetabolite drug having antifungal activity. It inhibits fungal protein

CELLULAR MECHANISMS OF ANTIFUNGAL RESISTANCE
➢ Change to more resistant species of *Candida* e.g replacement by *C. krusei* or *C.glabrata*
➢ Change to a more resistant strain of *C. albicans*
➢ Genetic alterations that render a strain resistant. Drug pressure leads to a generation of resistant cells with specific random mutations
➢ Transient gene expression which leads a cell to alter its phenotype to become resistant in the presence of drug
➢ Cellular mechanisms of drug resistance

Table 4: List of cellular factors which contribute to drug resistance

MOLECULAR MECHANISMS OF ANTIFUNGAL RESISTANCE
➢ Alteration in drug import by change in sterol components of the plasma membrane
➢ Alteration in intracellular drug processing Modification Degradation
➢ Genetic changes in target enzyme, *ERG11* including Point mutations Over-expression Gene amplification (leads to over-expression) Gene conversion or mitotic recombination
➢ Alteration in other enzymes in ergosterol biosynthetic pathway
➢ Increased efflux of drugs attributed to ABC transporters (*CDR* genes) MFS transporters (*MDR1* gene)

Table 5: List of Molecular factors which contribute to drug resistance

while acquired resistance results from a failure to metabolize 5-FC to 5-FUTP and 5-synthesis by replacing uracil with 5-flurouracil in fungal RNA. Flucytosine also inhibits thymidylate synthetase via 5-fluorodeoxy-uridine monophosphate and thus interferes with fungal DNA synthesis. Primary resistance to 5-FC is a common phenomenon. Resistance may occur due to the deficiency or lack of enzymes involved in the uptake or metabolism of 5-FC, or may be due to the deregulation of the pyrimidine biosynthetic pathway, whose products can compete with the fluorinated metabolites of 5-FC [Kerridge and Whelan, 1984]. Detailed investigations on the molecular mechanisms of resistance to 5-FC have shown that intrinsic resistance in fungi can be due to a defect in cytosine permease (with the exception of *C. albicans*), FdUMP, or from the loss of feedback control of pyrimidine biosynthesis [Andriole, 1999; Wynn *et al.*, 2003].

1.4.3.1.2 Resistance to Polyenes

Polyene resistance has not been a major clinical problem to date, although polyene resistant isolates have been isolated and characterized. The polyene antifungal agents include nystatin and AmpB which are fungicidal and have a broad spectrum of antifungal activity. Acquired resistance to AmpB is often associated with alteration of membrane lipids, especially sterols. Most polyene resistant clinical *Candida* isolates have greatly reduced ergosterol content in their membranes [Hitchcock *et al.*, 1987; Hitchcock *et al.*, 1987; White *et al.*, 1998]. There is evidence to suggest that alterations in the membrane structure or in the sterol-to-phospholipid ratio in the membrane may be associated with resistance. Recently, clinical isolates of *C. albicans* resistant to AmpB were described lacking ergosterol and accumulating 3-β-ergosta-7, 22-dienol and 3-β-ergosta-8-enol, typical for a defect in the sterol $\Delta^{5,6}$ desaturase system [Kelly *et al.*, 1997]. Such a defect is known in laboratory yeasts (*S. cerevisiae*) harbouring a defect in the $\Delta^{5,6}$ desaturase gene *ERG3* [Kelly *et al.*, 1994; Geber *et al.*, 1995].

1.4.3.1.3 Resistance to Allylamines

Squalene epoxidase (product of the *ERG1* gene) is the target enzyme of the commonly used allylamines; naftifine and terbinafine [Favre and Ryder, 1997]. Both are used mainly to treat dermatophytosis. The gene encoding squalene epoxidase

(*ERG1*) has been cloned in *S. cerevisiae*. Deletion of this gene affected viability of *S. cerevisiae* during aerobic growth. Resistance of yeasts to allylamines has been reported only rarely however the potential to develop resistance by the action of multidrug efflux transporters does exist. For example, *CDR1* and *CDR2* genes, and *CaMDR1* gene of *C. albicans* when over-expressed in *S. cerevisiae* can confer resistance to terbinafine thus showing that this compound is a substrate for these transporters. Moreover, deletion of the *CDR1* gene in *C. albicans* renders cells hypersusceptible to the same drug [Sanglard *et al.*, 1996]. Several *C. albicans* isolates resistant to azole antifungal agents are also less susceptible to terbinafine. Since such isolates are resistant to azole derivatives by the mechanism of multidrug efflux transporter gene over-expression, the cross-resistance to terbinafine could perhaps be explained by this phenomenon.

1.4.3.1.4 Resistance to Morpholines

Amorolfine is the only morpholine derivative in clinical use. It inhibits at least two enzymes Δ^{14}-reductase (product of the *ERG24* gene) and $\Delta^{8,7}$ isomerase (product of the *ERG2* gene), in the post-lanosterol steps of the ergosterol biosynthesis pathway. Acquired resistance to morpholine derivatives has not been reported so far in yeast pathogens and this is probably due to the limited use of this antifungal for the treatment of superficial fungal infections. However, resistance to morpholine derivatives in *S. cerevisiae* can be due to the over-expression of the *ERG24* or *ERG4* (sterol C-24 (28) reductase) genes [White *et al.*, 1998]. Moreover, previously published studies have pointed out that amorolfine, like terbinafine, could be a substrate of multidrug efflux transporters of the ABC superfamily. This was concluded from results showing that: (i) over-expression of the *C. albicans CDR1* and *CDR2* genes in *S. cerevisiae* could render cells resistant to amorolfine [Sanglard *et al.*, 1997], (ii) *C. albicans* multidrug transporter mutants were hypersusceptible to this antifungal agent [Sanglard *et al.*, 1996], and (iii) *C. albicans* clinical isolates resistant to azole antifungal agents over-expressing the *CDR1* and *CDR2* genes were less susceptible to amorolfine. Therefore, the potential for developing resistance to this agent does exist.

1.4.3.1.5 Resistance to 1, 3 β–glucan synthase inhibitors

The echinocandins and their analogs, the pneumocandins, represent the newest class of antifungal drugs. They inhibit the synthesis of 1,3-β-D-glucan, a fundamental component of the fungal cell wall by the inhibition of 1,3 β-D-glucan synthase, an enzyme complex that forms glucan polymers in the cell wall and is absent in mammalian cells. In *S. cerevisiae*, β-(1,3)-glucan synthase is a multienzyme complex with two subunits encoded by the *FKS1* and *FKS2* genes. Deletion of both genes in this yeast results is lethal [Onishi *et al.*, 2000; Douglas *et al.*, 1997; Kelly *et al.*, 2000]. Resistance to these compounds is possible, since spontaneous mutants resistant to the echinocardin L-733560 have been isolated *in vitro* in *S. cerevisiae* [Onishi *et al.*, 2000; Douglas *et al.*, 1997], and in *C. albicans* [Kurtz *et al.*, 1996]. The mechanism of resistance in these two yeast species is thought to be a lower affinity of echinocandin to the β-(1,3)-glucan synthase produced in these mutants. Resistance to echinocandin may not be relevant in clinical situations, since it was shown that *C. albicans* resistant mutants exhibited attenuated virulence in animal experiments [Kurtz *et al.*, 1996].

1.4.3.2 Mechanisms of azole mediated resistance

Azole antifungal agents are by far the most commonly used drugs to treat infections caused by *C. albicans*. The target for azole antifungal agents in yeast is a cytochrome P-450. This enzyme is involved in the 14α-demethylation of lanosterol which is an important step in the biosynthesis of ergosterol. Azole drugs interact in the active site of the target enzyme by binding to the heme moiety and thus acting as competitive inhibitors of the substrate. Figure 3 depicts the molecular mechanisms of azole resistance that are commonly present in the pathogenic yeast *C. albicans*. Nevertheless, other unknown mechanisms of azole resistance may still be found in clinical isolates. All these mechanisms have been discussed in the following sections.

1.4.3.2.1 Permeability resistance

Defects in drug import are a common mechanism of drug resistance. Many hydrophilic drugs, for example the anticancer antimetabolite methotrexate, cannot easily diffuse through the plasma membrane and have to use specific transporters for

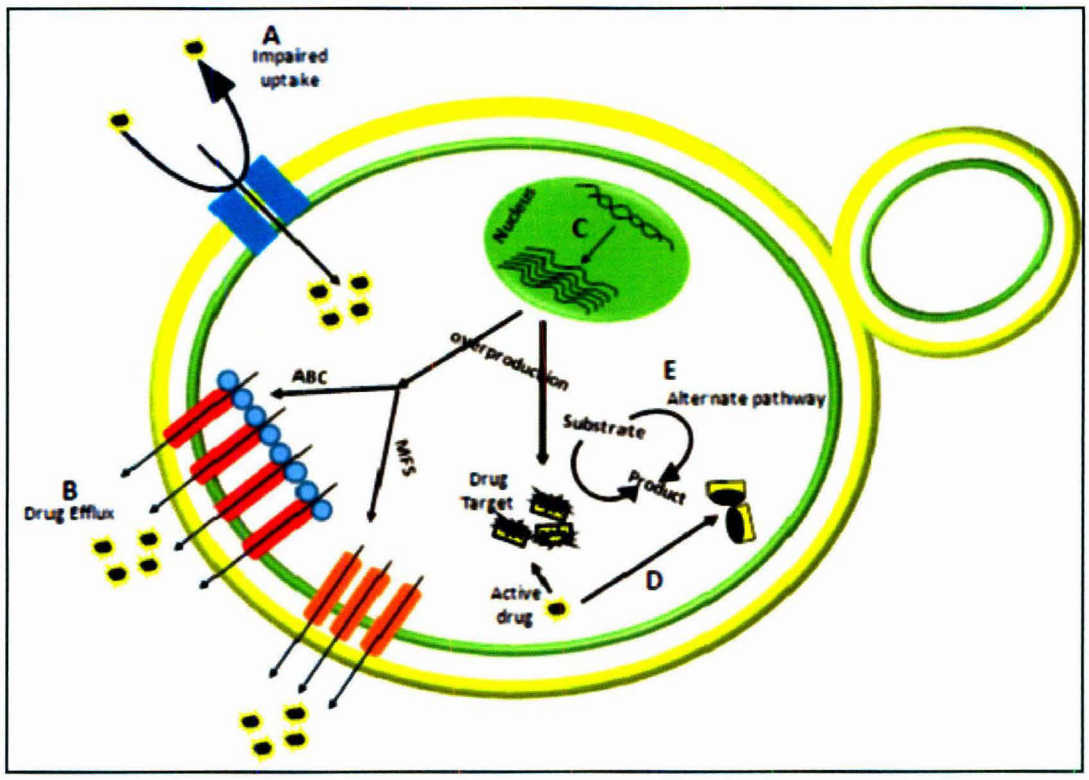

Figure 3: Predominant drug resistance mechanisms in yeast.
(A) Reduced drug uptake (import) due to compositional changes in the cell wall or plasma membrane. (B) Rapid efflux of drugs mediated by the ABC or MFS transporters. (C) Over-expression of the genes encoding drug target *ERG11 and* or of efflux pumps e.g. *CDR1, CDR2* and *CaMDR1*. (D) Mutation in drug target Erg11p (P45014DM) leads to reduction or loss in drug binding. (E) Activation of alternate ergosterol pathways such as $\Delta^{5,6}$-desaturase.

this purpose. Alterations in these transporters often lead to reduced influx of drugs. In the case of Methotrexate, resistance is found to be associated with alterations in the folate transporter [Skovsgaard *et al.,* 1994]. Decreased toxicity can also be caused due to changes in the lipid composition of the membranes leading to a decrease in permeability. The decreased permeability and fluidity of the membranes results from cis- to trans- isomerization of their saturated fatty acids. Resistance to the polyene systemic antifungal such as amphotericin B which interacts with membrane ergosterol to form pores in membranes results in most cases, from defects in the ergosterol biosynthetic pathway, leading to decreased ergosterol levels in the plasma membrane [Kelly *et al.,* 1997]. Several studies have demonstrated that when the ergosterol component of the plasma membrane is eliminated or reduced in favor of other sterol components such as 14α-methyl sterols, there are concomitant permeability changes in the plasma membrane and a lack of fluidity [Bossche *et al.,* 1987]. These changes may lower the capacity of azole drugs to enter the cell. Most amphotericin B resistant

isolates contain abnormally low number of ergosterol molecules in their plasma membrane thereby limiting the number of available binding sites for the polyene and thus preventing membrane damage. Existence of other mechanisms of polyene resistance not linked to sterol alterations has also been suggested [Joseph-Horne and Hollomon, 1997]. Another kind of permeability barrier in *C. albicans* involves formation of biofilms, which are large masses of cells. They have taken centre stage with the increasing recognition of their role in human infections. In the protected microenvironment of biofilms, the pathogens are more resistant to antimicrobial therapies [Reynolds and Fink, 2001]. However, reduction of membrane permeability due to changes in the membrane biophysical properties is not a very efficient way of resistance, unless it is accompanied by another resistance mechanism, such as active efflux or enzymatic activation, which often is the case.

1.4.3.2.2 Molecular alterations in ergosterol pathway genes

Most of the currently used antifungal drugs are directed against the enzymes of the ergosterol pathway (Figure 4). Modifications in the ergosterol pathway are likely to generate resistance not only to the drug to which cells are likely to generate resistance but also to related drugs. DeBacker *et al.,* 2001 have used the DNA chip technology to study cellular responses to perturbations of ergosterol biosynthesis caused by the broad-spectrum antifungal agent itraconazole. A global up-regulation of *ERG* genes in response to azole treatment was observed. *ERG11* and *ERG5* were found to be upregulated approximately 12 fold. In addition, a significant up-regulation was observed for *ERG1, ERG2, ERG3, ERG4, ERG6, ERG9, ERG10, ERG25, ERG26, IDIII, HGMS, NCPI*, and *FEN2*, all of which are genes known to be involved in ergosterol biosynthesis. Azoles inhibit a specific step in the ergosterol biosynthesis in fungi by binding to and inhibiting P45014DM [Wilkinson *et al.,* 1972; Wilkinson *et al.,* 1974]. This leads to high levels of 14-methylated sterols causing disruption of membrane structures. Azole derivatives have been shown to interact with the heme molecule in P45014DM where unhindered nitrogen atom of the azole ring (N3 in imidazole or N4 in derivatives) binds to the heme iron at the sixth co-ordinate position. The blocking of this position that is normally occupied by activated oxygen prevents initiation of the hydroxylation reaction. The affinity and selectivity of the azoles for their target(s) are also determined by their structure, lipophilicity and

stereochemical orientation of the N-1 side chain. Azole derivatives also fit in P45014DM substrate pocket, which normally accepts lanosterol as a natural substrate. The import of azoles inside the cell still remains unresolved although it has been suggested that the hydrophobicity of these drugs could facilitate their entry. Once the drug enters the cell its interaction with P45014DM can be modified in two ways; target alteration and over-expression. Certain point mutations in the gene for P45014DM (ERG11) make the enzyme less sensitive to the drug. The over-expression of enzyme, which necessitates the need for a higher dose of azoles, as compared to a susceptible strain represents another mechanism [White, 1997; Marichal, 1999; White, 1997].

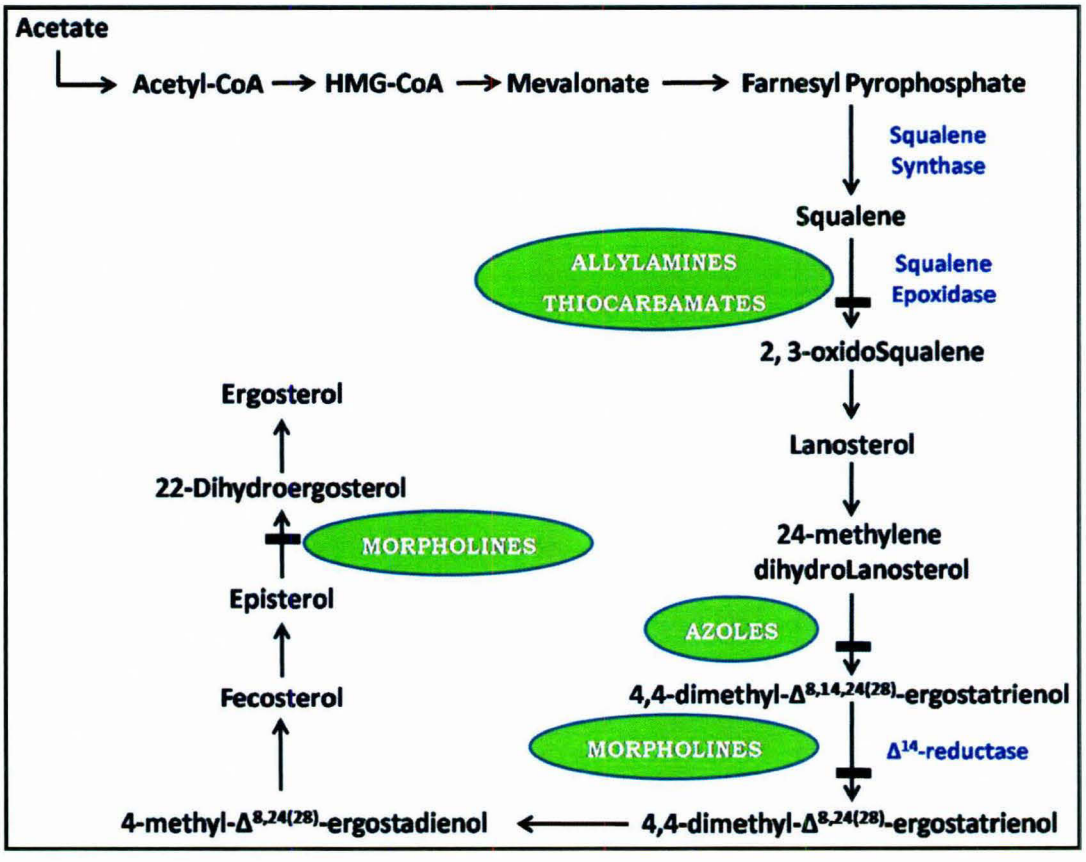

Figure 4: Ergosterol biosynthetic pathway showing the sites of inhibition by different antifungals.

1.4.3.2.2.1 Alterations in Erg11p

Since Erg11p is the target of azole derivatives, it can be expected that amino acid substitution could affect the affinity of this drug. Indeed, many studies have documented point mutations in P45014DM (*ERG11*) gene, which resulted in changes

in the affinity of the azoles to its target protein leading to resistance [Sanglard *et al.*, 1998; Favre *et al.*, 1999; Marichal *et al.*, 1999]. White's group who analyzed a series of C. albicans strains which were earlier isolated by Redding *et al.*, 1994 from a single HIV patient over a period of two years and identified a single amino acid substitution viz., R467K in Erg11p. Since this mutation is close to amino acid cysteine that participates in the coordination of the iron atom in the heme cofactor of enzyme, it has been proposed that the mutation causes structural changes associated with the heme. It has been further reported that R467K alone can confer azole resistance by reducing the affinity of the enzyme for fluconazole [White, 1997]. Based on the architecture of the active site of the enzyme, Lamb *et al.*, 2000 introduced a point mutation T315A in Erg11p and observed that mutant variant protein had higher MIC values for fluconazole and ketoconazole [Lamb *et al.*, 2000]. The purified mutated protein exhibited reduced enzyme activity and affinity for azoles thus providing an example of a single amino acid change in the target protein leading to azole resistance. There are several reports wherein in response to azoles, many point mutations in Erg11p have been identified [Marichal *et al.*, 1999]. The known point mutation in *C. albicans*, have been compiled in a graphical representation by Marichal *et al.*, 1999, to show the frequency and position of each substitution. It is observed that four mutations D116E, K128T, E266D and G464S occurred with highest frequency whereas G464S was the only substitution, which was exclusively seen in azole resistant isolates. The exact placement of these mutations in a 3-D model of the protein show that these mutations are not randomly distributed but rather clustered in three hot spot regions between amino acid residues 105-165, 266-287 and 405-488 [Marichal et al., 1999].

1.4.3.2.2.2 Upregulation of ERG11

Resistance to fluconazole in many clinical isolates has often been associated with the transcriptional activation of *ERG11* (gene encoding target protein P45014DM) [Harry *et al.*, 2002]. However, it has been difficult to correlate the up regulation of the gene with the observed fluconazole resistance mainly due to the simultaneous occurrence of mutations in *ERG11* or due to the over expression of the efflux pumps encoding genes. Gene amplification is one of the common mechanisms of resistance in eukaryotic cells [Stark and Wahl, 1984; Van der Bliek *et al.*, 1988]. However, over expression of *ERG11* in *C. albicans* has not been linked to gene amplification [Bossche *et al.*, 1992; Vanden *et al.*, 1994; Marichal *et al.*, 1997]. In a

clinical isolate of *C. glabrata*, increased level of P45014DM was shown to be associated with the amplification of the *ERG11* gene [Bossche *et al.*, 1992; Vanden *et al.*, 1994; Marichal *et al.*, 1997]. The amplification of the *ERG11* gene in this isolate was linked to chromosomal duplication, which in turn resulted in high levels of P45014DM protein [Marichal *et al.*, 1997]. That gene conversion or mitotic recombination could also play a role in fluconazole resistance in *C. albicans*, was apparent from a study done by White's group where additional genetic variations in a clinical isolate of *C. albicans* with R467K substitution have been reported [White, 1997]. It was shown that all allelic differences present in sensitive isolates of *C. albicans* were eliminated in the resistant isolates from the *ERG11* by gene conversion or mitotic recombination [White, 1997]. The resulting strain had an R467K mutation in both the copies of *ERG11* and was more resistant to azoles as compared to a strain with single allelic substitution.

1.4.3.2.3 Molecular alterations in other *ERG* genes

In addition to the alterations in lanosterol demethylase, another common mechanism of resistance is an alteration in other enzymes of the same pathway. Till date *ERG1*, *ERG2*, *ERG3*, *ERG4*, *ERG7* and *ERG11* have been cloned from *C. glabrata* and *ERG11* has been cloned from *C. krusei* [White *et al.*, 1998]. The *ERG3* and *ERG11* genes of *C. glabrata* have been studied in some detail. The double deletion mutant of ERG3 and ERG11 in *C. glabrata* has been shown to be aerobically viable, accumulates 14α-methylfecosterol and lanosterol and is resistant to azoles and AmpB.

1.4.3.2.3.1 $\Delta^{5,6}$-desaturase (ERG3)

Another enzyme of ergosterol biosynthesis pathway, $\Delta^{5,6}$-desaturase (*ERG3*), has been shown to contribute to azole resistance. A defect in *ERG3* leads to the accumulation of 14α-methylfecosterol instead of 14α- methylergosta-8, 24(28)-dien-3β, 6-α diol. Accumulation of sufficient amounts of 14α-methylfecosterol compensates for ergosterol in the membranes and thus contributes to azole resistance in *C. albicans* [White *et al.*, 1998; Ghannoum and Rice, 1999]. The lethality of *S. cerevisiae* disruptant of *ERG11* can be suppressed by $\Delta^{5,6}$-desaturase [Kelly *et al.*, 1997]. The decrease in ergosterol content due to a defect in $\Delta^{5,6}$-desaturase in

fluconazole resistant clinical isolates of *C. albicans* also results in cross-resistance to amphotericin B [Kelly *et al.*, 1997].

1.4.3.2.3.2 Δ^{22}-desaturase (ERG5)

Another cytochrome P450, Δ^{22}-desaturase (CYP61 and also *ERG5*) has been purified from an *ERG11* (P45014DM) disrupted strain of *C. glabrata* [Lamb *et al.*, 1999]. The purified enzyme showed desaturase activity in a reconstituted system. Δ^{22}-desaturase and its homologues have also been identified in *C. albicans* and *Schizosaccharomyces pombe*. The spectral analyses obtained with azole antifungal compounds viz., ketoconazole, fluconazole and itraconazole in reconstituted Δ^{22}-desaturase suggests that these drugs directly interact with the cytochrome heme [Lamb *et al.*, 1999].

1.4.3.2.3.3 Membrane Lipid Composition

In addition to membrane ergosterol, which mainly provides rigidity, stability and resistance to physical stresses, there are other membrane lipid components, which also affect drug susceptibilities of *Candida* cells [Loffler *et al.*, 2000; Mukhopadhyay *et al.*, 2002]. Of note, it is well documented that clinical as well as adopted azole resistant isolates of *C. albicans* exhibit altered membrane phospholipids as well as sterol composition [Loffler *et al.*, 2000; Mukhopadhyay *et al.*, 2002]. Additionally, recent reports suggest that the interactions between membrane ergosterol and sphingolipid are important determinants of drug susceptibilities of *C. albicans* cells [Mukhopadhyay *et al.*, 2002]. In a recent study, close interactions between ergosterol and sphingolipid, which appeared to be disrupted in *erg* mutants, were found to be critical for drug sensitivity of *C. albicans* cells. It is observed that *Candida* cells, when grown in presence of fumonisin B1 (specific inhibitor of sphingolipid synthesis), had lower sphingolipid content. These were similar to *ERG* mutant cells and became hypersensitive to the tested drugs [Mukhopadhyay *et al.*, 2004].

1.4.3.2.4 Import of drugs

The hydrophobic nature of drugs permits their easy import by passive diffusion. However, the contribution of drug import to the overall scenario of MDR is not well established since technically it has not been possible to separate efflux of

drugs from their import. Nonetheless, there are a few studies particularly with mammalian cells where passive diffusion of drugs through a lipid bilayer has been shown to be an important determinant of MDR [Ferte, 2000]. The variations in membrane fluidity are expected to affect passive diffusion of drugs and in turn their sensitivity. The enhanced fluidity has been linked to enhanced diffusion of drugs [Mukhopadhyay *et al.*, 2002]. Of note, there are factors, other than membrane fluidity, which can also influence passive diffusion of drugs across the membrane bilayer thus affecting drug susceptibilities [van den Hazel *et al.*, 1999].

Mutation of the genes necessary for 5FC toxicity has been studied in detail in *C. lusitaniae*, especially because these mutations can cause cross resistance to fluconazole. 5FC is imported by a cytosine permease (Fcy2p); it is then deaminated by a cytosine deaminase (Fcy1p) to 5FU. 5FU is converted to 5-fluorouridine monophosphate by a phosphoribosyltransferase (Fur1p) [Marie and White, 2009]. Inactivation of any of these genes confers resistance to 5FC. *FCY1* and *FCY2* mutants also display fluconazole resistance in the presence of subinhibitory 5FC concentrations but not to fluconazole alone. Two hypotheses have been proposed to explain this cross-resistance. The first is that extracellular 5FC acts as a competitive inhibitor of FLC uptake [Papon *et al.*, 2007], however, this does not explain cross-resistance mediated by Fcy1p. More recently it has been proposed that cross-resistance is mediated by the accumulation of fluorinated cytosine within the cell by an unknown mechanism. 5FC enters cells with mutant *FCY2* permeases through other lower affinity permeases [Chapeland-Leclerc *et al.*, 2005], indicating that *FCY2* mutation does not abolish 5FC import. The import of drugs and its impact on drug resistance needs to be analyzed more carefully. It is expected that with better experimental design, the contribution of import of drugs in MDR can be established.

1.4.3.2.5 Efflux of drugs

Active efflux by specific or MDR transporters is a strategy to prevent the access of toxic compounds to their intracellular targets [Kolaczkowski and Goffeau, 1997]. It is also used to excrete products of intracellular metabolism of endo- and xenobiotics flagged by glutathione, glucuronide, or sulfate. The potential danger of this type of mechanism lies in the fact that a single protein can confer resistance to a

plethora of compounds from different chemical classes. Many membrane transport systems have been demonstrated to play an important role in both bacteria and eukaryotes by conferring multidrug resistance to various compounds. For instance, in human cancer cells, resistance to antitumor chemotherapeutic agents is commonly mediated by the P-glycoprotein efflux pump [Gottesman and Pastan, 1993], and in bacterial pathogens, resistance to antibiotics and antiseptics is frequently due to extrusion of the drug [Li and Nikaido, 2004]. The most important MDR transporters belong either to the ATP-binding cassette family or to the Major Facilitator Superfamily, which differ in the way they are energized. The ABC and MFS superfamilies are designated by Transport Commission (TC) system as TC 3.A.1 and TC 2.A.1, respectively [Busch and Saier Jr., 2002]. Whereas the ABC transporters bind ATP and require ATP hydrolysis for transport activity, the MFS mediated transport is driven by the proton-motive force. Members of both classes are found in all three kingdoms of life and are apparently involved in transport of solutes across the plasma membrane or across intracellular membranes. Subfamilies have been defined on the basis of structural and functional criteria [Pao *et al*, 1998; Saier and Paulsen, 2001], but only for a few transporters the physiological substrates are known. Both ABC and MFS transporters are encoded by large gene families that have been characterized extensively [Decottignies and Goffeau, 1997; Goffeau *et al*, 1997; Nelissen *et al*, 1997; Bauer *et al*, 1999; Wolfger *et al*, 2001; Sa-Correia and Tenreiro, 2002]. Members of both classes can have broad and overlapping substrate specificities. A schematic representation of the two major classes of multidrug transporters is shown in Figure 5.

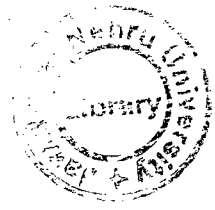

1.4.3.2.5.1 ABC superfamily

ABC proteins constitute one of the largest and most highly conserved superfamilies and are found in large numbers across organisms in all the three kingdoms of life. It comprises about 5% of the genome in *Escherichia coli* and with currently more than 1000 members represents the largest protein family known till date [Higgins, 1992]. The signposting of ABC transporters as a Superfamily with a core structure of four domains was made in 1986 and was followed in 1992 by an encyclopaedic review on ABC transporters [Higgins, 1992]. Despite the plenitude of solute types and processes with which they are involved, ABC transporters comprise a

conserved core structure of two transmembrane domains (TMDs) and two cytosolic ABCs, also commonly known as nucleotide-binding domains (NBDs). The acronym 'ABC' derives from ATP binding cassette [Hyde *et al.*, 1990]. The TMDs contain 6-11 hydrophobic segments, which span the membrane and form the transmembrane channel. The various topologies commonly found in ABC transporters are shown in Figure 6. The typical ABC transporter, also called a full size protein, has two membrane domains (TMDs) comprising of six transmembrane segments (TMS) each and two nucleotide-binding domains (NBD). On the other hand the half-size, ABC proteins have only one membrane domain comprising of five to ten transmembrane segments and one nucleotide-binding domain. Some ABC proteins do not possess a transmembrane domain and are probably soluble proteins [Higgins, 1992; Dean and Allikmets, 1995]. The latter must form either homodimers or heterodimers to form a functional transporter. ABC genes are widely dispersed in eukaryotic genomes and are highly conserved between species, indicating that most of these genes have existed since the beginning of eukaryotic evolution. The genes can be divided into subfamilies based on similarity in gene structure (half versus full transporters), order of the domains, and on sequence homology in the NBD and transmembrane domains.

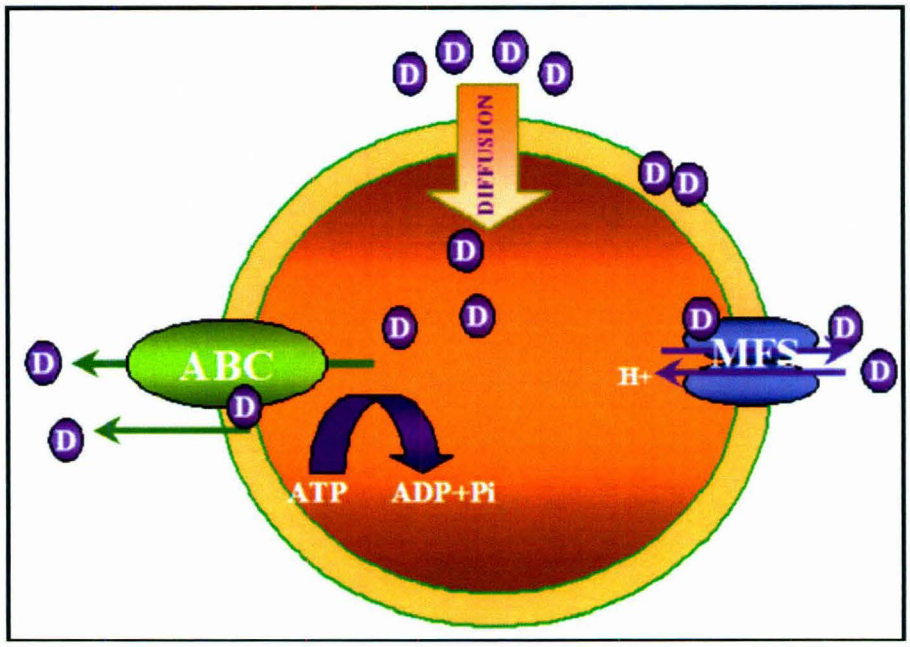

Figure 5: Schematic representation of the two major classes of multidrug transporters: ABC transporters utilize the free energy of ATP hydrolysis to pump drugs out of the cell while MFS transporters mediate the diffusion of structurally unrelated drugs in a coupled exchange with protons.

There are seven mammalian ABC gene subfamilies, five of which are found in the *S. cerevisiae* genome [Bauer *et al.*, 1999]. The primary sequences of the TMDs are markedly variable compared with those of the NBDs. The NBDs contain characteristic motifs (Walker A and B), separated by approximately 90–120 amino acids, found in all ATP binding proteins (Figure 7). ABC genes also contain an additional element, the Signature C motif, located just upstream of the Walker B site [Higgins, 1992; Endicott and Ling, 1989]. This acts as the diagnostic signature sequence of ABC proteins. While the TMDs are thought to contain the substrate binding sites, the NBDs are molecular motors that transform the chemical potential energy of ATP into protein conformational changes.

The best-characterized ABC superfamily transporter is the multidrug efflux pump, P-glycoprotein, encoded by the human or rodent *mdr1* gene, which mediates resistance to a broad range of cytotoxic drugs via ATP dependent export [Endicott and Ling, 1989; Gottesman and Pastan, 1993]. Homologs within this family have also been proposed to be involved in ATP dependent export-mediated MDR to antimalarial agents in *Plasmodium falciparum* [Foote *et al.*, 1989]; to emetine, iodoquinol, and diloxanide in *Entamoeba histolytica* [Samuelson *et al.*, 1990; Samuelson *et al*, 1992]; and to leptomycin B and other cytotoxic drugs in *Schizosaccharomyces pombe* [Nishi *et al.*, 1992]. Homologs of ABC transporters involved in MDR have also been identified by sequence analysis in such diverse organisms as *Arabidopsis thaliana*, *Caenorhabditis elegans*, *Drosophila melanogaster*, *E. coli*, *Haemophilus influenzae*, *Saccharomyces cerevisiae*, *Staphylococcus aureus*, and *Xenopus laevis* [Allikmets *et al.*, 1993; Castillo *et al.*, 1995; Dudler and Hertig, 1992; Fleischmann *et al.*, 1995; Henze and Berger-Bachi, 1995; Wilson *et al.*, 1994; Wu *et al.*, 1991]. Several mammalian ABC proteins are medically important, because mutations in corresponding genes cause severe genetic diseases such as Cystic fibrosis [Harris and Argent, 1993], Adrenoleukodystrophy [Mosser *et al.*, 1993] and Zeweller syndrome [Gartner and Valle, 1993], Dubin-Johnson syndrome [Paulusma *et al.*, 1996], familial hyperinsulinemic hypoglycaemia of infancy, hepatic choleostasis and Stargardt's mascular dystrophy of the eye [Klein *et al.*, 1999].

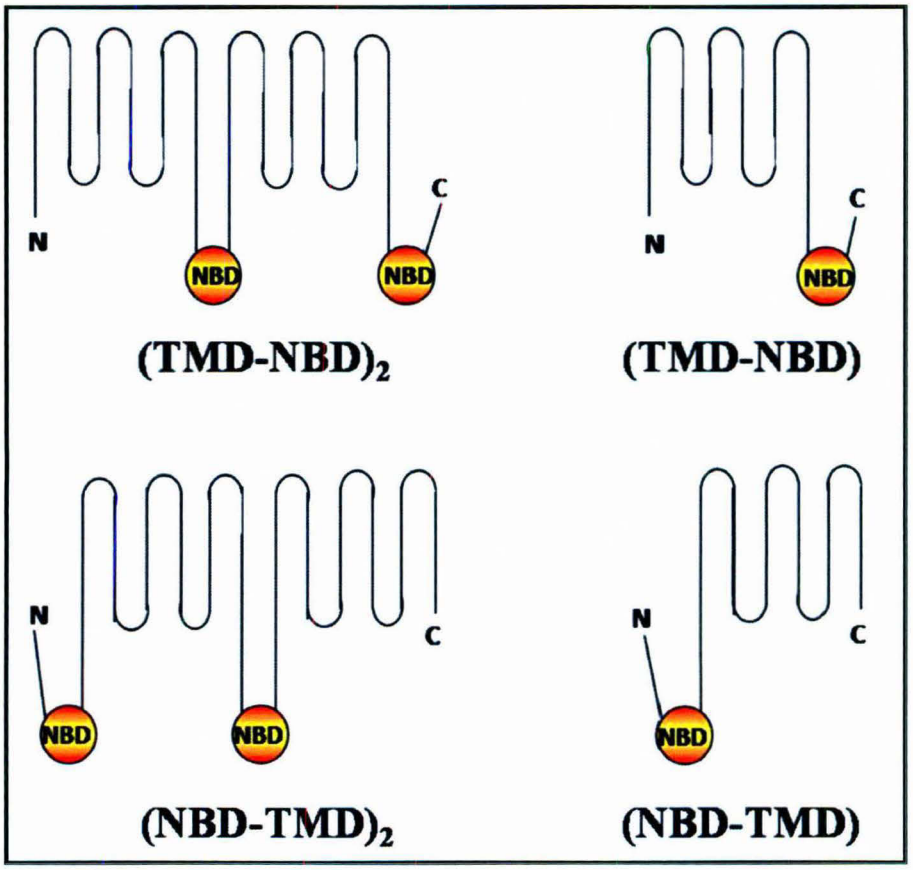

Figure 6: Predicted topology of the principal ABC proteins.
Figure shows both full and half ABC transporters. The TMD domain consists of six predicted transmembrane spans. The NBD domain is represented by the cytoplasmic loop comprising the ATP binding domain.

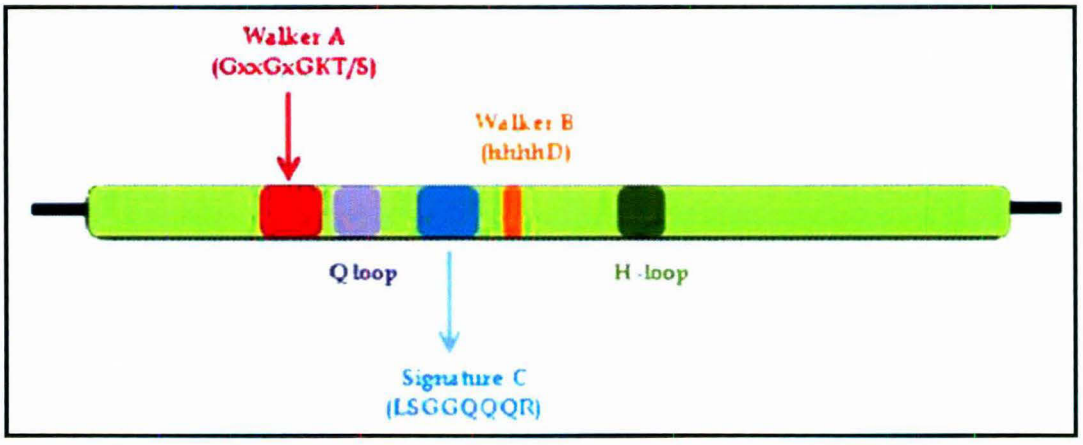

Figure 7: Linear representation of a prototype ABC domain, with assignment of the main functional sites.

1.4.3.2.5.2 MFS Transporters

Another class of efflux pumps / transporters that are structurally quite similar to ABC pumps but do not contain ATP-binding domains, are known as Major Facilitator Superfamily proteins. The MFS has originally been defined as a superfamily of permeases that are characterized by two structural units of six transmembrane spanning α-helical segments, linked by a cytoplasmic loop (Figure 8). The MFS proteins are involved in symport, antiport, or uniport of various substrates and are ubiquitously present from bacteria to higher eukaryotes [Marger and Saier, 1993]. MFS proteins are shown to be involved in (i) drug resistance, (ii) sugar uptake,

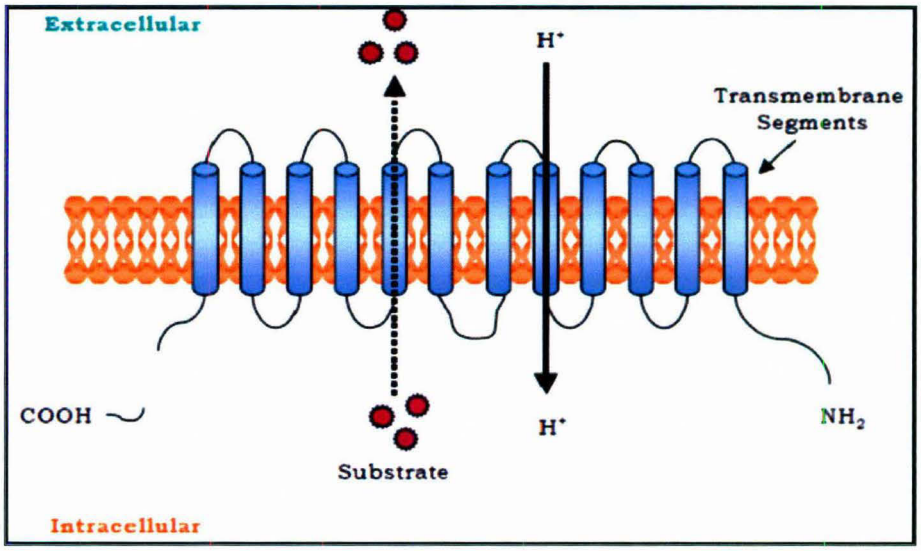

Figure 8: A diagrammatic representation of an MFS transporter.

(iii) uptake of Krebs cycle intermediates, (iv) phosphate ester/phosphate antiport, and (v) oligosaccharide uptake Marger and Saier 1993; Paulsen *et al.* 1996]. More than 300 individual proteins which belong to this superfamily have been identified [Paulsen *et al*, 1996]. It includes well-known and much studied proteins, such as the *E. coli* lactose permease LacY [Kaback, 1992; Kaback *et al*, 1994] and the human GLUT glucose transporters [Gould and Bell, 1990], which are often considered paradigms for secondary active transport and facilitative transport, respectively. The MFS drug resistance proteins are proton motive force (PMF)-dependent antiporters which efflux out drugs in exchange of one or more H^+ [Paulsen *et al.,* 1996]. The MFS-MDR transporters are classified into two families according to the number of predicted transmembrane spans: The Drug: H^+ Antiporter-1 (12-Spanner; DHA1)

Family, and the Drug: H^+ Antiporter-2 (14-Spanner; DHA2) Family (Figure 9). On average the DHA2 family is more variable between genomes than the DHA1 family and both are more variable than the ABC transporters.

In *S. cerevisiae*, 28 MFS proteins have been identified of which a few have been implicated to play a role in drug resistance [Goffeau *et al.,* 1997]. *FLR1* gene of *S. cerevisiae*, which encodes a MFS protein, has been shown to cause resistance to cycloheximide, fluconazole, cadmium and H_2O_2 [Alarco *et al.,* 1997]. *CaMDR1* (previously known as BENr) and *FLU1* are the two MFS genes identified in *C. albicans*. *CaMDR1* was initially identified as a gene, which conferred resistance to the tubulin binding agent benomyl and tetrahydrofolate reductase inhibitor, methotrexate [Fling *et al.,* 1991; Ben-Yaacov *et al.,* 1994]. *FLU1* on the other hand, was initially picked up as a clone that could confer resistance to fluconazole. *CaMDR1* is highly homologous to *FLR1*, while *FLU1* revealed high similarity to a *S. cerevisiae* putative MFS transporter YLL028Wp. *CaMDR1* expression in *S. cerevisiae* confers resistance to several unrelated drugs and its over-expression has been linked to azole resistance in *C. albicans*. The expression of *CaMDR1* in *C. albicans* cells was enhanced by benomyl, methotrexate and several other unrelated drugs, and was more pronounced in some of the azole resistant clinical isolates. This confirms that while *CaMDR1* over-expression is linked to fluconazole resistance, other efflux mechanisms are equally important [Gupta *et al.,* 1998].

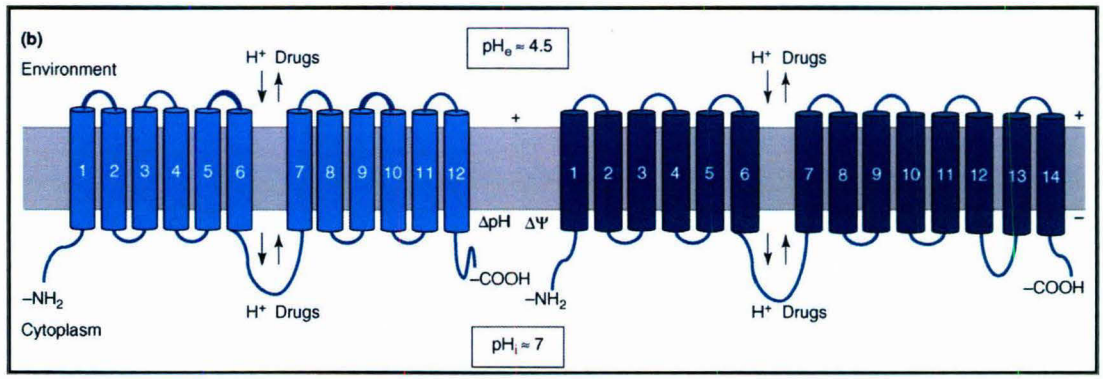

Figure 9: A Typical MFS-MDR transporter from the 12-spanner DHA1 (light blue) and 14-spanner DHA2 (dark blue) families.

Homologues of *CaMDR1* have been identified from *C. dubliniensis* and *C. glabrata* which are termed as *CdMDR1* and *CgMDR1*, respectively [Moran *et al.,*

1998; Sanglard *et al.,* 1999]. It appears that increased expression of *CdMDR1* is the main mechanism of fluconazole resistance involved in *C. dubliniensis* clinical isolates [Moran *et al.,* 1998]. Since *CgMDR1* confers specific resistance to fluconazole, its constitutive expression in *C. glabrata* may be responsible for the intrinsically low susceptibility of this yeast species to fluconazole [Sanglard *et al.,* 1999]. Interestingly, the ser-asn-asp rich domain present in CaMdr1p and its alleles was not found in CdMdr1p, Cyhrp (cycloheximide resistance protein from *C. maltosa*) and Flr1p from *S. cerevisiae* which are 93, 57 and 46% identical to CaMdr1p, respectively but do not confer resistance to benomyl [Moran *et al.,* 1998; Gupta *et al.,* 1998].

1.5 STRATEGIES TO COMBAT MDR

Considerable evidence has accumulated indicating that the multidrug efflux pumps (mainly *CDR1/CDR2* and *CaMDR1*) play a role in the development of simultaneous resistance to multiple antifungal drugs in clinical *C. albicans* isolates. In recent years, research to overcome this barrier in treatment of fungal infections has been focussed mainly on two areas: - (1) advanced and sensitive detection of multidrug efflux pumps mRNA or protein and their regulation and expression (2) development of inhibitors / modulators of these multidrug efflux pumps. The studies dealing with development of modulators / inhibitors need an in-depth structural and functional analysis of these efflux pumps.

1.6 STRUCTURAL AND FUNCTIONAL STUDIES ON EFFLUX TRANSPORTERS

1.6.1 Functional aspects of ABC Transporters

Several crystal structures of bacterial ABC transporters have now been described [Locher *et al.*, 2002; Dawson and Locher, 2006; Oldham *et al.*, 2007; Ward *et al.*, 2007; Pinkett *et al.*, 2007; Hollenstein *et al.*, 2007; Hvorup *et al.*, 2007; Gerber *et al.*, 2008; Kadaba *et al.*, 2008]. These bacterial ABC transporter structures include both importers and exporters that shuttle a wide variety of substrates. While the TMDs of these proteins differ significantly, a general theme prevails. Transport does indeed appear to be mediated by an alternating-access mechanism [Jardetzky, 1966], with motion of the TMDs shutting a substrate-binding cavity to one side of the

membrane and exposing the cavity to the other (Figure 10). This motion of the TMDs is coupled to association and dissociation of the NBDs [Davidson and Maloney, 2007; Hollenstein *et al.*, 2007; Sonne *et al.*, 2007]. Without nucleotide, the NBDs are apart or open, but when ATP binds to both NBDs they close to form a tight dimer with two ATPase active sites at the interface. A coupling helix from a TMD fits into a groove on an NBD, tethering each TMD to one of the NBDs, such that opening / dissociation and closing / association of the NBDs results in simultaneous movement of transmembrane helices [Hollenstein *et al.*, 2007]. When the NBDs are open, the substrate-binding cavity formed by the TMDs faces inwards toward the cytosolic NBDs. When the NBDs are bound to ATP and closed, the substrate binding cavity faces outwards. A cycle of ATP binding, hydrolysis, and product release can hence cause large conformational changes.

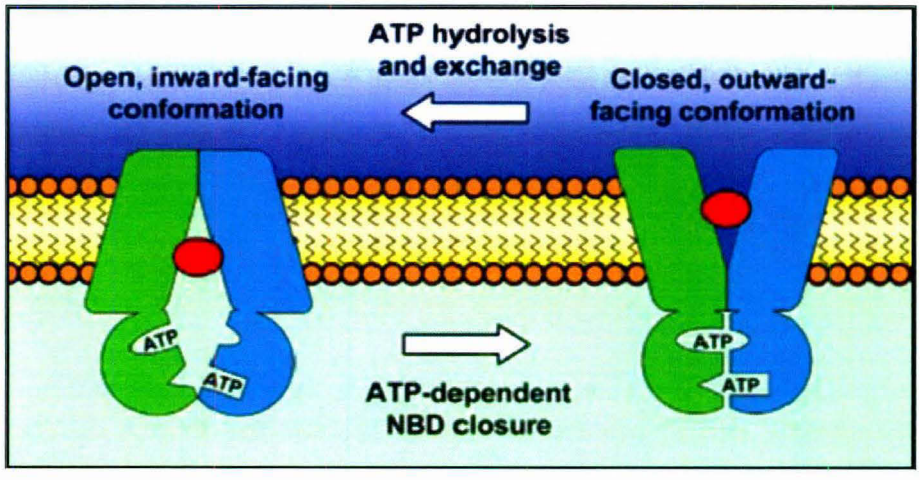

Figure 10: Kinetic mechanism of a typical ABC transporter.

Many bacterial ABC transporters function as importers, and binding of an extracytoplasmic substrate-binding protein to the outwardfacing conformation triggers ATP hydrolysis, thereby inducing substrate import by promoting the inward facing conformation. For exporters, a transport cycle might begin with substrate binding to an inward-facing, open NBD conformation of the ABC transporter. This is followed by ATP-dependent closure of the NBDs, which concomitantly changes the transporter to an outward-facing conformation and exposes the substrate for release on the other side of the membrane. Subsequent ATP hydrolysis now causes the NBDs to reopen and the transporter returns to the starting conformation.

Overlaid on this basic pathway are complexities associated with an individual or collection of transporters. Many ABC transporters have additional accessory domains that provide new functions, often for regulation. Furthermore, nearly half the mammalian heterodimeric transporters have nonequivalent ATPase active sites [Procko *et al.*, 2006]. While the ABC transporter literature contains numerous models and sometimes conflicting data, the strong trends among protein sequences and crystal structures provide compelling evidence of important generalities, even if some attributes are transporter-specific.

As introduced above, ABC transporters share the same basic core, comprising two TMDs and two NBDs. The different domains of an ABC transporter may be provided by one or more polypeptide chains, with most possible linkage permutations observed in nature. Mammalian ABC transporters display three dominant gene arrangements. In the case of TAP, two proteins, TAP1 and TAP2, each contribute a TMD and NBD, and form a functional heterodimer [Kelly *et al.*, 1992, Procko *et al.*, 2009]. Other ABC proteins, such as the drug efflux pump ABCG2, form functional homodimers, where each identical subunit has a TMD and NBD [Kage *et al.*, 2002; Bhatia *et al.*, 2005]. However, most mammalian ABC transporters are "fused heterodimers," and a single polypeptide contributes both TMDs and both NBDs. This last category includes the chloride channel CFTR, the sulfonylurea receptors SUR1 and SUR2, the various MRP drug exporters, and P-glycoprotein, another drug efflux pump. In all cases, ATP mediated conformational changes in the NBDs are transmitted to the TMDs to facilitate substrate transport. Most mammalian ABC transporters are therefore composed of two homologous but non-equivalent halves. Even in lower eukaryotes such as the yeast *S. cerevisiae*, the majority of ABC transporter genes encode all four domains in a fused heterodimer arrangement [Decottignies and Goffeau, 1997]. Although a number of bacterial ABC transporters also have distinct TMDs and / or NBDs [Lubelski *et al.*, 2006] thus far only one available crystal structure illustrates an ABC transporter with nonidentical halves-the transmembrane domains of the maltose transporter are encoded by two genes, MalF and MalG [Oldham *et al.*, 2007]. As the detailed mechanisms of different transporters, both homodimeric and heterodimeric, with and without ATPase site asymmetry, become better understood, we can now begin to clarify which features are broadly

applicable to this entire family, and which are specific to subgroups or even unique to particular transporters.

1.6.2 Functional aspects of MFS transporters

This superfamily is ubiquitous in all kingdoms of life and in all biological cells, and includes members of direct medical and pharmaceutical significance. Mechanistically, MFS transporters display three distinct kinetic mechanisms: there are (i) uniporters, which transport only one type of substrate and are energized solely by the substrate gradient; (ii) symporters, which translocate two or more substrates in the same direction simultaneously, making use of the electrochemical gradient of one of them as the driving force; and (iii) antiporters, which transport two or more substrates, but in opposite directions across the membrane. Individual members within the MFS show stringent specificity, yet as a group the superfamily accepts an enormous diversity of substrate types (ions, sugars, sugar phosphates, drugs, neurotransmitters, nucleosides, amino acids and peptides, to list a few). As a result, mechanistic studies of the MFS allows one to focus on fundamental questions related to how proteins recognize substrates and transport them across the membrane. Our understanding of these issues is well advanced in some model systems. This is especially true of the *E. coli* lactose: H^+ permease (LacY), an MFS symporter that has been the subject of intense experimental scrutiny for many decades by a number of laboratories [Abramson *et al.*, 2003; Guan and Kaback, 2006; Kaback and Wu, 1997].

Until the recent arrival of high-resolution three-dimensional (3D) structures of representatives of the MFS, the field relied on indirect methods, such as phylogeny and sequence analysis, as a guide to structure and function of these proteins [Chang *et al.*, 2004]. Hydropathy analysis of protein sequences and topological studies with gene-fusion constructs predicted that almost all MFS proteins possess a uniform topology of 12 transmembrane a-helices (TMs) connected by hydrophilic loops, with both their N- and C-termini located in the cytoplasm [Pao *et al.*, 1998; Saier, 1999; Saier, 2003]. Interestingly, the N-terminal half of the protein (TM1-TM6) displays weak sequence homology to the C-terminal half (TM7-TM12), suggesting that the molecule may have arisen following a gene duplication/fusion event [Maiden *et al.*, 1987]. This has implications, now confirmed, regarding an underlying structural

symmetry, as noted later. Exceptions to the 12-TM rule do exist - a few MFS families have 14-TMs, one representative has only six and yet another 24 [Pao *et al.*, 1998]. The extra two helices in the 14-TM members probably arose via insertion of the central cytoplasmic loop into the membrane, whereas the 24-TM member is likely a consequence of a gene fusion event [Saier, 2003]; one suspects that the lone example with six TMs functions as a homodimer.

MFS proteins typically consist of 400-600 amino acids, and analysis of their primary sequences revealed that within any single family, sequence similarity is highly significant [Pao *et al.*, 1998]. By contrast, at the level of the superfamily, individual MFS members share low sequence identity or similarity, and are united only by a pair of conserved signature sequences, DRXXRR, at equivalent positions in the N- and C-terminal halves of the proteins, in loops that join TM2 to TM3 and TM8 to TM9, respectively [Maiden *et al.*, 1987]. Along with the conserved transmembrane topology and the internal sequence homology between the two halves of the proteins, this duplicated signature sequence suggests a common ancestral gene for the MFS. The importance of these earlier studies to a structural perspective was underlined by the publication of high-resolution 3D crystal structures of *E. coli* GlpT [Huang *et al.*, 2003], LacY [Abramson *et al.*, 2003] and EmrD [Yin *et al.*, 2006], and a lower resolution structure of *O. formigenes* OxlT [Hirai *et al.*, 2002; Hirai *et al.*, 2004]. This revealed that all these MFS proteins - despite their sequence divergence - indeed share almost the same 3D structures. Essentially all existing biochemical and biophysical data for these and other MFS proteins are in agreement with these structures [Lemieux, 2007; Lemieux *et al.*, 2004; Mueckler *et al.*, 2006]. This leads to the notion of a shared fold that acts as a scaffold for all MFS proteins, irrespective of their particular function as a symporter, uniporter or antiporter.

Detailed 3D structural information is currently available for three MFS antiporters, all from prokaryotes [Hirai et al., 2002; Huang et al., 2003; Yin et al., 2006]. The structure of GlpT [Huang et al., 2003], along with that of the related LacY symporter [Abramson et al., 2003; Guan et al., 2007], has been determined in the inward facing or Ci conformation. Two additional structures - those of the oxalate exchanger, OxlT, and the multidrug transporter, EmrD – may represent transporters in an occluded state [Hirai et al., 2002; Huang et al., 2003; Yin et al., 2006], but there is

as yet no structure of an MFS transporter in the opposite, outward facing or Co conformation. Nevertheless, the available structures emphasize the general conservation of fold and architecture, consisting of two domains with a pore between them (Figure 11). Publication of these structures, in combination with previous mutagenesis, biochemical and biophysical studies [Ambudkar and Maloney, 1984; Ambudkar and Maloney, 1985; Ambudkar et al., 1986], has enabled a dramatic enrichment of our understanding of transporter mechanism.

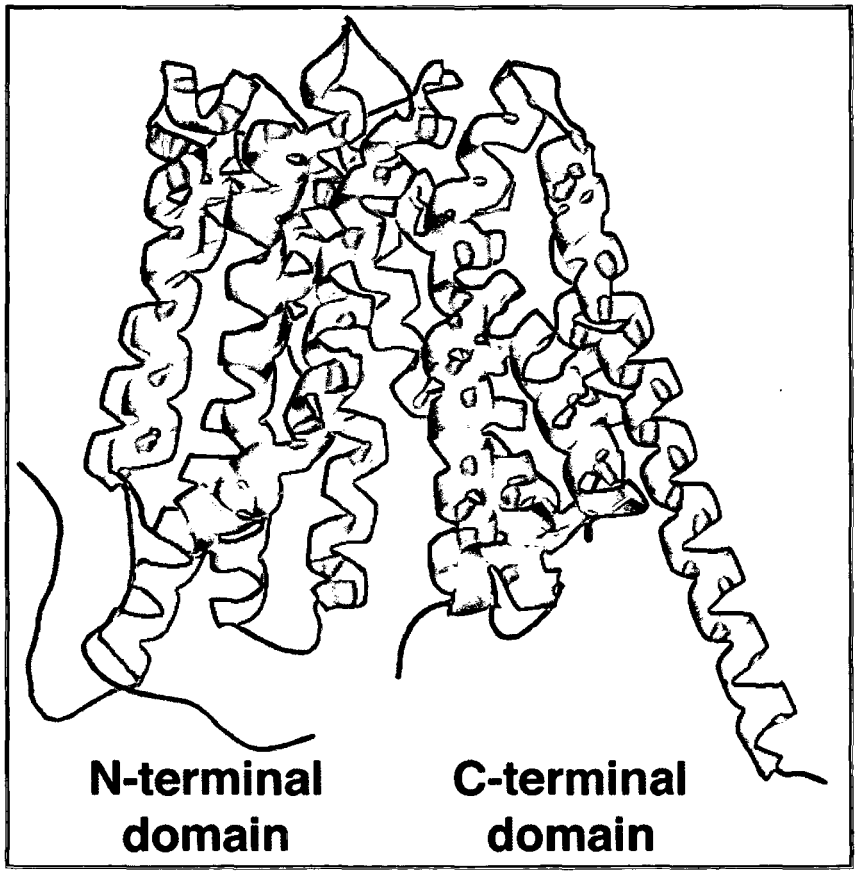

Figure 11: Typical 3D structure of an MFS transporter.

A fundamental problem encountered in the study of membrane transport concerns the mechanism of substrate translocation; following substrate binding, how can a membrane embedded protein catalyze movement of the substrate from one side of the membrane to the other? In both MFS antiporters and symporters, it is clear that the substrate-binding site has access to each side of the membrane in alternating fashion. This can now be seen as a direct consequence of domain movement that allows the N- and C-terminal portions of the transporter to rock back and forth against each along an axis that runs along the domain interface in the membrane. This

"rocker-switch" mechanism, implied from the crystal structures of GlpT [Huang *et al.*, 2003] and LacY [Abramson *et al.*, 2003], is the contemporary version of what Mitchell referred to as the 'mobile barrier' model, a name intended to replace the idea (and implications) of the 'mobile carrier' [Maloney, 1994]. Recent work on LacY has supported the notion of a global conformational change during substrate translocation [Majumdar *et al.*, 2007; Smirnova *et al.*, 2007]. The current model of GlpT-mediated transport invokes a single-binding site, alternating-access mechanism accompanied by rocker-switch type movement of the N- and C-terminal domains of the transporter; in kinetic terms, this reflects that interconversion between the C_i and C_o (and vice versa) conformations is favored upon substrate binding (Figure 12). Recent work using a combination of MD simulations and biochemical experiments suggests that formation and breaking of inter- and intradomain salt bridges is important in controlling the helical motions necessary for the large scale conformational change between C_i and C_o [Law *et al.*, 2008].

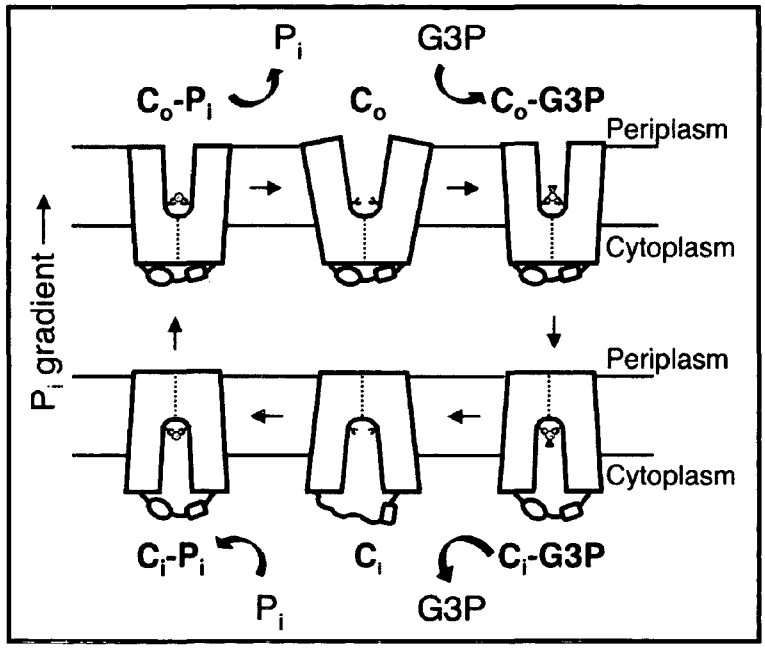

Figure 12: Schematic diagram of the single binding site, alternating access mechanism with a rocker-switch type of movement for the GlpT-mediated G3P-Pi exchange reaction. The diagram describes the proposed conformational changes that the transporter undergoes during the reaction cycle. C_o represents the protein in the outward facing conformation and C_i the inward facing one.

Thus, a set of principles apply equally to all MFS antiporters. a) All MFS proteins share essentially the same 3D structure, with two domains that saddle the

substrate-translocation pore. b) Conservation of the blueprint for the fold of MFS antiporters implies that the diversity of substrate preference seen in the MFS is a result of changes in only a few residues in the substrate-binding site and translocation pathway. c) Release of intrinsic binding energy upon binding of substrate lowers the activation energy barrier sufficiently to allow Brownian motion to drive substrate translocation across the membrane. d) Substrate translocation, via the rocker-switch mechanism, is accompanied by large, global conformational change of the protein that involves formation and breaking of inter- and intrahelical salt bridges [Law *et al.*, 2008].

Although a steady progress has been made in illuminating the biology of MFS antiporters, significant questions remain unanswered. We eagerly await the arrival of high-resolution structures of an MFS antiporter in the outward-facing C_o conformation, and in the C_i conformation with substrate bound. There is an urgent need to define the transition states in conformational space. Characterization of these states and the ability to achieve an individual state in vitro is the main hurdle to realizing a full structural characterization of any secondary active transporter.

1.7 APPROACHES FOR STRUCTURAL AND FUNCTIONAL ANALYSIS OF MULTIDRUG EFFLUX PUMPS

From the relative simplicity of bacterial cells, fungi and protozoa, to the complexity of human cancer cells, resistance has become problematic. Drug resistance decreases the chance of providing successful treatment against a plethora of diseases. A major mechanism of resistance in *C. albicans* as well as in cancer cells is the membrane protein catalyzed extrusion of drugs from the cell. P-gp (also known as ABCB1) has long been associated with drug resistance in many cancer types. This protein is a member of the ABC family and is believed to confer drug resistance in cancer cells by mediating the active outward efflux of chemotherapeutic drugs. Providing information on the nature of the drug-ABCB1 interaction has been a vital and synergistic pursuit alongside efforts to locate the drug-binding sites on the protein. The range and number of compounds 'recognized' by ABCB1 are astounding and there remains no conclusive explanation for this poly-specific behaviour. Numerous pharmacological studies utilizing equilibrium drug binding, hydrolysis of

ATP and steady-state accumulation assays have demonstrated that ABCB1 contains multiple sites for drug interaction. Moreover, complex allosteric interactions between sets of drugs have been demonstrated which may involve negative heterotrophy or conversely, permit the simultaneous binding of two drugs [Ferry *et al.*, 1992; Lugo and Sharom, 2005; Martin *et al.*, 2000; Orlowski *et al.*, 1996]. ABCB1 displays a complex mechanism of drug translocation across the membrane that requires coupling between the energy providing NBDs and TMDs, which contain the drug binding sites and the translocation conduit. There is considerable debate concerning the characteristics of coupling, specifically whether one or two ATP molecules are hydrolysed per transport event and whether ATP binding per se or the hydrolytic step is responsible for switching the binding site orientation during transport. Binding events are also not equal because interaction of certain compounds leads to transport and the stimulation of hydrolysis, whereas others are not transported and cause potent inhibition of ATPase activity. Elucidating the location and biophysical properties of the drug-binding sites would provide considerable input into the molecular interaction between substrates / inhibitors with ABCB1. Structural and pharmacological information of this ilk would facilitate the development of potent inhibitors of ABCB1 to restore the effectiveness of many anticancer agents [Crowley and Callaghan, 2010].

All this information is a result of continuous effort of many scientists and use of many approaches for structural and functional analysis of P-gp. This includes studying various aspects of these transporters ranging from catalysis of drug efflux to mapping the drug binding sites. Since 1989, a large number of research teams have employed numerous strategies to elucidate the precise location of drug-binding sites on ABCB1 and a summary of the major findings is presented in Table 6. This is not an exhaustive list, but does highlight many significant observations during the past two decades. Mutated forms of ABCB1 conferred a distinct resistance profile to the wild-type protein, which was thought to reflect alterations in drug binding or transport. Subsequent, more sophisticated, studies used directed mutagenesis to introduce mutations into targeted regions of the protein [Kajiji *et al.*, 1993; Loo and Clarke, 1993; Ma *et al.*, 1997]. The approaches used for structural and functional analysis of any multidrug efflux pump and can be classified into three broad categories shown in a pictorial representation in Figure 13.

Date	Comments
1989	**Strategy**: Photoaffinity labeling and protein digestion **Result**: Two sites or one with components in each half
1990-1991	**Strategy**: Labeling, digestion and antibody-mediated identification **Result**: 6 kDa fragment labeled within/close to TM11 and TM12
1993	**Strategy**: Phe → Ser mutations within TM11 followed by transport/cytotoxicity assays **Result**: TM11 contributes to DBS
1993	**Strategy**: Labeling, digestion and antibody-mediated identification **Result**: Labeling at two regions Cterminal to TM6/12
1993	**Strategy**: Phe → Ala mutations at nucleotides 335 (TM6) and 978 (TM12) **Result**: Mutations altered resistance profile, suggesting that TM6/12 contributes to binding and/or translocation
1994	**Strategy**: Theoretical – molecular simulations **Result**: Proposed that drugs intercalate between multiple Phe residues. Several helices contain Phe residues which shields drug from the aqueous environment – implicate TM3, TM5, TM8 and TM11 forming DBS
1995	**Strategy**: ABCB1 chimera assessed by cytotoxicity and photolabeling **Result**: Loop between TM11 and TM12 (EC3) modulates resistance spectrum & may be involved in translocation pathway
1997	**Strategy**: Site-directed mutagenesis and cytotoxicity **Result**: Mutations in TM6 alter the ability of cyclosporin A (not verapamil) to overcome resistance; TM6 involved in selectivity
1997	**Strategy**: Photolabeling and protein digestion **Result**: Differential effects of flupentixol on two [^{125}I]-IAAP labeling sites – nonidentical binding sites in N- & C-termini
1998	**Strategy**: Chemical structure-activity relationships for substrates **Result**: H-bonding patterns in substrates are key elements in drug recognition
1998	**Strategy**: Site-directed mutagenesis of TM12 **Result**: N-terminal region of TM12 influences transport specificity
2001	**Strategy**: IAAP labeling and chemical cleavage **Result**: Three regions of labeling found; TM4-5, TM7-8 and post-NBD2. Single site for IAAP comprising multiple spatial elements
2001	**Strategy**: Effects of TM9 mutations on cytotoxicity and photolabeling **Result**: Mutations in TM9 produce a distinct resistance pattern similar to TM6. TM9 and TM6 may co-operate in IAAP labeling
2005	**Ligand**: [^{3}H]propafenone and analogues **Strategy**: Photolabeling and identification with MALDI-TOF MS **Result**: Two binding regions – TM3/11 and TM6/8. MsbA-based model suggest the two sites are at TMD : TMD interfacial regions
2005	**Strategy**: Mapping R/H sites; fluorescence approach **Result**: H-site within bilayer leaflet region of ABCB1, whereas the R-site is in the cytosolic region. The R-site can bind two drugs simultaneously
2005	**Strategy**: Review of their site-directed mutagenesis studies **Result**: Suggest a common drug-binding site in the central cavity Interfaces at TM5/8 and TM2/11 form gates to the cavity and drugs negotiate passage through these gates
2006	**Strategy**: Theoretical study – MsbA based ABCB1 model **Result**: Propose a large central binding cavity with a lateral opening to lipid bilayer. Cavity helices include TM4, TM5, TM6, TM10, TM11 and TM12
2006	**Strategy**: Directed mutagenesis and drug labeling **Result**: Two studies suggesting that TM1/7 also contribute to the binding pocket in the central cavity
2006	**Strategy**: Simulations to probe drug-ABCB1 interaction **Result**: Argue that those residues at the interfacial region and that this is in contact with the polar head group region of the membrane
2007	**Strategy**: Sav186-based model used to characterize drug binding **Result**: Proposed several key residues from TM1, TM5 and TM6 in drug binding
2007	**Strategy**: Cysteine-directed mutagenesis of TM6 **Result**: Mutations did not alter initial drug binding however the helix was crucial in mediating TMD-NBD communication
2009	**Strategy**: MsbA-based model to dock drugs onto **Result**: Proposed a number of binding clusters dotted throughout the TMDs and that multiple drugs could interact simultaneously

Table 6: Time-line of the search for the location of drug-binding sites on P-gp. The time-line contains a summary of the strategies and observations obtained from studies specifically aimed at locating the sites of drug binding to P-glycoprotein.

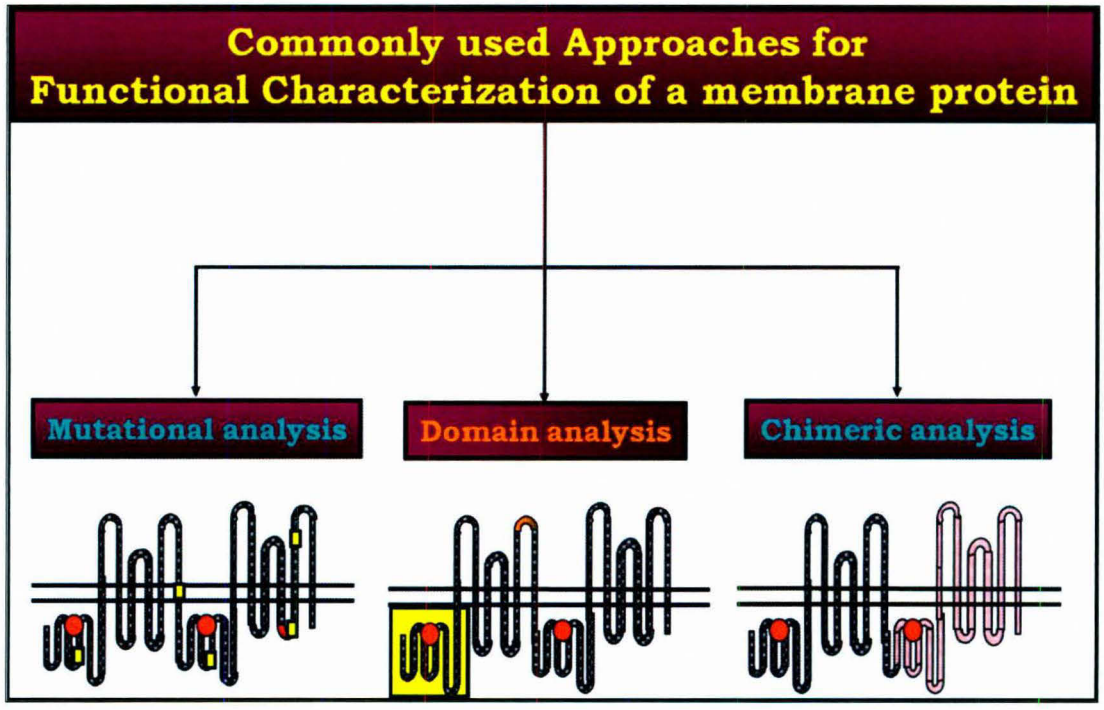

Figure 13: Strategies commonly used for structural and functional characterization of membrane proteins.

The functional consequences of the mutations were assessed using a range of assays including the ability of ABCB1 to confer cellular resistance, reduce intracellular drug accumulation, bind drug and / or display drug-stimulated ATPase activity. Frequently, a range of these assays was employed to provide a more detailed understanding of the contribution of specific residues to protein activity. A popular approach involved the mutagenesis of target residues to cysteine, which enables conjugation of thiol-reactive drug derivatives and exploration of the local environment and topography [Loo and Clarke, 2001; Loo and Clarke, 2001; Rothnie *et al.*, 2004; Storm *et al.*, 2007].

One of the most clinically significant mechanisms of azole resistance in pathogenic yeast *C. albicans* is the over-expression of multidrug transporter Cdr1p (Candida Drug Resistance) belonging to the ABC Superfamily of transporter and Mdr1p (Multiple Drug Resistance) belonging to the MFS transporters. Owing to the great deal of studies in other ABC transporters, there is much more known about the mechanism of ABC transporter Cdr1p as compared to the MFS transporter CaMdr1p.

The molecular mechanisms which govern CaMdr1p functions are not well-known and information is needed (1) to understand how the protein can bind to structurally diverse range of compounds (2) to define the drug-substrate binding (3) to determine how proton translocation is linked to the drug transport. The understanding of these issues is well-advanced in some model systems. Insight into the molecular details of mechanism is less advanced for antiporters as compared to the symporters. The above-mentioned three different strategies were employed for identifying critical residues of the antiporter CaMdr1p.

1.7.1 Random and Site-directed mutagenesis

Random and site-directed mutational strategies have been extensively used to understand the structure and function of the MDR efflux proteins. These strategies have helped us to identify several critical amino acid residues of an ABC transporter, ScPdr5p of budding yeast. These residues can bear a function of imparting substrate specificity and sensitivity to various inhibitors. Several point mutations led to significant changes in drug specificity and these were found to be distributed throughout the length of ScPdr5p. Site-directed mutagenesis followed by an elegant screen done by Golin's group has revealed interactions between TMS 2 and the NBD which may help to define at least part of the translocation pathway for coupling ATP hydrolysis to drug transport mediated by ScPdr5p. Recently, Ernst *et al.*, 2008 have elucidated the residues in H-loop of ScPdr5p which bear a function of coupling ATP hydrolysis with drug transport. Site-directed mutational analysis of multidrug ABC multidrug transporter CaCdr1p (a close homologue of ScPdr5p) has revealed insight into its drug binding and efflux properties. These studies have implicated some of the amino acid residues of TMS 5, 6, 11 and 12 as the components of the substrate binding pocket(s) of CaCdr1p [Shukla *et al.*, 2003; Saini et al., 2005; Puri *et al.*, 2009].

Site-directed mutagenesis is the only approach which has been exploited widely in studying the structural and functional details of MFS transporters. The strategy of introducing cysteine residues throughout the cavity-lining helices has yielded considerable mechanistic information on helical involvement in Lactose Permease function. The lactose permease, encoded by the *lacY* gene of *E. coli*,

catalyzes galactoside / H^+ symport and is an important model for secondary transport proteins in organisms from Archaea to the mammalian central nervous system that transduce free energy stored in electrochemical ion gradients into solute concentration gradients [Kaback, 1983; Kaback, 1989]. In a functional mutant devoid of native Cys residues, each residue has been replaced with Cys [Frillingos *et al.*, 1998]. Analysis of the mutant library has led to the following developments [Kaback and Wu, 1997; Kaback and Wu, 1999; Kaback and Wu, 1997; Frillingos *et al.*, 1998; Weinglass and Kaback, 1999]:

i. The great majority of the mutants are expressed normally in the membrane and exhibit significant activity, and only six side chains are clearly irreplaceable for active transport—Glu-126 (helix IV) and Arg-144 (helix V), which are indispensable for substrate binding, and Glu-269 (helix VIII), Arg-302 (helix IX), His-322, and Glu-325 (helix X), which are critical for H^+ translocation and coupling with substrate translocation.
ii. Helix packing and tilts, as well as ligand-induced conformational changes, have been determined by using site-directed biochemical and biophysical techniques.
iii. Positions that are accessible to solvent have been revealed.
iv. Positions where the reactivity of the Cys replacement is increased or decreased by ligand binding have been identified.
v. The permease has been shown to be a highly flexible molecule.
vi. A working model for lactose/H^+ symport has been formulated.

Alignment of the MFS transporters reveals that the central cytoplasmic loop is consistently longer than the other loops. Although this loop in LacY contains a portion of the binding site for the regulatory protein [Hastings *et al.*, 1990; Hoischen *et al.*, 1996; Seok *et al.*, 1997; Sondej *et al.*, 1999] Cys-scanning [Frillingos *et al.*, 1998] and insertional mutagenesis [McKenna *et al.*, 1992; Consler *et al.*, 1993] mutagenesis indicate that this region does not play an important role in the transport mechanism. Deletion of 5 residues (Δ5) from the central cytoplasmic loop of the lactose permease of Escherichia coli has no significant effect on expression or activity, whereas Δ12 leads to increased rates of permease turnover after membrane insertion and decreased transport activity, and Δ20 abolishes insertion and activity. By expressing Δ12 or Δ20 in two halves, both expression and activity are restored to

levels approximating wild-type. Replacing deleted residues with random hydrophilic amino acids also leads to full recovery. However, introduction of hydrophobic residues decreases expression and activity in a context-dependent manner. Thus, a minimum length of the central cytoplasmic loop is vital for proper insertion, stability, and efficient transport activity, because of constraints at the cytoplasmic ends of helices VI and VII. Furthermore, the results are consistent with the idea that the middle cytoplasmic loop provides a temporal delay between insertions of the first six helices into the membrane before insertion of the second six helices [Weinglass and Kaback, 2000].

The advent of crystal structures of three MFS antiporters shed light on their fundamental mechanism. Even with all this knowledge about MFS antiporters there are no considerable advances on the structural and functional aspects in MFS antiporters of higher organisms.

1.7.2 Domain analysis

Domains present one of the most useful levels at which to understand protein function, and domain family-based analysis has had a profound impact on the study of individual proteins. In absence of soluble domains in a MFS transporter, these studies where domains can be swapped with each other cannot be carried out. So, its use in structural and functional analysis of MFS transporters is negligible.

Typically, the predicted topology of Cdr1p exhibits the characteristic features of an ABC transporter; containing two highly hydrophobic MSDs and two cytoplasmically localized NBDs. NBDs are known to play a role in utilization of the energy of ATP hydrolysis to transport these substrates across the plasma membrane against the concentration gradient. The conserved NBDs located at the cytoplasmic periphery are the hub of such an activity. In prokaryotic ABC type transporters such as the histidine permease of *Escherichia coli*, both NBDs are functionally identical and equally contribute to the protein's activity. Inactivation of either one of these NBDs in the full protein results in a transporter that has its activities reduced to 50%. On the other hand, the NBDs of the eukaryotic transporters such as the human CFTR (Cystic Fibrosis Transmembrane conductance Regulator) and MRP1 do not appear to

be functionally complementary, as inactivation of either of them completely abolishes ATPase and transport activities of the protein [Azzaria *et al.*, 1989].

Advances in our understanding of the interactions of the drug-binding site and the NBDs of an ABC transporter have been greatly aided by the construction of a dimeric LmrA. The LmrA fusion protein transports fluorescent dyes, but disruption of either NBD inhibited the ATPase activity of the protein and abolished transport, indicating that LmrA functions as a homodimer in which there is co-operativity between the two NBDs and between these sites and the drug-binding site(s). This is consistent with studies of Pgp, where disruption of either NBD blocks ATP hydrolysis by both sites [Loo and Clarke, 1994], and it has been proposed that the NBDs function by an alternating-site mechanism in which the binding and hydrolysis of ATP by one site prevents the binding of ATP at other site [Senior *et al.*, 1995]. The above studies generally support a model in which the two NBDs are functionally equivalent, but where only one can undergo catalysis at any given time. However some studies have reported that the NBDs function asymmetrically. Co-operativity has been reported for several bacterial ABC transporters [Davidson *et al.*, 1996]. In case of *Salmonella typhimurium* histidine permease (His P), both subunits hydrolyze ATP and one subunit is activated by the other. In a heterodimer containing one wild-type and one hydrolysis defective subunit both hydrolysis and ligand translocation occurs at half the rate of the wild-type. Some reports suggest that 8-azido ATP preferentially label the N-terminal NBD of Pgp [Hrycyna *et al.*, 1999]. There is clear evidence to indicate asymmetry of function of the NBDs of MRP1 and CFTR1, which may reflect the much lower sequence similarity in the two NBDs of these transporters.

The functional relevance of these two hydrophilic domains i.e. NBD1 and NBD2 of Cdr1p was elucidated by swapping the two NBDs. An attempt was made to find out whether the two hydrophilic domains of Cdr1p are functionally complementary to each other by constructing *CDR1* having hydrophilic region comprised of two NBD1 rather than NBD1 and NBD2. Construction of Cdr1p with hydrophilic region comprised of two NBD1 led to trafficking problem that could be rescued by using substrates of Cdr1p and the surface localized protein retained the ability to bind the Cdr1p substrates but lost the ability to efflux them out [Saini et al., 2005].

1.7.3 Chimeric Analysis

This approach has been widely used in cases where the two proteins have a reasonable sequence identity but have widely different functions. These chimeric constructs help us to identify regions in a protein that a responsible for a specific function. As MFS transporters have no distinct domains, so the making of such constructs needs a suitable justification for mapping out the region for making a chimera. However, there are four distinct domains in case of ABC transporters like Cdr1p and Cdr3p, which gives us a demarcation for constructing the chimeras among them. Pair-wise sequence comparisons indicate that Cdr3p displays 56% sequence identity and 74% similarity with Cdr1p and 55% sequence identity and 75% similarity with Cdr2p, while Cdr1p and Cdr2p are 84% identical and 92% similar [Sanglard *et al.*, 1997]. The highest degree of sequence homology between Cdr1p and Cdr3p is found in the segments overlapping the two predicted intracellular domains that contain the ATP-binding sequences. Despite a high degree of sequence conservation with *C. albicans* Cdr1p and Cdr2p, *CDR3* does not transport *CDR1* substrates and thus is not involved in drug resistance [Balan *et al.*, 1997]. Rather Cdr3p has been shown to be involved in opaque-phase associated biological function in WO-1 opaque cells [Balan *et al.*, 1997] as well as lipid translocation [Smriti *et al.*, 2002]. This situation is reminiscent of the mammalian mdr gene family, which codes for the three highly homologous Pgp isoforms: *Mdr1*, *Mdr2* and *Mdr3* [Gros and Buschman, 1993]. Both *Mdr1* and *Mdr3* can confer drug resistance when over-expressed in mammalian cells while *Mdr2* cannot. It has been shown that *Mdr2* and *Mdr3* can function as phospholipid translocases, demonstrating that *Mdr2* can indeed function as transporter [Ruetz and Gros, 1994]. Furthermore, a functional analysis of chimeric proteins obtained by exchanging homologous domains between Mdr1 and Mdr2 proteins has shown that there is a functional difference detected between *Mdr1* and *Mdr2* in terms of the ability to confer drug resistance reside within predicted TMDs [Buschman and Gros, 1991]. In the case of human *MDR1* and *MDR2* also, it has been demonstrated that MDR1 residues Q330, V331 and L332 in transmembrane domain 6 are sufficient to allow an MDR2 backbone in the N-terminal half of Pgp to transport several MDR1 substrates [Zhou *et al.*, 1999]. Similar to *MDR1* and *MDR2*, the functional difference between *CDR1* and *CDR3* provides an opportunity to identify

the residues essential for broad substrate spectrum of *CDR1*. Various chimeras were made between *CDR1* and *CDR3* by exchanging homologous segments of *CDR1* and *CDR3*. The result suggested that replacement of either the N- or C-terminal half of *CDR1* with the corresponding region of *CDR3* resulted in non-functional chimeras as this replacement led to the trafficking problem, however exchanging only TM12 resulted in functional chimera as the residues predicted to participate in substrate interaction is highly conserved between *CDR1* and *CDR3* [Pawagi *et al.*, 1994] thus demonstrating the functional exchangeability of TM12 of *CDR1* with *CDR3*.

Such reports of chimeric studies are absent in MFS transporters thus leaving site-directed mutagenesis as the most popular and commonly used approach. Thus, there was a need to improve this approach so as to develop it into a rational mutational analysis of these proteins. This enables us to identify critical residues using computational tools which increase the efficacy of this approach.

1.8 AIMS, OBJECTIVES AND SCOPE OF THE PRESENT WORK

One of the most clinically significant mechanisms of azole resistance in pathogenic yeast *C. albicans* is the over-expression of multidrug transporter protein Cdr1p (Candida Drug Resistance), belonging to the ABC superfamily of transporters and CaMdr1p, belonging to Major Facilitator Superfamily. This is well-established with the reports from fluconazole resistant clinical isolates of C. albicans where the enhanced expression of Cdr1p and CaMdr1p has been shown to help the pathogen to efflux this therapeutic azole and hence facilitate its own survival. This mechanism of survival is certainly not the forte of this pathogen alone; tumor cells also utilize it in order to resist chemotherapy through over-expression of the Cdr1p homologs, i.e. P-glycoprotein (P-gp) / MDR1 and the multidrug resistance associated protein (MRP1).

Membrane proteins belonging to the MFS, transport molecules including drugs across the membrane and thus are known to be associated with drug resistance. CaMdr1p is one such MFS major multidrug efflux pump whose over-expression is linked to frequently encountered azole resistance in hospital isolates of C. albicans. CaMdr1p of C. albicans is a 564-aminoacid protein with 12 TMSs thus it belongs to Drug-proton antiporter-1 (DHA-1) family of MFS transporters. Amino acid residues critical for a protein's function, are conserved across members of the protein family.

However, the traditional measure of conservation is not a useful parameter in mapping a functionally important residue in membrane proteins e.g. hydrophobically conserved stretches, form helical transmembrane regions of the protein and are responsible for membrane localization, which individually have limited effect on binding and transport. A new method was developed that uses information theory to score the conservation of a residue relative to its context within the membrane and hypothesize that these residues would be critical for the protein's function. The relevance of predicted residues in the functioning of MFS is validated on CaMdr1p. The three sections of the thesis are titled as-

a) Random mutational analyses of the multidrug MFS transporter CaMdr1p

This chapter of the thesis deals with the elegant site-directed mutational analysis of CaMdr1p based on the traditional measure of conservation. Several residues important for function were identified and segregated into classes based on those which affected the drug sensitivity towards all drugs, had a differential effect or did not affect drug sensitivity at all. Biochemical analyses on the topology of transmembrane proteins include cysteine scanning mutagenesis which minimally perturbes the structure and function of the protein. Alanine scanning of all native cysteines present in CaMdr1p was done and results demonstrated that these cysteiens when replaced individually do not affect function. A cysless-CaMdr1p version was also constructed for in-depth structural and functional analysis. Analysis of the unique and unusually long N-terminal of CaMdr1p and elucidation of its role in PM localization of CaMdr1p is also a part of this chapter.

b) Membrane environment based rational computational approach for identification of family-wide-function specific residues of CaMdr1p

This Chapter II embodies results pertaining to the development of a new computational approach which worked efficiently for membrane proteins as it calculated the Relative Entropy of a residue of a membrane protein based on the environment where it was present. This gives us a rational way of mutational analysis which is much more efficient over the traditional measure of conservation. This method accurately predicts and validates family-wide-function residues not only of CaMdr1p but of all MFS member proteins. Based on a deduced 3D homology model

of CaMdr1p, results show that these residues have a role in maintaining the inter-helical interactions of this protein.

c) Identification of drug-proton antiporter function-specific residues of CaMdr1p by employing information theoretic measures

Chapter III of the thesis deals with moving a step further and predicting the residues important for drug-proton antiporter function. This was done by exploiting another information theoretic measure (CRE_S). This again provides rationality to the mutational analysis and the accuracy of prediction is definitely incomparable. These residues were predicted to be important for other members of the DHA1 family to which CaMdr1p belongs.

2.1 MATERIALS

Anti-GFP monoclonal antibody was purchased from BD Biosciences Clontech, Palo Alto, CA, USA and Anti-Pentahis monoclonal antibody were from Qiagen. DNA modifying enzymes and all other restriction enzymes were purchased from New England Biolabs (NEB Inc., USA) and MBI Fermentas (Fermentas Inc.). The drugs cycloheximide (CYH), 4-Nitroquinoline oxide (4-NQO), Methotrexate (MTX), Cerulenin (CER), Anisomycin (ANISO), Nile Red (NR) and Protease inhibitors (Phenylmethylsulfonyl fluoride, Leupeptin, Aprotinin, Pepstatin A, TPCK, TLCK) and other molecular grade chemicals were obtained from Sigma Chemicals Co. (St. Louis, MO, USA). All routine chemicals were obtained from Qualigens (Mumbai, India) and were of analytical grade. Anti-CaMdr1p polyclonal antibody was a kind gift by Prof. R. D. Cannon, New Zealand. Fluconazole (FLU) was generously provided by Ranbaxy Laboratories, India. [^{3}H] Fluconazole was custom prepared and [^{3}H] Methotrexate (MTX) was purchased from Amersham Biosciences, United Kingdom. Random primer labelling kit was also procured from Amersham. Zymolase T was from Seikagaku Corp. Japan. Media chemicals were obtained from HiMedia (Mumbai, India). Luria Bertani broth and agar media was purchased from Difco, BD Biosciences, NJ, USA. Ultra pure deoxyribonucleotides (dATP, dGTP, dCTP, dTTP) for PCR and the sequencing kit (Sequenase version 2.0 enzyme) were obtained from Amersham Biosciences Ltd. Oligonucleotides used were commercially synthesized from Sigma-Aldrich.

2.2 MEDIA AND STRAINS

Plasmids were maintained in *Escherichia coli* DH5α. *E coli* was cultured in Luria Bertani medium (Difco, BD Biosciences, NJ, USA) to which ampicillin was added (100 μg/ml). The yeast strains were cultured in YEPD broth (Bio101, Vista CA) or SD-URA$^-$ (Bio101, Vista CA). For agar plates 2.5% (w/v) bacto agar (Difco, BD Biosciences, NJ, USA) was added to the medium. The details of the composition of the respective media used are given in Appendix I. The list of plasmids and yeast strains used in this study are listed in Supplementary Table S1. All the yeast and bacterial strains were maintained at 30°C and 37°C respectively.

MATERIALS AND METHODS

2.3 OLIGONUCLEOTIDES

The oligonucleotides used in this study were custom synthesized from Sigma Aldrich, USA and are listed in Supplementary Table S2.

2.4 METHODS

2.4.1 COMPUTATIONAL METHODS

2.4.1.1 Multiple Sequence Alignments

561 MFS sequences having 12 TMS as predicted by TMHMM [Krogh *et al.*, 2001] were extracted from SWISSPROT release 56.2. Redundancy in the sequences is reduced to 90% on the basis of identity using BLASTclust by setting the identity threshold S to 90 and keeping all other parameters to default values (http://genomes.ucsd.edu/manuals/blast/blastclust.html). The resulting 342 sequences were then aligned by PRALINETM using TMHMM as the method for predicting transmembrane lengths and keeping all other parameters at their default values [Chen *et al.*, 2002; Pirovano *et al.*, 2008].

MFS sequences belonging to DHA1 (Drug-Proton Antiporters Class I) and SP (Sugar Porter) families were extracted from TCDB (http://www.tcdb.org/index.php). The resultant dataset thus included 37 members of DHA1 and 44 members of SP. Redundant sequences, if any, were identified using blastclust [Altschul *et al.*, 1990], by setting the identity threshold S to 90, L to 0.9 and keeping all other parameters to default values. The DHA1 and SP sequences were then aligned separately by PRALINETM [Pirovano *et al.*, 2008] using TMHMM as the method for predicting TM lengths [Krogh *et al.*, 2001] and keeping all other parameters at their default values. These resulting separate DHA1 and SP PRALINETM alignments were then aligned together by using the profile-profile alignment option of MUSCLE. Conservation of amino acids in a column, for the entire dataset and for each family individually, was calculated using the method described by Livingstone and Barton, 1993.

2.4.1.2 Calculation of Conservation Score and RE_M from Multiple Sequence Alignment of MFS transporters

Conservation of an amino acid in an alignment column was calculated using Jalview. For calculating RE_M, the available scoring schemes which are restricted to soluble proteins, were modified to accommodate different background probabilities for TM and inter-TM regions. RE_M was calculated as the deviation of the amino acid distribution $p_i(a)$ from a background disribution $f(a)$.

Relative Entropy, RE_M:

$$RE_M = \sum_{a=1..20} p_i(a) \log \frac{p_i(a)}{f(a)}$$

where $P_i(a)$ is the probability of the occurrence of amino acid a in column i of the MSA

$f(a)$ is the background probability of amino acid a and is classically estimated as the probability of occurrence of an amino acid in a large data set of proteins. In this method $f(a)=f(a)_{TM}$ or $f(a)_{iTM}$ where $f(a)_{TM}$ and $f(a)_{iTM}$ is the background probability calculated separately for TM and inter-TM regions of the alignment and replaced the background probability with this environment specific background frequency. A classical description of entropy also does not take into consideration the absence of data points which are gaps in the case of a multiple alignment column. The scaling factor was used which was equal to the number of amino acid positions is excluding gaps in column i divided by total number of sequences. The scores were then divided by this scaling factor to give scaled RE_M score.

2.4.1.3 Calculation of Scaled Cumulative Relative Entropy (CRE_S) score from a profile-profile alignment of DHA1 and SP families of MFS transporters

Alignments for each of these two families were extracted individually from the complete MSA. HMMbuild program of HMMER (http://hmmer.wustl.edu) was used to build profiles for these individual alignments. The probability of occurrence of each amino acid is read from the HMM profiles, for each alignment position and for both the subfamilies [Srivastava *et al.*, 2007].

Relative Entropy (RE) is calculated as the deviation of the amino acid distribution (for a particular column) of one subfamily from that of another subfamily in the complete alignment. RE for the two subfamilies y_1 and y_2 at column position *i*, is given by

$$RE_i y_1 \| y_2 = \sum_{x=1..20} P(x_i, y_1) \log \frac{(Px_i, y_1)}{(Px_i, y_2)} \qquad \text{Equation 1}$$

where, $P(x_i, y_n)$ is the probability of the occurrence of amino acid *x* in subfamily y_n at column *i* of the MSA

While CRE at column *i* is given by the Kullback-Liebler distance between the corresp onding *i*th columns

$$CRE_i = \left[\sum_{x=1..} P(x_i, y_1) \log \frac{(Px_i, y_1)}{(Px_i, y_2)} + \sum_{x=1..20} P(x_i, y_2) \log \frac{(Px_i, y_2)}{(Px_i, y_1)} \right] \qquad \text{Equation 2}$$

A classical description of entropy does not take into consideration the absence of data points which are gaps in the case of a multiple alignment column. Normalized CRE_i scores were obtained using a scaling factor which is equal to number of amino acid positions excluding gaps in column *i* divided by total number of sequences.

To select the alignment positions on the basis of both, high conservation across DHA1 and high CRE_i, the normalized CRE_i was further scaled with respect to the RE_{null} across DHA1, where $P(x_i, y_2)$ in Equation 1 above is the background probability of the amino acid, based on its occurrence in SWISSPROT. This was referred to as CRE_S and represented as per the following equation.

$$CRE_S = RE_{null} * normalized\_CRE_i \qquad \text{Equation 3}$$

All calculations were made using PERL scripts.

2.4.1.4 Molecular modeling of CaMdr1p

Structures of known MFS proteins [PDB id – 1pv6 [Abramson *et al.*, 2003], 1pw4 [Huang *et al.*, 2003] and 1zc7 [Yin *et al.*, 2006] were retrieved from Protein Data Bank (www.rscb.org) and aligned using Modeller9v5 [Sali and Blundell, 1993]. MFS sequences containing CaMdr1p aligned earlier with PRALINETM were aligned to this structure alignment after removing the sequences which corresponded to known structures. These were aligned using the profile-profile alignment option of ClustalW. The Profile alignment was then manually refined based on helix packing information of known MFS structures. Manual refinement was restricted to incorporating gaps in the loop regions without disturbing either the structural alignment or PRALINE sequence alignment. The homology model for the target sequence CaMdr1p was generated using MODELLER9V5 [Sali and Blundell, 1993] using 1pv6, 1pw4 and 1zc7 as template sequences. The initial 90 residues from N-terminal of CaMdr1p did not align with any of the templates, and were omitted from further study. The model was evaluated and validated by PROCHECK.

2.4.1.5 Generating the contact map

The contact map of CaMdr1p is plotted between all the residues vs all the residues. It displays the distances between Cβ of one residue and Cβ of every other residue within 8 A° distance (Cα is considered in case of glycine). Using the homology model a symmetric contact map for CaMdr1p was generated using a PERL program.

2.4.2 MOLECULAR BIOLOGY PROTOCOLS

2.4.2.1 Site-specific mutagenesis and development of transformants

Site-directed mutagenesis was performed by using the Quick-Change mutagenesis system from Stratagene (La Jolla, CA, USA). The mutations were introduced into the plasmid pRPCaMDR1-GFP according to the manufacturer's instructions. The desired alterations in the nucleotide sequence were confirmed by the automated sequencing of the ORF. The mutated plasmid pRPCaMDR1-GFP, after linearizing with *Xba I*, was used to transform AD1-8u$^-$ cells for uracil prototrophy, by

lithium acetate transformation protocol. Integration was confirmed by Southern blot analysis.

2.4.2.2 Bacterial miniprep DNA isolation

3 ml of bacterial culture (harbouring the desired plasmid) was centrifuged for 5 min at 10,000 rpm. Plasmid DNA was isolated using alkaline lysis method (0.2N NaOH and 1% SDS). Contaminating proteins and *E. coli* genomic DNA was removed by extraction with phenol: chloroform: isoamylalcohol (25:24:1) twice. The plasmid DNA was then precipitated with 0.6 volumes of isopropanol plus one-tenth volume sodium acetate (pH 5.2). Precipitated DNA pellet was subjected to 70% ethanol wash and then dried under vacuum and resuspended in 50 µl TE buffer (10mM Tris.HCl pH 8.0; 1 mM EDTA).

2.4.2.3 Integrative and episomal DNA transformation

LiAc method: The *S. cerevisiae* cells were grown in 10 ml YEPD medium overnight at 30°C with shaking at 200rpm. From this primary culture an aliquot was inoculated in 50 ml of YEPD medium to an initial O.D of 0.4. The culture was allowed to grow till an O.D of 1.4-1.6 was reached. The cells were then harvested in a sterile 50 ml centrifuge tube at 5000 rpm for 5 min. The cells were resuspended in 25 ml of sterile water and centrifuged again. After discarding the supernatant, the cells were resuspended in 1.0 ml of 100 mM LiAC (lithium acetate) and were transferred to a 1.5 ml eppendorf tube. The cells were pelleted at top speed and LiAc was removed with a micropipette. Finally, the cells were resuspended to a final volume of 500 µl in 100 mM LiAc. This cell suspension was vortexed and 50 µl samples were transferred to labelled microfuge tubes. After pelleting the cells and removing the LiAc the basic transformation mix components were added in the order given below:

240 µl PEG (50% w/v)

36 µl 1.0 M LiAc

15 µl of 10 mg/ml of salmon sperm DNA (boil ss-DNA for 10 mins)

65 µl of DNA (linearized DNA fragment or plasmid DNA) + water mix

The contents of the tube were vortexed vigorously until the cell pellet was mixed completely. These were then incubated at 30°C for 30 min. Heat shock was then given

to the cells at 42°C for 25 min after which the cells were centrifuged at 6000 rpm for 15 sec. The transformation mix was removed with the micropipette and the cells were resuspended in 100 µl of sterile water. The mix was then plated on SD-URA$^-$ plates and incubated at 30°C for 2-4 days.

For integrative transformation in *S. cerevisiae* 2 µg of linear DNA fragment was used while for episomal transformations 10 µg of plasmid DNA was used.

Electroporation: The cells were grown in 10 ml of YEPD media overnight at 30°C for primary culture. For secondary culture, 5 µl of primary culture was inoculated in 50 ml of YEPD media and allow it to grow for 14 hrs (mid-log phase) and then harvested at 3,000 rpm for 5 min after checking the OD (1.6-1.8) of the cells. The pellet was then resuspended in 8 ml of ice cold sterile MQ water, 1 ml of 10X TE (Tris-EDTA) and 1 ml of 1M LiAC. The cells were kept at 30°C for 1 hr shaking and then added 250 µl of 1 M DTT and kept it again at 30°C for 30 min in a shaking incubator. The cells were washed with ice cold MQ water twice at 3,000 rpm for 5 min. The pellet was resuspended in 25 ml of 1 M sorbitol and after centrifugation the supernatant was discarded and the pellet was dissolved in minimum volume of sorbitol left in the tube. 40 µl of the cells were taken for electroporation in each cuvette and mixed with the linearized gel eluted DNA. The cells were dissolved in 1 ml of 1 M sorbitol after giving electric pulse at 1800V. After centrifugation the cells were dissolved in 1 ml of YEPD and allow it to grow at 30°C for 4-5 hrs. The cells were dissolved in minimum volume of YEPD and plated on the SD-URA$^-$ agar plates for uracil prototrophy. The plates were then grown for 1-2 days for colonies which were then inoculated for genomic DNA isolation.

2.4.2.4 Yeast Genomic DNA isolation

The *S. cerevisiae* cells were allowed to grow in 15 ml of YEPD media for 12-16 hrs, harvested at 3000 rpm for 5 min and were washed once with 1 ml of SOE (1M Sorbitol and 0.1 M EDTA). SOE was then added to the cells to make final volume 500 µl. 20 µl of 10 mg/ml solution of Zymolyase was added and the tubes were incubated at 37°C. The tubes were then turned upside down gently after every 15 min. The contents of the tube were then centrifuged at 2000 rpm for 1 min until the cells were just pelleted enough. The supernatant was discarded and the cells were

resuspended by vortexing thoroughly for 1 min in 500 µl of 50 mM Tris, 20-mM EDTA mix. 50 µl of 10% SDS was added to the above suspension and incubated at 65°C for 30 min. 200 µl of cold 5.0 M potassium acetate was added and the tubes were chilled on ice for 60 min after vortexing to mix the contents. After incubation on ice the cell suspension was centrifuged for 5 min at 4°C. The supernatant was recovered in fresh tubes after centrifugation and 1 volume of isopropanol was added. The tubes were inverted several times to get a pellet of DNA. Eventually centrifuging briefly pelleted the DNA down. The pellet was semi-dried in a speedvac and resuspended in 150 µl of TE. The DNA was kept at 65°C till it dissolved completely. 1.5 µl of RNase A solution (10 mg/ml) was added and the tubes were incubated at 37°C for 30 min. The tubes were chilled on ice and then centrifuged for 5 minutes at 4°C. The supernatant was transferred to fresh tubes and the DNA was precipitated with 2.5 volumes of ethanol and 1/10 volumes of 3.0 M sodium acetate (pH 5.2). The DNA pellet was washed with 70% ethanol and dried in a speedvac. The DNA pellet was finally resuspended in 100-200 µl of sterile MQ water.

Alternatively, the *S. cerevisiae* cells were allowed to grow in 10 ml of YEPD media for 12-16 hrs. The cells were then collected by centrifugation and resuspended in 500 µl of MQ water. The supernatant was decanted and the tubes were briefly vortexed to resuspend the pellet in the residual liquid. 200 µl of TENTS (2% Triton X-100, 1% SDS, 100 mM NaCl, 10 mM Tris pH 8.0, 1 mM EDTA), 200 µl of PCI and 200 µl of glass beads were then added to the cell suspension. The glass beads were prepared by soaking them in conc. HNO_3 for 1 hr, washing extensively with water and baking until dry. The cells were then broken in the breaker. The tubes were then centrifuged at 10,000 rpm for 5 min at 4°C. The supernatant was then taken and RNase treatment was given for 5-10 min at 37°C. 10 µl of 4 M ammonium acetate solution was then added. The tubes were then completely filled with chilled absolute ethanol and were inverted to mix properly and then incubated at room temperature for 5-10 min. Subsequently centrifugation was done to pellet down the DNA which was then washed with 70% ethanol. The pellet was then semidried and suspended in 100-200 µl of MQ water.

2.4.2.5 Southern blot analysis of genomic DNA

5-10 µg of the genomic DNA was digested with the appropriate enzyme and loaded on a 1% agarose gel (Tris-Acetate-EDTA buffer). After the digested DNA was separated, the gel was denatured in a 1.5 M NaCl, 0.5 M NaOH solution for 30 min followed by its treatment in the neutralization solution (1.5 M NaCl, 0.5 M Tris pH 7.2, 1 mM EDTA) for 30 min. The gel was then transferred to a Hybond^{TM}-N^{+} membrane with 20X SSC by capillary transfer overnight. The membrane was cross-linked in a UV cross linker and then was put for pre-hybridization for at least 4 hrs at 65°C in 3 ml 0.1 M Sodium phosphate buffer, 7 ml of 10% SDS and 200 µl of 0.5M EDTA. The probe product was labelled by random primed labelling method using the Amersham MegaPrime labeling kit, according to the manufacturer's instructions (Amersham Biosciences). The labelled probes were purified using Sephadex G-50 and then added into the prehybridization buffer. Membranes were thus hybridized with this α-^{32}P dATP labelled CaMDR1 specific probe for 12-16 hrs at 65°C. These membranes were then washed under high stringency condition at 65°C. These washed membranes were quantified by exposure of the hybridized membranes in a FLA5000 Fuji Phosphoimager system.

2.4.2.6 Plasma membrane preparation and Immunodetection

CMs were prepared from *S. cerevisiae* cells grown in YEPD to late exponential phase. The cells were broken with glass beads by vortexing the cells 4 times for 30 sec each followed by intermittent cooling for 30 sec on ice. The homogenization medium contained 50 mM Tris pH 7.5 and 2.5 mm EDTA and the protease inhibitor cocktail (1mM PMSF, 1µg/ml leupeptin, pepstatin A and aprotinin). The CM was recovered by centrifuging at 1000 X g to remove unbroken cells and finally pelleting the CM by ultracentrifugation at 100,000 X g for 1 hr. The CM was resuspended in buffer having 20 mM Tris pH 7.5, 150 mM NaCl, 20% glycerol and protease inhibitors at concentrations mentioned above. Plasma membrane (PM) fractions were obtained from CM fractions by sucrose gradient centrifugation as described by Monk *et al.*, 1991. The protein samples (20 µg) were separated on 8% SDSPAGE gel and either stained with colloidal Coomassie G250 or electroblotted (40V, 1h, 4°C) on to nitrocellulose membranes (Invitrogen Life Technologies, CA,

USA). The membranes were incubated with either 1:5000 dilution anti-GFP Monoclonal antibodies, 1:1000 anti-CaMdr1p antibodies or 1:4000 anti-PentaHis Monoclonal antibodies. Immunoreactivity was detected with HRP labelled goat antimouse antibody at 1:10,000 dilution in 5% fat-free milk for GFP antibody. Protein on immunoblots was visualized using the enhanced chemiluminescence assay system (ECL kit, Amersham Biosciences, Arlington Heights, IL, USA).

2.4.2.7 Protein gel electrophoresis (SDS-PAGE)

SDS-polyacrylamide gel electrophoresis was performed as described by Laemmli, 1970. A 5-12% polyacrylamide gel was run at 80-120 V for 2 hours in Bio-Rad Mini Gel apparatus. The samples were prepared according to the method of Holzer and Hammes [Holzer and Hammes, 1989]. Protein aliquots were mixed with 5X sample loading buffer and incubated at 90°C for 10 min. After electrophoresis, the gel was visualized by silver staining.

2.4.2.8 Confocal microscopy

The cells were grown in YEPD media to late log phase, washed and resuspended in appropriate volume of 50 mM HEPES pH 7.0. The cells were then directly viewed with 100X oil immersion objective on a Biorad confocal microscope (Radiance 2100, AGR, 3Q/BLD, Biorad, UK).

2.4.2.9 Flow Cytometry

Flow cytometric analysis of the CaMDR1-GFP and its mutant variants was performed with a FACSort flow cytometer (Becton-Dickinson Immunocytometry Systems, San Jose, Calif.). Cells were grown to mid-log phase, and 10^6 cells were harvested and washed with 50 mM HEPES (pH 7.0). Cells were resuspended in 500 µl of 50 mM HEPES (pH 7.0). Ten thousand cells were analyzed in acquisition. Analysis was performed with CellQuest software (Becton-Dickinson Immunocytometry Systems). The mean fluorescence intensity was calculated using the histogram stat program.

2.4.3 RESISTOTYPING

2.4.3.1 Drug Resistance assays

The susceptibilities of yeast cells to different drugs were determined by three different methods. The following stock solutions were prepared: The drugs used were (solvent used is given in parenthesis): Cycloheximide (water); 4-nitrosoquinoline-N-oxide (DMSO); Fluconazole (methanol); Anisomycin (DMSO); cerulenin (DMSO); methotrexate (Tris-HCl). The solvents used to solubilize different drugs were also tested and there was no inhibition of growth due to the solvents used. Three different methods can be listed as follows:

- Filter disc assay
- Spot test
- Antifungal susceptibility testing using NCCLS method M27A

Following is a detailed description of these different methods and the drugs along with their respective solvents used in this study are listed in Appendix IV.

2.4.3.1.1 Filter Disc assay

The drug resistance profile of yeast cells was determined as described earlier [Daum *et al.*, 1998]. Cells were grown in YEPD broth or SD-URA$^-$ media as described above. Yeast strains ($6x10^5$ cells ml^{-1}) were mixed with molten media with agar (~40°C) and poured in a petriplate. After solidifying, the filter discs were kept on the plate and drugs were spotted on to the discs. The amount of drugs (in μg) was applied on disc in 5-10 μl volume. The diameter of zone of inhibition was scored after 48 hrs and compared with that of WT strain. The zones of inhibition have been reported in 'cms' at a concentration where maximum difference between the WT and the mutants was visible.

2.4.3.1.2 Microtitre / microdilution assay

The relative azole susceptibility of was essentially determined using NCCLS 27A method [Espinell-Ingroff *et al.*, 1998; Martins and Rex, 1997; Rex *et al.*, 1997] modified microdilution test [Talibi and Raymond, 1999] in YEPD or SD-URA$^-$ media containing SD-URA drop out mix. The scheme is depicted in Figure 14. Briefly, cells were grown on YEPD plates for 24 hrs at 30°C to obtain single colonies, which were

resuspended in saline solution to give an A_{600} of 0.1. The cells were then diluted 100-fold in YEPD medium. The diluted cell suspensions were added to the wells of round bottom 96-well microtitre plates (100 µl/well) containing equal volumes of medium (100 µl/well) and different concentrations of drugs [Kohli *et al.*, 2002; Talibi and Raymond, 1999]. A drug free control was also included. The plates were incubated at 30°C for 48 hrs. The MIC test end point was evaluated by reading A_{600} in a microplate reader and is defined as a lowest drug concentration that gave >80% inhibition of growth compared with the growth of the drug free control.

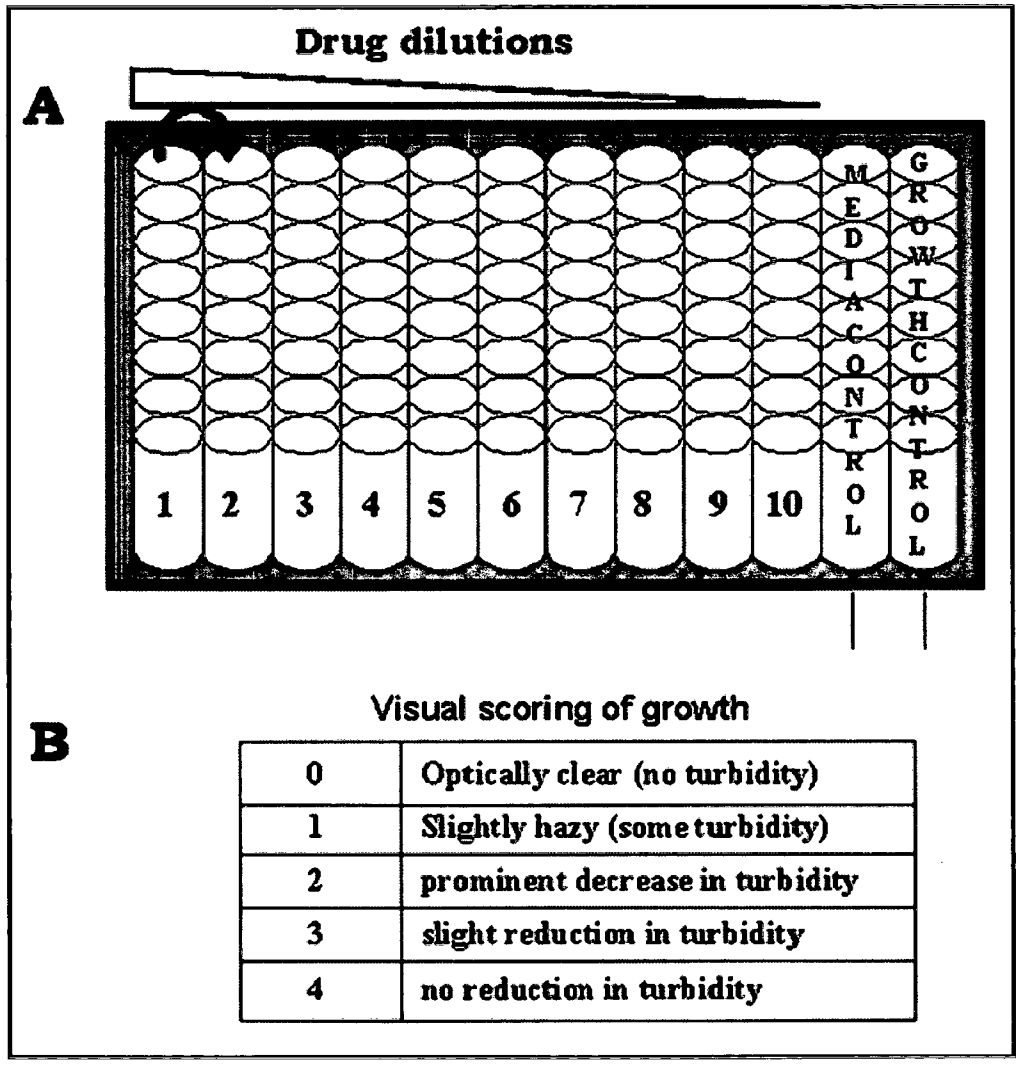

Figure 14: Antifungal susceptibility testing of yeast.
(A) Scheme: From a stock solution of drug, doubling dilutions of drugs are prepared in RPMI or YEPD media to which 0.1 ml of inoculum is added at a final concentration of 2×10^3 cells ml-1. Well 12 of each row is the growth control and contain inoculum w/o drug. Column 11 has no drug / no inoculum and represents the medium control.
(B) The MIC may be determined by the eye by scoring turbidity or may be checked spectrophotometrically at A_{619} using a microtiter plate scanner.

2.4.3.1.3 Spot assay

The yeast cells were grown overnight on YEPD plates. The cells were then resuspended in normal saline to an A_{600} of 0.1. Five microlitres of fivefold serial dilutions of each strain was spotted on to YEPD plates in the absence (control) and presence of the following drugs, Fluconazole, Cycloheximide, 4-nitrosoquinoline-N-oxide, Anisomycin, Methotrexate and Cerulenin. Growth differences were recorded following incubation of the plates for 48 hrs at 30°C. Growth was not affected by the presence of the solvents used for the drugs. These assays with each drug were repeated at least 3-4 times.

2.4.4 BIOCHEMICAL TECHNIQUES

2.4.4.1 [^{3}H]-Fluconazole and [^{3}H]-Methotrexate accumulation

The accumulation of [^{3}H] FLU and [^{3}H] MTX accumulation was determined by modification of method described elsewhere [Sanglard *et al.*, 1996]. Cells from midlog phase were centrifuged at 500 X g for 3 minutes and resuspended in fresh YNB medium as a 5% cell suspension. 1.5 ml of cell suspension was incubated in shaking water bath for 150 rpm at 30°C and [^{3}H] FLU or [^{3}H] MTX was added to a final concentration of 100 nM [10X stock was prepared by mixing 990 µl of 1µM cold FLU+10 µCi [^{3}H] FLU, (specific activity 20 Ci mmol^{-1})] and 25µM [10X stock was prepared by mixing 99 µl of 2.5 mM cold MTX + 8 µl [^{3}H] MTX, (specific activity 20 Ci mmol^{-1}) + 893 µl of 10 mM Tris-Cl] respectively. A 100 µl aliquot of cells was taken after 45 min, filtered rapidly and washed twice with 10 mM PBS, pH 7.4 on Millipore manifold filtration assembly using 0.45 µm cellulose nitrate filters (Millipore, USA). The filter discs were dried and put in scintillation cocktail-O for radioactivity measurement by using a liquid scintillation counter (Packard, USA). The [^{3}H] FLU and [^{3}H] MTX accumulation was expressed as pmoles mg^{-1} dry weight.

2.4.4.2 Transport of Nile Red

The accumulation of NR in cells expressing WT or mutant variant CaMdr1p-GFP was measured by flow cytometry with a FACSort flow cytometer (Becton-Dickinson Immunocytometry Systems, San Jose, Calif.) as described previously [Ivnitski-Steele *et al.*, 2009]. Briefly 0.1 OD_{600} cells were inoculated and were

incubated at 30°C with shaking until the cultures reached an OD_{600} of 0.25. Cells were then harvested to be resuspended as 5% cell suspension in diluted medium (containing one part YEPD and two parts water). NR was added to a final concentration of 7 μM and cells were incubated in shaking water bath at 150 rpm at 30°C for 30 minutes. The cells were then harvested, washed and then resuspended in the diluted medium. Ten thousand cells were analyzed in acquisition. Analysis was performed with CellQuest software (Becton-Dickinson Immunocytometry Systems). The mean fluorescence intensity was calculated using the histogram stat program.

2.4.4.3 Statistical analysis

Data are the means ± S.D from duplicate samples of at least three independent experiments. Differences between the mean values were analyzed by Student's t-Test and results were considered significant when $P < 0.001$.

RESULTS AND DISCUSSION

SECTION-I

3.1 RANDOM MUTATIONAL ANALYSES OF THE MULTIDRUG MFS TRANSPORTER CaMdr1p

3.1.1 INTRODUCTION

The incidences of developing resistance to various antifungal drugs by the opportunistic pathogenic fungus *C. albicans* have increased considerably over the past few decades. Various studies have proved that evolving resistance to such a wide range of antifungals is a multifactorial phenomenon. The drug efflux is one of the major strategies adopted by *Candida* to become resistant to drugs, in particular to azoles, which are frequently used in treating candidiasis. Among the identified and well-studied MDR transporters in *C. albicans,* are CaCdr1p and CaCdr2p, belonging to the ABC superfamily and CaMdr1p belonging to the MFS transporter proteins [Lopez-Ribot *et al.*, 1999; Prasad *et al.*, 2002; Sanglard and Odds, 2002].

Random and Site-directed mutational strategies have been extensively used to understand the structure and function of these MDR efflux proteins. For example, random mutational analysis of an ABC transporter, ScPdr5p of budding yeast identified several amino acid residues that alter its substrate specificity and sensitivity to various inhibitors [Egner *et al.*, 1998; Egner *et al.*, 2000; Golin *et al.*, 2003; Tutulan-Cunita *et al.*, 2005; Ernst *et al.*, 2008]. Site-directed mutational analysis of multidrug ABC multidrug transporter CaCdr1p (a close homologue of ScPdr5p) has revealed insight into its drug binding and efflux properties. These studies have implicated some of the amino acid residues of TMS 5, 6, 11 and 12 as the components of the substrate binding pocket(s) of CaCdr1p. Together, these studies suggest that the drug binding sites in CaCdr1p are scattered throughout the protein and probably more than one residue of different helices are involved in binding and extrusion of drugs [Krishnamurthy *et al.*, 1998; Dogra *et al.*, 1999; Shukla *et al.*, 2003; Saini *et al.*, 2005; Puri *et al.*, 2009]. However, there is still insufficient information available to predict where and how exactly the most common antifungals such as azoles bind and how are they extruded by CaCdr1p.

CaMdr1p, which is a major multidrug transporter of *C. albicans* remains poorly understood. CaMdr1p belongs to MFS superfamily which consists of membrane transport proteins from bacteria to higher eukaryotes and involved in

symport, antiport or uniport of various substances. One of the 17 families of MFS transporters uses the proton motive force to drive drug transport. These proteins are likely to operate as multidrug / proton antiporters and have been identified in both prokaryotes and eukaryotes [Pao *et al.*, 1998]. CaMdr1p belongs to this DHA1 drug efflux family which is widely distributed and includes both drug-specific and multidrug efflux pumps. An over-expression of CaMdr1p is associated with an increased resistance to a variety of drugs particularly to fluconazole, benomyl and methotrexate. CaMdr1p has a unique and conserved antiporter motif also called as 'motif C' in TMS 5. Alanine scanning of 'motif C' highlighted its importance in drug transport. The putative helical wheel projection showed clustering of functionally critical residues to one side and thus suggesting an asymmetric nature of TMS 5 [Pasrija *et al.*, 2007].

In this study an *In silico* analysis was done which reveals that CaMdr1p possesses many conserved residues scattered throughout the length of the protein. The conserved residues were deduced by whole sequence alignment of fungal MFS transporters. These residues of CaMdr1p were analyzed systematically and checked for their role in the functionality of the protein. For this, all the residues were subjected to site-directed mutagenesis and were replaced with alanine. A comparison of drug resistance profile of individual mutant variants revealed the specificity of critical residues.

The structures of many important proteins, as well as key aspects of protein regulation and dynamics, are not yet accessible to high resolution methods. Site-directed cysteine and disulfide chemistry provides an approach that can in many cases addresses these challenging questions by analyzing the structure and dynamics of a given protein in its native environment [Frillingos *et al.*, 1998]. The most prevalent application of site-directed cysteine and disulfide chemistry has been in the structural studies of membrane protein systems and large multiprotein complexes. The structures of large, insoluble, complicated systems are often the most difficult to analyze high-resolution structural methods, making the structural constraints provided by the present chemical approach quite valuable. The approach can give solutions to various problems: - (a) to map secondary, tertiary and quaternary structure (b) analyze conformational changes and the structural basis of regulation by covalently trapping

specific conformational or signaling states (c) to uncover the spatial and temporal aspects of thermal fluctuations by detecting backbone and domain dynamics. These two approaches together led an insight into the structural and functional aspects of CaMdr1p.

3.1.2 RESULTS

3.1.2.1 SITE-DIRECTED MUTATIONAL ANALYSIS OF CONSERVED RESIDUES OF CaMdr1p

3.1.2.1.1 Sequence alignment of fungal MFS transporters with CaMdr1p reveals several conserved residues

Various sequences of known fungal MFS transporters such as CaMDR1, CdMDR1, CtMDR1, CmCYHR, ScFLR1, spBsu1, ScTPO1 were taken from SWISSPROT and aligned using CLUSTALW. The multiple whole sequence alignment of fungal MFS transporters highlighted the conservation of certain amino acid residues throughout the protein (Figure 15).

In an effort to develop an understanding about the molecular details of the functioning of these conserved residues of CaMdr1p, in this study, several mutant variants of the protein were generated where these residues were substituted with alanine by site-directed mutagenesis. All existing alanines were replaced with glycines. The glycine residues were also replaced with leucine wherever replacement with alanines did not affect the functioning. All CaMdr1p mutant variants were stably over-expressed as GFP-tagged variants in a heterologous hyper-expression system developed by Cannon's group by integrating it at *PDR5* locus downstream from the *PDR5* promoter in the *S. cerevisiae* strain AD1-8u$^-$. The host AD1-8u$^-$ constructed by Goffeau's group was derived from a *Pdr1-3* mutant strain with a gain of function mutation in the transcription factor Pdr1p, resulting in constitutive hyperinduction of the *PDR5* promoter. Single copy integration of each transformant at the *PDR5* locus was confirmed by Southern hybridization (Figure 16). Two positive clones of each mutant were selected to rule out clonal variations.

MULTIPLE SEQUENCE ALIGNMENT

```
CaMDR1  ---------------------------MHYRFLRDSFVGRVTYHLSKHKYFAHPEEAK---  31
CdMDR1  ---------------------------MHYRFLRDSFVGRVVYHLSKHKYFAHPEEAK---  31
CtMDR1  ------------------------------------------------------------
CYHR    ----------------------------MAAFIKDSFWGQIIYRLSGRKLFRHNDELP---  30
FLR1    --------------------------MVYTSTYRHTIVVDLLEYLGIVSNLETLQSAR---  32
Bsu1    ------------------------------------MASKIASLFSPSETASKDQHEN---  22
TPO1    MSDHSPISNKENHLLPSDSSRSSSSDMHSTGTTGTTGVEPVDFTGEGAKYTTATEGNGGA  60

CaMDR1  DYIVPEKYLADYKPTLADDTSINFEKEEIDNQGEPNSSQSSSSNNTIVDNNNNNNDNDVD  91
CdMDR1  DYIVPEKYLADYKPTLGDDTSINFEKEEIDNEGEPNSTQSSS-NNTVVSNTNED------  84
CtMDR1  ------------------------------------------------------------
CYHR    DYVVPEKYLLDPKEEVLNSS----DKSQSSENKEQTEGDQATIQNEPAS-----------  75
FLR1    EDETRKPENTDKKECKPDYDIECGPNRSCSESSTDSDSSGSQIEKN--------------  78
Bsu1    ---VAEDLELGTASSQSDGIHETNSEYDEKKREESPE----------------------  56
TPO1    DLAIQRTTTMNSAAESEVNITRRLTKILTGSVNEPDRVEVDYTNCAPMGGDRPYPPSLPS 120

CaMDR1  GDKIVVTWDGDDDPENPQNWPTLQKAFFIFQISFLTTSVYMGSAVYTPGIEELMHDFGIG 151
CdMDR1  -DKIIVTWDGDDDPENPQNWPALQKAFFIFQISFLTTSVYMGSAVYTPGIEELMHDFGIG 143
CtMDR1  ------------------------------------------------------------
CYHR    -EHIIVTWDGDDDPENPYNWPFAWKAIAAMQIGFLTVSVYMASAIYTPGVEEIMNQFNIN 134
FLR1    -DPFRVDWNGPSDPENPQNWPLLKKSLVVFQIMLLTCVTYMGSSIYTPGQEYIQEEFHVG 137
Bsu1    -VIDISNLISSDHPAHPQNWHWAKRWSIVFMFCLMQIYVIWTSNGFGSIEYSVMAQFNVS 115
TPO1    RDLYEVTFDGPNDPLHPFNWPMKKKVLLCLVLCLDSIAIAMCSSIFASAVPQICEIYHVI 180

CaMDR1  RVVATLPLTLFVIGYGVGPLVFSPMSENAIFGRTSIYIITLFLFVILQIPTALVNNIAGL 211
CdMDR1  RVVATLPLTLFVIGYGVGPLVFSPMSENAIFGRTSIYIVTLFLFVILQIPTALVNNIAGL 203
CtMDR1  ---------LFVIGYGVGPMIFSPMSENAIFGRTSIYIVTLAIFVILQVPTALVKNIAGL  51
CYHR    STLATLPLTMFVIGYGIGPLFWSPLSENSRIGRTPLYIITLFIFFILQIPTALSNHIAGL 194
FLR1    HVVATLNLSLYVLGYGLGPIIFSPLSETARYGRLNLYMVTLFFFMIFQVGCATVHNIGGL 197
Bsu1    AQVATLCLSMNILGSGLGPMFLGPLS--DIGGRKPVYFCSIFVYTVFNISCALPRNIVQM 173
TPO1    EVVAILGITLFVLGFAASPVIYAPLS--ELYGRKGVLVLSAFGFALFQFAVATAENLQTI 238

CaMDR1  CILRFLGGFFASPCLATGGASVADVVKFWNLPVGLAAWSLGAVCGPSFGPFFGSILTVK- 270
CdMDR1  CILRFLGGFFASPCLATGGASVADVVKFWNLPVGLAAWSLGAVCGPSFGPFFGSILTVK- 262
CtMDR1  CILRFLGGFFASPCLATGGASVADVVNFWNAPIGISVWSLGAVCGPSLGPFFGSILTVK- 110
CYHR    SVLRVIAGFFAAPALSTGGASYGDFIAMHYYSIALGVWSIFAVAGPSIGPLIGAAVINRS 254
FLR1    IVMRFISGILCSPSLATGGGTVADIISPEMVPLVLGMWSAGAVAAPVLAPLLGAAMVDA- 256
Bsu1    IISHFIIGVAGSTALTNVAGGIPDLFPEDTAGVPMSLFVWACAGGAIGAPMATGVDINAK 233
TPO1    FICRFFGGFIGAAPMAVVPAAFADMFDTNVRGKAIALFSLGVFVGPILSPVMGSYIAQR- 297

CaMDR1  ---ASWRWTFWFMCIISGFSFVMLCFTLPETFGKTLLYRKAKRLRAITGNDRITSEGEIE 327
CdMDR1  ---ASWRWTFWFMCIISGFSFVMLCFTLPETFSKTLLYRKAKRLRAITGNNRITSEGEIE 319
CtMDR1  ---AGWRWTFWFMCIISGFSLFMLAFTLPESFSKTLLRRKAQRLRAVTGNDRITSDGEVE 167
CYHR    HDADGWRWSFWFMAILSGVCFIVLSFSLPETYGKTLLRRKAERLRKLTGNNRIISEGELE 314
FLR1    ---KNWRFIFWLLMWLSAATFILLAFFFPETQHHNILYRRALKLRKETGDDRYYTEQDKL 313
Bsu1    ---YGWRWLYYIN-IIVGGFFLIVILIIPETLPIKVITRYENAKGR-------IVEGIPK 282
TPO1    ---TTWRWLEYVVGCFASAVFVAIVLFFEETHHPTILVNKAKQMRKQSNN--WGIHAAHE 352
```

```
CaMDR1  NSKMTSHELIIDTLWRPLEITVMEPVVLLINIYIAMVYSILYLFFEVFPIYFVGVKHFTL 387
CdMDR1  NSKMTSHELIIDTLWRPLEITVMEPVVLLINIYIAMVYSILYLFFEVFPIYFIGVKHFTL 379
CtMDR1  NSKMTTHELIVDTLWRPLEITIMEPVVLLIDIYIAMVYSILYLFFEVFPIYFVGVRGFTL 227
CYHR    DGHKTTSQVVSSLLWRPLEITMLEPVVFLIDIYIALVYSIMYLIFESVPIVYAGIHHFTL 374
FLR1    DREVDARTFLINTLYRPLKMIIKEPAILAFDLYIAVAYGCFYLFFEAFPIVFVGIYHFSL 373
Bsu1    NNLKEVLKKCKFVTTMGFRMMLTEPIILSMGLYNFYAYGISYFFLTAIWPVFYDTYKMSE 342
TPO1    DVELSIKDIVQKTVTRPIIMLFVEPLLLFVTIYNSFVYGILYLLLEAYPLVFVEGYGFTE 412
        :                 : : . ** :: . :*   .*.  *:::      :     ::

CaMDR1  VELGTTYMSIVIGIVIAAFIYIPVIRQKFTKPILRQEQVFPEVFIPIAIVGGILLTSGLF 447
CdMDR1  VELGTTYMSIVIGIVIAAFIYIPVIRQKFTKPILREEQVFPEVFIPIAIVGGILLTSGLF 439
CtMDR1  VELGTTFFSVLIGIVVACSIYLPIIKRIFTDRILRKEPVFPEVFIPLAIVGGCLLTGGLF 287
CYHR    VEMGATYVSTIIGIIIGGAIYLPTVYYKFTKKLLAGQNVTPEVFLPPAIFGAICMPIGVF 434
FLR1    VEVGLAYMGFCVGCVLAYGLFG-ILNMRIIVPRFRNGTFTPEAFLIVAMCVCWCLPLSLF 432
Bsu1    MGASCTYLSGFVASTLLFLYQPIQDWIFRRDKAKNNGVARPEARFTSALFITLLFPAGMF 402
TPO1    NGE-LPYIALIIG-MMVCAAFIWYMDNDYLKRCRAKGKLVPEARLYAMVIAGTVFPIGIL 470
             .:..  :.  :                          **. :   :     :. .::

CaMDR1  IFGWSANR--TTHWVGPLFGAATTASGAFLIFQTLFNFMGASFKPHYIASVFASNDLFRS 505
CdMDR1  IFGWSANR--TTHWVGPLFGAAITASGAFLIFQTLFNFMGASFKPHYIASVFASNDLFRS 497
CtMDR1  IFGWSATR--TTHWIGPLFGAAVTSSGAFIIFQTLFNYMGASFQPIYIASVFASNDLFRS 345
CYHR    IFGWTSSP--DINWFVPLIGMALFAVGAFIIFQTLFNYMAVSFKVEYLASVFSSNAFFRS 492
FLR1    LFGWTAR----VHWILPVISEVFFVLAVFNIFQATFAYLATCY-PKYVASVFAGNGFCRA 487
Bsu1    LFAFTCHP--PFPWMSPIVGNSMVTVANGHNWMCILNYLTDSY-PLLSGSAVAAFTLPSF 459
TPO1    WFCWTGYYPHKIHWMVPTVGGAFIGFGLMGIFLPCLNYIIESY-LLLAASAVAANTFMRS 529
         * ::        *. * ..      .    :   : ::  .:     .*..:.  :

CaMDR1  VIASVFPLFGAPLFDNLATPEYPVAWGSSVLGFITLVMIAIPVLFYLNGPKLRARSKYAN 565
CdMDR1  VIASVFPLFGAPLFDNLATPEYPVAWGSSVLGFITLLMIAIPVLFYLNGPKLRARSKYAN 557
CtMDR1  TVASVFPLFGAPLFNNLATPNYPVAWGKP------------------------------ 374
CYHR    VSAGAFPLFGRALYNNLSIDKFPVGWGSSILGFISLGMIAIPVFFYLNGPKLRARSKYAY 552
FLR1    SFACAFPLFGRAMYDNLATKNYPVAWGSSLVGFLTLGLAIIPFILYKYGPSLRTRSSYTE 547
Bsu1    IGATVFAHVSQIMFNNMS-----VKWAVATMAFISISIPFIIYTFYFFGQRIRALSSLTG 514
TPO1    AFGACFPLFAGYMFRGMG-----IGWAGLLLGLFAAAMIPVPLLFLKYGESIRKKSKYAY 584
         .  *. ..  :: .:.     : *.

CaMDR1  ------------
CdMDR1  ------------
CtMDR1  ------------
CYHR    ------------
FLR1    E----------- 548
Bsu1    NKALKYLPLENN 526
TPO1    AA---------- 586
```

Figure 15: Multiple sequence alignment of MFS transporters showing conserved residues.

The MFS sequences were aligned using clustalw. Completely conserved residues which are marked by a star underneath and were further studied.

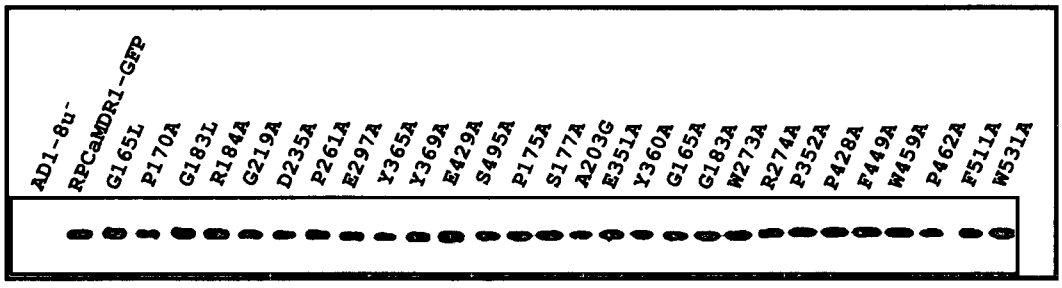

Figure 16: Southern Blot Hybridization confirming integrated mutant variants of conserved residues in CaMdr1p.
Genomic DNA was extracted from all the mutant variants and then digested with Spe I, loaded and separated by electrophoresis. The gel was then transferred to the nylon membrane and the blot was probed with CaMDR1 specific probe. Southern Blot Analysis confirms single-copy integration of the mutant variants of CaMDR1-GFP. The negative (AD1-8u$^-$) and positive (RPCaMDR1-GFP) controls are also shown for comparison.

3.1.2.1.2 Mutant variants of the conserved residues display different levels of sensitivity to various drugs tested

Confirmed positive mutants were screened for their sensitivity towards different substrates by microdilution and spot assays. Based on the sensitivity pattern as shown in Figure 17, these mutant variant could be divided into three categories:

1. **Class I**- This included twelve variants of CaMdr1p; G165L, P170A, G183L, R184A, G219A, D235A, P261A, E297A, Y365A, Y369A, E429A and S495A which showed severely decreased susceptibility to all the drugs tested. The glycine residues which did not show effect upon mutation to alanines were replaced with leucines to check for their importance of function.
2. **Class II**- This category included five variants P175A, S177A, A203G, E351A and Y360A which showed selective resistance. These mutants continued to display resistance to FLU, MTX and ANISO but became sensitive to CYH and 4-NQO.
3. **Class III**- This included eleven mutant variants; G165A, G183A, W273A, R274A, P352A, P428A, F449A, W459A, P462A, F511A and W531A which were when replaced with alanine, showed level of resistance comparable to WT-CaMdr1p.

The drug sensitivities as revealed by spot assays matched well with the microdilution assay results (Table 7). The locations of the mutated residues are shown in the pictorial representation of secondary structure of CaMdr1p (Figure 18).

CLASS I

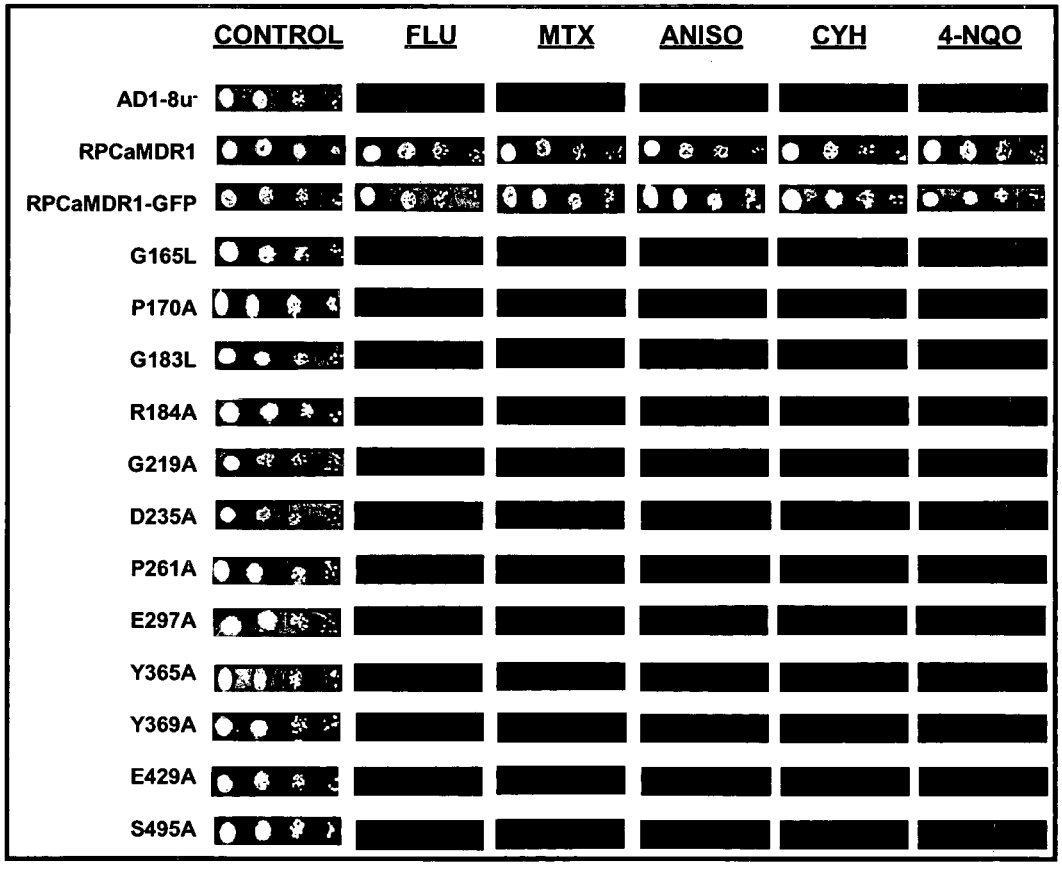

CLASS II

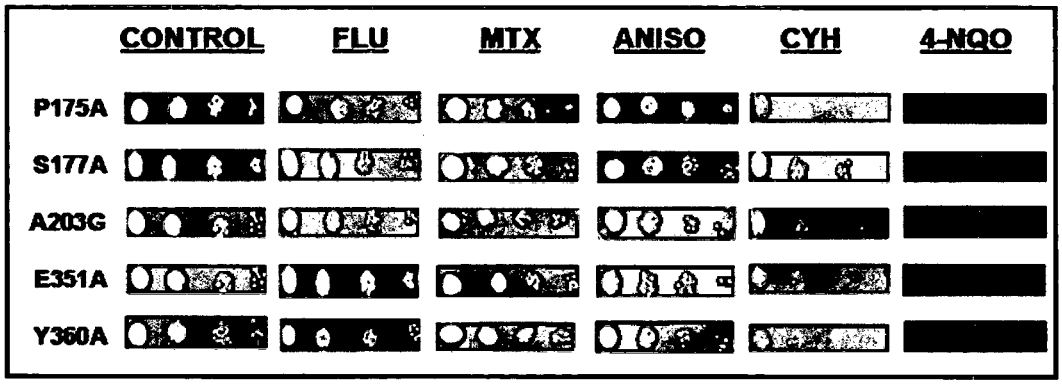

CLASS III

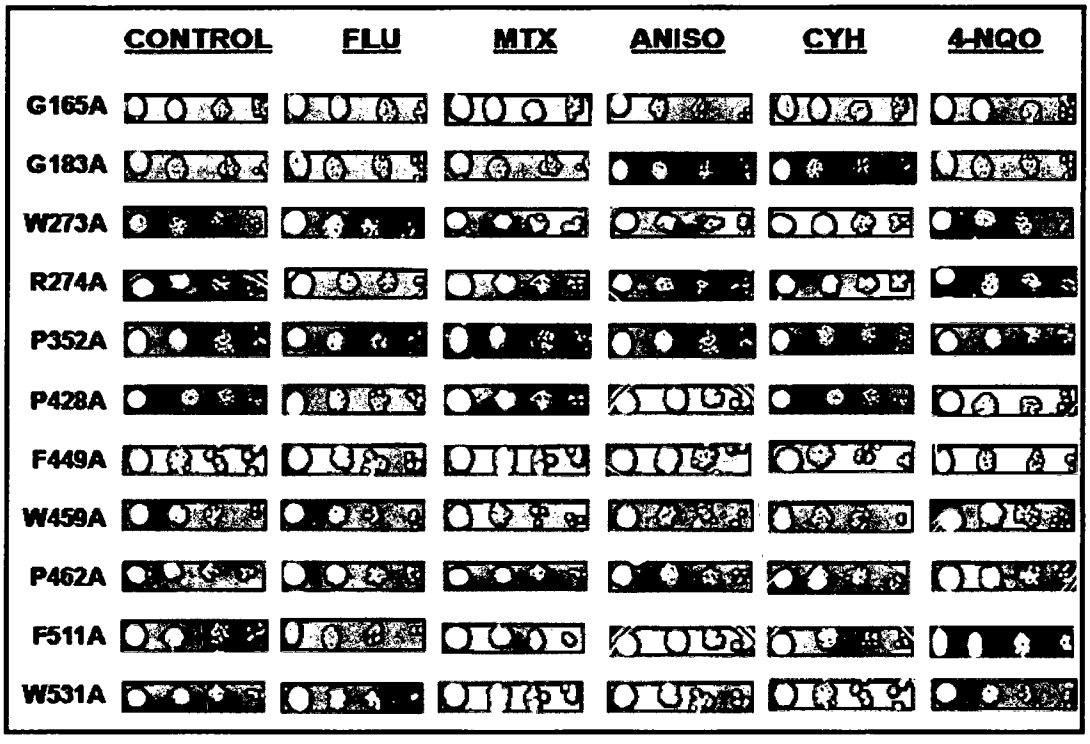

Figure 17: Drug resistance profile of wild-type and conserved residues mutant CaMDR1 strains determined by the spot assay.
Cells were spotted on to YEPD plates in the absence (control) and presence of the following drugs used- FLC (0.6 μg/ml), MTX (65 μg/ml), ANISO (3 μg/ml), CYH (0.2 μg/ml) and 4-NQO (0.2 μg/ml). Growth differences were recorded following incubation of the plates for 48 hrs at 30°C. Growth was not affected by the presence of the solvents used for the drugs (data not shown).

Strain	MIC $_{80}$(µg/ml)				
	FLU	**MTX**	**ANISO**	**CYH**	**4-NQO**
AD1-8u$^-$	0.5	16	0.5	0.015	0.03
RPCaMDR1	16	128	32	0.5	1
RPCaMDR1-GFP	16	128	32	0.5	1
Class I					
G165L	0.5	16	0.5	0.015	0.03
P170A	0.5	16	0.5	0.015	0.03
G183L	0.5	16	0.5	0.015	0.03
R184A	0.5	16	0.5	0.015	0.03
G219A	0.5	16	0.5	0.015	0.03
D235A	0.5	16	0.5	0.015	0.03
P261A	0.5	16	0.5	0.015	0.03
E297A	0.5	16	0.5	0.015	0.03
Y365A	0.5	16	0.5	0.015	0.03
Y369A	0.5	16	0.5	0.015	0.03
E429A	0.5	16	0.5	0.015	0.03
S495A	0.5	16	0.5	0.015	0.03
Class II					
P175A	16	128	32	0.06	0.125
S177A	16	128	32	0.03	0.125
A203G	16	128	32	0.03	0.125
E351A	16	128	32	0.03	0.125
Y360A	16	128	32	0.03	0.125
Class III					
G165A	16	128	32	0.5	1
G183A	16	128	32	0.5	1
W273A	16	128	32	0.5	1
R274A	16	128	32	0.5	1
P352A	16	128	32	0.5	1
P428A	16	128	32	0.5	1
F449A	16	128	32	0.5	1
W459A	16	128	32	0.5	1
P462A	16	128	32	0.5	1
F511A	16	128	32	0.5	1
W531A	16	128	32	0.5	1

Table 7: MIC$_{80}$ (µg/ml) values of the mutant variants of conserved residues of CaMdr1p. Minimum Inhibitory Concentration (MIC$_{80}$ µg/ml) of various mutant variants of the conserved residues for the different drugs tested in comparison to AD1-8u$^-$ and RPCaMDR1 (GFP-tagged and untagged variants).

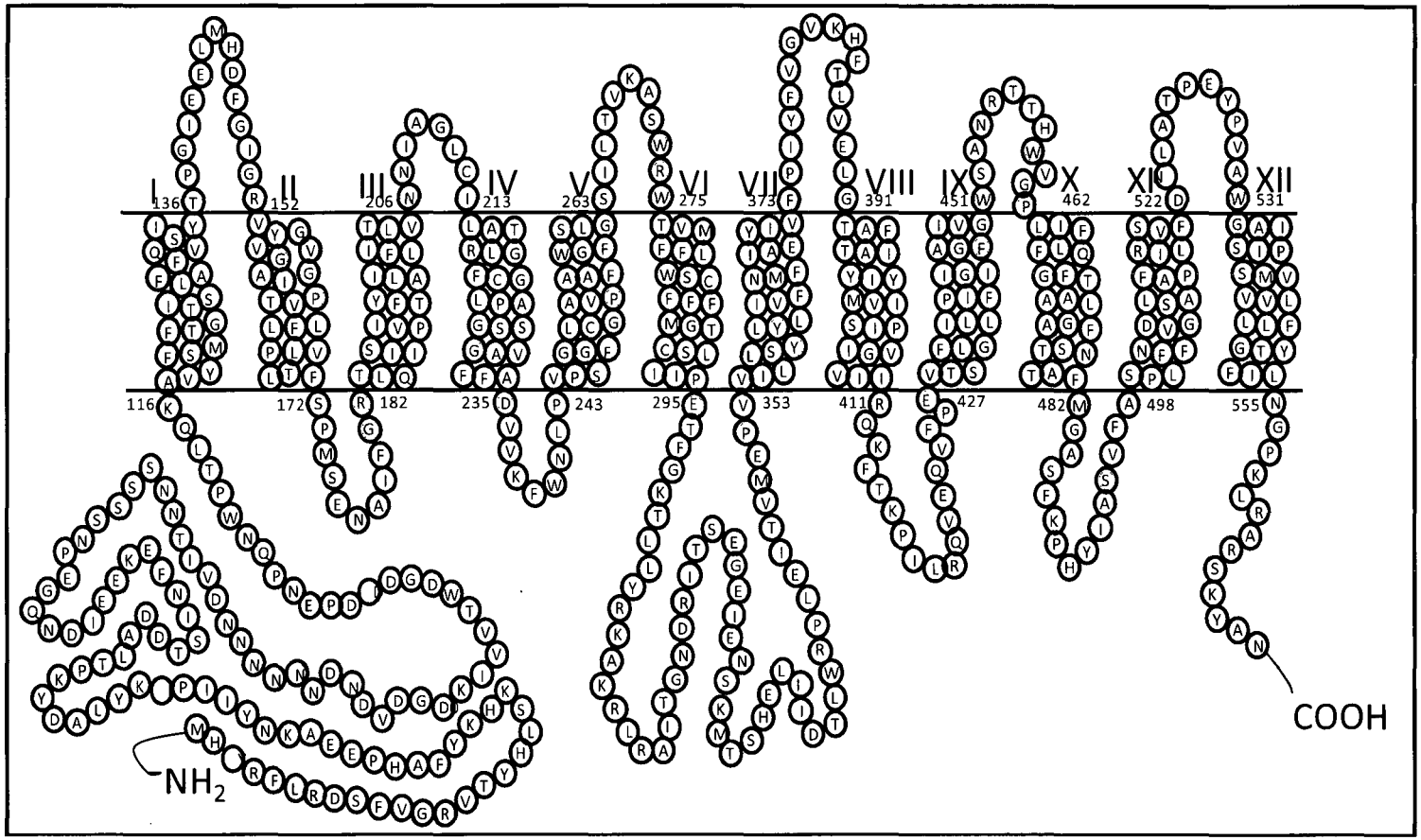

Figure 18: Predicted topology of the CaMdr1p with conserved residues shown in color.
The mutated positions are marked in colour in the secondary structure of CaMdr1p. The colour codes follow the classification mentioned above, such as residues of Class I are marked in red, Class II are marked in yellow while that of Class III are marked in green.

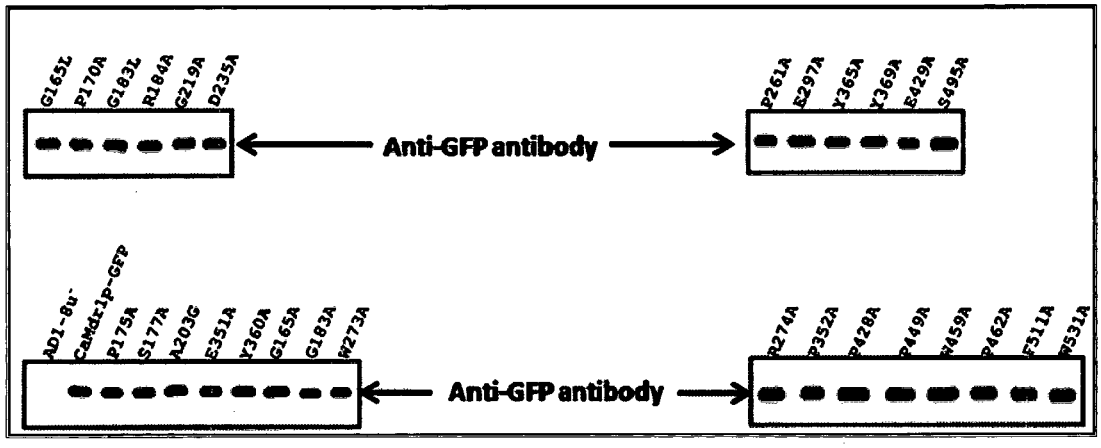

Figure 19: Comparison of protein expression profiles of CaMdr1p-GFP and its mutant variants of conserved residues in *S. cerevisiae*.
The PM fraction of mutant variants showed expression levels similar to WT-CaMdr1p-GFP on Western Blot analysis with anti-GFP antibody.

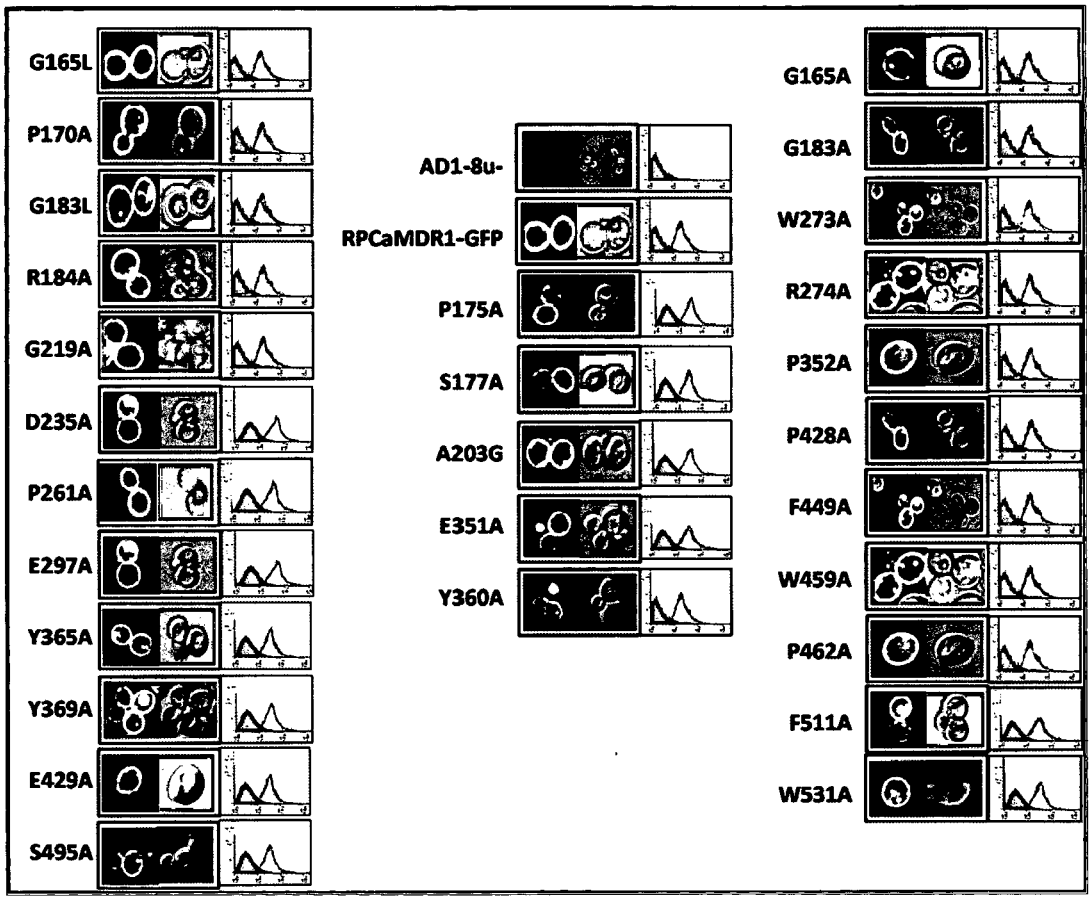

Figure 20: Surface localization of CaMdr1p-GFP and its mutant variants of conserved residues.
Confocal images and FACS analysis of the all the mutant variants to check their localization in comparison to AD1-8u$^-$ (negative control) and RPCaMDR1-GFP (positive control).

3.1.2.1.3 All mutant variants of CaMdr1p showed Cell Surface Expression and localization similar to the wild-type

To confirm that the susceptibility observed in the variants was not due to mislocalization, the surface expression and localization of RPCaMDR1-GFP was compared with its mutant variants. Similar levels of expression in the wild-type and the mutant variants were also confirmed by Western Blot analysis (Figure 19). Confocal images showed proper rim localization of GFP-tagged CaMdr1p mutant variants which was further confirmed by FACS analysis (Figure 20).

3.1.2.1.4 Accumulation of drugs [^{3}H] MTX and [^{3}H] FLU by selected mutant variants is enhanced

All the mutant variants were further analyzed for their functionality by measuring the intracellular accumulation of [^{3}H] MTX and [^{3}H] FLU. It has been earlier shown that MTX and FLU are substrates of CaMdr1p [Pasrija *et al.*, 2007]. The first category of mutants G165L, G183L, R184A, G219A, D235A, P261A, E297A, Y365A, Y369A, E429A and S495A showed complete abrogation of function and accordingly a relative increase of 50-70% in accumulation of [^{3}H] MTX and [^{3}H] FLU (decreased efflux) was observed. The second class of mutants which included P175A, S177A, E351A, Y360A, P512A and L513A and showed selective resistance, however, had levels of accumulation of [^{3}H] MTX and [^{3}H] FLU similar to WT-CaMdr1p. Coinciding with the drug susceptibility assay, the third class of mutants; G165A, G183A, W273A, R274A, P352A, P428A, F449A, P462A, and F511A showed drug efflux comparable to WT-CaMdr1p (Figure 21).

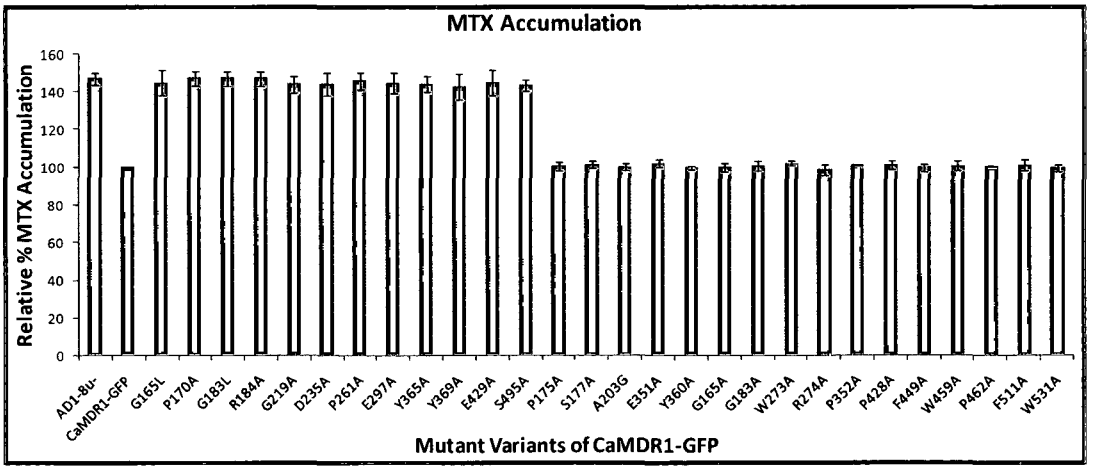

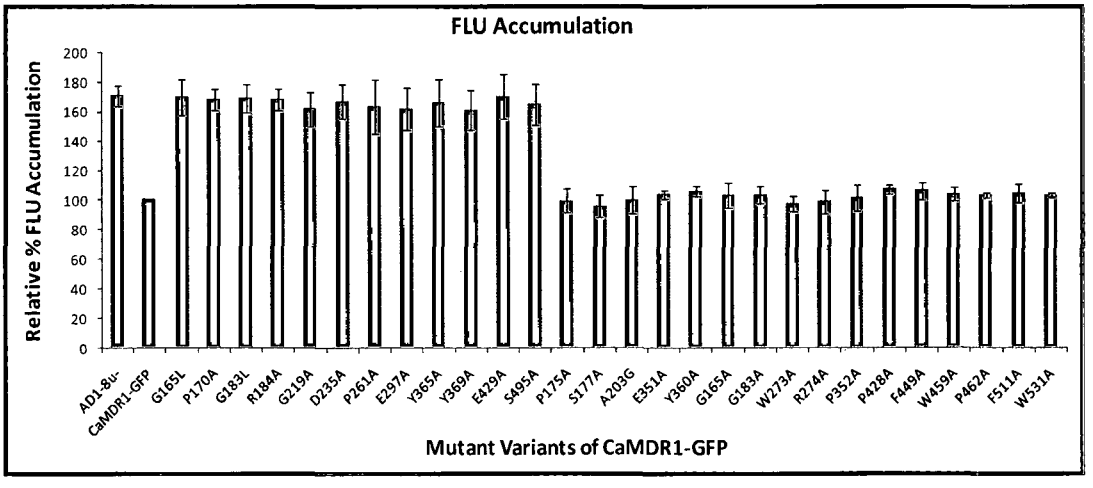

Figure 21: [^{3}H] MTX and [^{3}H] FLU accumulation in wild-type and in different mutant variants of conserved residues.

The graph shows accumulation levels of these substrates relative to RPCaMDR1-GFP. Controls AD1-8u- and CaMdr1p-GFP have also been included for comparison. The results are means $\pm$ standard deviations for three independent experiments.

3.1.2.2 CYSTEINE-SCANNING MUTAGENESIS

3.1.2.2.1 Location of cysteines marked on the secondary structure of CaMdr1p

The multidrug MFS protein CaMdr1p has 5 cysteine residues located in the N-terminal half of the protein. The location of the cysteine residues is marked in the pictorial representation of the protein below (Figure 22).

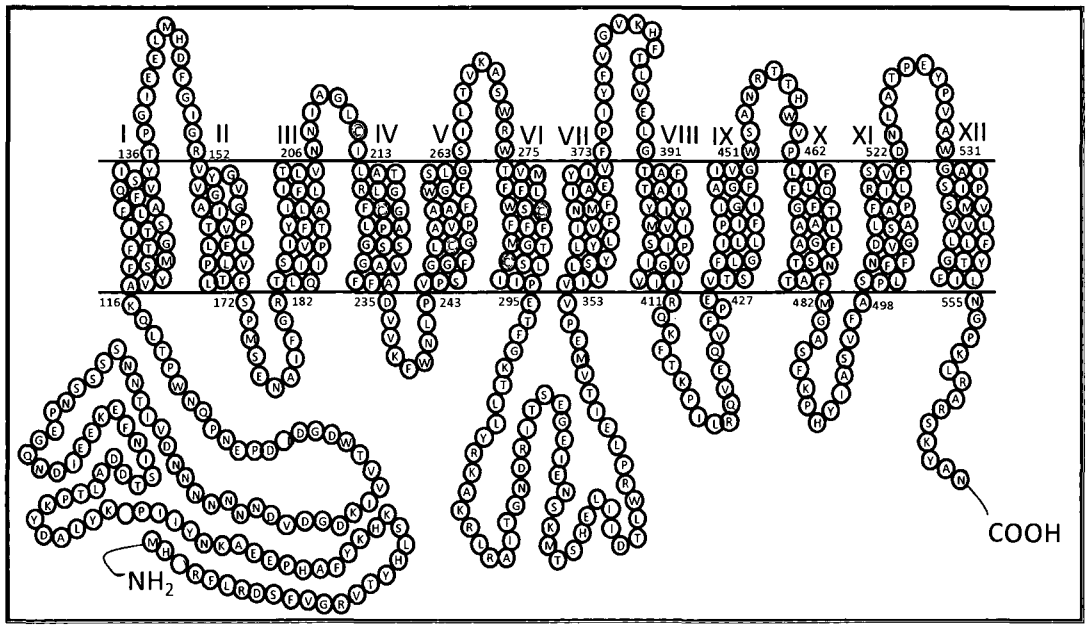

Figure 22: Secondary structure of the CaMdr1p with positions of cysteine residues marked therein.
The figure displays the positions of all the 5 cysteine residues marked in green.

All the 5 cysteines in CaMdr1p were replaced individually with alanines to explore their structural and functional role. Followed by this individual replacement of cysteine with alanine, a cys-less version of RPCaMDR1-GFP was generated (KKCLCaMDR1-GFP) to develop a tool wherein the cysteine-scanning approach could be exploited for further studies. All these mutant variants were stably over-expressed as GFP-tagged variants in a heterologous hyper-expression system developed by Cannon's group by integrating it at *PDR5* locus downstream from the *PDR5* promoter in the *S. cerevisiae* strain AD1-8u⁻. Single copy integration of each transformant at the *PDR5* locus was confirmed by Southern hybridization as described earlier (Figure 23). Two positive clones of each cysteine mutants as well as in case of cysless variant were selected to rule out clonal variations.

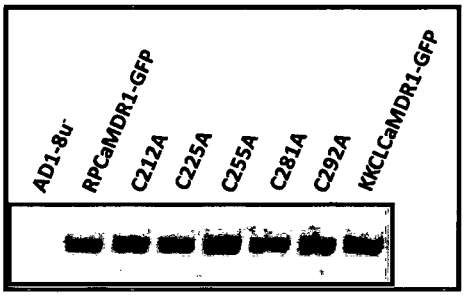

Figure 23: Southern Hybridization showing integration of mutant variants of cysteine residues and cysless variant of CaMdr1p-GFP.
Genomic DNA was extracted from all the cysteine mutant variants as well as from the cysless CaMDR1 (KKCLCaMDR1-GFP) and then digested with Spe I, loaded and separated by electrophoresis. The gel was then transferred to the nylon membrane and the blot was probed with CaMDR1 specific probe. Southern Blot Analysis confirms single-copy integration of the mutant variants of CaMDR1-GFP. The negative (AD1-8u-) and positive (RPCaMDR1-GFP) controls are also shown for comparison.

3.1.2.2.2 Cloning of cysless-CaMDR1-$(His)_{10}$ in the hyper-expression system

A cysless CaMDR1 without the GFP tag was also cloned in the same hyper-expression system. This was done to ensure that GFP, being a huge tag, is not affecting the functioning of the cysless variant of CaMDR1. For detection purposes, deca-histidines were tagged at the C-Terminal end of cysless-CaMdr1p. For this, the cysless CaMdr1p was amplified from KKCLCaMDR1-GFP using the primers mentioned in Materials and Methods. The reverse primer harbored ten histidine residues for tagging at the C-terminal end of cysless-CaMdr1p. This was then cloned at the *SpeI* site in the pSK-PDR5PPUS vector. The resultant construct was sequenced which confirmed the right orientation. It further confirmed that all the 5 cysteines were mutated to alanine and ten histidines were tagged at the C-terminal.

The expression system developed by Cannon's group was exploited wherein cys-less-CaMdr1p-$(HIS)_{10}$ is stably over-expressed from the genomic *PDR5* locus in a *S. cerevisiae* mutant AD1-8u⁻ as described earlier. This strategy for over-expression is shown in Figure 24. Single copy integration of CLCaMDR1-$(His)_{10}$ at the *PDR5* locus was confirmed by Southern hybridization (Figure 25). The resulting strain over-expressing His-tagged cysless-CaMDR1 was designated as KKCLCH10. It was further ensured that the introduction of 10 histidines at C-terminal does not lead to improper surface localization and impaired functional activity.

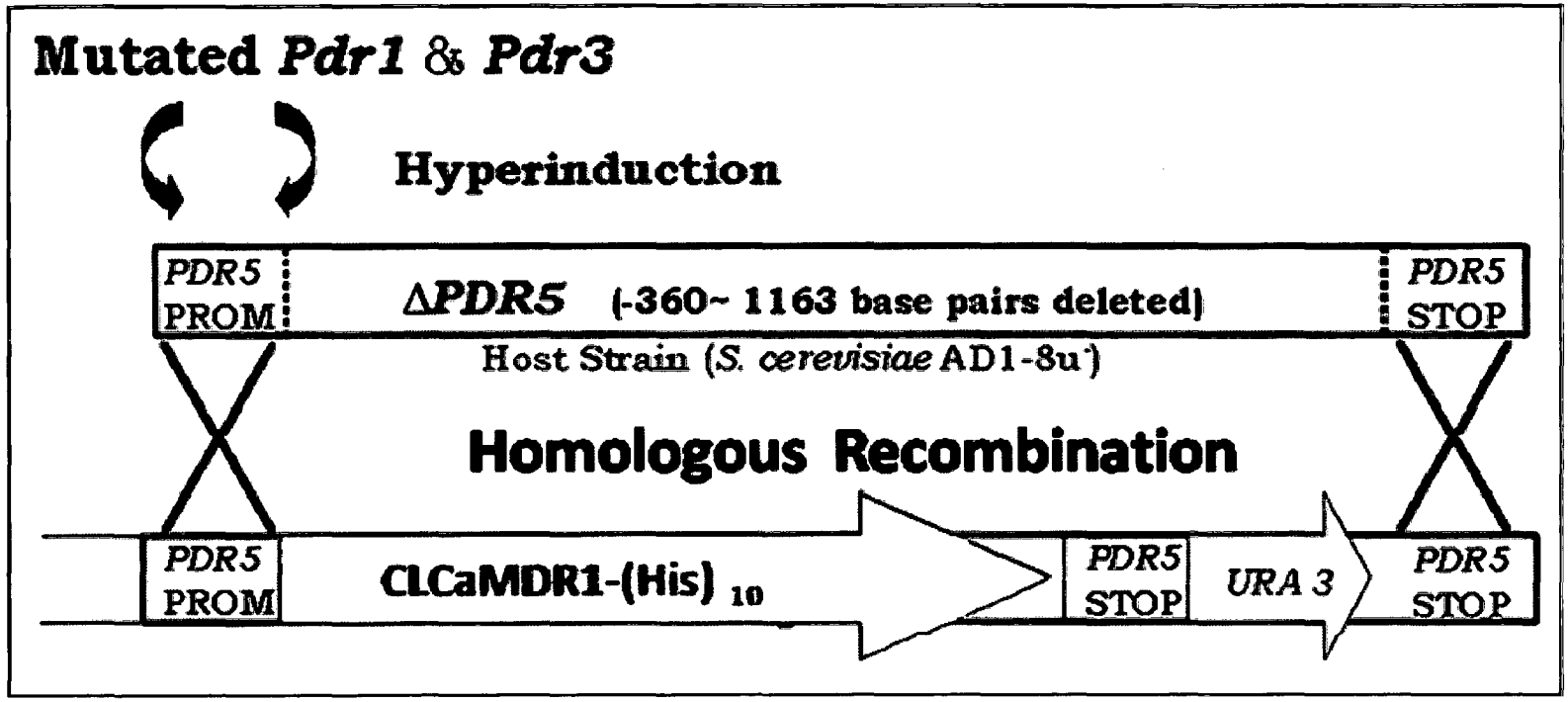

Figure 24: Strategy showing the integration of CLCaMDR1-(His)$_{10}$.
CLCaMDR1-(His)$_{10}$ was integrated at the PDR5 locus in the over-expression strain of *S. cerevisiae* AD1-8u-, derived from a pdr1-3 mutant strain with a gain-of-function mutation in the transcription factor Pdr1p, resulting in constitutive hyperinduction of the PDR5 promoter.

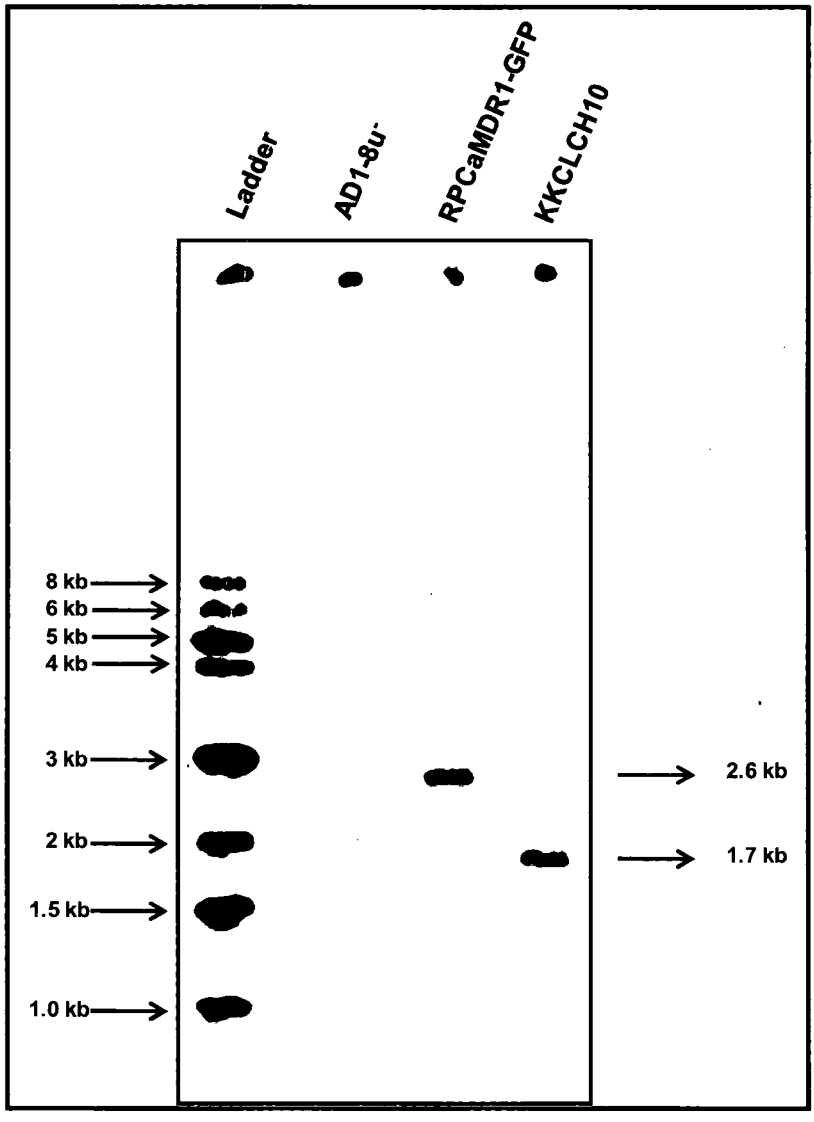

Figure 25: Southern Hybridization confirming integration of CLCaMDR1-$(His)_{10}$. Genomic DNA was extracted from the cysless versions of CaMDR1 (KKCLCH10) and then digested with Spe I, loaded and separated by electrophoresis. The gel was then transferred to the nylon membrane and the blot was probed with CaMDR1 specific probe. Southern Blot Analysis confirms single-copy integration of the mutant variants of CaMDR1-GFP. The negative (AD1-8u-) and positive (RPCaMDR1-GFP) controls are also shown for comparison.

3.1.2.2.3 Drug resistance profile of individual cysteine mutant variants and the cysless constructs

The drug susceptibility for the individual cysteine mutants and the cys-less-CaMdr1p (GFP and His tagged) was checked in the presence of varied drugs (Figure 26). Both the cysless variants KKCLCaMDR1-GFP and KKCLCH10 showed increased susceptibility towards drugs as compared to RPCaMDR1-GFP. It was seen that the GFP tag did not affect the phenotype exhibited by cys-less-CaMdr1p and that both GFP and His-tagged constructs behaved the same. These results of spot assay were corroborated by the results of microdilution assay as shown in Table 8.

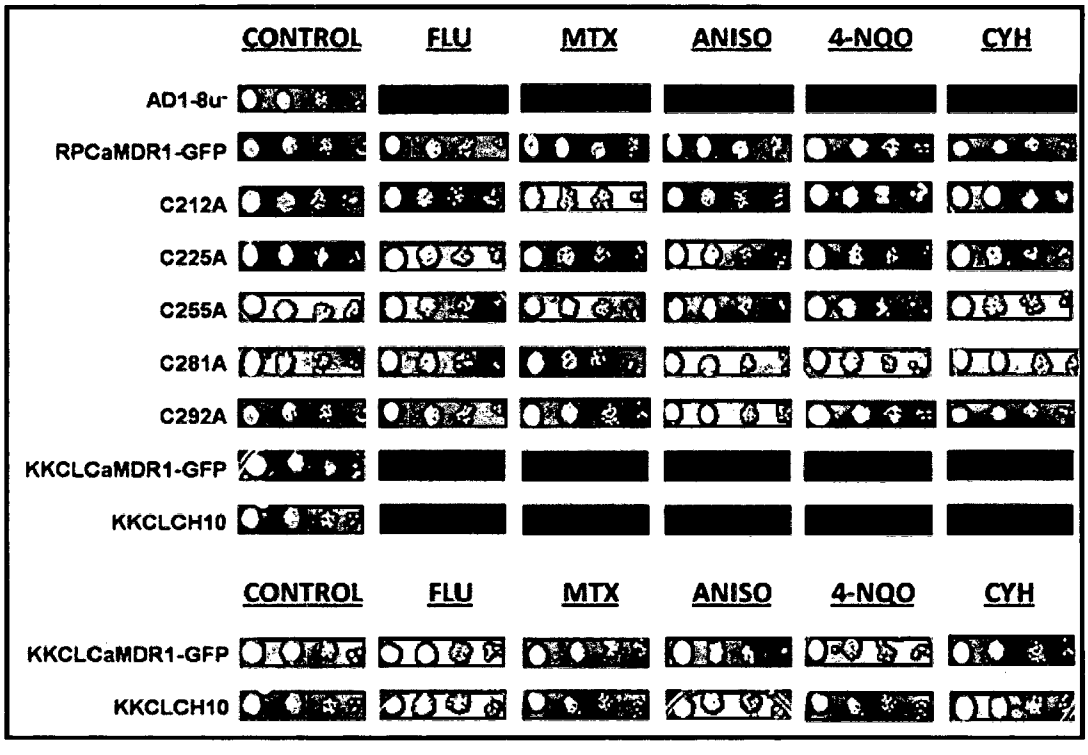

Figure 26: Drug resistance profile of wild-type, cysteine mutant variants and cysless variants of CaMDR1 determined by the spot assay.
Cells were spotted on to YEPD plates in the absence (control) and presence of the various drugs (concentrations mentioned earlier). For the cysless variants a range of concentrations were tried. Cells were spotted on to YEPD plates in the absence (control) and presence of the following drugs- FLC (0.22 μg/ml), MTX (45 μg/ml), ANISO (1 μg/ml), CYH (0.045 μg/ml) and 4-NQO (0.045 μg/ml). The results are shown in the bottom panel of the figure.
Growth differences were recorded following incubation of the plates for 48 hrs at 30°C. Growth was not affected by the presence of the solvents used for the drugs (data not shown).

Strain	MIC $_{80}$(µg/ml)				
	FLU	MTX	ANISO	CYH	4-NQO
AD1-8u$^-$	0.5	16	0.5	0.015	0.03
RPCaMDR1-GFP	16	128	32	0.5	1
C212A	16	128	32	0.5	1
C225A	16	128	32	0.5	1
C255A	16	128	32	0.5	1
C281A	16	128	32	0.5	1
C292A	16	128	32	0.5	1
KKCLCaMDR1-GFP	2	32	8	0.06	0.125
KKCLCH10	2	32	8	0.06	0.125

Table 8: MIC$_{80}$ (µg/ml) values of individual cysteine mutant variants and the cysless variants of CaMdr1p.
Minimum Inhibitory Concentration (MIC$_{80}$ µg/ml) of cysteine mutant variants and cysless CaMdr1p (both GFP and His-tagged) for the different drugs tested. These values were compared to the AD1-8u$^-$ (negative control) and RPCaMDR1-GFP (positive control).

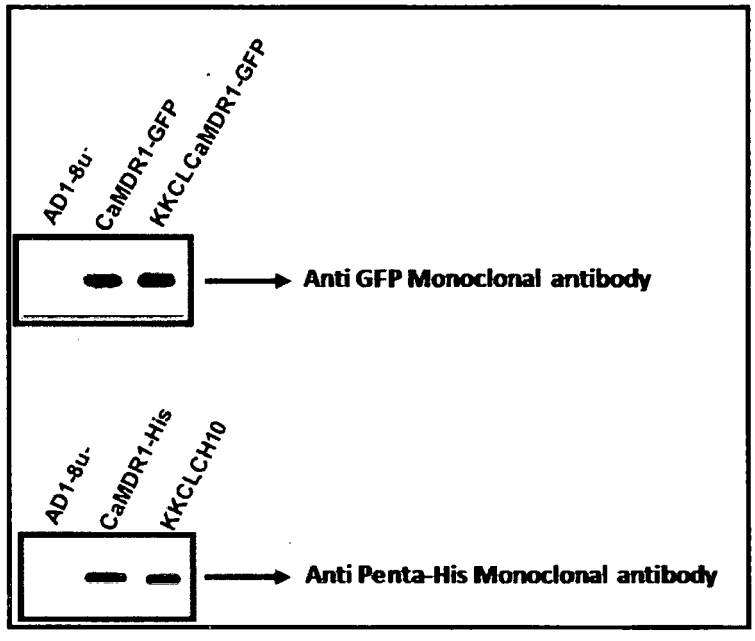

Figure 27: Protein expression profiles of KKCLCaMDR1-GFP and KKCLCH10 in comparison to CaMDR1-GFP and CaMDR1-His in *S. cerevisiae*.
The PM fraction of cysless variants having GFP or His-tag showed expression levels similar to WT-CaMdr1p-GFP and CaMdr1p-His respectively upon immunodetection with anti-GFP and anti-PentaHis antibody, as described in Materials and Methods.

3.1.2.2.4 All cysteine mutants as well as cysless-CaMdr1p showed Cell Surface Expression and localization similar to the wild-type

The cell surface expression was checked for all the cysteine mutant variants as well as the cysless version of CaMdr1p. For cysless-CaMdr1p the expression was checked in the absence and presence of GFP-tag. It was shown that introduction of GFP or His-tag does not affect the expression of CaMdr1p and it remains similar to WT-CaMDR1-GFP (Figure 27). The localization of RPCaMDR1-GFP and the cysteine mutant variants was also comparable. Confocal images showed proper rim localization of GFP-tagged cysteine mutants which was further confirmed by FACS analysis. Also the susceptibility of KKCLCaMDR1-GFP was not attributed to mislocalization as it was comparable to that of WT-CaMDR1-GFP (Figure 28).

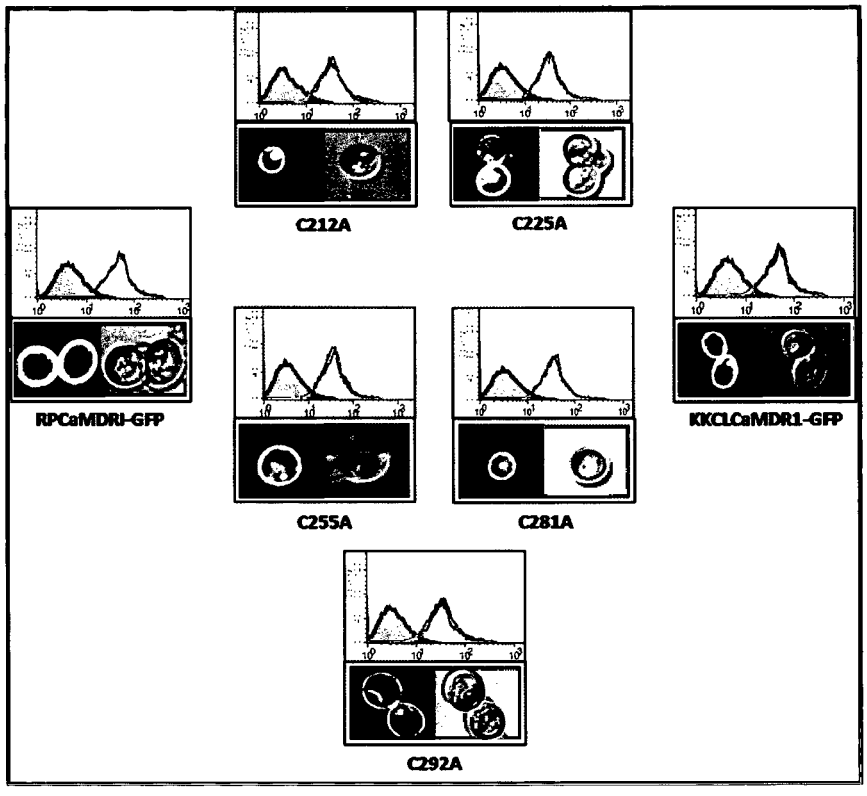

Figure 28: Confocal images and FACS analysis of the all the cysteine mutant variants and KKCLCaMDR1-GFP.
These figures showed localization of these cysteine mutants and the cysless variants similar to that of RPCaMDR1-GFP.

3.1.2.3 CHARACTERIZATION OF UNIQUE N-TERMINAL OF CaMdr1p

Earlier, the identification and molecular characterization of seven mutant alleles of *CaMDR1* (*CaMDR1*-1 to *1*-7) by the complete sequencing revealed several in-frame point mutations leading to a change in amino-acid residues wherein insertion/replacement of an aspartate residue in a serine-asparagine-aspartate rich domain (^{68}SSQSSSSNNTIVDNNNNNNDNDVDGD---DDD^{104}) was most noteworthy [Gupta *et al.*, 1998]. Interestingly, these alleles showed a distinct drug resistance profile. The expression of *CaMDR1,* or of its alleles, in *C. albicans* cells was enhanced by benomyl, methotrexate and several other unrelated drugs, and was more pronounced in at least one of the azole-resistant clinical isolates [Gupta *et al.*, 1998]. The complete sequencing of all the mutant alleles revealed that they were 99% identical to *CaMDR1* (BENr, benomyl resistance) cloned earlier [Fling *et al.*, 1991]. However, there were many in-frame point mutations scattered over the entire sequence of all the alleles (Figure 29).

A closer analysis of a Multiple Sequence alignment of MFS trasporters reveals that N-terminal part of fungal sequences is much longer as compared to MFS tranporters of other organisms. Furthermore, CaMdr1p, a MFS antiporter has a unique N-terminal which is about 90 residues long and harbors a ^{68}SSQSSSSNNTIVDNNNNNNDNDVDGD---DDD^{104} stretch (Figure 30). This stretch has repetitive ser-asn-asp residues and is unique to CaMdr1p since other fungal MFS members including its close homologues such as CdMdr1p of *C. dubliniensis*, Cyhrp of *C. maltosa* and Flr1p of *S. cerevisiae* which are 93, 57 and 46% identical to CaMdr1p, respectively, do not have this motif. Interestingly, the unique ^{68}SSQSSSSNNTIVDNNNNNNDNDVDGD---DDD^{104} stretch was observed in all the alleles and there were polymorphisms seen in this stretch [Gupta *et al.*, 1998]. The curiosity of such a unique arrangement led us to elucidate the importance of this unusually long N-terminal of CaMdr1p and decipher its role in the functioning of this protein. The site-directed mutational analysis of the unique ^{68}SSQSSSSNNTIVDNNNNNNDNDVDGD---DDD^{104} stretch was carried out. All the Serine, Asparagines and Aspartate residues of this unique stretch in the N-terminal of CaMdr1p were mutated to alanines. These mutant variants were then stably over-expressed as GFP-tagged variants in a heterologous hyper-expression system as

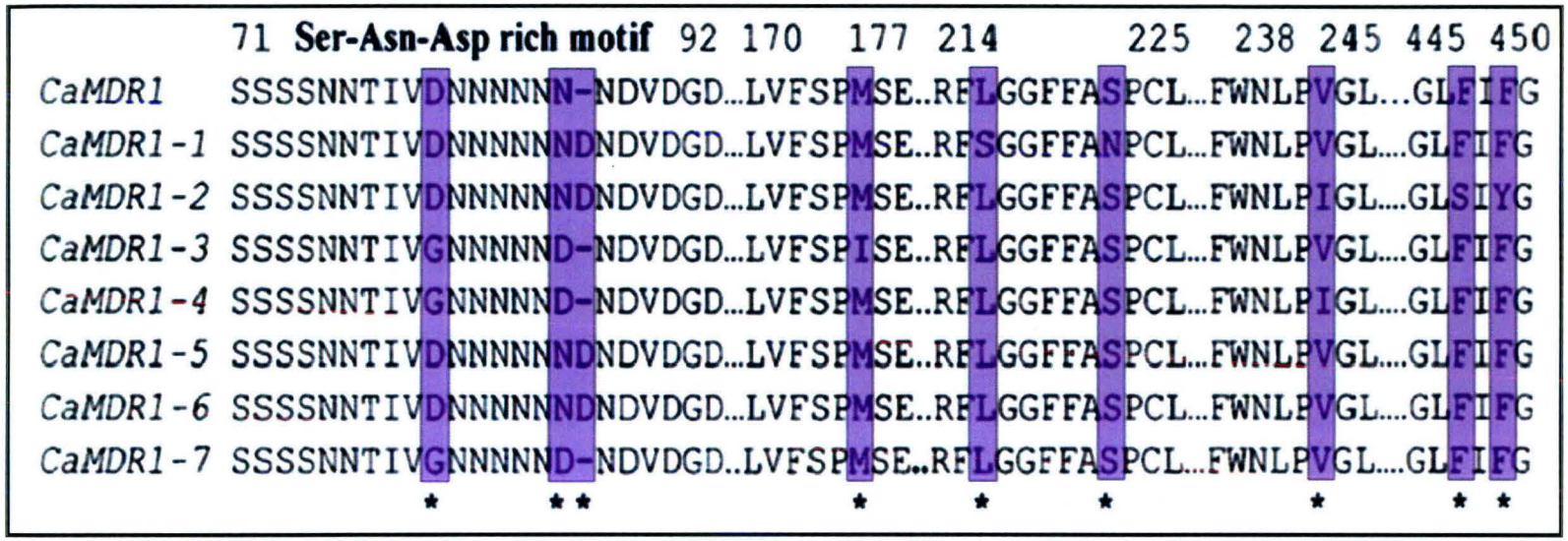

Figure 29: Multiple sequence alignment of different CaMDR1 polymorphic alleles.
The amino-acid variation is depicted by *. The alignment columns are highlighted by purple boxes.

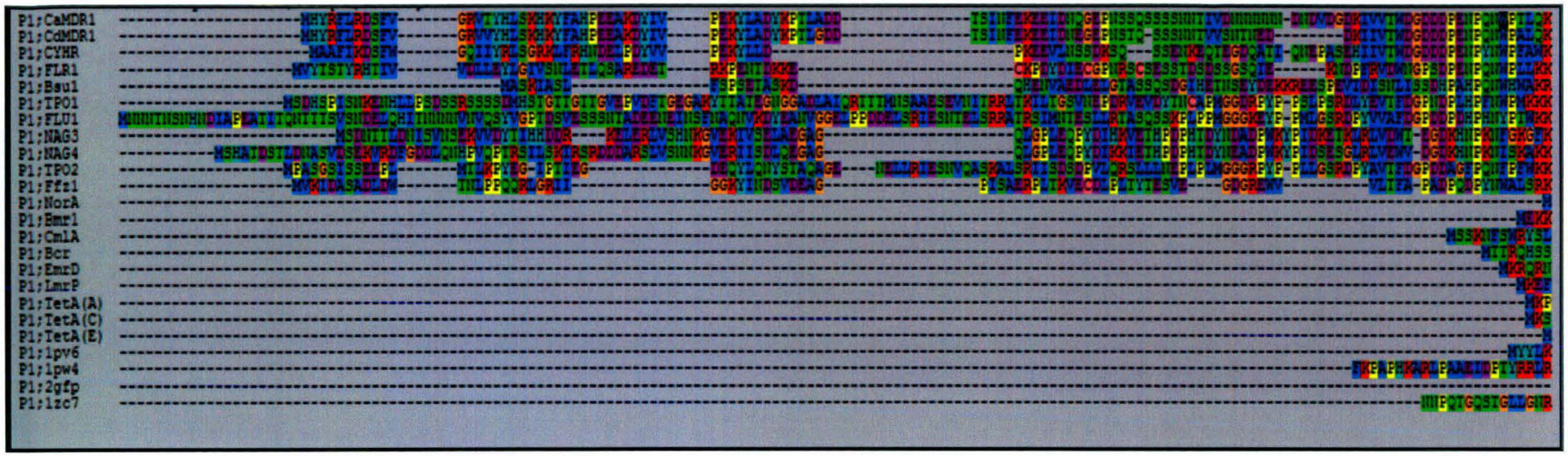

Figure 30: N-terminal portion of a Multiple Sequence Alignment of MFS sequences.
The sample portion shows the N-terminal region of various MFS sequences. The fungal sequences have a longer N-terminal as compared to MFS transporters in other organisms. Moreover CaMdr1p has a unique ser-asn-asp stretch which is not present in any other MFS transporter.

described earlier. Single copy integration of each transformant at the *PDR5* locus was confirmed by Southern hybridization (Figure 31). Two positive clones of each mutant were selected to rule out clonal variations.

3.1.2.3.1 Drug resistance profile of individual mutant variants of Serine, Asparagine and Aspartate residues in the (^{68}SSQSSSSNNTIVDNNNNNNDNDVDGD---DDD^{104}) stretch

This study shows that any of the individual replacements of these repetitive residues with alanine in the unique ^{68}SSQSSSSNNTIVDNNNNNNDNDVDGD---DDD^{104} stretch do not have a remarkable effect on the functioning of the protein. The drug susceptibility towards the entire spectrum of substrates for majority of these mutant variants remained unchanged and exhibits a phenotype like the wild-type. D104A was the only mutant variant where the drug susceptibility was affected. This was seen by both spot (Figure 32) and Microtitre plate assay (Table 9).

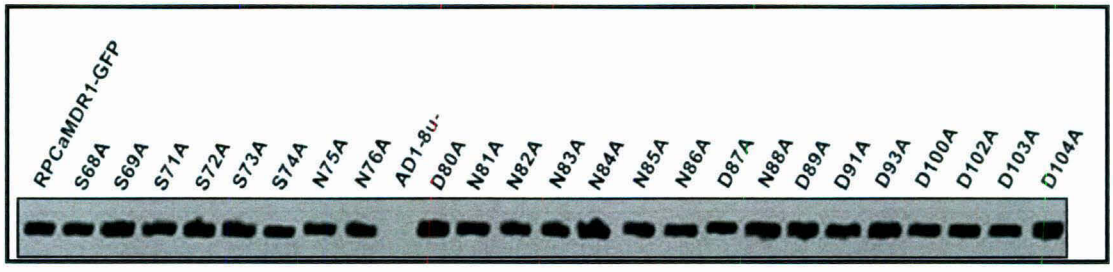

Figure 31: Southern Blot Hybridization confirming integrated mutant variants of Serine, Asparagine and Aspartate residues of unique stretch of CaMdr1p.
Genomic DNA was extracted from all the mutant variants and then digested with Spe I, loaded and separated by electrophoresis. The gel was then transferred to the nylon membrane and the blot was probed with CaMDR1 specific probe. Southern Blot Analysis confirms single-copy integration of the mutant variants of CaMDR1-GFP. The negative (AD1-8u-) and positive (RPCaMDR1-GFP) controls are also shown for comparison.

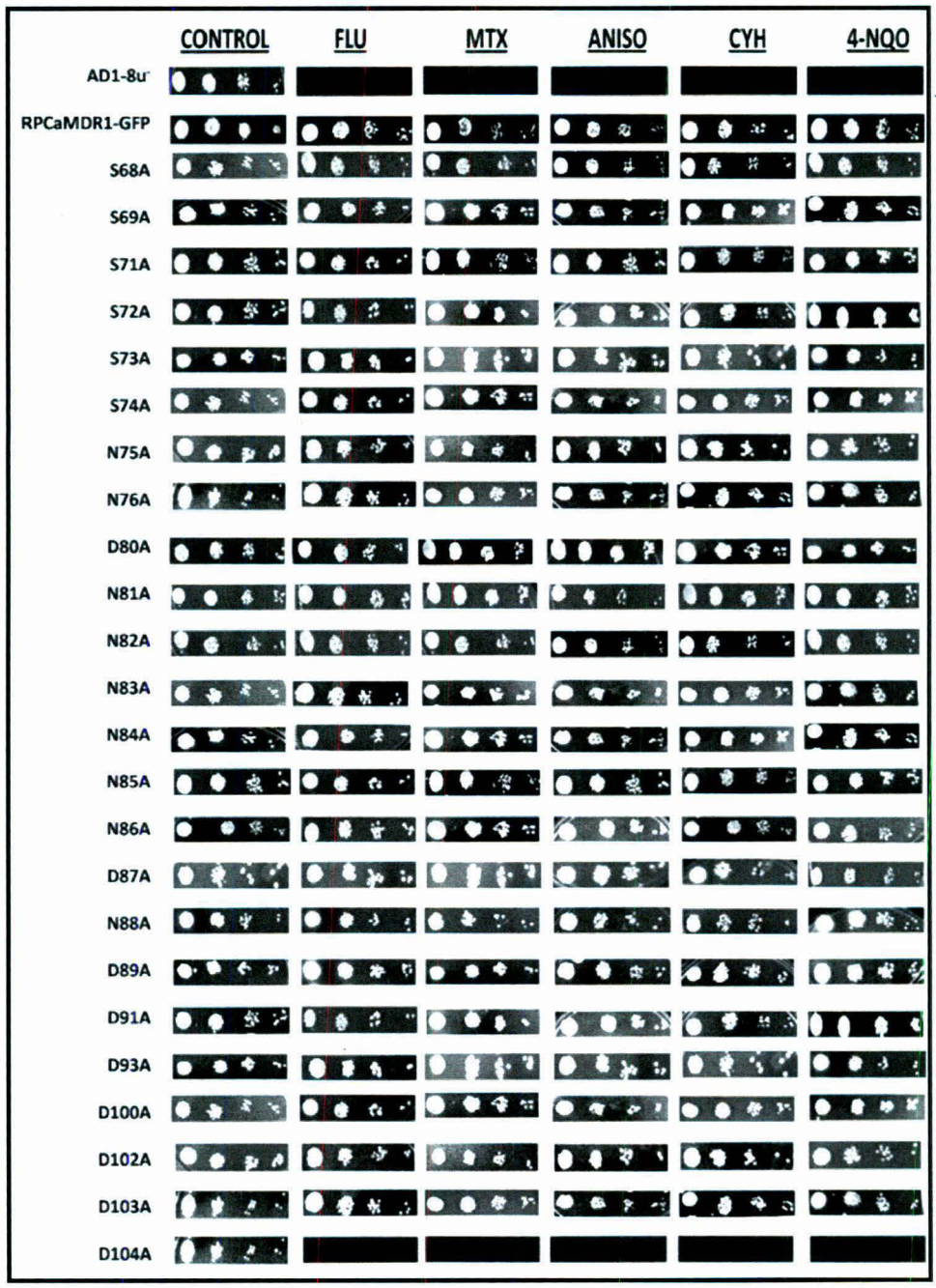

Figure 32: Drug resistance profile of wild-type CaMDR1-GFP and mutant variants of Serine, Asparagine and Aspartate residues in unique stretch of CaMdr1p as determined by the spot assay.

Cells were spotted on to YEPD plates in the absence (control) and presence of the following drugs- FLC (0.6 µg/ml), MTX (65 µg/ml), ANISO (3 µg/ml), CYH (0.2 µg/ml) and 4-NQO (0.2 µg/ml). The growth differences are compared against AD1-8u⁻ (negative control) and RPCaMDR1-GFP (positive control). Growth differences were recorded following incubation of the plates for 48 hrs at 30°C. Growth was not affected by the presence of the solvents used for the drugs (data not shown).

Strain	MIC $_{80}$(µg/ml)				
	FLU	MTX	ANISO	CYH	4-NQO
AD1-8u$^-$	0.5	16	0.5	0.015	0.03
RPCaMDR1-GFP	16	128	32	0.5	1
S68A	16	128	32	0.5	1
S69A	16	128	32	0.5	1
S71A	16	128	32	0.5	1
S72A	16	128	32	0.5	1
S73A	16	128	32	0.5	1
S74A	16	128	32	0.5	1
N75A	16	128	32	0.5	1
N76A	16	128	32	0.5	1
D80A	16	128	32	0.5	1
N81A	16	128	32	0.5	1
N82A	16	128	32	0.5	1
N83A	16	128	32	0.5	1
N84A	16	128	32	0.5	1
N85A	16	128	32	0.5	1
N86A	16	128	32	0.5	1
D87A	16	128	32	0.5	1
N88A	16	128	32	0.5	1
D89A	16	128	32	0.5	1
D91A	16	128	32	0.5	1
D93A	16	128	32	0.5	1
D100A	64	128	32	0.5	1
D102A	16	128	32	0.5	4
D103A	16	128	32	0.5	1
D104A	0.5	16	0.5	0.015	0.03

Table 9: MIC_{80} (µg/ml) values of the mutant variants of the Serine, Asparagine and Aspartate residues in the unique stretch of CaMdr1p.

Minimum Inhibitory Concentration (MIC_{80} µg/ml) of mutant variants of unique stretch for the different drugs tested. These values were compared to the AD1-8u- (negative control) and RPCaMDR1-GFP (positive control).

3.1.2.3.2 Expression and localization of CaMdr1p-GFP in the mutant variants remains unaffected

The cell surface expression of these mutant variants was checked by Western Blot analysis which revealed that none of these replacements affected the cell surface expression of the mutant version of CaMdr1p-GFP. Similar levels of expression of CaMdr1p-GFP were observed in the wild-type and all the mutant variants (Figure 33). Confocal images further showed proper localization of GFP-tagged CaMdr1p mutant variant protein as a rimmed appearance at the plasma membrane. These results were also corroborated by FACS analysis (Figure 34).

3.1.2.3.3 Accumulation assay of [^{3}H] MTX and [^{3}H] FLU exhibits that the activity of mutant variants is similar to wild-type

All these mutant variants were assessed for their activity by measuring the intracellular accumulation of [^{3}H] MTX and [^{3}H] FLU. Except D104A which showed complete abrogation of function and exhibited a relative increase of 70-90% in accumulation of both [^{3}H] MTX and [^{3}H] FLU (decrease efflux) all the other mutant variants showed drug efflux comparable to RPCaMDR1-GFP (Figure 35).

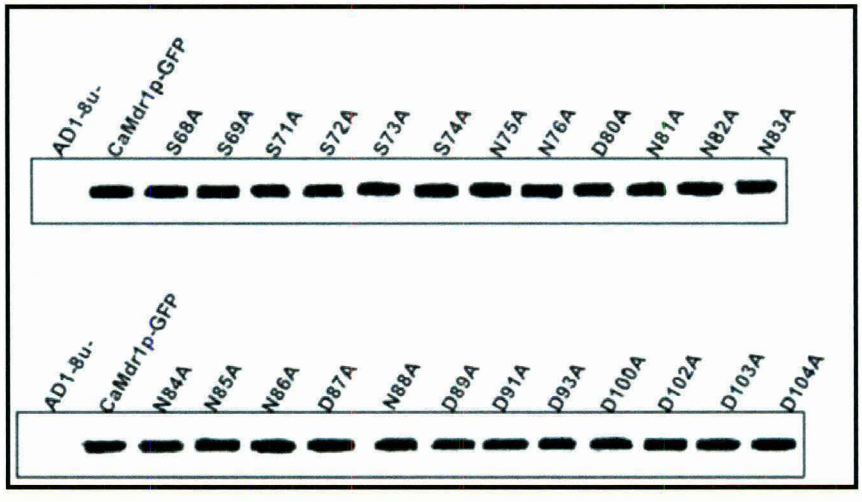

Figure 33: Protein expression profiles of CaMdr1p-GFP and its mutant variants of Serine, Asparagine and Aspartate residues of unique stretch in *S. cerevisiae*.
The PM fraction of mutant variants showed expression levels similar to WT-CaMdr1p-GFP on Western Blot analysis with anti-GFP antibody.

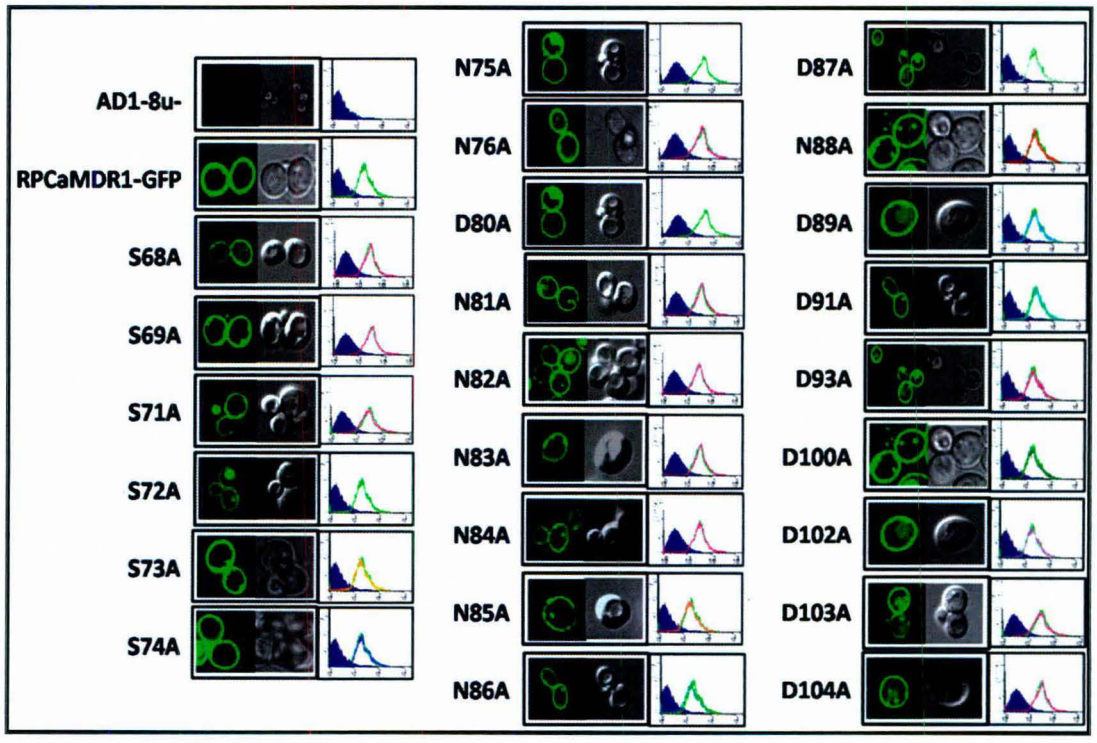

Figure 34: Surface localization of CaMdr1p-GFP and its mutant variants of residues in unique stretch of its N-terminal.

Confocal images and FACS analysis of the all the mutant variants to check their localization in comparison to AD1-8u- (negative control) and RPCaMDR1-GFP (positive control).

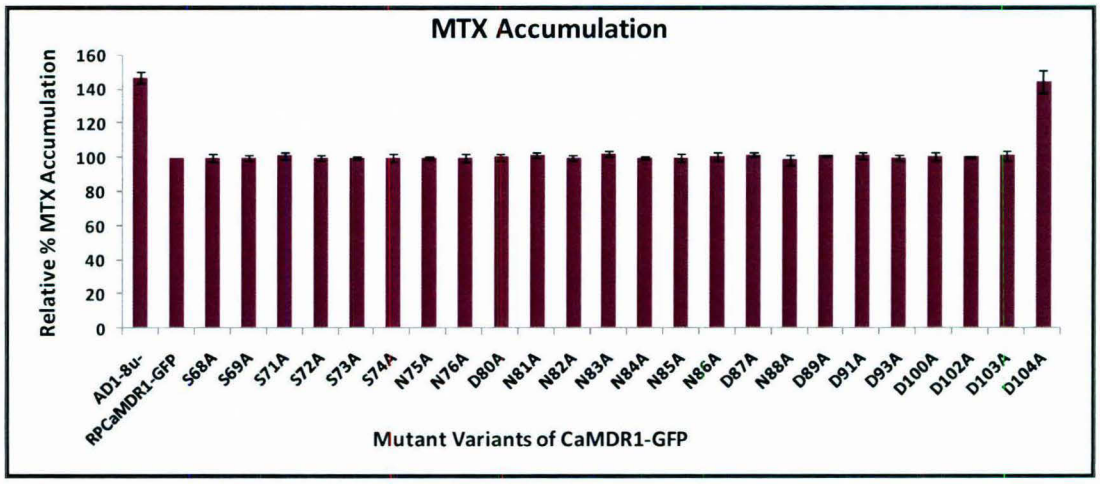

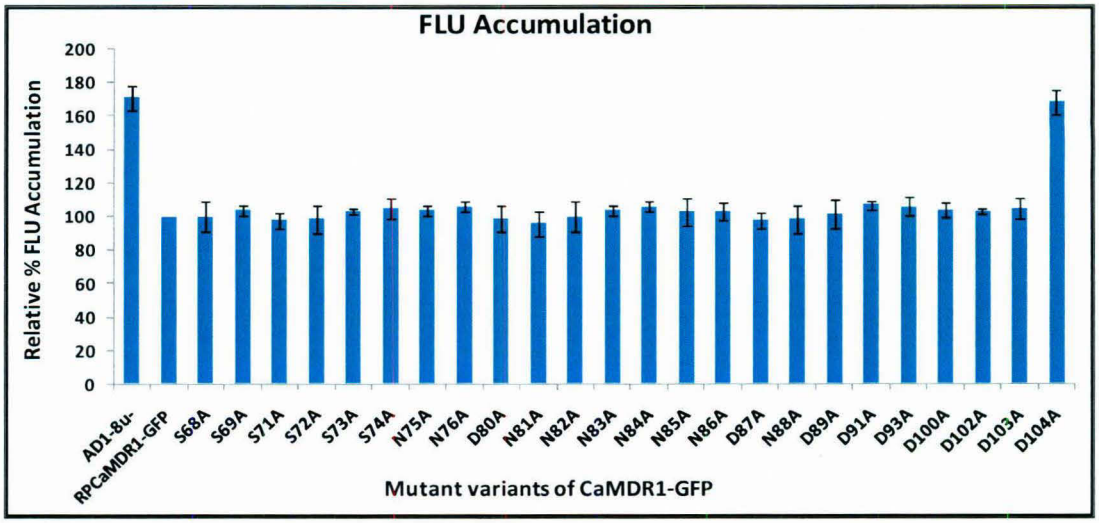

Figure 35: [^{3}H] MTX and [^{3}H] FLU accumulation in the different mutant variants of residues in N-terminal of CaMdr1p-GFP in *S.cerevisiae*.

The graph shows accumulation levels of the [3H] MTX and [3H] FLU (Red and Blue bars respectively) in the mutant variants. Controls AD1-8u- and RPCaMDR1-GFP have also been included for comparison. The results are means + standard deviations for three independent experiments.

3.1.2.3.4 Deletion Mutants of the unusually long N-terminal of CaMdr1p

As the replacement in the ^{68}SSQSSSSNNTIVDNNNNNNDNDVDGD---DDD^{104} stretch with alanines did not reveal any noteworthy phenotype, the deletion mutants were created. The entire 90 amino acid long N-terminal which also harbors ^{68}SSQSSSSNNTIVDNNNNNNDNDVDGD---DDD^{104} stretch was deleted as a whole as well as in parts. The deletion mutants were named according to the stretch of amino acids deleted from the CaMdr1p sequence. Del 90 had the initial 90 amino acids deleted from the N-terminal while Del 7-30, Del 31-60 and Del 61-111 had deletions from 7^{th}-30^{th}, 31^{st}-60^{th} and 61^{st}-111^{th} amino acid respectively (Figure 36). All CaMdr1p deletion mutant variants were stably over-expressed as GFP-tagged variants in a heterologous hyper-expression system as described earlier. Single copy integration of each transformant at the *PDR5* locus was confirmed by Southern hybridization. Two positive clones of each mutant were selected to rule out clonal variations (data not shown).

3.1.2.3.5 Drug resistance profile of the N-terminal deletion mutants

These *S. cerevisisae* cells over-expressing GFP-tagged deletion mutants of the N-terminal were then checked for their drug susceptibility against a spectrum of drugs. Their growth profile was compared to wild-type RPCaMDR1-GFP. It was seen that Del 90 and Del 7-30 were sensitive to all the drugs. Del 31-60 exhibited sensitivity towards FLU and MTX and had no phenotype against other drugs. Contrastingly, Del 61-111 behaved similar to the wild-type (Figure 37). Similar results were seen by microdilution assays (Table 10).

3.1.2.3.6 Reduced expression of CaMdr1p-GFP in the deletion mutants due to mislocalization as checked by Western Blot Analysis

It was further checked if the drug sensitivity of these deletion mutants could be attributed to surface localization and expression of the GFP-tagged truncated protein. Western Blot analysis with anti-CaMdr1 antibody reveals that these over-expressing deletion mutants of CaMdr1p-GFP had lower levels of surface expression as compared to the wild-type (Figure 38).

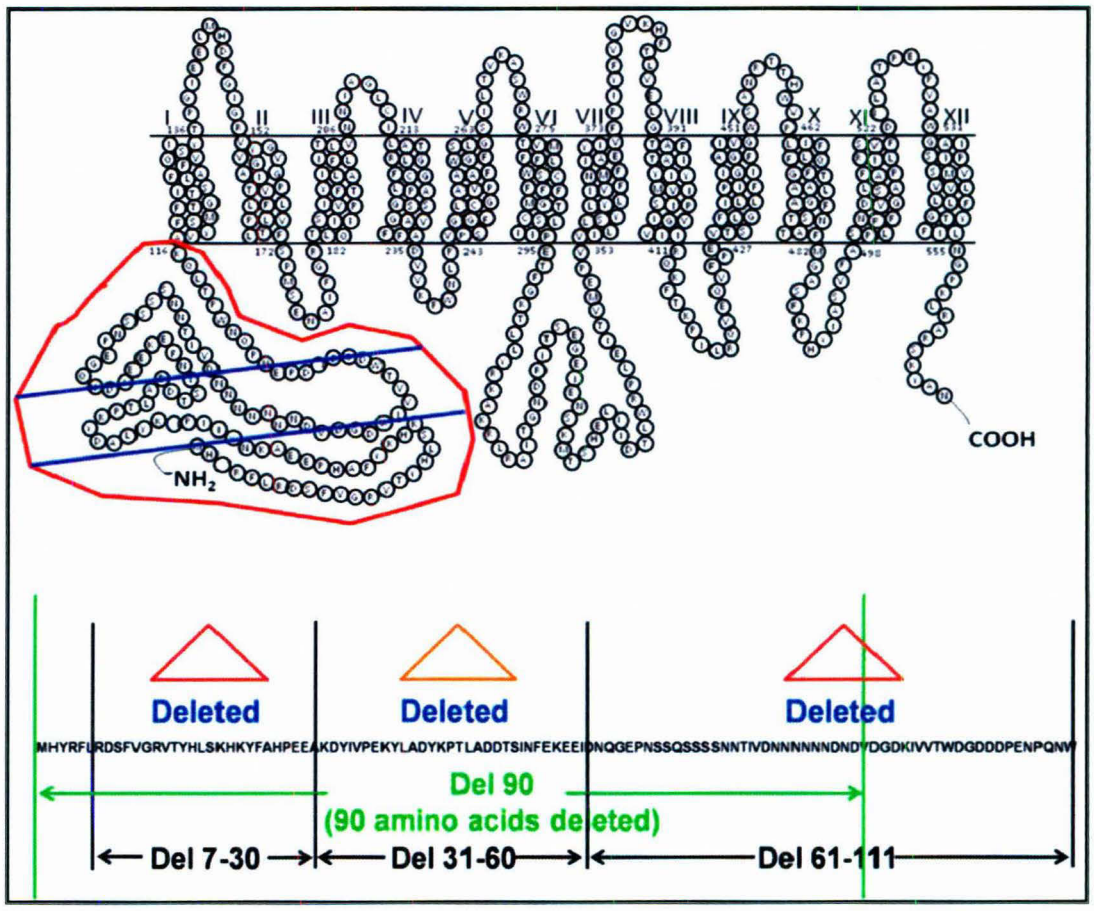

Figure 36: The secondary structure of CaMdr1p highlights the N-terminal region where the deletion constructs are made.
A blow up of the highlighted region shows the demarcations for each of these deletion constructs.

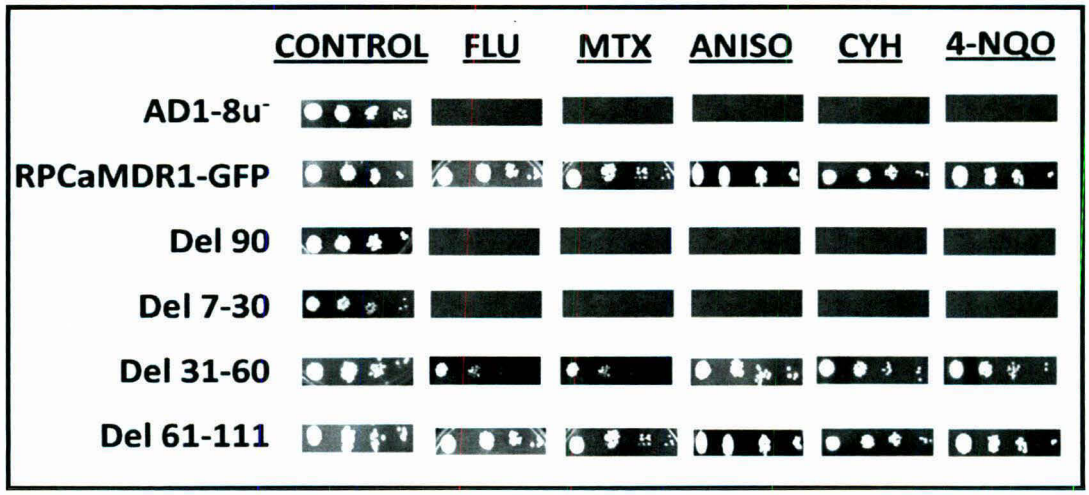

Figure 37: Drug resistance profile of CaMdr1p deletion mutant variants of the N-terminal compared to RPCaMDR1-GFP (positive control) and AD1-8u⁻ (negative control).

Cells were spotted on to YEPD plates in the absence (control) and presence of the following drugs- FLC (0.6 µg/ml), MTX (65 µg/ml), ANISO (3 µg/ml), CYH (0.2 µg/ml) and 4-NQO (0.2 µg/ml). Growth differences were recorded following incubation of the plates for 48 hrs at 30 °C. Growth was not affected by the presence of the solvents used for the drugs (data not shown).

Strain	MIC $_{80}$(µg/ml)				
	FLU	MTX	ANISO	CYH	4-NQO
AD1-8u⁻	0.5	16	0.5	0.015	0.03
RPCaMDR1-GFP	16	128	32	0.5	1
Del 90	0.5	16	0.5	0.015	0.03
Del 7-30	0.5	16	0.5	0.015	0.03
Del 31-60	4	32	16	0.125	0.25
Del 61-111	16	128	32	0.5	1

Table 10: MIC_{80} (µg/ml) values of the deletion mutants with truncations in the N-terminal of CaMdr1p.

Minimum Inhibitory Concentration (MIC_{80} µg/ml) of deletion mutant variants of the N-terminal of CaMdr1p for the different drugs tested. These values were compared to the AD1-8u- (negative control) and RPCaMDR1-GFP (positive control).

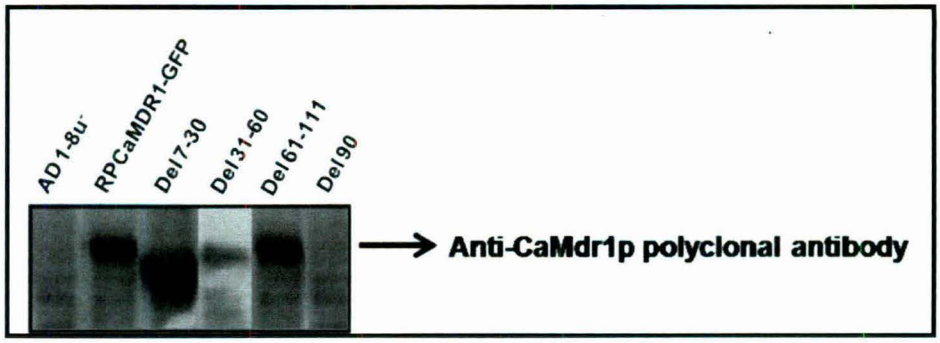

Figure 38: Protein expression profiles of the wild-type compared to the deletion mutant variants of N-terminal of CaMdr1p-GFP.
The PM fraction of the deletion mutants of the N-terminal of CaMdr1p-GFP showed reduced expression levels in comparison to RPCaMDR1-GFP. Immunodetection was done using anti-CaMdr1p polyclonal antibody, as described in Materials and Methods.

3.1.2.3.7 The deletion mutants of N-terminal of CaMdr1p-GFP show poor surface localization

The surface localization of these N-terminal deletion mutants was checked by FACS and Confocal imaging. Confocal images show that these deletion mutants were not properly surface localized as compared to RPCaMDR1-GFP (wild-type). It was seen that Del 90 failed completely in localizing to the PM while Del 7-30 is severely trapped at various stages in different organelles inside the cell. Del 31-60 was seen to have a beaded and punctuated appearance though it still exhibited resistance towards few drugs. On the contrary Del 61-111 was observed to be properly localized on the plasma membrane and behaved like the wild-type (Figure 39). FACS analysis of the live cells showed lower fluorescense intensity in Del 90, Del 7-30 and Del 31-60. The fluorescense intensity of Del 61-111 was comparable to wild-type RPCaMDR1-GFP (Figure 40). Taken together, these results suggest that there was almost no expression of mutant CaMdr1p-GFP in Del 90 while there was minimal expression in Del 7-30 and in both these cases there was a complete drug sensitivity and loss in activity. There was a marginal expression in case of Del 31-60 which was sufficient to confer drug resistance towards selective drugs as seen in the susceptibility assays. Del 61-111 behaved like the wild-type in all respects. Thus, it would be fair to mention that the signals for localization lie in the N-terminal of CaMdr1p. The localization signals might mainly reside in the first half of the deletion stretch. Also, the second half though is not essentially required for localization but definitely required for imparting an environment for proper localization, expression and activity of CaMdr1p. The third half might be dispensable for the protein.

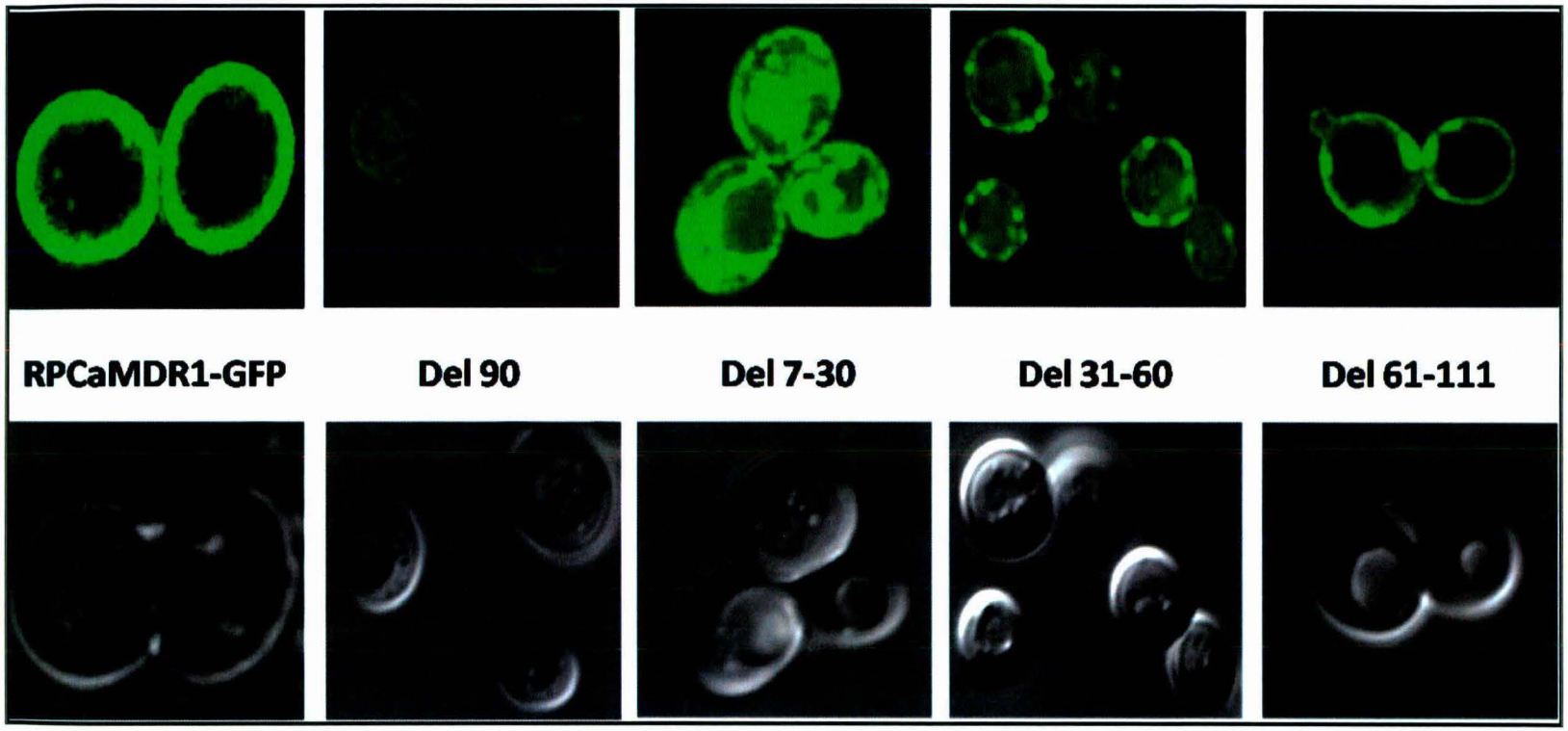

Figure 39: Confocal images of the deletion constructs of the N-terminal of CaMdr1p.
Del 90, Del 7-30 and Del 31-60 shows mislocalization as compared to RPCaMDR1-GFP while Del 61-111 shows a proper surface localization.

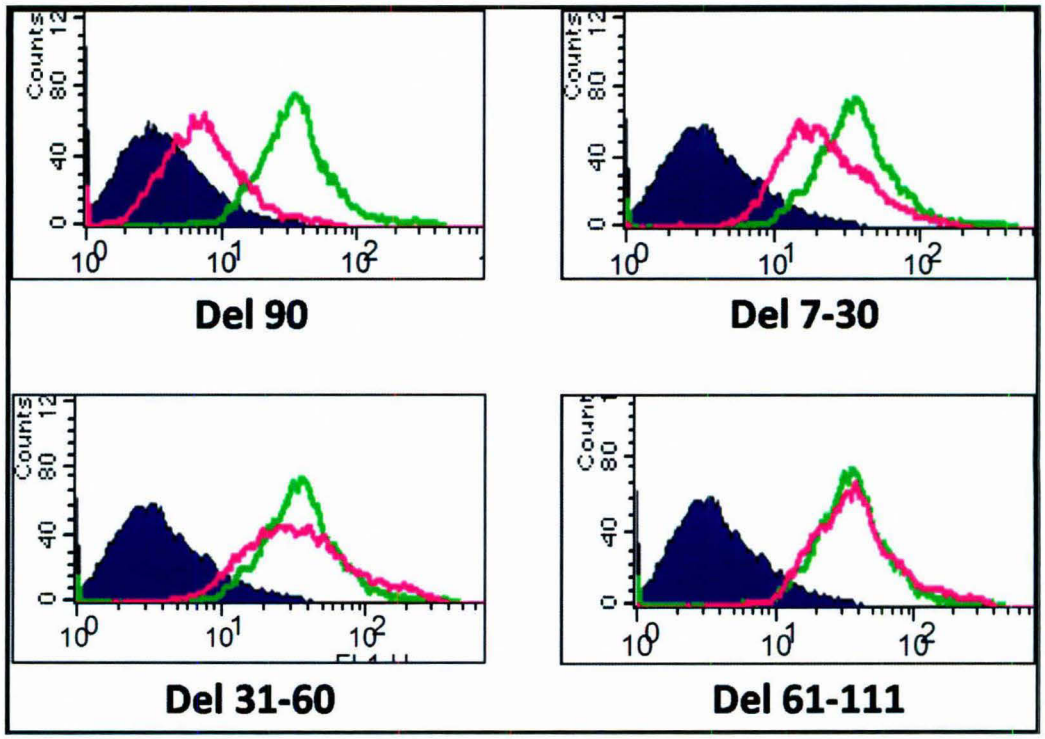

Figure 40: Comparison of Flow cytometry analysis of cells expressing CaMdr1p-GFP and its deleted versions.

FACS analysis reveals lower fluorescence intensity in the deletion mutants (pink lines) when compared to the wild-type (green line). In case of Del 90 the fluorescence intensity is as low as that of the unstained (negative control) (blue area).

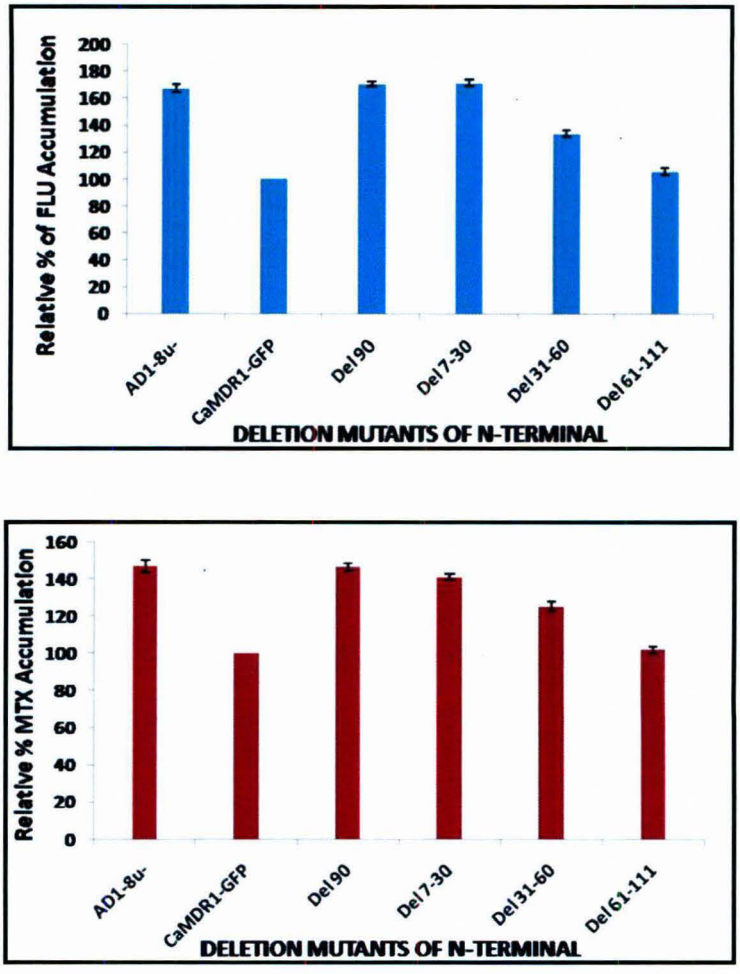

Figure 41: [^{3}H] MTX and [^{3}H] FLU accumulation in the deletion mutant variants of CaMDR1-GFP.

The graph shows an increased accumulation of the radiolabeled substrates which can be attributed to loss of efflux activity in of these deletion mutants. Del 61-111 has activity similar to the wild-type. The results are mean $\pm$ standard deviations for three independent experiments.

3.1.2.3.8 Accumulation assay of [^{3}H] MTX and [^{3}H] FLU shows aborted activity of CaMdr1p-GFP in these deletion mutants

All the deletion mutant variants were further analyzed for their functionality by measuring the intracellular accumulation of [^{3}H] MTX and [^{3}H] FLU. All the deletion mutants except Del 61-111 show higher levels of accumulation of the radiolabeled substrates which points to their reduced efflux by these deleted variants. Thus the efflux activity was completely aborted in all these deletion mutants. Taken together, it can be said that the increased susceptibility towards different drugs and the loss in efflux activity observed in the case of Del 90, Del 7-30 and Del 31-60 can be attributed to poor surface localization and reduced expression of truncated CaMdr1p-GFP. Del 61-111, on the other hand, continues to efflux the substrates like the wild-type and thus has no effect on the activity of the deleted protein (Figure 41).

3.1.3 DISCUSSION

The critical residues of CaMdr1p were identified based on their conservation in a multiple sequence alignment. These conserved residues of GFP tagged CaMdr1p were subjected to alanine scanning and the effect was analyzed on the basis of the functionality of this drug-proton antiporter. On the basis of these observations, the mutant variants were bunched into 3 classes: - Mutants belonging to Class I; G165L, G183L, R184A, G219A, D235A, P261A, E297A, Y365A, Y369A, E429A and S495A which showed complete loss in drug resistance and also showed increased relative % accumulation of [^{3}H] MTX and [^{3}H] FLU. The second class of mutant variants which included P175A, S177A, E351A, Y360A, P512A and L513A showed selective resistance but showed decreased accumulation of [^{3}H] MTX and [^{3}H] FLU. As deciphered from the drug susceptibility assays, the third category of mutant variants G165A, G183A, W273A, R274A, P352A, P428A, F449A, P462A, and F511A showed accumulation of [^{3}H] MTX and [^{3}H] FLU comparable to that of RPCaMDR1-GFP. Figure 3 summarizes the sensitivity profiles of the mutant variants with different drugs. The observed decrease in drug resistance was not due to poor expression or localization of these mutant variants. This possibility was ruled out by subjecting each mutant variant to confocal and FACS analyses. It was revealed that all

the mutant variants showed proper localization of fluorescence in confocal microscopy which was also validated by FACS data.

The previous studies could demonstrate that although FLU and MTX are extruded by this transporter but are unable to compete with each other. This implied that these two drug substrates share different binding sites [Pasrija *et al.*, 2007]. Thus the mutant variants of conserved residues which showed sensitivity to the tested drugs i.e Class I might be involved in forming a binding pocket for all these drugs tested while the residues belonging to Class II might be responsible for binding only to CYH and 4-NQO. This suggested the presence of overlapping binding sites. The residues which are predicted to be critical might be involved in a range of functions of this protein. These can be either family-wide specific functions or transporter specific functions. For example, the residues forming the helix might be responsible for at least one or more of the following functions: - a) proper surface localization of the protein on the membrane contributed majorly by hydrophobic residues which might have similar function in other MFS proteins as well b) specificity for binding of substrates c) proton translocation.

This study shows that individual replacement of each of the 5 cysteines in CaMdr1p did not affect the functioning of the protein. A cys-less CaMdr1p was also constructed which provides an ideal platform to conduct cross-linking experiments. In view of the limited availability of information about the structure and function of CaMdr1p, it was difficult to decide a rationale for conducting cross-linking experiments with this cysless-CaMdr1p.

The Multiple Sequence Alignment revealed that CaMdr1p habors a unique ^{68}SSQSSSSNNTIVDNNNNNNDNDVDGD---DDD^{104} stretch in its N-terminal which had repetitive Serine, Asparagine and Aspartate residues. As this arrangement was not observed in any other fungal MFS transporter, an alanine scanning of this stretch was done so as to reveal the structural and functional information. Surprisingly, all these mutant variants behaved like the wild-type. However, further analysis by making deletion mutants of the complete N-terminal of CaMdr1p revealed that this stretch may be important in trafficking of CaMdr1p to plasma membrane. These deletion mutants had defects in trafficking and this leads us to elucidate the role of the unusually long N-terminal of CaMdr1p.

All these random mutational strategies which either followed the criteria of conservation of a residue, or cysteine mutagenesis or the unique occurrence of repetitive stretches, though put some light on the critical residues of CaMdr1p but were not really efficient. Designing of a cys-less-CaMdr1p gave an efficient tool for further analysis of the protein but in the absence of literature available on fungal MFS transporters, it seems to be a far-sighted goal. Similarly, the repetitive stretches in the N-terminal of CaMdr1p though seemed to be unique and exciting, did not lead us anywhere. Deletion mutants of the complete N-terminal give us only a rough idea of the existing targeting signals and these needs to be rigorously studied.

Site-directed mutational strategies rely on conservation of residues in a Multiple Sequence Alignment (MSA). The conservation of a residue is calculated from the amino acid frequency distribution in the corresponding column of a MSA. However, the physicochemical conservation is not necessarily responsible for a protein's structure and function but could reflect a more general function such as membrane localization. The conservation alone is not sufficient to distinguish between residues responsible for the protein function and a general property such as membrane localization. This can be clearly seen from the fact that even though there is complete conservation in few columns, yet upon site-directed mutagenesis, no significant loss in function can be observed. Thus, MSA has limitations, particularly since the criteria of conservation cannot precisely predict the important residues across the alignment. Moreover the sequence similarity can lead to redundancy and thus the residues picked up as conserved might be an erroneous representation of the data set. Nonetheless, a more generalized function for each of these classes of mutant variants could be stated but in the absence of any information about its structure, it was difficult to predict a more specific role for a residue that shows to be critical. For example, a residue that abolishes the activity of CaMdr1p upon mutation to alanine could be important for the general functioning of any MFS transporter or could hold a more specific function like drug binding and translocation or proton transport. For such an analysis a more structured approach was demanded so as to select residues based on their importance.

SECTION-II

3.2 MEMBRANE ENVIRONMENT BASED RATIONAL COMPUTATIONAL APPROACH FOR IDENTIFICATION OF FAMILY-WIDE-FUNCTION SPECIFIC RESIDUES OF CaMdr1p

3.2.1 INTRODUCTION

The transporters belonging to MFS, consists of membrane proteins from bacteria to higher eukaryotes and these are involved in symport, antiport or uniport of various substrate [De *et al.*, 2002; Ginn *et al.*, 2000). One of the 17 families of MFS transporters uses the proton motive force to drive drug transport and has been identified in both prokaryotes and eukaryotes [Paulsen *et al.*, 1996]. Crystal structures of MFS proteins such as lactose permease (LacY), glycerol-3-phosphate (GlpT), EmrD and oxalate: formate antiporter (OxlT), suggest high structural resemblance among this family of proteins [Law *et al.*, 2008]. These consist of 12 TMS, arranged with a similar predicted topology, strongly supporting a common structural architecture or fold across all the MFS transporters [Abramson *et al.*, 2003; Huang *et al.*, 2003; Yang *et al.*, 2005; Yin *et al.*, 2006]. The fungal MFS members particularly those involved in drug transport are poorly explored in terms of their structure and function. The multidrug MFS transporter CaMdr1p belongs to DHA1 family which is widely distributed and includes both drug-specific and multidrug efflux pumps [Sa-Correia *et al.*, 2009].

Random and site-directed mutational strategies have been extensively used to understand the structure and function of these MDR efflux proteins. Tutulan-Cunita *et al.*, 2005 observed that several point mutations led to significant changes in drug specificity of ScPdr5p which are distributed throughout the length of the protein [Egner *et al.*, 2000]. Site-directed mutagenesis followed by an elegant screen done by Golin's group has revealed interactions between TMS 2 and the NBD which may help to define at least part of the translocation pathway for coupling ATP hydrolysis to drug transport mediated by ScPdr5p. Recently, Schmitt *et al.* have elucidated the role of H1068 in H-loop of ScPdr5p which couples ATP hydrolysis with drug transport [Ernst *et al.*, 2008].

Site-directed mutational strategies rely on conservation of residues in a Multiple Sequence Alignment (MSA). The conservation of a residue is calculated

from the amino acid frequency distribution in the corresponding column of a MSA. However, the physicochemical conservation is not necessarily responsible for a protein's structure and function but could reflect a more general function such as membrane localization. The conservation alone is not sufficient to distinguish between residues responsible for the protein function and a general property such as membrane localization. Membrane proteins differ from soluble proteins because of their inter-TM hydrophilic and TM hydrophobic propensities, which have allowed the development of efficient membrane protein TM prediction methods [Krogh *et al.*, 2001] and of membrane protein specific substitution matrices [Ng *et al.*, 2000].

A new method using information theory was developed and employed to rationalize mutation strategies and also applied it to MFS multidrug transporter CaMdr1p [Valdar, 2002]. Claude Shannon founded information theory in 1940s and this theory has long been known to be closely related to thermodynamics and physics. In 1991, Sander and Schneider extended Shannon entropy derived scores to proteins for positional conservation in alignment [Sander]. The commonly used information theoretic scores are entropy (H) and relative entropy (RE). Relative Entropy (RE) or the Kullback-Liebler divergence is an information theoretic measure of the difference between two probability distributions and has been increasingly applied in bioinformatics to identify functional residues [Valdar, 2002; Cover and Thomas, 2009]. The use of RE with background frequencies [Shannon, 1997] can improve the prediction of a protein's functional residues [Wang and Samudrala, 2006; Hannenhalli and Russell, 2000; Srivastava *et al.*, 2007; Reva *et al.*, 2007; Li *et al.*, 2003; Fischer *et al.*, 2008] as well as detect residues that determine the functional subtype of proteins [Hannenhalli and Russell, 2000]. This method calculates Relative Entropy (RE_M) for all the positions in a MSA. The RE_M scoring scheme has been improved by treating TM and inter-TM regions of MFS proteins separately which has drastically increased the credibility over the existing methods [Capra and Singh, 2008]. The predictions were validated by replacing the predicted highest RE_M positions of CaMdr1p with alanine by site-directed mutagenesis. It was seen that most of these residues when replaced with alanine showed decreased resistance to drugs which was corroborated by abrogated efflux of drugs. Additionally, it could be further confirmed that the functional relevance of each of these high RE_M residues by predicting their location in deduced 3D model of CaMdr1p and their role in maintaining apparent inter-helical

interactions. With this approach, the method enabled us to accurately predict and validate important residues not only of CaMdr1p but of all MFS member proteins in a large data set.

3.2.2 RESULTS

3.2.2.1 RE_M considers conservation as well as the background probability of each alignment position of a MSA

A comprehensive non-redundant data set, sourced from all MFS sequences present in the 56.2 release, was generated. This data set was then aligned using a membrane-specific multiple alignment program, which stacked the helices appropriately. The complete alignment in clustalw format is shown in Supplementary Dataset DS1. A highly conserved residue in a multiple alignment is predicted to have a functional significance. The conservation values were calculated using the algorithm from Jalview. Residues shown to be conserved dominate the TM helices, and on closer evaluation are largely hydrophobic residues associated with membrane localization. The traditional relative entropy and this modified treatment of the method (RE_M) were calculated on the same alignment using scripts written in-house. (Figure 42 shows a representative section of the alignment along with the RE_M, RE and conservation scores; see Supplementary Table S3 for the RE_M, RE and conservation scores for the entire MSA).

Notably the dominant signal using a conventional conservation measure lies in the TM helices and traditional RE also issues high scores to these residues which are less frequent in nature. This treatment of using RE_M dampens the membrane localization signals further increasing the signal from atypically occurring conserved residues (Figure 43). Since RE_M considers conservation as well as the background probability of a residue at a particular alignment position, it is an improved index of the functional significance of a residue. The distribution curve generated on the basis of RE_M from the MSA is shown in Figure 44A. To emphasize the above-mentioned fact, thirty residues with highest values were short-listed each from the conservation list, RE list and RE_M list. On comparison, it was found that there are thirteen residues shortlisted as both conserved and with high RE while it was found that only nine out of these short-listed columns are both conserved and have high RE_M (Supplementary

Table S4). The thirty alignment positions with high RE_M were further studied to assess their functional relevance. Expectedly, all residues predicted using RE_M, are not present in every protein in the family. In CaMdr1p, 16 residues were identical with the most frequently occurring residue in the thirty highest scored alignment columns, and were mutated to alanine to directly validate the prediction (Figure 44B).

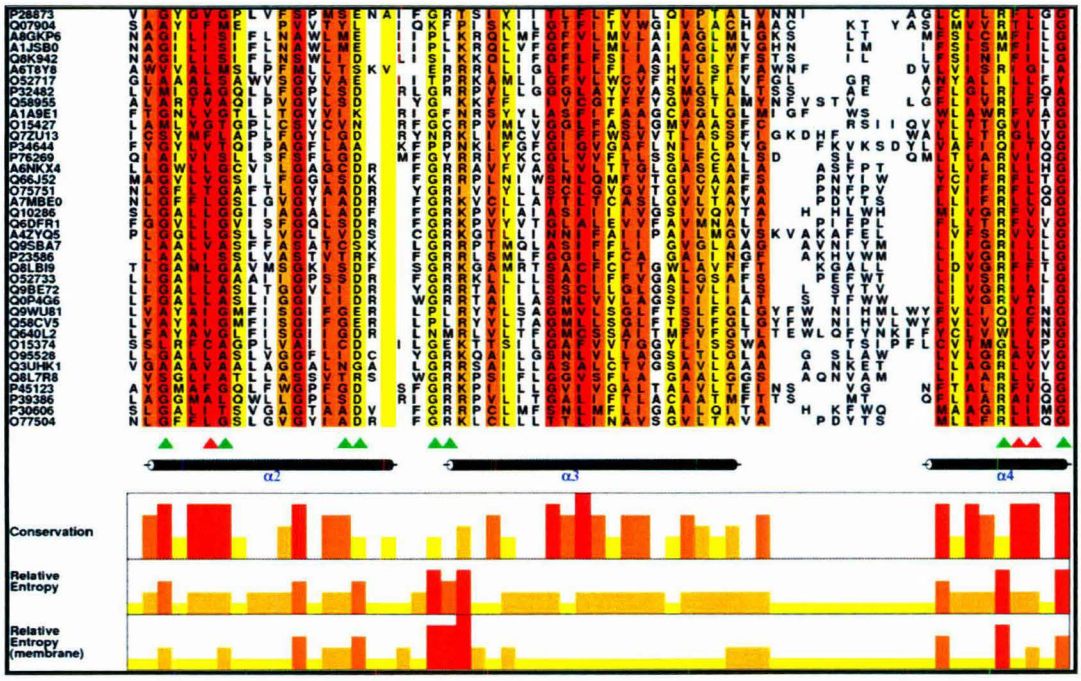

Figure 42: A portion of Multiple SequenceAlignment showing conservation and RE_M for each column.

Figure showing a representative portion of the alignment of MFS sequences and is generated using Alscript [Barton, 1993]. The alignment is coloured in a gradient from red to yellow on the basis of decreasing conservation score. Conservation was calculated using a method by Livingstone *et al.*, 1993 and the scores are shown as a histogram. The histogram compares the conservation, RE and the RE_M scores for the alignment columns shows in the figure. Results of selected mutations in CaMdr1p are indicated by triangles, green being sensitive while red are resistant. RE_M scores are better indicators of functional relevance than physicochemical conservation.

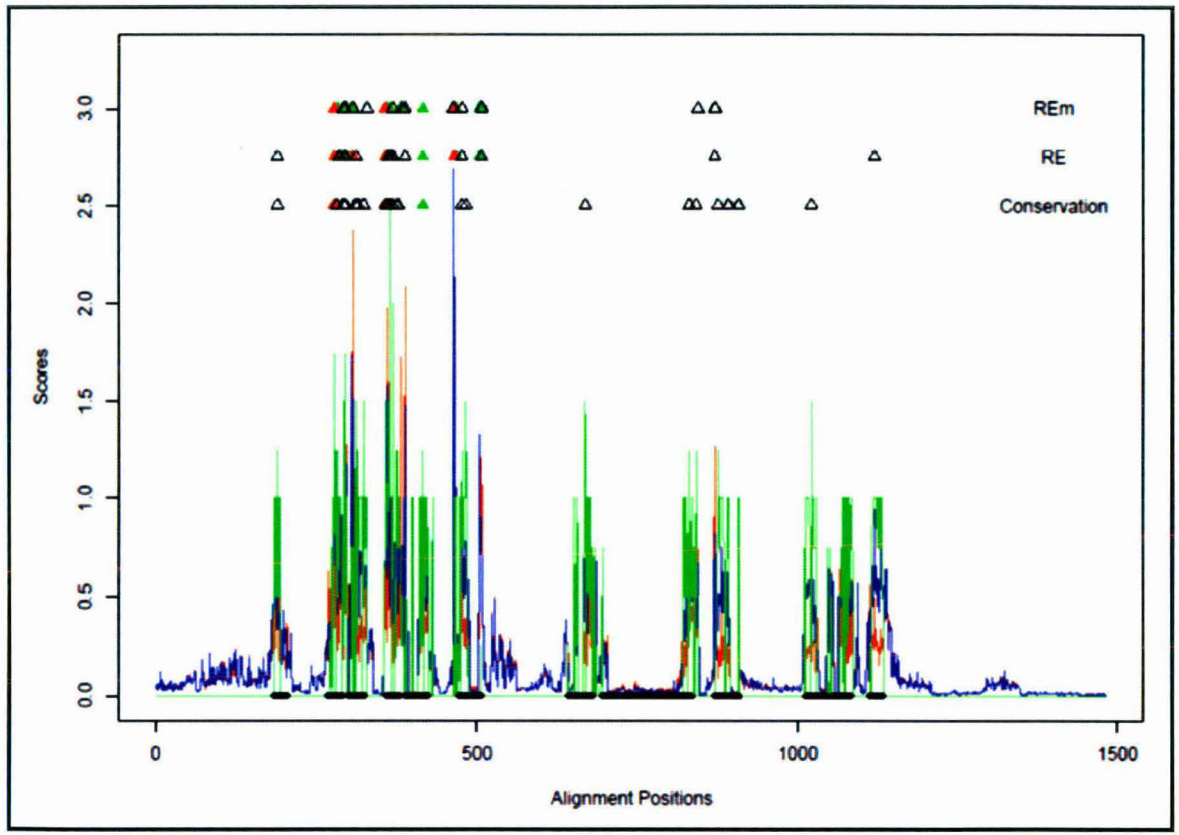

Figure 43: Comparative plot of conservation (red), RE (green) and RE_M (blue) across the entire alignment.
The conservation scores are scaled for comparison with RE and RE_M. Positions of the highest scoring alignment columns by each method are shown above the graph, along with the results of mutation of the matching residues. Out of these top scoring positions by three different calculations, the mutated positions showing resistant phenotype are marked in red triangles, those showing sensitive on all drugs are marked in green triangles while those which were not mutated are marked by empty triangles. Locations of the transmembrane regions are marked by black bars on the x-axis.

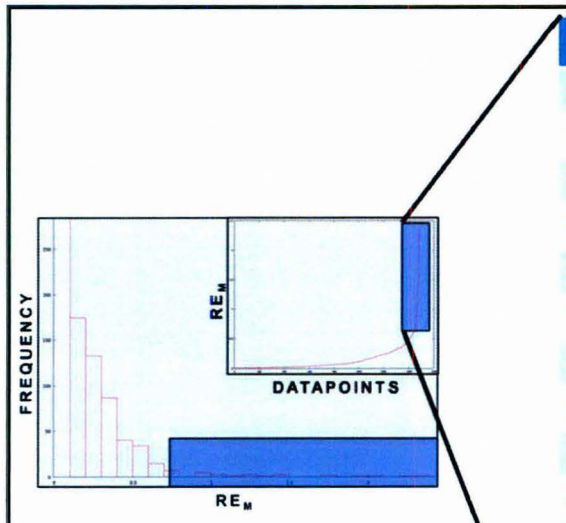

RE_M	RESIDUE	LOCATION
2.2	W273	Loop
1.9	R215	TMS 4
1.7	G183	Loop
1.7	D235	TMS 4
1.4	R184	TMS 4
1.3	P296	Loop
1.2	E178	TMS 2
1.0	R274	Loop
1.0	T160	TMS 2
0.94	F277	TMS 6
0.94	E297	Loop
0.91	G256	TMS 5
0.72	T298	Loop
0.72	L211	TMS 4
0.71	G165	TMS 2

Figure 44: Distribution curve of RE_M values of complete MSA.

A) Histogram of the RE_M scores (+ve/background frequency) vs frequency for all positions of MSA of the MFS transporters. The top 30 RE_M positions depicted in the boxed region were selected for further analysis. The inset represents the same data by a line graph.

B) The table shows 16 out of the top 30 high RE_M alignment positions where the residue in CaMdr1p matched with the most frequent amino acid at that particular position in a MSA of 342 MFS members. Their predicted location with respect to CaMdr1p is also displayed in the next column.

3.2.2.2 Residues with high RE_M are part of the known motifs of Major Facilitator Superfamily

These sixteen out of the top thirty positions, wherein the residue in CaMdr1p matched with the most occurring residue across that alignment position in MSA were analyzed for further studies by site-directed mutagenesis. Interestingly, most of the sixteen residues with high RE_M turned out to be part of the well-known motifs of the MFS. These motifs are identified as Motif A (GxLaDrxGrkxxl), Motif B (lxxxRxxqGxgaa) which are conserved throughout the MFS, Motif C (gxxxGPxxGGxl) only in 12 and 14-TMS family and Motif D2 exclusive to 12-TMS family [Paulsen *et al.*, 1996]. Three out of the sixteen residues short-listed for CaMdr1p; E178, G183 and R184 are a part of Motif A; residues L211, R215 and G219 are a part of Motif B and G256 is a part of motif C. In addition to the known motifs mentioned above, two new motifs have been identified by this study. The

residues in these stretches ^{273}Wrxxf^{277} and ^{296}Pespr^{300} have high RE_M scores. However, the known motif D2 does not appear to be highly conserved in the alignment and is thus not predicted to be family-wide function-specific.

3.2.2.3 Site-specific mutagenesis of residues with high RE_M shows that they are functionally critical

All the sixteen residues selected on the basis of high RE_M were mutated to alanine by employing site-directed mutagenesis except G165, G183 and G256 which were replaced by leucine. For functional analysis of the mutant variants, a heterologous hyper-expression system, where GFP-tagged CaMdr1p (CaMDR1-GFP) was stably over-expressed from a genomic *PDR5* locus in a *S. cerevisiae* mutant AD1-8u$^-$, was used [Nakamura *et al.*, 2001]. The host AD1-8u$^-$ developed by Goffeau's group, was derived from a *Pdr1-3* mutant strain with a gain-of-function mutation in the transcription factor Pdr1p, resulting in constitutive hyper-induction of the *PDR5* promoter [Pasrija *et al.*, 2007]. These mutant variants of the residues with high RE_M score showed increased drug susceptibility and abrogated efflux of substrates such as [^{3}H] MTX and [^{3}H] FLU (Figure 45 and 46). Of note, there were few exceptions to the list of residues with high RE_M. For example residues T160, L211, W273 and R274 have high RE_M values but do not appear to be critical for function of CaMdr1p since the drug susceptibility and efflux are not affected upon replacement of these residues with alanine.

3.2.2.4 All these mutant variants are properly surface localized

To confirm that the change in susceptibility observed in the mutant variants was not due to their poor expression or mislocalization, the localization of GFP-tagged version of CaMdr1p (CaMDR1-GFP) and its mutant variants was compared using FACS and confocal imaging. A proper localization of all the mutant variants was confirmed by both these methods which showed proper rimmed appearance of GFP-tagged CaMdr1p. The Western Blot analysis further confirmed that the expression levels of CaMdr1p of all the mutant variants were similar thus corroborating FACS and confocal data (Figure 47).

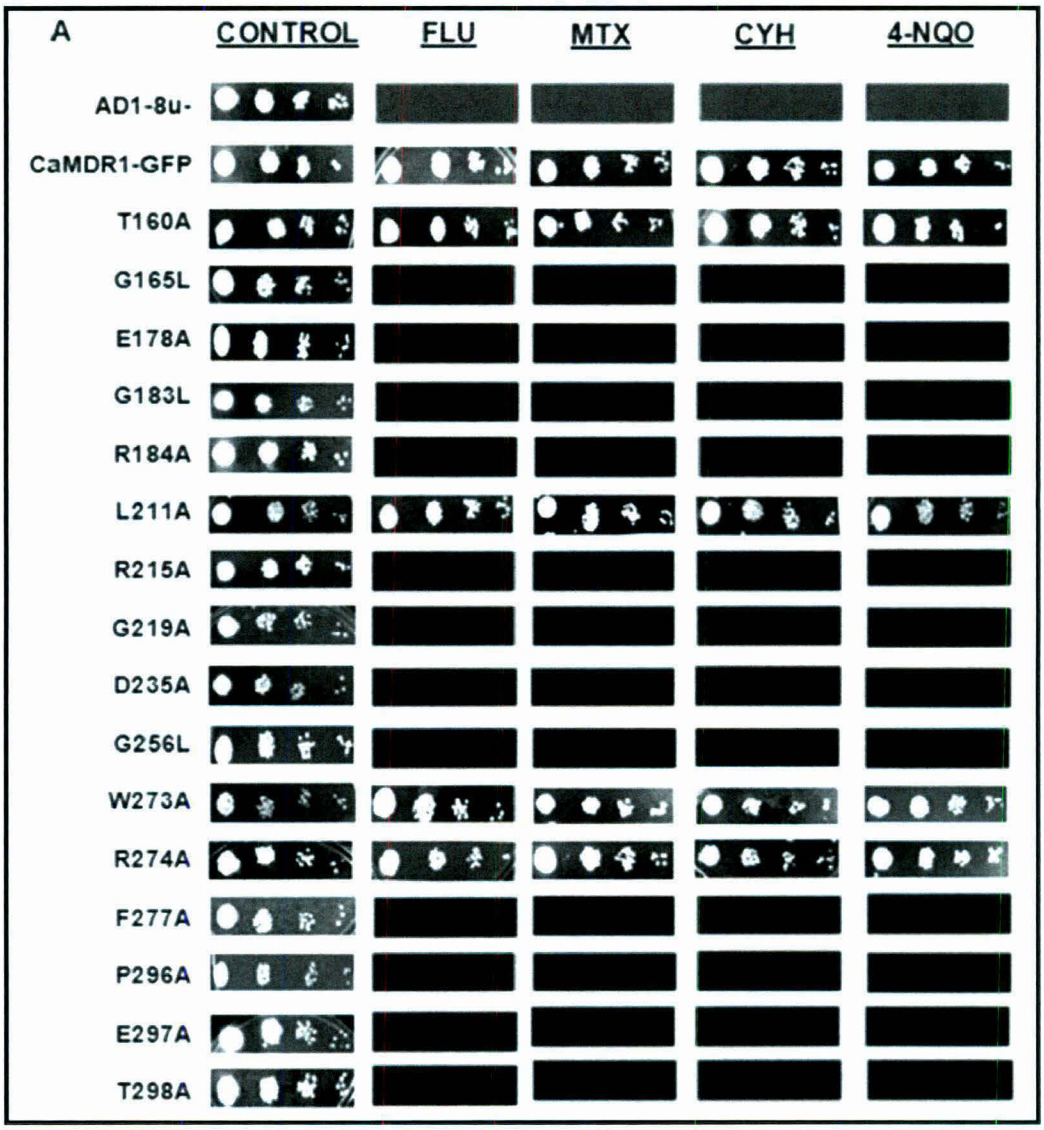

Figure 45: Drug susceptibility assay of mutant variants of high RE_M residues in CaMdr1p-GFP in *S. cerevisiae*.

Drug resistance profile of wild-type and mutant CaMDR1-GFP yeast strains determined by spot assay. For spot assay, cells were freshly streaked, grown overnight and then resuspended in normal saline to an A_{600} of 0.1 ($1X10^6$ cells) and Each strain was spotted on to YEPD plates in the absence (control) and presence of the following drugs: FLU (0.20 µg/ ml), CYH (0.20 µg/ ml), 4-NQO (0.20 µg/ ml) and MTX (65 µg/ ml). Growth differences were recorded following incubation of the plates for 48 hrs at 30°C. Growth was not affected by the presence of the solvents used for the drugs (data not shown).

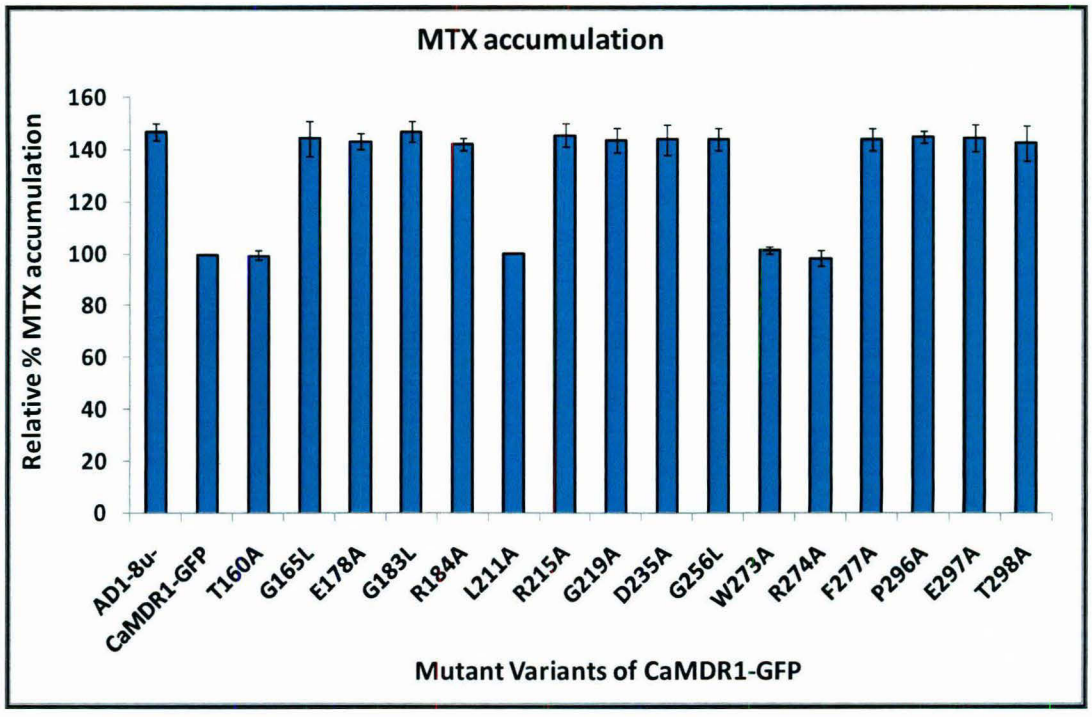

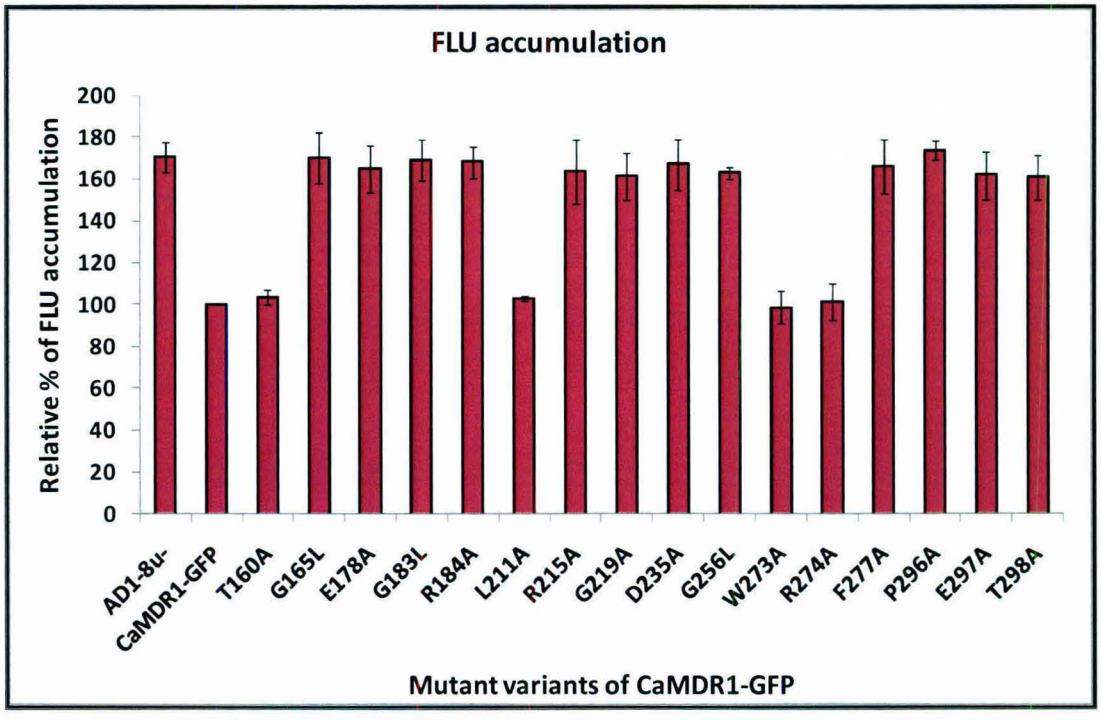

Figure 46: [^{3}H] MTX and [^{3}H] FLU accumulation in the mutant variants of high RE_M residues of CaMdr1p-GFP. Controls AD1-8u$^-$ and RPCaMDR1-GFP have also been included for comparison. The results are means $\pm$ standard deviations for three independent experiments.

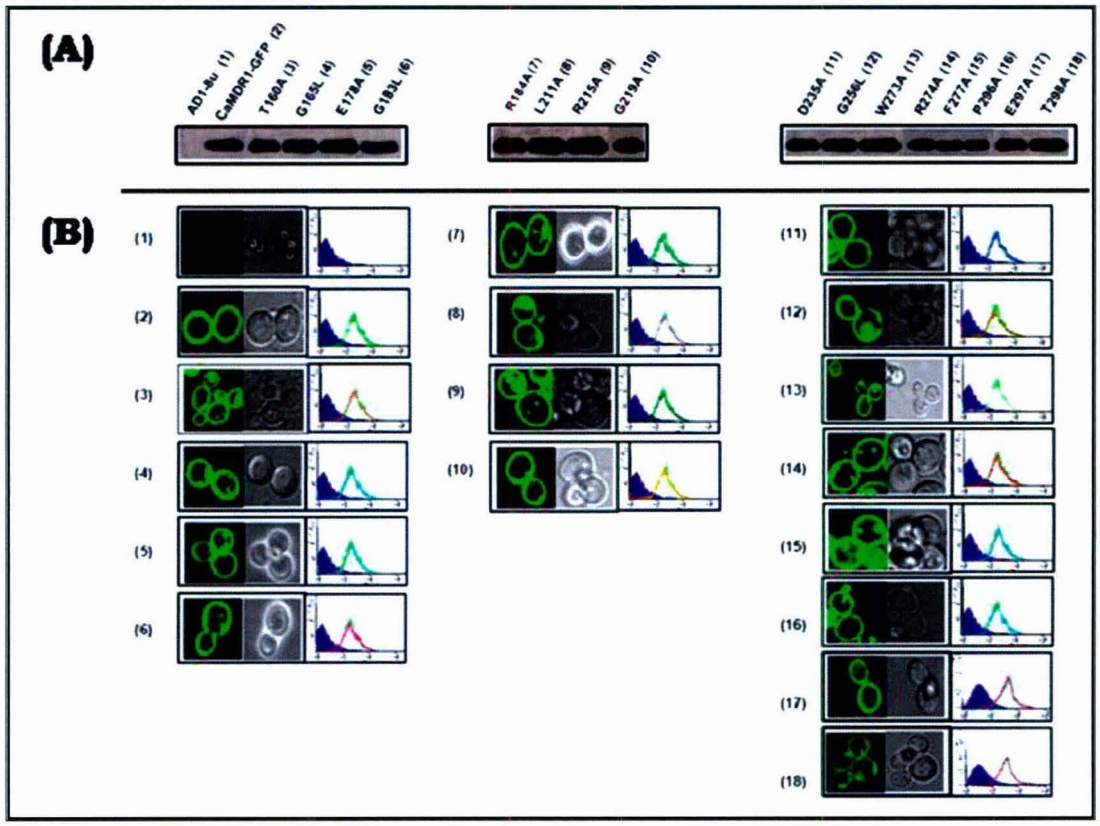

Figure 47: Protein expression profiles of CaMdr1p-GFP and its mutant variants of high RE_M residues in *S. cerevisiae*.

A) Western Blot analysis of the PM fraction of mutant variants with anti-GFP antibody.

B) Confocal and FACS analysis of the all the mutant variants to check their expression and localization in comparison with AD1-8u⁻ (negative control) and RPCaMDR1-GFP (positive control) [Shukla *et al.*, 2003].

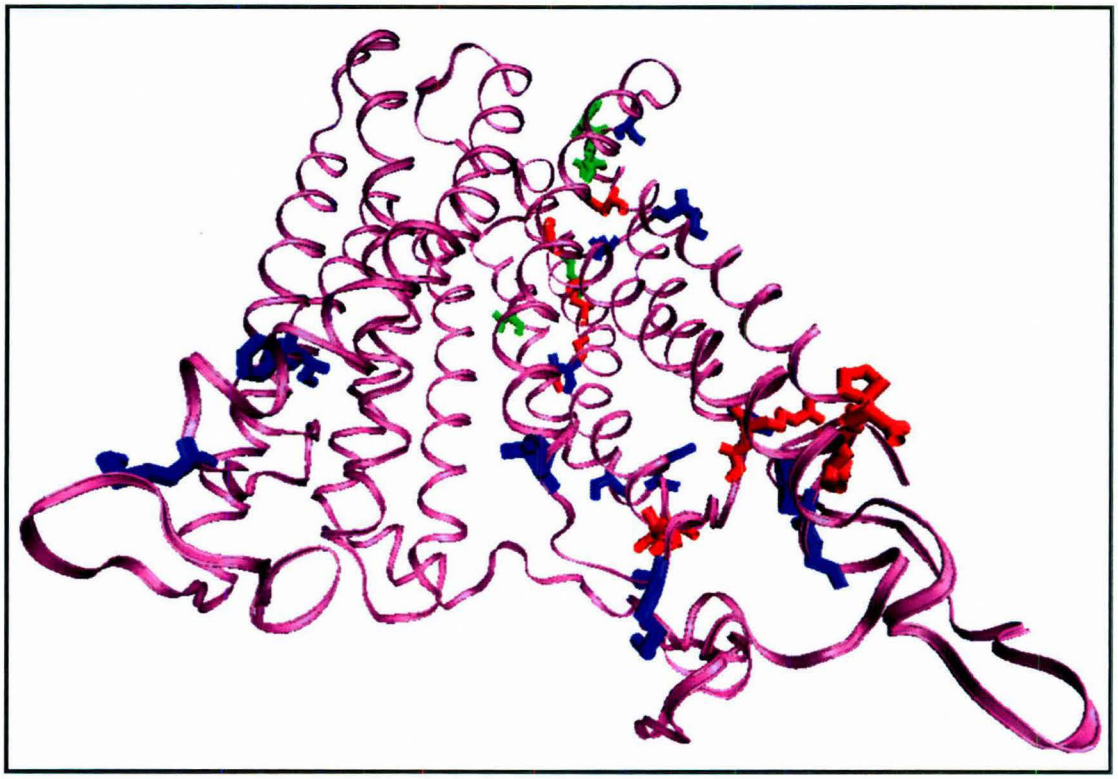

Figure 48: The 3D deduced homology model of CaMdr1p.
The 3D homology model of CaMdr1p wherein the mutated residues are marked onto the model and are colored on the basis of the phenotypes exhibited upon mutation. Red denotes sensitive, green shows resistant and blue marks a position predicted to be important but not mutated as the CaMdr1p residues did not match the conserved residue in that alignment position. The structure is viewed using Visual Molecular Dynamic (VMD) software.

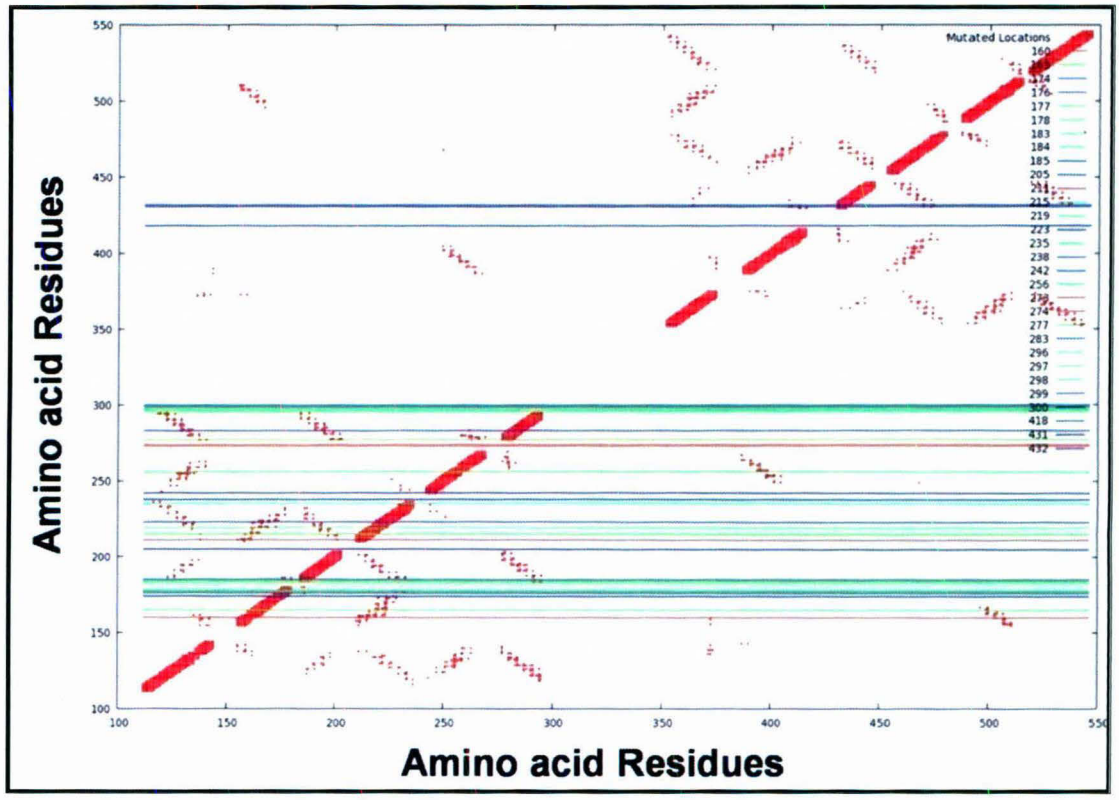

Figure 49: The contact map derived from the 3D homology model of CaMdr1p.
The contact map of CaMdr1p is plotted as described in Materials and Methods. The lines represent the top thirty high RE_M residues and are coloured on the basis of the phenotypes where green represents the residues that are sensitive upon mutation while red are the ones that do not show any phenotype. The blue lines mark the residues in CaMdr1p that did not match with the most frequent residue in that particular column of the MSA.

RESIDUES	LOCATION	PREDICTED INTERHELICAL INTERACTIONS
G165	TMS2	TMS4
R184	TMS3	TMS6
R215	TMS4	TMS1
		TMS2
		TMS3
G219	TMS4	TMS1
		TMS2
		TMS3
G256	TMS5	TMS1
		TMS8
F277	TMS6	TMS1
		TMS3
		TMS5

Table 11: Summary of inter-helical interactions via high RE_M residues.
The table summarizes predicted inter-helical interactions mediated via selected residues with high RE_M. More than one residue pair is predicted to be involved in maintaining the interactions between the helices.

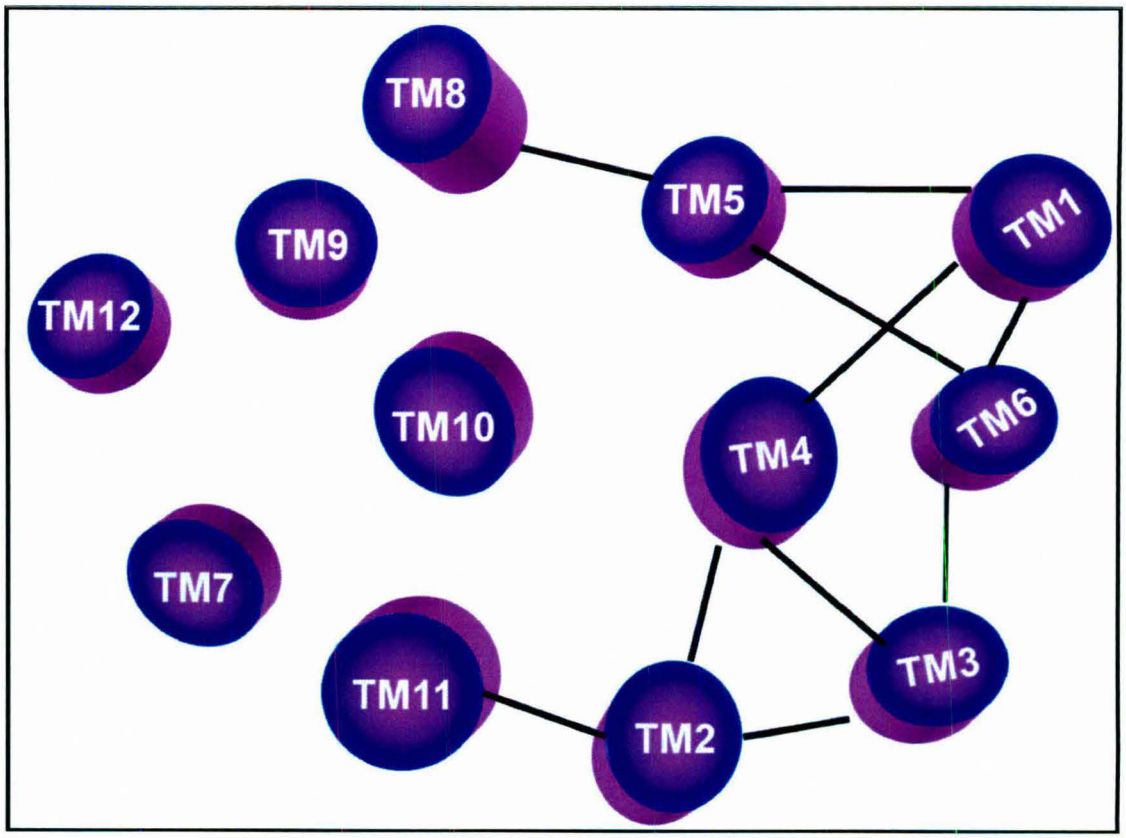

Figure 50: Pictorial representation of inter-helical interactions via these high RE_M residues.
Figure shows that the residues involved in these interactions are majorly confined to the N-terminal half of the protein.

3.2.2.5 Distance plot of CaMdr1p from deduced 3D homology model reveals inter-helical interactions

For evaluating the relevance of high RE_M residues in CaMdr1p, 3D deduced homology model was constructed using available crystal structures of lac permease of *E. coli* (1pv6), glycerol-3-phosphate of *E. coli* (1pw4) and oxalate:formate transporter of *O. formigenes* (1zc7) as described in Materials and Methods (Figure 48). All the top thirty positions of highest RE_M are marked in the model which mostly lie in the N-terminal half of the protein (Figure 48). Using the homology model, a symmetric contact map of CaMdr1p was generated as discussed in Materials and Methods (Figure 49). This distance plot was exploited to ascertain the role of these residues with high RE_M.

It is apparent that residues L211, R215 and G219 in TMS 4 are within 8 A° distance to many residues of TMS 1, 2 and 3. For example, it can be seen that residue G219 on TMS 4 lies on the same face of the helix and is within 8 A° to the residues G165 and G169 on TMS 2. Indeed, the mutation of predicted G165 and G169 on TMS 2 resulted in abrogated drug susceptibility and transport (data not shown). All the predicted inter-helical interactions are summarized in Table 11 and shown in a pictorial representation of the homology model in Figure 50.

3.2.3 DISCUSSION

The multidrug MFS transporter CaMdr1p harbors a conserved antiporter 'motif C' within TMS 5. The previous study has revealed that the conserved and critical residues of this motif and of TMS 5 are bunched together on the same face of its helical wheel projection and are critical in drug efflux [Pasrija *et al.*, 2007]. However, the structural and functional aspects of this major multidrug transporter remain poorly understood. To address some of these questions, in this study, the conventional mutational strategy was rationalized by applying computational approach to predict functionally critical residues of CaMdr1p.

The sequence set described in this manuscript represents a comprehensive non-redundant coverage of annotated MFS sequences from SWISSPROT. Many methods have been developed to improve the MSA of membrane protein families for

accurate predictions of residues critical for structure and function [Pirovano *et al.*, 2008]. Membrane proteins have fold signals which are easily mapped to the primary sequence as TM and inter-TM stretches. Considering the differences in physico-chemical properties of these two regions, membrane protein specific substitution matrices have been developed [Ng *et al.*, 2000]. However, it was argued that a conservation score on the basis of identity or physico-chemical similarity still remains inadequate as the background frequencies of their immediate environmental milieu are radically different with respect to hydrophilic and hydrophobic propensities. This is also apparent from the conservation scores of the MSA wherein a large proportion of the conserved columns correspond to hydrophobic TM regions. Notably, two CaMdr1p residues (F216 and L217) with high conservation but low RE_M (taken as controls) when replaced with alanine showed no change in the phenotype (see Supplemenatry Table S4). One of the most basic fold specific signals is the hydrophobic core in globular proteins, and the TM region in membrane proteins. Unlike globular proteins, the hydrophobic TM region is continuous in the membrane protein's primary structure, and indeed this still remains one of the preferred methods to identify membrane proteins, and map their TM regions. While it is intuitive that the synchronous stretch of hydrophobic residues is responsible for membrane localization, the application of a scoring method that can distinguish these residues from family-wide alignment columns associated with other functions has not yet been deployed. In essence, a method was required that can objectively separate the TM signals from other signals. To overcome these limitations, we improved existing method(s) of information theory wherein RE_M was calculated on the basis of MSA of MFS proteins, keeping in mind the differences in the environmental milieus. The TM and inter-TM regions were treated by different background probabilities for calculation of RE_M. These RE_M scores helped us to predict those sites which have amino acid distributions very different from the respective background distribution and are thereby statistically predicted to be functionally critical. Not all the residues predicted using RE_M, are present in every protein in the family. In CaMdr1p, 16 residues were identical with the most frequently occurring residue in the thirty highest scored alignment columns, and were mutated to directly validate the prediction (Figure 44B). The results of drug susceptibility assays revealed that almost all of these matched residues with high RE_M when replaced with alanine displayed sensitivity to the tested drugs and showed abrogated drug transport (Figure 45). Interestingly, upon

mutation of these residues which had high conservation values but lower RE_M values (negative control), none showed alterations in drug susceptibilities and thus did not retain the functionally critical stringency as was evident from residues with higher RE_M. For example, analysis of a few conserved columns of the MSA, such as F216, L217 and L171 having RE_M values between 0.57-0.44 revealed that their replacement with alanine did not affect the function of CaMdr1p. This strengthens the fact that this method takes into account the conservation along with the background frequency and thus lists out residues which affect the function. Also, to check the efficiency of the method, another negative control used was to mutate residues which are have conservation and low RE_M values but lie in the vicinity of one of the 16 selected high RE_M residues. For example, when C225 which is closer to the critical G219 and D235, was mutated to C225A, the functioning of the protein was not affected (data not shown). Similarly, for critical G256, when residues A248, A253 and V254 which are within its vicinity were mutated as A248G, A253G and V254A, the mutant variants continued to behave as WT-CaMDR1-GFP [Pasrija *et al.*, 2007].

To further elucidate the role of predicted residues in the functionality of CaMdr1p, a homology model based on the available crystal structures of lac permease, glycerol-3-phophate and oxalate: formate transporter was deduced [Abramson *et al.*, 2003; Huang *et al.*, 2003; Yin *et al.*, 2006]. The RE_M method predicts the relative importance of a residue purely from sequence analysis and is independent of the protein's structure. However, the role a residue plays in the protein's function is not readily apparent from its sequence. The protein's 3D model was exploited as a guide to reason why a residue is functionally critical. The deduced 3D model suggested that similar to other MFS structures, the 12 TM helices of the CaMdr1p span the membrane in such a way that they form the channel pore particularly aligned by residues of TMS 2, 4, 5, 7, 8, 10 and 11. From the deduced homology model of CaMdr1p, a symmetric contact map was generated to highlight the inter-helical interactions of the protein (Figure 48). Based on the predictions from the distance map, it could be shown that many high RE_M residues are indeed a part of inter-helical interactions (Figure 49). It is apparent that more than one residue pair is predicted to be involved in maintaining the interactions between helices (Table 11).

This study aims to develop this method so as to identify residues with high specificity which would play a critical role across this entire MFS protein family. Although signals associated with antiporter motifs have been identified using this method, a finer granularity in function such as substrate specificity determining residues is not expected, as these signals would not be family-wide. Since the enlisted residues with high RE_M values which are functionally critical for CaMdr1p are expected to be family-wide function-specific and thus critical for the entire MFS protein data set, their relevance was validated from the earlier published work. It is known that Motif A of the MFS transporters span an eight residue long loop between TMS 2 and 3 and is suggested to be involved in maintaining a β-turn linking the adjacent TM helices [Pao *et al.*, 1998]. In the present study, G183 and R184 in the loop between TMS 2 and TMS 3 of CaMdr1p were picked up as family-wide function-specific residues thus corroborating that these residues are a part of Motif A (GxLaDrxGrkxxl) which holds importance throughout the MFS transporters. The hypothesized rocking motion in MFS presumably requires conformational changes in the TMS and the β–turns. In this, the transporter inter-converts between C_i (inward facing) and C_o (outward facing) states for translocation of substrates. In glycerol-3-phosphate of *E. coli*, it was seen that D88 was involved in inter-conversion between these C_i and C_o states of the protein [Huang *et al.*, 2003]. Interestingly, D88 corresponds to E178 of CaMdr1p which also lies in Motif A which upon mutation to alanine turns out to be critical for drug susceptibility and efflux (Table 12).

Motif B (lxxxRxxqGxgaa) of all MFS has a role in energy coupling which spans the N-terminal half of TMS 4 [Paulsen *et al.*, 1996]. CaMdr1p contact map reveals that residues in Motif B interface with residues ^{165}GxxxG^{169} on TMS 2. Motifs rich in glycine and proline residues promote formation of special backbone conformation including kinks in TMS, tight interactions between TMS and very flexible β-turns. In human VAchT, Motif B and the adjacent sequences contain a total of nine notch signatures. A notch allows two helical TMS to approach each other unusually closely because small side chains are located at the interface. R124 of PcaK of *Pseudomonas putida* which is equivalent to high RE_M R215 of CaMdr1p of *C. albicans* is shown to be critical for helix packing [Ditty and Harwood, 1999]. Interestingly, G111 of LacY of *E.coli* which also occupies a position in the same alignment column is also critical and earlier shown to be a residue at a kink.

MFS TRANSPORTER	ORGANISM	CRITICAL RESIDUE (RE_M)	LOCATION	FUNCTION
LacY	*E.coli*	G111 (1.9)	TMS4	Kink
LacY	*E.coli*	G150 (0.91)	TMS5	Kink
PcaK	*Pseudomonas putida*	R124 (1.9)	TMS4	Helix Packing
PcaK	*Pseudomonas putida*	E144 (0.76)	TMS4	Helix Packing
MdfA	*E.coli*	D77 (1.2)	TMS2	Topology
EmrD	*E.coli*	R118 (0.59)	TMS4	Topology

Table 12: High RE_M alignment positions shown to be critical for function in other MFS members.
The residues with high RE_M positions and their predicted roles in the case of other MFS members are enlisted. The residues of CaMdr1p at the same position in the alignment are shown to be critical in this study.

Residues from Motif C (gxxxGPxxGGxl) which is exclusive to 12-TMS family are also picked up by these calculations [Paulsen *et al.*, 1996]. G150 of LacY of *E.coli* which is equivalent to high RE_M G256 of CaMdr1p is function-specific for LacY protein [Guan and Kaback, 2006]. A stretch of conserved residues ^{296}Pespr^{300}, previously unidentified, at the end of TMS 6 were also predicted with high RE_M. The equivalent residues P296A, E297A and T298A of CaMdr1p that overlap with the consensus residues in the stretch were mutated and it was found that cells expressing these mutated variants displayed increased sensitivity to drugs. However, the functional significance of these residues is yet to be established.

There are a few exceptions which emerged from usage of this method. For example, this method did not pick up any residue of Motif D2. This could be an artifact of the method used for alignments in earlier studies. In this study a membrane protein specific alignment was employed whereas earlier reports have used standard multiple alignments substitution matrices with smaller data sets. However, when the alignment was done using MUSCLE [Edgar, 2004] and with other standard substitution matrix (Blosum 62) [Henikoff and Henikoff, 1992] on the complete data set, the motif still did not appear (data not shown). Motif D2 is assumed to have a structural significance as it holds a major kink within TMS 1 but mutations in this motif do not alter the backbone conformation. As an example of the possibly

insignificant role of the motif, in human VAchT, the mutation of L49G in this motif completely eliminates propensity for a kink or notch and abolishes activity while normally a glycine itself is expected to be present at this position and is supposed to be involved in maintaining a major kink in this motif [Chandrasekaran et al., 2006].

Out of the 16 residues that were mutated, T160A, L211A, W273A and R274A did not lead to any phenotypic changes. It is known that for some of the positions in alignment, the most frequent amino acid does not match with the residue of CaMdr1p at that site. One reason for this could be that some of the functionally important residues co-evolve i.e., these residues may mutate, with compensatory mutation occurring elsewhere in the protein to regain function [Martin et al., 2005]. T160 where the most frequent residue is a serine at that position may be one such case. Another reason may be that the alignment used in this study involved prediction of TMS with the possibility of errors in demarcating the edges of TM helices. Residues from columns lining the edges of the helices may be wrongly assigned to TM and inter-TM regions. This probably explains the lack of any effect of mutation on residues T160 of TMS 2 and L211 of TMS 4 which lie at the edge of the respective TMS. Other exceptions in the predictions are the mutation of W273 and R274 which though highly conserved and probably a part of the new motif but do not abrogate function upon mutation. Although a few tryptophans in an ABC transporter MRP1, have been shown to be involved in substrate binding and transport [Koike et al., 2002], generally, in a membrane protein tryptophan residues located on the surface of the molecule are mainly positioned to form hydrogen bonds with the lipid head groups while their hydrophobic rings are immersed in the lipid part of the bilayer [Schiffer et al., 1992]. It can be predicted that W273 and R274 may be associated with membrane helix orientation and this function may not be perturbed by mutating them individually through alanine scanning. Alternatively, the tryptophan-arginine residues could be functionally critical in tandem and compensate each other for the loss of either one of them.

Of note, in the predictions made by this study, it can be seen that substrate-specific residues which predominantly occur in C-terminal of MFS proteins are not picked up with high REM. It should be mentioned that since this alignment considers the entire MFS, residues responsible for substrate specificity would only be

selectively conserved within a subfamily and would not have sufficiently strong signals to be visible in this present family-wide study. For this, the same method may be applied to a data set classified on the basis of substrate selectivity to identify residues critical to the functioning of that subfamily.

There are a number of conservation methods known but none has yet achieved both biological and statistical rigor. This study uses RE_M to separate conserved residues from the background function of TM localization. The interpretations support the well-known fact that MFS has a conserved N-terminal half which has residues important for maintenance of a specific fold for this class of proteins while C-terminal half has a more specific role in substrate binding and recognition [Paulsen *et al.*, 1996]. Taken together, this study provides an insight into the molecular details of MFS transporters in general and CaMdr1p in particular. This method of scaled RE_M calculations improves its performance over other information theoretic methods. Additionally, this study also provides a method for rational mutational analysis not only for MFS proteins but can be applied to any class of membrane proteins and thus makes it possible to predict and locate family-wide functionally relevant residues.

SECTION-III

3.3 IDENTIFICATION OF DRUG-PROTON ANTIPORTER FUNCTION SPECIFIC RESIDUES OF CaMdr1p BY EMPLOYING INFORMATION THEORETIC MEASURES

3.3.1 INTRODUCTION

A significant mechanism of azole resistance includes an over-expression of membrane proteins that actively efflux the incoming drugs [Prasad and Kapoor, 2005] Among the 28 putative ATP-Binding Cassette (ABC) transporter genes and 95 putative MFS transporter genes identified in the *C. albicans* genome, only CaCdr1p and CaCdr2p among the ABC transporters and CaMdr1p among the MFS transporters are multidrug transporters involved in clinically encountered azole resistance of this fungal pathogen. Thus, azole resistant clinical isolates mostly show an increased expression of the plasma membrane efflux pumps encoding genes, viz. *CaCDR1, CaCDR2 and CaMDR1* [Gaur *et al.*, 2005; Gaur *et al.*, 2008].

MFS is one of the largest families of transporters and includes members that function as uniporters, symporters or antiporters. Structural studies of MFS transporters revealed that the members of this superfamily share structural homology but have relatively weak sequence similarities. MFS transporters are an important superfamily of membrane proteins which import or export diverse substrates and catalyze different modes of transport using unique combinations of functional residues [Paulsen *et al.*, 1996]. In comparison to ABC transporters, the structural and functional aspects of MFS multidrug transporters are only beginning to emerge. The structural studies conducted so far suggest the possibility that the fold of these transporters constitutes a scaffold for all MFS members with 12 helices. Although the fold is conserved, the specific function is obtained by varying sets of amino acids at the substrate binding and translocation domains. This is quite evident from the structural differences between Lactose Permease (LacY) of *E.coli* (symporter) and Glycerol-3-Phosphate (GlpT) of *E.coli* (antiporter) [Law *et al.*, 2008]. The previous study identifies residues important for the entire MFS family irrespective of its mechanism of transport, however, the method did not differentiate between family-wide function-specific and subfamily specific residues [Kapoor *et al.*, 2009].

Predicting functionally important residues from a Multiple Sequence Alignment (MSA) by using conservation and then employing site-directed mutagenesis for validation has been a common approach. Multiple methods for scoring the conservation of a residue are being used frequently [Valdar, 2002]. However, this process has serious limitations, particularly since the criterion of conservation across the sequence alignment, does not necessarily predict the functional importance of a residue for a given protein. A residue shown to be conserved across MSA can be important for the entire class and can have a role in maintaining the fold of the protein rather than playing a more specific role in its function [Kapoor *et al.*, 2009]. Moreover, the sequence similarity can lead to redundancy and thus the residues picked up as conserved might be an erroneous representation of the data set.

To predict function-specific residues of CaMdr1p this study used the modifications of Relative Entropy (RE) or the Kullback-Liebler divergence, a well-known information theoretic measure [Cover and Thomas, 2009; Shannon, 1997]. The method has been increasingly applied in bioinformatics to identify functional residues. Given an alignment, and a set of proteins grouped into sub-families, according to some definition of function, such as catalytic activity, the method identifies positions that are indicative of these functional differences between the mentioned sub-families [Valdar, 2002]. In view of this, the information theoretic measure scaled cumulative RE (CRE_S) were used over the traditional conservation measures, to predict residues important for CaMdr1p, and extrapolated it to other members of its family. The DHA1; a family of drug-proton antiporters, with Sugar Porter (SP); a family of symporters were contrasted to identify the residues important for a drug-proton antiporter exclusively, on the basis of CRE_S. Since CRE_S is a better score over traditional conservation [Hannenhalli and Russell, 2000], thirty residues with highest CRE_S were selected for analysis. Selected residues were subjected to site-directed mutagenesis and replaced with alanines or leucines. Notably, the mutant variants of these residues showed abrogation of resistance to either all or to selected drugs. The enhanced susceptibility of these mutant variants to the drugs was corroborated with abrogated efflux of the substrates. The predictions were validated from previously published data and it was seen that the equipositional residues in other members of the DHA1 family are also functionally critical. This study shows

that the use of CRE_S provides an impartial score to select differentially conserved residues, which can be evaluated for their functional significance.

3.3.2 RESULTS

3.3.2.1 CRE_S scores predict functionally important residues of CaMdr1p

This study is an attempt to rationalize the site-directed mutational strategy in order to predict functionally critical residues of CaMdr1p. As CaMdr1p belongs to DHA1 family; a family of drug-proton antiporters, its sequences were contrasted with another family of MFS transporters having totally different function. It was speculated that such a comparison will predict residues exclusively important for DHA1 family. For this sort of comparison, SP family, a family of symporters, was chosen as it completely differs from DHA1 in terms of mechanism of transport as well as its substrate specificity. The dataset included 37 of DHA1 and 44 of SP sequences with no redundancy. Other such contrasting families of MFS have very few members and were not included since the use of a smaller dataset is prone to statistical errors. This study then employed a well-known information theoretic measure, CRE with this comprehensive non-redundant dataset. The complete alignment in clustalw format is shown in Supplementary Dataset DS2. The RE within a family (conservation across a subfamily) and CRE_S scores across all columns of this profile MSA were calculated (Supplementary Table S5). Figure 51 shows a representative part of this profile alignment with Cumulative Relative Entropy (CRE_S), Relative Entropy (RE) and conservation scores for each alignment position. It was predicted that for a residue to be functionally critical, it should not only have a high CRE score but should also be highly conserved in the DHA1 family. Thus, a criterion of selection which took both the conservation score and the CRE score in consideration was required. For this, a scaled CRE score (CRE_S), a product of conservation across only DHA1 (measured using RE_{null}), and CRE between the two families was calculated. A residue position with high CRE_S was predicted to be either differentially conserved across the two families or exclusively conserved in the DHA1 family vis-à-vis the SP family and thus was predicted to impart functional specificity to DHA1. The distribution curve generated on the basis of CRE_S scores of the entire MSA is shown in Figure 52A. The thirty residues with highest CRE_S were shortlisted for further studies. The range of selection spanned from a scaled score of 6.12-1.96 and is highlighted in Figure 52B.

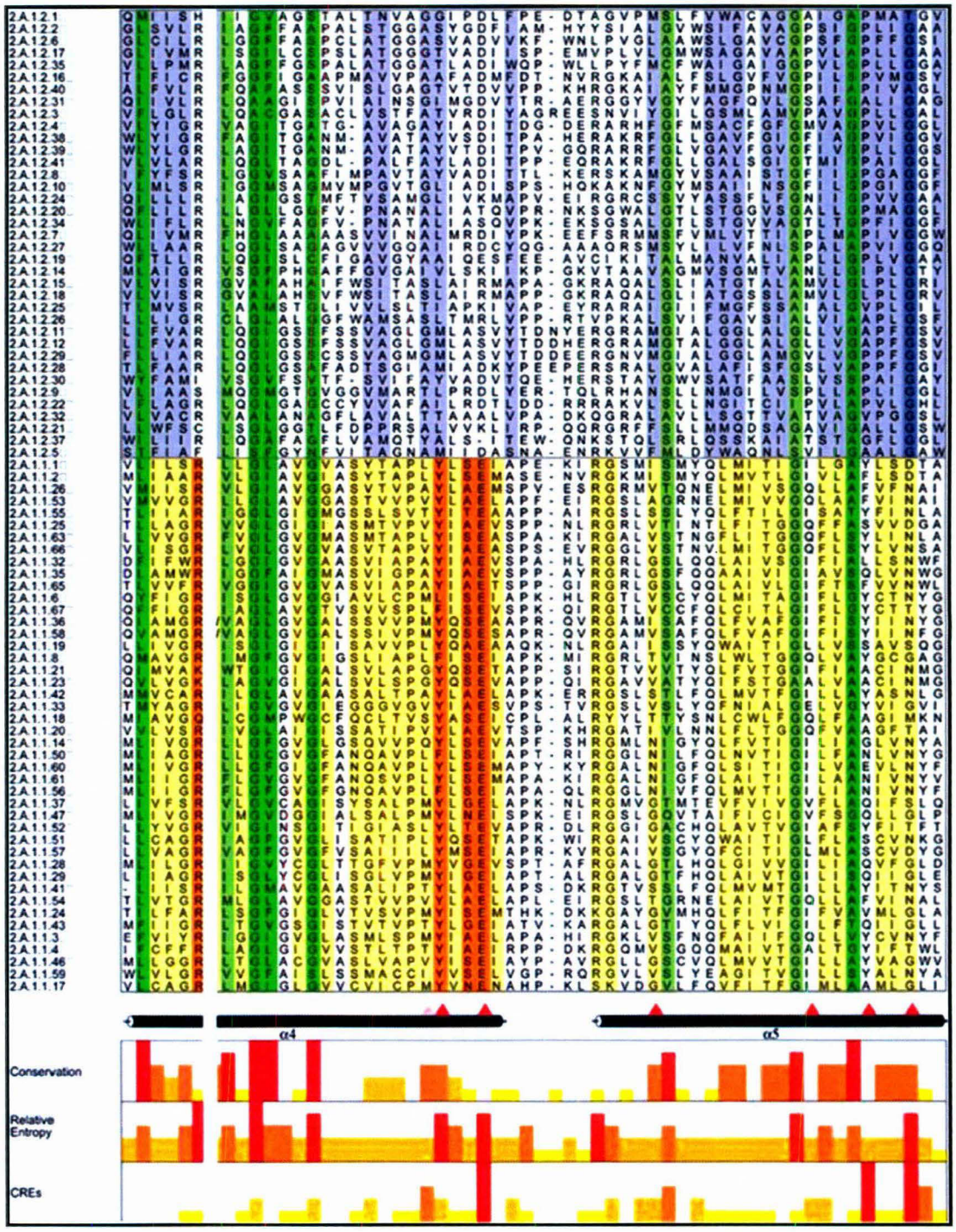

Figure 51: Representative alignment of DHA1 and SP families of MFS transporters. Figure showing a representative portion of the MSA of the MFS sequences and is generated using Alscript. The top 37 sequences belong to the DHA1 family and the next 44 belong to the SP family. The part of the MSA spanning helix 4 and 5 is highlighted in the figure. Alignment columns are coloured in a gradient based on the degree of conservation. TCDB ID of CaMdr1p Sequence is 2.A.1.2.6 and is third from the top. Green columns denote family-wide conservation, while conserved columns in DHA1 and SP family are coloured in blue and yellow respectively. A comparison of conservation, RE and CRE_S scores are shown as histograms. CRE_S identifies columns which are differentially conserved in the DHA1 family. The phenotypes of the mutated positions in CaMdr1p are indicated by triangles, red being sensitive and pink being differential.

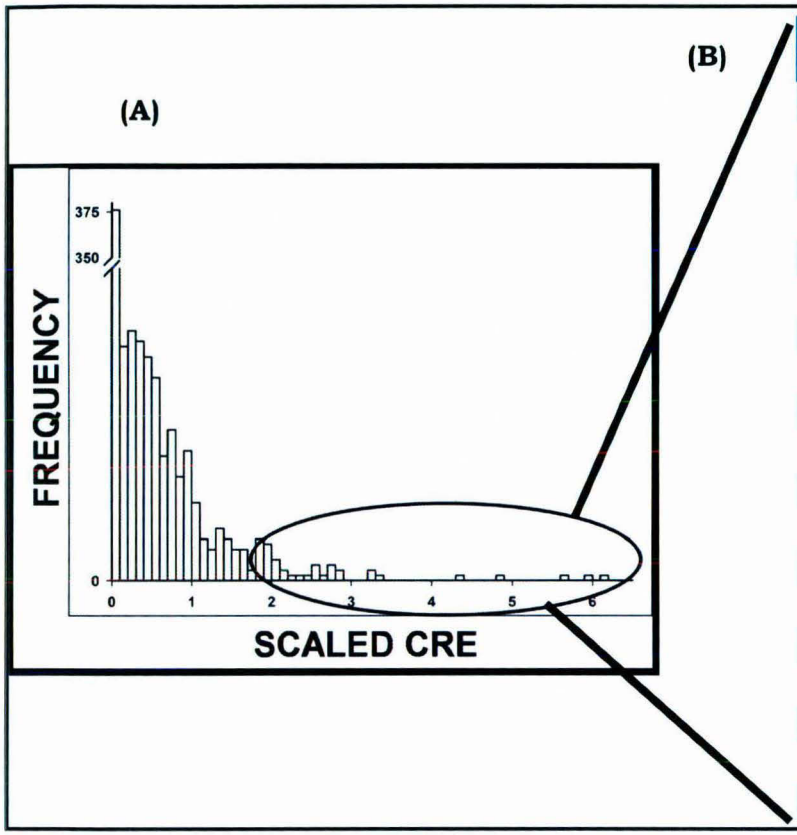

Conservation Score in DHA1	CRE_S	CaMDr1p Residues	Location
1.319	6.12	D235	TMS 4
2.559	5.901	G264	TMS 5
1.671	5.634	P261	TMS 5
1.132	4.891	G133	TMS 1
1.579	3.321	A231	TMS 4
0.936	3.247	G472	TMS 10
0.655	2.892	V364	TMS 7
0.626	2.887	Y369	TMS 7
1.22	2.787	G391	TMS 8
1.008	2.732	G515	TMS 11
0.826	2.711	M132	TMS 1
1.918	2.508	F277	TMS 6
1.516	2.333	P139	TMS 1
0.901	2.143	L246	TMS 5
1.13	2.083	P512	TMS 11
0.814	2.073	S232	TMS 4
0.457	2.046	S505	TMS 11
0.742	1.983	P257	TMS 5
0.92	1.977	V496	TMS 11

Figure 52: Distribution curve of CRE_S values from the complete MSA.

A) Histogram of the CRE_S scores for all positions of an MSA of DHA1 and SP family. The 30 highest scoring CRE_S positions depicted in the marked region were selected for further analysis.

B) The table shows 19 out of the 30 highest scoring CRE_S alignment positions wherein the CaMdr1p residue matched with the most frequent amino acid at that position in the MSA. Their predicted location with respect to CaMdr1p is also displayed in the next column.

3.3.2.2 Site-specific mutagenesis confirms CRE_S based selection of functionally critical residues

Nineteen out of the thirty highest CRE_S alignment positions had the most frequent amino acid matching with the CaMdr1p residue. These are listed in Figure 51B and include D235, G264, P261, G133, A231, G472, V364, Y369, G391, G515, M132, F277, P139, L246, P512, S232, S505, P257 and V496. These residues which were predicted to be functionally relevant were subjected to site-directed mutagenesis and were replaced with alanine. In the cases where glycines were present, they were replaced with leucine while the existing alanines were replaced with glycines. For functional analysis of the mutant variants, a heterologous hyper-expression system was used where GFP-tagged CaMdr1p (CaMDR1-GFP) was stably over-expressed from a genomic *PDR5* locus in AD1-8u$^-$, a *S. cerevisiae* mutant. The host AD1-8u$^-$ developed by Goffeau's group, was derived from a *Pdr1-3* mutant strain with a gain-of-function mutation in the transcription factor Pdr1p, resulting in constitutive hyper-induction of the *PDR5* promoter. A single-copy integration of each transformant at the *PDR5* locus was confirmed by Southern hybridization (data not shown). Two positive clones of each mutant were selected to rule out clonal variations.

The mutant variants of CaMdr1p were analyzed for their drug susceptibility by employing microtiter plate and spot assays. All the high CRE_S residues except P139A showed decreased resistance to tested drugs. Though all the cells expressing mutant variant CaMdr1p, grew poorly on solid as well as in liquid media, a closer look revealed the variation in specificity of residues to drugs and their magnitude of resistance. On the basis of selective sensitivity to various drugs, these mutant variants could be grouped into three classes. Class I included the mutant variants such as D235A, G264L, G133L, G472L, Y369A, G391L, G515L, F277A and S232A which displayed sensitivity towards all the drugs. Notably, P261A, L246A and P257A belong to antiporter motif which also bunched within this class. The residues which showed selective increase in sensitivity towards the considered spectrum of drugs were grouped in Class II. The six mutant variants A231G, M132A, P512A, V496A, S505A and V364A of this class showed selective decrease in resistance at differential levels for various drugs. For example, mutant variants A231G, M132A, P512A and V496A continued to display resistance to FLU, MTX, ANISO, CER but exhibited

sensitivity towards CYH and 4-NQO. S505A was susceptible to ANISO along with CYH and 4-NQO. V364A, on the other hand was different from these as it was resistant only to FLU and MTX while showed sensitivity towards, CER, ANISO, CYH and 4-NQO. The mutant variant P139A which behaved like WT-CaMdr1p-GFP was placed under Class III (Figure 53). The spot assay results were confirmed by microtiter assays as well. The MIC80 values of these mutant variants listed in Table 13 are the index of their susceptibility in the liquid medium.

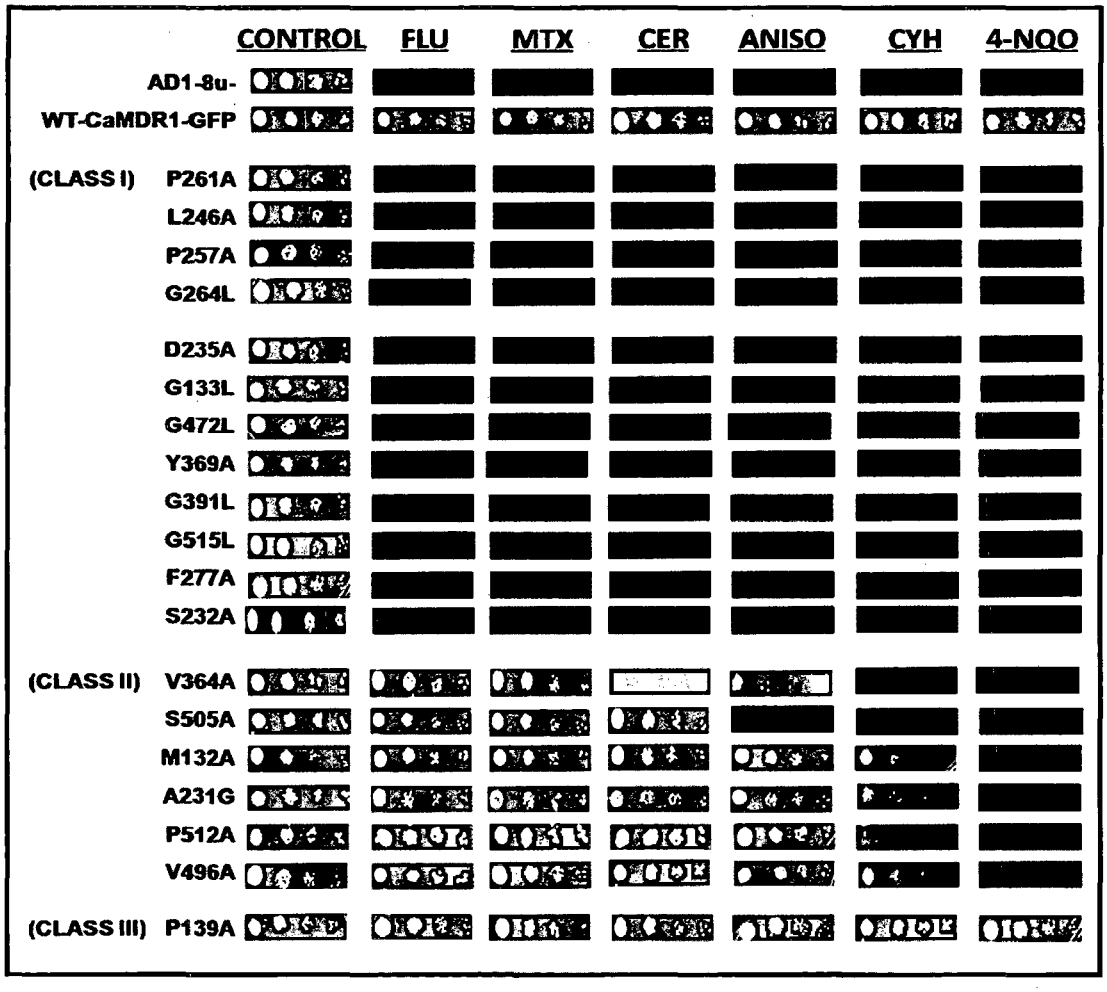

Figure 53: Drug susceptibility assay of mutant variants of high CRE_S residues in CaMdr1p-GFP.

Drug resistance profile of wild-type and mutant CaMDR1-GFP yeast strains as determined by spot assay. 5 µl of five-fold serial dilutions, namely 1 (1:5), 2 (1:25), 3 (1:125) and 4 (1:625), of each strain was spotted on to YEPD plates as described previously in the absence (control) and presence of the following drugs: FLU (0.20 µg/ ml), MTX (65 µg/ ml), CER (3 µg/ ml), ANISO (3 µg/ ml), CYH (0.20 µg/ ml) and 4-NQO (0.20 µg/ ml). Growth differences were recorded following incubation of the plates for 48 hrs at 30°C. Growth was not affected by the presence of the solvents used for the drugs (data not shown).

	MIC_{80} (µg / ml)					
STRAIN	**FLU**	**MTX**	**ANISO**	**CER**	**CYH**	**4-NQO**
AD1-8u-	0.5	16	0.5	0.5	0.015	0.03
WT-CaMDR1-GFP	16	128	32	8	0.5	1.0
CLASS I						
Residues in Antiporter motif						
P261A	0.5	16	0.5	0.5	0.015	0.03
L246A	0.5	16	0.5	0.5	0.015	0.03
P257A	0.5	16	0.5	0.5	0.015	0.03
G264L	0.5	16	0.5	0.5	0.015	0.03
Other Residues						
D235A	0.5	16	0.5	0.5	0.015	0.03
G133L	0.5	16	0.5	0.5	0.015	0.03
G472L	0.5	16	0.5	0.5	0.015	0.03
Y369A	0.5	16	0.5	0.5	0.015	0.03
G391L	0.5	16	0.5	0.5	0.015	0.03
G515L	0.5	16	0.5	0.5	0.015	0.03
F277A	0.5	16	0.5	0.5	0.015	0.03
S232A	0.5	16	0.5	0.5	0.015	0.03
CLASS II						
A231G	8	64	8	4	0.125	0.06
M132A	4	64	32	4	0.125	0.03
P512A	8	64	4	4	0.125	0.06
V496A	8	64	16	2	0.125	0.06
S505A	8	64	0.5	4	0.03	0.06
V364A	4	32	2	1	0.03	0.03
CLASS III						
P139A	16	128	32	8	0.5	1.0

Table 13: MIC_{80} (µg/ml) values of the mutant variants of high CRE_S residues in CaMdr1p.

The residues at high CRE_S positions were tested for their drug susceptibility and their Minimum inhibitory concentration values are listed in comparison with the WT-CaMDR1-GFP and AD1-8u- (Negative control). More than 2-well difference in Microtiter plates was considered as significant, which matched with the results reported on the solid medium in the spot assays [Pasrija *et al.*, 2007].

3.3.2.3 All the mutant variants of CaMdr1p are normally expressed and properly localized

To confirm that the change in susceptibility of mutant variants to various drugs was not due to their poor expression or surface localization, a comparison of the surface expression and localization of GFP-tagged version of CaMdr1p (CaMDR1-GFP) and its mutant variants was done. Notwithstanding the fact that all the mutant variants displayed decreased resistance to drugs, their expression levels matched with that of WT-CaMdr1p-GFP as confirmed by Western Blot Analysis (Figure 54A) while both FACS and confocal imaging confirmed their proper surface localization (rimmed appearance of GFP-tagged CaMdr1p) (Figure 54B).

3.3.2.4 High CRE_S residues displayed abrogated efflux

To validate the drug susceptibility data of the mutant variants, efflux measurements were done by employing three substrates, fluorescent NR, and radiolabel [^{3}H] FLU and [^{3}H] MTX. All the three compounds have been shown to be the substrates of CaMdr1p [Kapoor *et al.*, 2009; Ivnitski-Steele *et al.*, 2009]. The intracellular concentration of these substrates was determined with respect to time. It was observed that there was minimum accumulation of substrates at 30 minutes. Hence a time point of 30 minutes was selected for checking intracellular accumulation of all these three substrates in the mutant variants and then compared with host AD1-8u$^-$. Notably, the level of intracellular accumulation of [^{3}H] FLU, [^{3}H] MTX and NR is indicative of high (low accumulation) or low (high accumulation) efflux activity of the cell mediated by CaMdr1p. Site-directed mutant variants of these high CRE_S positions showed increased accumulation at 30 minutes as compared to that of WT-CaMdr1p and thus indicating a decrease in their ability to efflux NR, [^{3}H] FLU and [^{3}H] MTX. The increased accumulation of NR and [^{3}H] MTX in mutant variants D235A, G264L, P261A, G133L, G472L, Y369A, G391L, G515L, F277A, L246A, S232A and P257A, was attributed to the loss of efflux activity upon mutation. All the other mutant variants which though exhibited different levels of sensitivity to various drugs i.e. V364A, M132A, A231G, P512A and V496A or which remained resistant to all drugs i.e. P139A, continued to efflux these three substrates as efficiently as WT-CaMdr1p. Exceptionally, S505A, which exhibited differential sensitivity towards the

drugs also showed differential accumulation of these substrates. For example, S505A displaying decreased accumulation in case of [^{3}H] FLU and [^{3}H] MTX, showed no change in NR accumulation which was comparable to AD1-8u$^-$ cells (Figure 55).

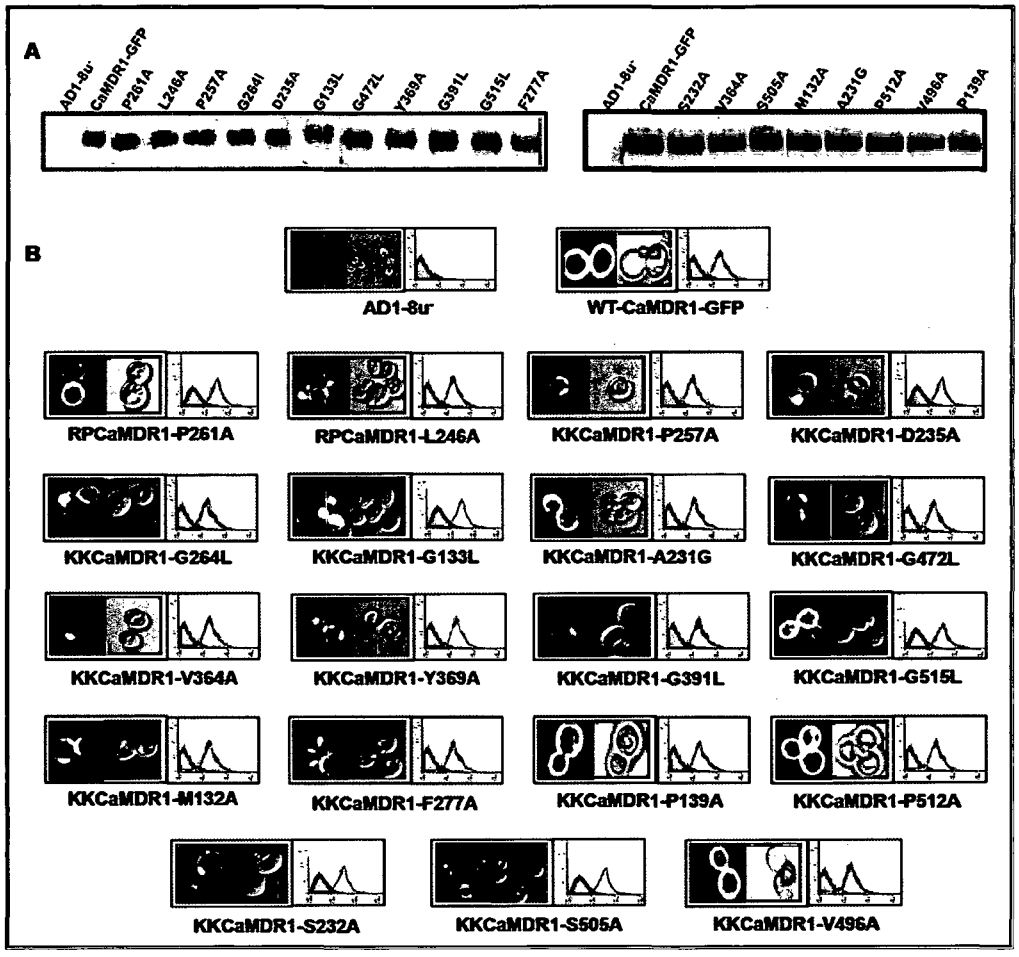

Figure 54: Expression profiles of CaMdr1p-GFP and its mutant variants of high CRE$_S$ residues.

A) Western Blot analysis of the PM fraction of the mutant variants with anti-GFP antibody.

B) Confocal and FACS analysis of the all the mutant variants to check their expression and localization in comparison with AD1-8u$^-$ (negative control) and WT-CaMDR1-GFP (positive control).

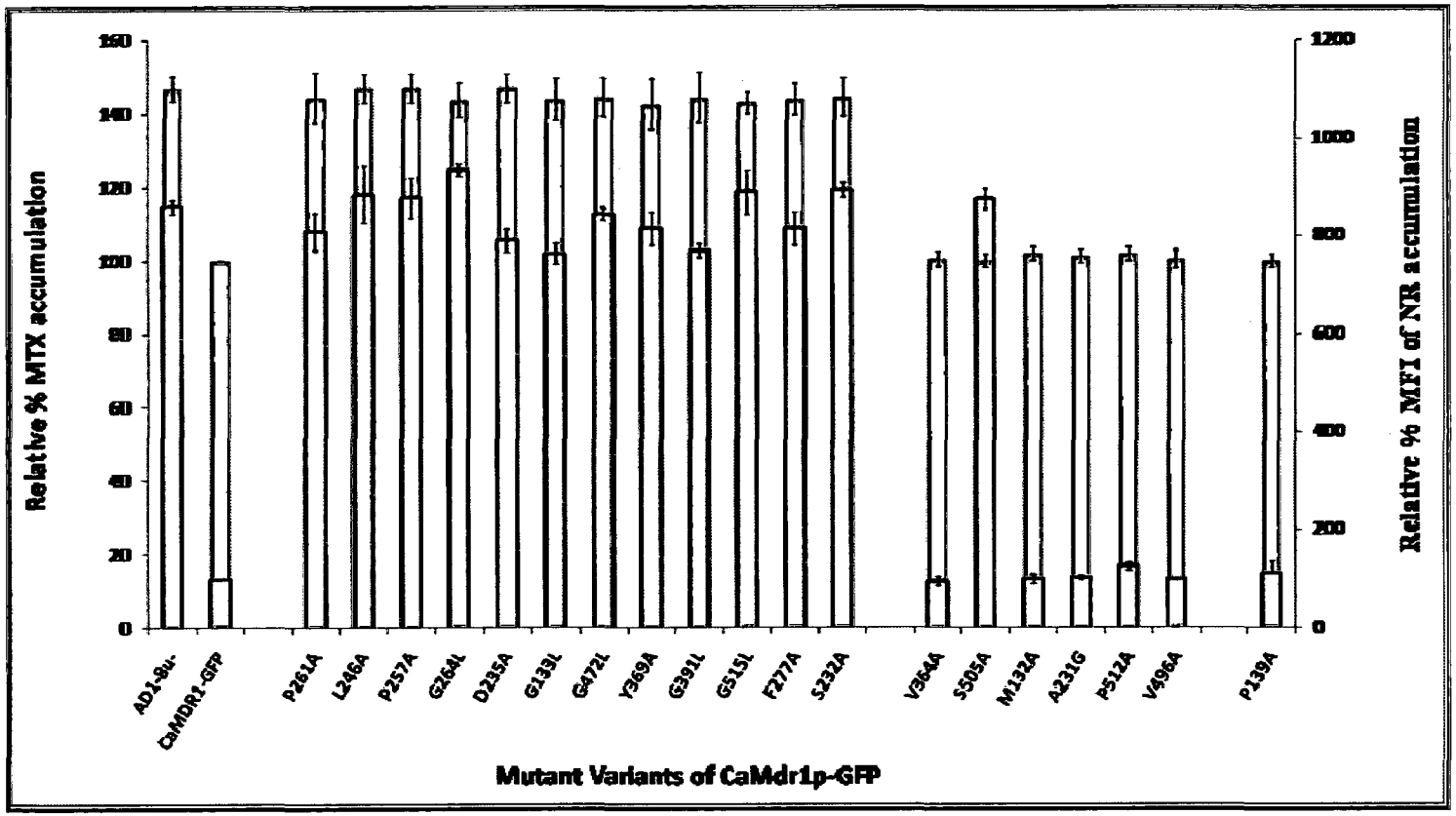

Figure 55: [^{3}H] MTX and NR accumulation in the mutant variants of high CRE$_S$ residues in CaMdr1p-GFP.
The graph shows accumulation levels of these substrates relative to WT-CaMDR1-GFP. The grey colored bars (no border) indicate levels of accumulation for [^{3}H] MTX while empty bars (black border) indicate that for NR. Controls AD1-8u$^-$ and CaMdr1p-GFP have also been included for comparison. The accumulation assays with [^{3}H] FLU gave similar results as [^{3}H] MTX for all the mutant variants (data not shown). The results are means $\pm$ standard deviations for three independent experiments.

3.3.3 DISCUSSION

CaMdr1p is one of the major MDR transporter involved in frequently occurring azole resistance in *C. albicans*. The efflux pump proteins display promiscuity towards substrate specificity wherein a very large number of structurally diverse compounds can be extruded by the transporter. In-depth knowledge of protein structure and function is essential for any logical approach to block the activity of such protein in MDR isolates of *C. albicans*. This study represents an attempt in that direction wherein a rational approach is applied to predict functionally critical amino acids of this transporter. For this, the information theoretic measures were employed which provide objectivity in scoring the differentially conserved residues between two contrasting families [Chakrabarti *et al.*, 2007]. While it is intuitive to select these conserved residues across the subfamily, by a visual analysis of a multiple alignment, however, one tends to miss out the residues which may have a lower conservation but still are functionally important. As CaMdr1p is an antiporter and belongs to DHA1 family, a contrast of DHA1 (antiporters) and SP family (symporters) was done to identify residues differentially conserved between these two families. The CRE across the two families was scaled with respect to the conservation in DHA1 which helped us to enlist the alignment positions on the basis of high CRE as well as high conservation across the entire DHA1 family. This enabled us to identify residues conserved exclusively in DHA1 and those which were differentially conserved among the two families.

The thirty highest CRE_S scoring residues were selected and a further short-listing was done for those which were present in CaMdr1p. The 19 such residues of CaMdr1p D235, G264, P261, G133, A231, G472, V364, Y369, G391, G515, M132, F277, P139, L246, P512, S232, S505, P257 and V496 were subjected to site-directed mutagenesis. The analysis revealed that all the mutant variants except P139A displayed decreased resistance to the tested drugs though at varying degree and specificity. This ranged from having twelve mutant variants D235A, G264L, P261A, G133L, G472L, Y369A, G391L, G515L, F277A, L246A, S232A and P257A showing hypersensitivity to all the drugs, to six variants A231G, V364A M132A, P512A, S505A and V496A which displayed loss in resistance to only selective drugs. The efflux of MTX, FLU and NR by mutant variants was abrogated which matched well

with the loss in drug resistance. It was ensured that such changes were not related to poor expression and surface localization of mutant variant proteins (Figure 54).

As an exception, the criteria of CRE_S also picked up two residues D235 and F277, which were earlier reported to be family-wide function-specific [Kapoor *et al.*, 2009]. This could probably be because the program does not discriminate between the nature of amino acid present in DHA1 and SP families at a given alignment position. Some positions that are scored using this method may be actually excluded using the knowledge of amino acid similarity. For example, at position 235 of CaMdr1p, an aspartate is present. However, a glutamate occurs with same frequency at the respective alignment position in the SP family. This has been identified to be differentially conserved in DHA1 and SP. Another exception, P139, though predicted to be important, failed to show any effect when replaced with alanine.

This study puts forward a list of residues important for DHA1, drug-proton antiporters, when compared against SP, a symporter family. Since functionally critical residues of CaMdr1p are predicted to be DHA1 family specific, this was validated by comparing observations from previously published studies. In VAChT, a human vesicular acetylcholine transporter, a member of DHA1 family, six glycine and proline rich motifs are predicted to promote the formation of special backbone conformations including kinks in TMS, tight interactions between TMS and very flexible β-turns. The hypothesized rocking motions in the MFS family presumably require conformational changes in TMS and β-turns which occur due to the presence of these kinks and notches in the protein [Chandrasekaran *et al.*, 2006]. Interestingly, an analysis of the twelve mutant variants of CaMdr1p which displayed complete sensitivity to all the drugs, and also show abrogated efflux, reveals that most of these are glycines and prolines. Taken together, it can be hypothesized that these residues might be important for functions such as proton-antiport, rocker-switch mechanism or drug binding and translocation and if replaced, would result in a non-functional protein displaying susceptibility to all the drugs. This high propensity for kinks and notches are robustly predicted for motif D2 (lgxxxxxPvxP), motif C (gxxxGPxxGGxl) and motif C' (GxxxGPL). Interestingly, most of these nineteen residues of CaMdr1p with high CRE_S turned out to be part of the well-known motifs of the antiporters. These motifs are identified as Motif C and Motif C'. It is known

that the two halves of the protein must have been formed due to a gene duplication event and thus Motif C' of C-terminal is degenerated as compared to Motif C of N-terminal. Four out of the nineteen residues L246, P257, P261 and G264 are a part of Motif C, a characteristic motif of the antiporters [Ginn *et al.*, 2000], while residues S505, P512 and G515 are a part of Motif C'. Their corresponding positions in VAChT, L214, S225, P229 and G232 in Motif C and V420, P436 and A439 in Motif C' are predicted to form a notch which allows two helical TMS to approach each other closely because small side chains are located at the interface. Motif D2 is located where it might help block non-specific leakage of protons. It is known to hold a kink, which might be involved in bend or swivel during conformational transitions, also called as "molecular hinges". M132 and G133 of CaMdr1p lie in this motif D2. Notably, different levels of sensitivity seen in six other mutant variants A231G, V364A, M132A, P512A, S505A and V496A points to the fact that even though there is a single pore for proton antiport and drug binding and translocation, yet there are residues which impart selectivity in drug recognition along with those which affect the transport of all the drugs. Of note, most of these residues with high CRE_S are located in or near the pore in the 3D homology model of CaMdr1p, thus validating their relevance (Figure 56). The application of this method to another MFS-MDR transporter EmrD of *E. coli* further reveals that few of its functionally critical residues with high CRE_S score could be matched with equipositional residues of CaMdr1p. For example, P257, P261 and S505 of CaMdr1p which correspond to P145, P149 and G340 of EmrD, respectively, are predicted to be non-cavity lining residues as explained by the known crystal structure of EmrD [Jeon *et al.*, 2009]. Thus, the predictions are not only valid for CaMdr1p but could be extended to the entire DHA1 family.

Conservation, RE_{null} and CRE_S are three different scores which are routinely used to predict functionally critical residues of a protein. Figure 57 shows a comparison among them and reveals an interesting correlation. Traditional conservation, which uses amino acid similarity, selects residues indiscriminately across the transmembrane regions of the protein. These regions are predominantly hydrophobic, as required for optimal positioning within the hydrophobic environment of the lipid membrane. RE_{null} helps in subtracting these background conservation signals but can allow us to select only the residues which are important for family-

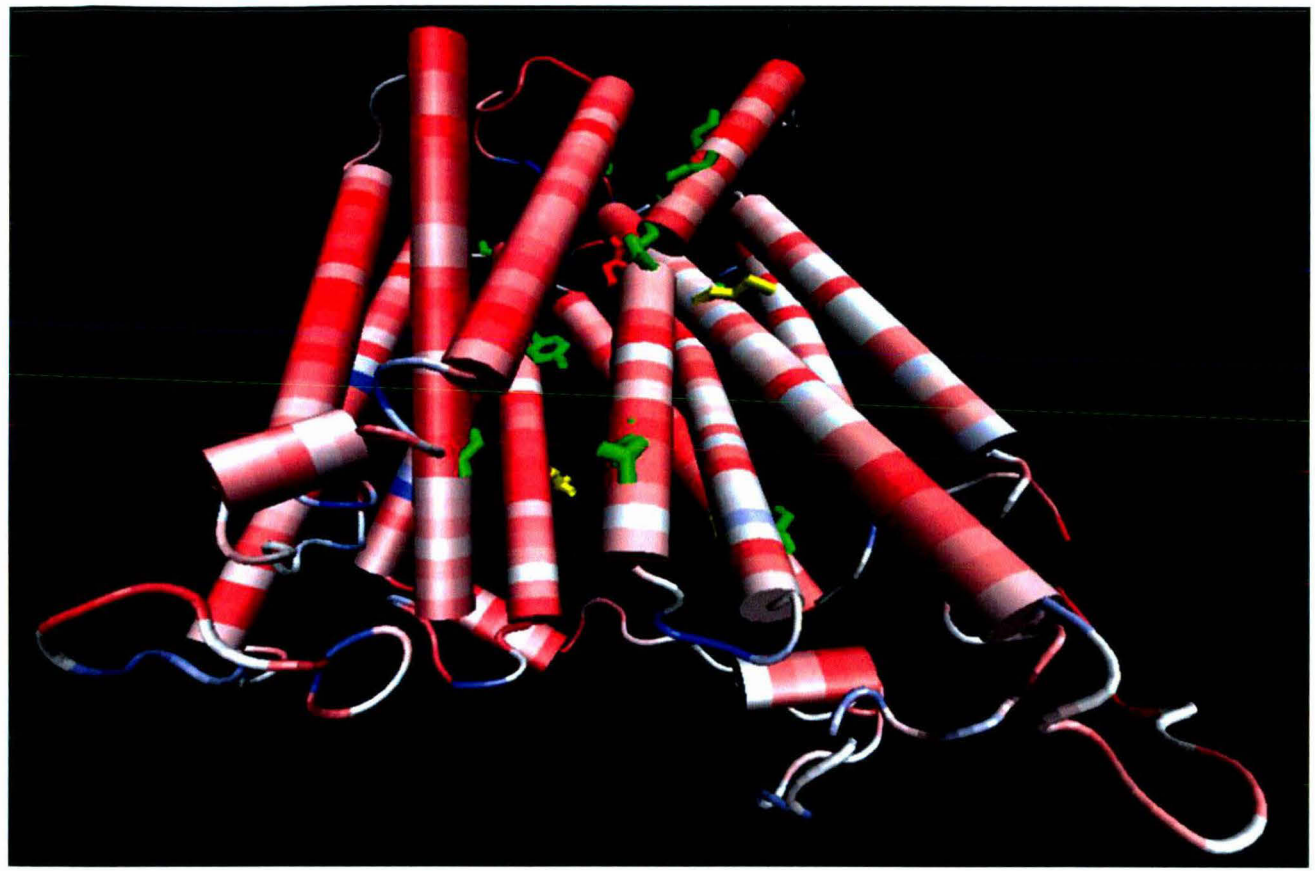

Figure 56: The deduced 3D homology model of CaMdr1p highlighting the positions of the mutated high CRE_S residues.
The 3D homology model of CaMdr1p wherein the mutated residues are marked onto the model and are coloured on the basis of the phenotypes exhibited upon mutation. Green denotes sensitive, red shows resistant while yellow marks the residues which exhibit differential sensitivity towards drugs upon mutation. The structure is viewed using Visual Molecular Dynamic (VMD) software.

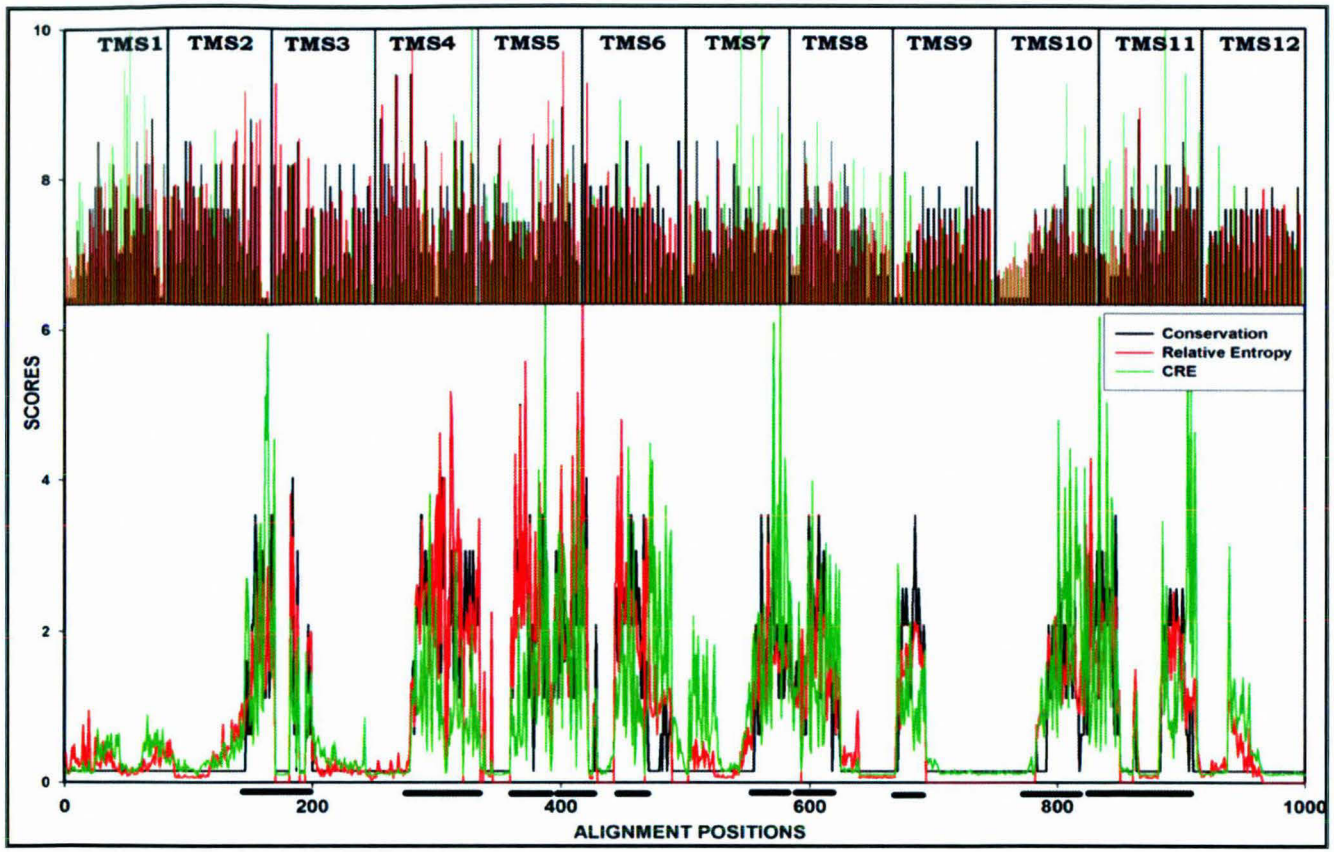

Figure 57: Comparative plot of Conservation, RE_{NULL} and CRE_S across the entire alignment.
Conservation in DHA1 family (black), REnull across DHA1 family (red) and CRES (green) are drawn as a line graph for all the alignment positions in the bottom panel of the Figure. Locations of the TMS are marked by black bars on the x-axis. These twelve TMS are shown separately as an inset in the top panel so to highlight the effectiveness of CRE_S over RE and traditional conservation.

wide function [Kapoor *et al.*, 2009]. Discernible from the Figure 57, is that the RE_{null} of DHA family is higher in the N-terminal half as compared to the C-terminal half of the protein, which supports the hypothesis that MFS proteins after duplication, have concentrated family-wide function specific residues in the N-terminal half, while allowing divergence in the C-terminal half for more specific function such as substrate binding and translocation [Paulsen *et al.*, 1996]. A comparison of an antiporter-specific alignment with a symporter-specific alignment further helped us to subtract MFS family-wide signals, so as to highlight residues, responsible for antiporter specificity. From this differential comparison, a concentration of signals around TMS 5-a known "antiporter motif" is seen where residues are highlighted by the use of CRE_S and this provides internal validation for the method. Other high-scoring residues are distributed over both the N-terminal and the C-terminal halves thus satisfying the earlier observation that substrate specificity is contributed by residues in the C-terminal, and providing a much sought after selection of novel residues, which are predicted to be important for drug antiporter function.

In conclusion, this study shows that by using an information theoretic measure, it is possible to rationally conduct structure and functional study of a major MFS antiporter Mdr1p of *C. albicans*. The function-specific residues identified therein are not only critical for CaMdr1p but are valid for the entire DHA1 family. This analysis effectively shows that few residues in or around the pore differ on the basis of the mechanism of an MFS transporter and are thus specific for a particular family. Such residues are important for classifying a sequence to be a MFS-MDR transporter as validated from CaMdr1p. Owing to the limited studies done on CaMdr1p, this study opens up new options for designing inhibitors / modulators to block the activity of this important transporter. However, that remains a challenging task.

SUMMARY

SUMMARY

From the relative simplicity of bacterial cells, fungi and protozoa to the complexity of human cancer cells, MDR has become problematic and decreases the chance of providing successful treatment against a plethora of diseases. *Candida albicans* is an opportunistic diploid fungus that causes infection in immunocompromised and debilitated patients [Odds, 1988]. Wide spread and prolonged usage of azoles in recent years has led to the rapid development of the phenomenon of azole resistance which poses a major threat to antifungal therapy [Calderone, 2002; White *et al.*, 1998]. MDR is a multifactorial phenomenon where a combination of mechanisms could contribute to drug resistance [White, 1997; Franz *et al.*, 1998; Lopez-Ribot *et al.*, 1998]. One of the most clinically significant mechanisms of azole resistance in pathogenic yeast *Candida albicans* is the over-expression of the drug extrusion pump encoding genes belonging to either ABC Superfamily, e.g. *CDR1* and *CDR2* or MFS e.g. Ca*MDR1* [Fling *et al.*, 1991; Ben-Yaacov *et al.*, 1994; Prasad *et al.*, 1995; Sanglard *et al.*, 1997]. The ABC and MFS superfamilies are designated by Transport commission (TC) system as TC 3.A.1 and TC 2.A.1, respectively [Busch and Saier, 2002]. Whereas the ABC transporters bind ATP and require ATP hydrolysis for transport activity, the MFS mediated transport is driven by the proton-motive force. Members of both classes are found in all three kingdoms of life and are apparently involved in transport of solutes across the plasma membrane or across intracellular membranes. Subfamilies have been defined on the basis of structural and functional criteria [Pao *et al.*, 1998; Saier, 1999] but the physiological substrates are known only for a few transporters. Both ABC and MFS transporters are encoded by large gene families that have been characterized extensively [Decottignies and Goffeau, 1997; Goffeau *et al.*, 1997; Nelissen *et al.*, 1997; Bauer *et al.*, 1999; Wolfger *et al.*, 2001; Sa-Correia and Tenreiro, 2002]. Members of both classes can have broad and overlapping substrate specificities. Owing to the fact that all eukaryotic genomes encode several gene families capable of encoding MDR functions, among which the ABC and MFS transporters are the largest, the number of candidate MDR genes in both these superfamilies means that study of the drug resistance properties of an organism cannot be effectively carried out without taking a wider perspective. In comparison to ABC transporters Cdr1p and Cdr2p which are well-studied, the MFS transporter CaMdr1p is poorly explored

[Shukla *et al.*, 2003; Saini *et al.*, 2005; Gupta *et al.*, 1998; Pasrija *et al.*, 2007]. In-depth knowledge of structure and function of CaMdr1p is necessary for an effective designing of modulators or inhibitors of this efflux transporter.

1. Random mutational analyses of the multidrug MFS transporter CaMdr1p

- A random mutational analysis of MFS transporter CaMdr1p using the traditional measure of conservation as the criteria for selection of the residues was followed. The conserved residues of CaMdr1p were mutated to alanine to elucidate their role in the functioning of CaMdr1p.
- The drug susceptibility assays classify the mutant variants of these conserved residues under three classes. Class-I G165L, P170A, G183L, R184A, G219A, D235A, P261A, E297A, Y365A, Y369A, E429A and S495A were extremely sensitive to all the drugs tested. Class-II P175A, S177A, A203G, E351A and Y360A had differential sensitivity towards the spectrum of drugs. Class-III G165A, G183A, W273A, R274A, P352A, P428A, F449A, W459A, P462A, F511A and W531A which were when replaced with alanine, showed level of resistance comparable to WT-CaMdr1p.
- Localization and expression of mutant CaMdr1p variants remained unaltered: All mutant CaMdr1p variants were localized at the plasma membrane and showed similar expression levels.
- The Class I mutant variants showed an increase in accumulation of [^{3}H] MTX and [^{3}H] FLU while Class II and III mutant variants had levels like that of the wild-type.
- Cysteine-scanning was employed so as to assess the structure-function relationship of this protein. Individual cysteine mutations to alanine did not lead to any effect on the drug susceptibilities of these mutant variants. A cysless-CaMdr1p was created which opens up as plethora of options to explore the mechanistic details of this MFS antiporter. It was sensitive to drugs as compared to the wild-type but still exhibited a considerable resistance towards these drugs.
- Localization of these individual cysteine mutant variants as well as the cysless-CaMdr1p was not affected.

- An analysis of the unique N-terminal of CaMdr1p revealed by site-directed mutagenesis followed by construction of deletion mutants predicts its role in surface localization of this protein.
- Of note, this random site-directed mutational study reveals the structural and functional details of this transporter but a better approach was required for identifying the critical residues for specific function of CaMdr1p. Moreover, efficacy of site-directed mutagenesis was comparatively low. Taken together, a more rationalized approach was needed to be developed which involved the usage of bioinformatics.

2. Membrane environment based rational computational approach for identification of family-wide-function specific residues of CaMdr1p

- A rational mutational analysis was done which uses a membrane environment based computational approach to predict the functionally critical residues of CaMdr1p. For this, Information theoretic scores which are variants of Relative Entropy (Modified Relative Entropy RE_M) were calculated from Multiple Sequence Alignment (MSA) of 361 MFS sequences, by separately considering distinct physico-chemical properties of transmembrane (TM) and inter-TM regions.
- The residues of CaMdr1p with high RE_M which were predicted to be significantly important were subjected to site-directed mutational analysis. Interestingly, heterologous host *S. cerevisiae*, over-expressing these mutant variants of CaMdr1p wherein these high RE_M residues were replaced by either alanine or leucine, demonstrated increased susceptibility to tested drugs.
- The hypersensitivity to drugs was supported by abrogated substrate efflux mediated by mutant variant proteins and was not attributed to their poor expression or surface localization.
- Additionally, by employing a distance plot from a 3D deduced model of CaMdr1p, the role of these functionally critical residues could be predicted in maintaining apparent inter-helical interactions to provide the desired fold for the proper functioning of CaMdr1p.

- Residues predicted to be critical for function across the family were also found to be vital from other previously published studies, implying its wider application to other membrane protein families.
- This study provides an insight into the molecular details of MFS transporters in general and CaMdr1p in particular. This method of scaled RE_M calculations improves its performance over other information theoretic methods.
- Additionally, this study also provides a method for rational mutational analysis not only for MFS proteins but can be applied to any class of membrane proteins and thus makes it possible to predict and locate family-wide functionally relevant residues.

3. Identification of drug-proton antiporter function specific residues of CaMdr1p by employing information theoretic measures

- This study employs information theoretic measures to present a structure and functional analysis of this multidrug-proton antiporter Mdr1p of *Candida albicans* by predicting residues important for drug-proton antiporter function.
- Since CaMdr1p belongs to drug-proton antiporter (DHA1) family of MFS transporters, this DHA1 family (antiporters) was contrasted with Sugar Porter family (symporters). Cumulative Relative Entropy (CRE) calculated for these two sets of alignments enabled us to selectively identify conserved residues of not only CaMdr1p but for the entire DHA1 family.
- Based on CRE, the highest scoring thirty positions were selected and predicted to impart functional specificity to CaMdr1p as well as to other drug-proton antiporters. Nineteen positions wherein the CaMdr1p residue matched with the most frequent amino acid at a particular alignment position of DHA1 members were subjected to site-directed mutagenesis and were replaced with either alanine or leucine.
- All these residues, except one, displayed either complete or selective sensitivity to the tested drugs. The enhanced susceptibility of these mutant variants was corroborated with the simultaneously abrogated efflux of substrates. Taken together, based on scaled CRE between two MFS sub-families, this study could accurately predict the functionally relevant residues of CaMdr1p.

- An extrapolation of these predictions to the entire DHA1 family as validated from previously published data shows that the equipositional residues in other members of the DHA1 family are also functionally critical.
- This analysis effectively shows that few residues in or around the pore differ on the basis of the mechanism of an MFS transporter and are thus specific for a particular family. Such residues are important for classifying a sequence to be a MFS-MDR transporter as validated from CaMdr1p.
- In conclusion, this study shows that by using an information theoretic measure, it is possible to rationally conduct structure and functional study of a major MFS antiporter CaMdr1p. The function-specific residues identified therein are not only critical for CaMdr1p but are valid for the entire DHA1 family.

REFERENCES

REFERENCES

Abramson, J., Smirnova, I., Kasho, V., Verner, G., Kaback, H.R. & Iwata, S. 2003, "Structure and mechanism of the lactose permease of *Escherichia coli*", *Science,* vol. 301, no. 5633, pp. 610-615.

Alarco, A.M., Balan, I., Talibi, D., Mainville, N. & Raymond, M. 1997, "Ap1-mediated multidrug resistance in *Saccharomyces cerevisiae* requires FLR1 encoding a transporter of the major facilitator superfamily", *Journal of Biological Chemistry,* vol. 272, no. 31, pp. 19304-19313.

Allikmets, R., Gerrard, B., Stewart, C., White, M. & Dean, M. 1993, "Identification of P-glycoprotein/multidrug resistance genes from model organisms", *Leukemia,* vol. 7, no. SUPPL. 2, pp. S13-S17.

Altschul, S.F., Gish, W., Miller, W., Myers, E.W. & Lipman, D.J. 1990, "Basic local alignment search tool", *Journal of Molecular Biology,* vol. 215, no. 3, pp. 403-410.

Ambudkar, S.V. & Maloney, P.C. 1984, "Characterization of phosphate:hexose 6-phosphate antiport in membrane vesicles of *Streptococcus lactis*", *Journal of Biological Chemistry,* vol. 259, no. 20, pp. 12576-12585.

Ambudkar, S.V. & Maloney, P.C. 1985, "Reconstitution of anion exchange from *Streptococcus lactis*", *Federation proceedings,* vol. 44, no. 5.

Ambudkar, S.V., Larson, T.J. & Maloney, P.C. 1986, "Reconstitution of sugar phosphate transport systems of *Escherichia coli*", *Journal of Biological Chemistry,* vol. 261, no. 20, pp. 9083-9086.

Andriole, V.T. 1999, "Current and future antifungal therapy: New targets for antifungal agents", *Journal of Antimicrobial Chemotherapy,* vol. 44, no. 2, pp. 151-162.

Azzaria, M., Schurr, E. & Gros, P. 1989, "Discrete mutations introduced in the predicted nucleotide-binding sites of the *mdr1* gene abolish its ability to confer multidrug resistance", *Molecular and cellular biology,* vol. 9, no. 12, pp. 5289-5297.

Balan, I., Alarco, A.M. & Raymond, M. 1997, "The *Candida albicans* CDR3 gene codes for an opaque-phase ABC transporter", *Journal of Bacteriology,* vol. 179, no. 23, pp. 7210-7218.

Barton, G.J. 1993, "ALSCRIPT: A tool to format multiple sequence alignments", *Protein engineering,* vol. 6, no. 1, pp. 37-40.

Bauer, B.E., Wolfger, H. & Kuchler, K. 1999, "Inventory and function of yeast ABC proteins: About sex, stress, pleiotropic drug and heavy metal resistance", *Biochimica et Biophysica Acta - Biomembranes,* vol. 1461, no. 2, pp. 217-236.

Ben-Yaacov, R., Knoller, S., Caldwell, G.A., Becker, J.M. & Koltin, Y. 1994, "*Candida albicans* gene encoding resistance to benomyl and methotrexate is a multidrug resistance gene", *Antimicrobial Agents and Chemotherapy,* vol. 38, no. 4, pp. 648-652.

Bhatia, A., Schäfer, H.-. & Hrycyna, C.A. 2005, "Oligomerization of the human ABC transporter ABCG2: Evaluation of the native protein and chimeric dimers", *Biochemistry,* vol. 44, no. 32, pp. 10893-10904.

Biedler, J.L. & Riehm, H. 1970, "Cellular resistance to actinomycin D in Chinese hamster cells in vitro: cross-resistance, radioautographic, and cytogenetic studies", *Cancer research,* vol. 30, no. 4, pp. 1174-1184.

Bossche, H.V., Marichal, P., Odds, F.C., Le Jeune, L. & Coene, M.-. 1992, "Characterization of an azole-resistant *Candida glabrata* isolate", *Antimicrobial Agents and Chemotherapy,* vol. 36, no. 12, pp. 2602-2610.

Busch, W. & Saier Jr., M.H. 2002, "The Transporter Classification (TC) system, 2002", *Critical reviews in biochemistry and molecular biology,* vol. 37, no. 5, pp. 287-337.

Buschman, E. & Gros, P. 1991, "Functional analysis of chimeric genes obtained by exchanging homologous domains of the mouse *mdr1* and *mdr2* genes", *Molecular and cellular biology,* vol. 11, no. 2, pp. 595-603.

Calderone R.A. 2002, "*Candida* and Candidiasis", ASM Press, Washington, D.C.

Capra, J.A. & Singh, M. 2008, "Characterization and prediction of residues determining protein functional specificity", *Bioinformatics,* vol. 24, no. 13, pp. 1473-1480.

Castillo, G., Shen, H.J. & Horwitz, S.B. 1995, "A homologue of the mammalian multidrug resistance gene (*MDR*) is functionally expressed in the intestine of *Xenopus laevis*", *Biochimica et Biophysica Acta - Gene Structure and Expression,* vol. 1262, no. 2-3, pp. 113-123.

Chakrabarti, S., Bryant, S.H. & Panchenko, A.R. 2007, "Functional Specificity Lies within the Properties and Evolutionary Changes of Amino Acids", *Journal of Molecular Biology,* vol. 373, no. 3, pp. 801-810.

Chandrasekaran, A., Ojeda, A.M., Kolmakova, N.G. & Parsons, S.M. 2006, "Mutational and bioinformatics analysis of proline- and glycine-rich motifs in vesicular acetylcholine transporter", *Journal of neurochemistry,* vol. 98, no. 5, pp. 1551-1559.

Chang, A.B., Lin, R., Studley, W.K., Tran, C.V. & Saier Jr., M.H. 2004, "Phylogeny as a guide to structure and function of membrane transport proteins", *Molecular membrane biology,* vol. 21, no. 3, pp. 171-181.

Chapeland-Leclerc, F., Bouchoux, J., Goumar, A., Chastin, C., Villard, J. & Noël, T. 2005, "Inactivation of the *FCY2* gene encoding purine-cytosine permease promotes cross-resistance to flucytosine and fluconazole in *Candida lusitaniae*", *Antimicrobial Agents and Chemotherapy,* vol. 49, no. 8, pp. 3101-3108.

Chen, C.P., Kernytsky, A. & Rost, B. 2002, "Transmembrane helix predictions revisited", *Protein Science,* vol. 11, no. 12, pp. 2774-2791.

Consler, T.G., Persson, B.L., Jung, H., Zen, K.H., Jung, K., Prive, G.G., Verner, G.E. & Kaback, H.R. 1993, "Properties and purification of an active biotinylated lactose permease from *Escherichia coli*", *Proceedings of the National Academy of Sciences of the United States of America,* vol. 90, no. 15, pp. 6934-6938.

Crowley, E. & Callaghan, R. 2010, "Multidrug efflux pumps: Drug binding-gates or cavity?", *FEBS Journal,* vol. 277, no. 3, pp. 530-539.

Davidson, A.L. & Maloney, P.C. 2007, "ABC transporters: how small machines do a big job", *Trends in microbiology,* vol. 15, no. 10, pp. 448-455.

Davidson, A.L., Laghaeian, S.S. & Mannering, D.E. 1996, "The maltose transport system of *Escherichia coli* displays positive cooperativity in ATP hydrolysis", *Journal of Biological Chemistry,* vol. 271, no. 9, pp. 4858-4863.

Dawson, R.J.P. & Locher, K.P. 2006, "Structure of a bacterial multidrug ABC transporter", *Nature,* vol. 443, no. 7108, pp. 180-185.

De Backer, M.D., Ilyina, T., Ma, X.J., Vandoninck, S., Luyten, W.H.M.L. & Bossche, H.V. 2001, "Genomic profiling of the response of *Candida albicans* to itraconazole treatment using a DNA microarray", *Antimicrobial Agents and Chemotherapy,* vol. 45, no. 6, pp. 1660-1670.

De Rossi, E., Arrigo, P., Bellinzoni, M., Silva, P.E.A., Martín, C., Aînsa, J.A., Guglierame, P. & Riccardi, G. 2002, "The multidrug transporters belonging to major facilitator superfamily (MFS) in *Mycobacterium tuberculosis*", *Molecular Medicine,* vol. 8, no. 11, pp. 714-724.

Dean, M. & Allikmets, R. 1995, "Evolution of ATP-binding cassette transporter genes", *Current Opinion in Genetics and Development,* vol. 5, no. 6, pp. 779-785.

Decottignies, A. & Goffeau, A. 1997, "Complete inventory of the yeast ABC proteins", *Nature genetics,* vol. 15, no. 2, pp. 137-145.

Ditty, J.L. & Harwood, C.S. 1999, "Conserved cytoplasmic loops are important for both the transport and chemotaxis functions of PcaK, a protein from *Pseudomonas putida* with 12 membrane-spanning regions", *Journal of Bacteriology,* vol. 181, no. 16, pp. 5068-5074.

Dogra, S., Krishnamurthy, S., Gupta, V., Dixit, B.L., Gupta, C.M., Sanglard, D. & Prasad, R. 1999, "Asymmetric distribution of phosphatidylethanolamine in *C. albicans*: Possible mediation by CDR1, a multidrug transporter belonging to ATP binding cassette (ABC) superfamily", *Yeast,* vol. 15, no. 2, pp. 111-121.

Douglas, C.M., D'Ippolito, J.A., Shei, G.J., Meinz, M., Onishi, J., Marrinan, J.A., Li, W., Abruzzo, G.K., Flattery, A., Bartizal, K., Mitchell, A. & Kurtz, M.B. 1997, "Identification of the *FKS1* gene of *Candida albicans* as the essential target of 1,3-β-D-glucan synthase inhibitors", *Antimicrobial Agents and Chemotherapy,* vol. 41, no. 11, pp. 2471-2479.

Dudler, R. & Hertig, C. 1992, "Structure of an mdr-like gene from *Arabidopsis thaliana.* Evolutionary implications", *Journal of Biological Chemistry,* vol. 267, no. 9, pp. 5882-5888.

Edgar, R.C. 2004, "MUSCLE: Multiple sequence alignment with high accuracy and high throughput", *Nucleic acids research,* vol. 32, no. 5, pp. 1792-1797.

Edgar, R.C. 2004, "MUSCLE: Multiple sequence alignment with improved accuracy and speed", , pp. 728.

Egner, R., Bauer, B.E. & Kuchler, K. 2000, "The transmembrane domain 10 of the yeast Pdr5p ABC antifungal efflux pump determines both substrate specificity and inhibitor susceptibility", *Molecular microbiology,* vol. 35, no. 5, pp. 1255-1263.

Egner, R., Rosenthal, F.E., Kralli, A., Sanglard, D. & Kuchler, K. 1998, "Genetic separation of FK506 susceptibility and drug transport in the yeast Pdr5 ATP-binding cassette multidrug resistance transporter", *Molecular biology of the cell,* vol. 9, no. 2, pp. 523-543.

Endicott, J.A. & Ling, V. 1989, "The biochemistry of P-glycoprotein-mediated multidrug resistance", *Annual Review of Biochemistry,* vol. 58, pp. 137-171.

Ernst J.F, Schmidt A. 2000, "Dimorphism in Human pathogenic and apathogenic yeasts". Karger, Switzerland.

Ernst, R., Kueppers, P., Klein, C.M., Schwarzmueller, T., Kuchler, K. & Schmitt, L. 2008, "A mutation of the H-loop selectively affects rhodamine transport by the yeast multidrug ABC transporter Pdr5", *Proceedings of the National Academy of Sciences of the United States of America,* vol. 105, no. 13, pp. 5069-5074.

Espinel-Ingroff, A., Barchiesi, F., Hazen, K.C., Martinez-Suarez, J.V. & Scalise, G. 1998, "Standardization of antifungal susceptibility testing and clinical relevance", *Medical Mycology, Supplement,* vol. 36, no. 1, pp. 68-78.

Favre, B. & Ryder, N.S. 1997, "Cloning and expression of squalene epoxidase from the pathogenic yeast *Candida albicans*", *Gene,* vol. 189, no. 1, pp. 119-126.

Favre, B., Didmon, M. & Ryder, N.S. 1999, "Multiple amino acid substitutions in lanosterol 14α-demethylase contribute to azole resistance in *Candida albicans*", *Microbiology,* vol. 145, no. 10, pp. 2715-2725.

Ferry, D.R., Russell, M.A. & Cullen, M.H. 1992, "P-glycoprotein possesses a 1,4-dihydropyridine-selective drug acceptor site which is allosterically coupled to a vinca-alkaloid-selective binding site", *Biochemical and biophysical research communications,* vol. 188, no. 1, pp. 440-445.

Ferté, J. 2000, "Analysis of the tangled relationships between P-glycoprotein-mediated multidrug resistance and the lipid phase of the cell membrane", *European Journal of Biochemistry,* vol. 267, no. 2, pp. 277-294.

Fischer, J.D., Mayer, C.E. & Söding, J. 2008, "Prediction of protein functional residues from sequence by probability density estimation", *Bioinformatics,* vol. 24, no. 5, pp. 613-620.

Fleischmann, R.D., Adams, M.D., White, O., Clayton, R.A., Kirkness, E.F., Kerlavage, A.R., Bult, C.J., Tomb, J.F., Dougherty, B.A., Merrick, J.M., McKenney, K., Sutton, G., FitzHugh, W., Fields, C., Gocayne, J.D., Scott, J., Shirley, R., Liu, L.-. & Venter, J.C. 1995, "Whose-genome random sequencing and assembly of *Haemophilus influenzae* Rd", *Science,* vol. 269, no. 5223, pp. 496-521.

Fling, M.E., Kopf, J., Tamarkin, A., Gorman, J.A., Smith, H.A. & Koltin, Y. 1991, "Analysis of a *Candida albicans* gene that encodes a novel mechanism for resistance to benomyl and methotrexate", *Molecular and General Genetics,* vol. 227, no. 2, pp. 318-329.

Foote, S.J., Thompson, J.K., Cowman, A.F. & Kemp, D.J. 1989, "Amplification of the multidrug resistance gene in some chloroquine-resistant isolates of *P. falciparum*", *Cell,* vol. 57, no. 6, pp. 921-930.

Franz, R., Michel, S. & Morschhäuser, J. 1998, "A fourth gene from the *Candida albicans* CDR family of ABC transporters", *Gene,* vol. 220, no. 1-2, pp. 91-98.

Frillingos, S., Sahin-Tóth, M., Wu, J. & Kaback, H.R. 1998, "Cys-scanning mutagenesis: A novel approach to structure-function relationships in polytopic membrane proteins", *FASEB Journal,* vol. 12, no. 13, pp. 1281-1299.

Gärtner, J. & Valle, D. 1993, "The 70 kDa peroxisomal membrane protein: An ATP-binding cassette transporter protein involved in peroxisome biogenesis", *Seminars in Cell and Developmental Biology,* vol. 4, no. 1, pp. 45-52.

Gaur, M., Choudhury, D. & Prasad, R. 2005, "Complete inventory of ABC proteins in human pathogenic yeast, *Candida albicans*", *Journal of Molecular Microbiology and Biotechnology,* vol. 9, no. 1, pp. 3-15.

Gaur, M., Puri, N., Manoharlal, R., Rai, V., Mukhopadhayay, G., Choudhury, D. & Prasad, R. 2008, "MFS transportome of the human pathogenic yeast *Candida albicans*", *BMC genomics,* vol. 9, pp. 579.

Geber, A., Hitchcock, C.A., Swartz, J.E., Pullen, F.S., Marsden, K.E., Kwon-Chung, K.J. & Bennett, J.E. 1995, "Deletion of the *Candida glabrata ERG3* and *ERG11* genes: Effect on cell viability, cell growth, sterol composition, and antifungal susceptibility", *Antimicrobial Agents and Chemotherapy,* vol. 39, no. 12, pp. 2708-2717.

Gerber, S., Comellas-Bigler, M., Goetz, B.A. & Locher, K.P. 2008, "Structural basis of trans-inhibition in a molybdate/tungstate ABC transporter", *Science,* vol. 321, no. 5886, pp. 246-250.

Ghannoum, M.A. & Rice, L.B. 1999, "Antifungal agents: Mode of action, mechanisms of resistance, and correlation of these mechanisms with bacterial resistance", *Clinical microbiology reviews,* vol. 12, no. 4, pp. 501-517.

Ginn, S.L., Brown, M.H. & Skurray, R.A. 2000, "The TetA(K) tetracycline/H+ antiporter from *Staphylococcus aureus*: Mutagenesis and functional analysis of motif C", *Journal of Bacteriology,* vol. 182, no. 6, pp. 1492-1498.

Goffeau, A., Park, J., Paulsen, I.T., Jonniaux, J.L., Dinh, T., Mordant, P. & Saier Jr., M.H. 1997, "Multidrug-resistant transport proteins in yeast: Complete inventory and phylogenetic characterization of yeast open reading frames within the major facilitator superfamily", *Yeast,* vol. 13, no. 1, pp. 43-54.

Golin, J., Ambudkar, S.V., Gottesman, M.M., Habib, A.D., Sczepanski, J., Ziccardi, W. & May, L. 2003, "Studies with novel Pdr5p substrates demonstrate a strong size dependence for xenobiotic efflux", *Journal of Biological Chemistry,* vol. 278, no. 8, pp. 5963-5969.

Gottesman, M.M. & Pastan, I. 1993, "Biochemistry of multidrug resistance mediated by the multidrug transporter", *Annual Review of Biochemistry,* vol. 62, pp. 385-427.

Gros, P. & Buschman, E. 1993, "The mouse multidrug resistance gene family: Structural and functional analysis", *International review of cytology,* vol. 137 C, pp. 169-197.

Guan, L., Kaback, H.R. 2006, "Lessons from lactose permease", *Annual Reviews in . Biophysical and Biomolecular Structures,* vol. 35, pp. 67-91.

Guan, L., Mirza, O., Verner, G., Iwata, S. & Kaback, H.R. 2007, "Structural determination of wild-type lactose permease", *Proceedings of the National Academy of Sciences of the United States of America,* vol. 104, no. 39, pp. 15294-15298.

Gupta, V., Kohli, A., Krishnamurthy, S., Puri, N., Aalamgeer, S.A., Panwar, S. & Prasad, R. 1998, "Identification of polymorphic mutant alleles of *CaMDR1*, a major facilitator of *Candida albicans* which confers multidrug resistance, and its in vitro transcriptional activation", *Current genetics,* vol. 34, no. 3, pp. 192-199.

Hannenhalli, S.S. & Russell, R.B. 2000, "Analysis and prediction of functional sub-types from protein sequence alignments", *Journal of Molecular Biology,* vol. 303, no. 1, pp. 61-76.

Harris, A. & Argent, B.E. 1993, "The cystic fibrosis gene and its product CFTR", *Seminars in Cell and Developmental Biology,* vol. 4, no. 1, pp. 37-44.

Harry, J.B., Song, J.L., Lyons, C.N. & White, T.C. 2002, "Transcription initiation of genes associated with azole resistance in *Candida albicans*", *Medical Mycology,* vol. 40, no. 1, pp. 73-81.

Hastings Wilson, T., Yunker, P.L. & Hansen, C.L. 1990, "Lactose transport mutants of *Escherichia coli* resistant to inhibition by the phosphotransferase system", *Biochimica et Biophysica Acta - Biomembranes,* vol. 1029, no. 1, pp. 113-116.

Henikoff, S. & Henikoff, J.G. 1992, "Amino acid substitution matrices from protein blocks", *Proceedings of the National Academy of Sciences of the United States of America,* vol. 89, no. 22, pp. 10915-10919.

Henze, U.U. & Berger-Bachi, B. 1995, "*Staphylococcus aureus* penicillin-binding protein 4 and intrinsic β- lactam resistance", *Antimicrobial Agents and Chemotherapy,* vol. 39, no. 11, pp. 2415-2422.

Higgins, C.F. 1992, "ABC Transporters: From microorganisms to man", *Annual Review of Cell Biology,* vol. 8, pp. 67-113.

Hirai, T. & Subramaniam, S. 2004, "Structure and transport mechanism of the bacterial oxalate transporter OxlT", *Biophysical journal,* vol. 87, no. 5, pp. 3600-3607.

Hirai, T., Heymann, J.A.W., Shi, D., Sarker, R., Maloney, P.C. & Subramaniam, S. 2002, "Three-dimensional structure of a bacterial oxalate transporter", *Nature structural biology,* vol. 9, no. 8, pp. 597-600.

Hitchcock, C.A., Barrett-Bee, K.J. & Russell, N.J. 1987, "The lipid composition and permeability to azole of an azole- and polyene-resistant mutant of *Candida albicans*", *Journal of Medical and Veterinary Mycology,* vol. 25, no. 1, pp. 29-37.

Hitchcock, C.A., Russell, N.J. & Barrett-Bee, K.J. 1987, "Sterols in *Candida albicans* mutants resistant to polyene or azole antifungals, and of a double mutant *C. albicans* 6.4.", *Critical reviews in microbiology,* vol. 15, no. 1, pp. 111-115.

Hoischen, C., Levin, J., Pitaknarongphorn, S., Reizer, J. & Saier Jr., M.H. 1996, "Involvement of the central loop of the lactose permease of *Escherichia coli* in its allosteric regulation by the glucose-specific enzyme IIA of the phosphoenolpyruvate-dependent phosphotransferase system", *Journal of Bacteriology,* vol. 178, no. 20, pp. 6082-6086.

Hollenstein, K., Dawson, R.J. & Locher, K.P. 2007, "Structure and mechanism of ABC transporter proteins", *Current opinion in structural biology,* vol. 17, no. 4, pp. 412-418.

Hollenstein, K., Frei, D.C. & Locher, K.P. 2007, "Structure of an ABC transporter in complex with its binding protein", *Nature,* vol. 446, no. 7132, pp. 213-216.

Holzer, K.P. & Hammes, G.G. 1989, "Cloning and expression of the yeast plasma membrane ATPase in *Escherichia coli*", *Journal of Biological Chemistry,* vol. 264, no. 24, pp. 14389-14395.

Hrycyna, C.A., Ramachandra, M., Germann, U.A., Cheng, P.W., Pastan, I. & Gottesman, M.M. 1999, "Both ATP sites of human P-glycoprotein are essential but not symmetric", *Biochemistry,* vol. 38, no. 42, pp. 13887-13899.

Huang, Y., Lemieux, M.J., Song, J., Auer, M. & Wang, D.-. 2003, "Structure and mechanism of the glycerol-3-phosphate transporter from *Escherichia coli*", *Science,* vol. 301, no. 5633, pp. 616-620.

Hvorup, R.N., Goetz, B.A., Niederer, M., Hollenstein, K., Perozo, E. & Locher, K.P. 2007, "Asymmetry in the structure of the ABC transporter - Binding protein complex BtuCD-BtuF", *Science,* vol. 317, no. 5843, pp. 1387-1390.

Ivnitski-Steele, I., Holmes, A.R., Lamping, E., Monk, B.C., Cannon, R.D. & Sklar, L.A. 2009, "Identification of Nile red as a fluorescent substrate of the *Candida albicans* ATP-binding cassette transporters Cdr1p and Cdr2p and the major facilitator superfamily transporter Mdr1p", *Analytical Biochemistry,* vol. 394, no. 1, pp. 87-91.

Jardetzky, O. 1966, "Simple allosteric model for membrane pumps", *Nature,* vol. 211, no. 5052, pp. 969-970.

Jeon, J., Yang, J.-. & Kim, S. 2009, "Integration of evolutionary features for the identification of functionally important residues in major facilitator superfamily transporters", *PLoS Computational Biology,* vol. 5, no. 10.

Joseph-Horne, T. & Hollomon, D.W. 1997, "Molecular mechanisms of azole resistance in fungi", *FEMS microbiology letters,* vol. 149, no. 2, pp. 141-149.

Kaback H.R. 1989, *Harvey Lectures,* vol. 83, pp. 77–103.

Kaback, H.R. & Wu, J. 1997, "From membrane to molecule to the third amino acid from the left with a membrane transport protein", *Quarterly reviews of biophysics,* vol. 30, no. 4, pp. 333-364.

Kaback, H.R. & Wu, J. 1999, "What to do while awaiting crystals of a membrane transport protein and thereafter", *Accounts of Chemical Research,* vol. 32, no. 9, pp. 805-813.

Kaback, H.R. 1983, "The lac carrier protein in *Escherichia coli*", *Journal of Membrane Biology,* vol. 76, no. 2, pp. 95-112.

Kaback, H.R. 1992, "The lactose permease of *Escherichia coli*: A paradigm for membrane transport proteins", *Biochimica et Biophysica Acta - Bioenergetics,* vol. 1101, no. 2, pp. 210-213.

Kaback, H.R., Frillingos, S., Jung, H., Jung, K., Prive, G.G., Ujwal, M.L., Weitzman, C., Wu Jianhua & Zen, K. 1994, "The lactose permease meets Frankenstein", *Journal of Experimental Biology,* vol. 196, pp. 183-195.

Kaback, H.R., Voss, J. & Wu, J. 1997, "Helix packing in polytopic membrane proteins: The lactose permease of *Escherichia coli*", *Current opinion in structural biology,* vol. 7, no. 4, pp. 537-542.

Kadaba, N.S., Kaiser, J.T., Johnson, E., Lee, A. & Rees, D.C. 2008, "The high-affinity *E. coli* methionine ABC transporter: Structure and allosteric regulation", *Science,* vol. 321, no. 5886, pp. 250-253.

Kage, K., Tsukahara, S., Sugiyama, T., Asada, S., Ishikawa, E., Tsuruo, T. & Sugimoto, Y. 2002, "Dominant-negative inhibition of breast cancer resistance protein as drug efflux pump through the inhibition of S-S dependent homodimerization", *International Journal of Cancer,* vol. 97, no. 5, pp. 626-630.

Kajiji, S., Talbot, F., Grizzuti, K., Van Dyke-Phillips, V., Agresti, M., Safa, A.R. & Gros, P. 1993, "Functional analysis of P-glycoprotein mutants identifies predicted transmembrane domain 11 as a putative drug binding site", *Biochemistry,* vol. 32, no. 16, pp. 4185-4194.

Kapoor, K., Rehan, M., Kaushiki, A., Pasrija, R., Lynn, A.M. & Prasad, R. 2009, "Rational mutational analysis of a multidrug MFS transporter CaMdr1p of *Candida albicans* by employing a membrane environment based computational approach", *PLoS Computational Biology,* vol. 5, no. 12.

Kelly, A., Powis, S.H., Kerr, L.-., Mockridge, I., Elliott, T., Bastin, J., Uchanska-Ziegler, B., Ziegler, A., Trowsdale, J. & Townsend, A. 1992, "Assembly and function of the two ABC transporter proteins encoded in the human major histocompatibility complex", *Nature,* vol. 355, no. 6361, pp. 641-644.

Kelly, R., Card, D., Register, E., Mazur, P., Kelly, T., Tanaka, K.I., Onishi, J., Williamson, J.M., Fan, H., Satoh, T. & Kurtz, M. 2000, "Geranylgeranyltransferase I of *Candida albicans*: Null mutants or enzyme inhibitors produce unexpected phenotypes", *Journal of Bacteriology,* vol. 182, no. 3, pp. 704-713.

Kelly, S.L., Lamb, D.C., Kelly, D.E., Manning, N.J., Loeffler, J., Hebart, H., Schumacher, U. & Einsele, H. 1997, "Resistance to fluconazole and cross-resistance to amphotericin B in *Candida albicans* from AIDS patients caused by defective sterol Δ5,6-desaturation", *FEBS letters,* vol. 400, no. 1, pp. 80-82.

Kelly, S.L., Lamb, D.C., Taylor, M., Corran, A.J., Baldwin, B.C. & Powderly, W.G. 1994, "Resistance to amphotericin B associated with defective sterol Δ(8→7)

isomerase in a Cryptococcus neoformans strain from an AIDS patient", *FEMS microbiology letters,* vol. 122, no. 1-2, pp. 39-42.

Kerridge, D. & Whelan, W.L. 1984, "The polyenes macrolide antibiotics and 5-fluorocytosine: molecular actions and interactions", *Mode of action of antifungal agents,* Cambridge University Press, Cambridge, pp. 343-375.

Kerridge, D. 1985, "The protoplast membrane and antifungal drugs", *Fungal protoplasts: applications in biochemistry and genetics.* NewYork, pp. 135-169.

Kerridge, D. 1986, "Mode of action of clinically important antifungal drugs", *Advances in Microbial Physiology,* vol. 27, pp. 1-72.

Khan, Z.K. & Gyanchandani, A. 1998, "Candidiasis-a review", CDRI Commun. B64: pp. 1-34.

Klein, I., Sarkadi, B. & Váradi, A. 1999, "An inventory of the human ABC proteins", *Biochimica et Biophysica Acta - Biomembranes,* vol. 1461, no. 2, pp. 237-262.

Klepser, M.E., Ernst, E.J. & Pfaller, M.A. 1997, "Update on antifungal resistance", *Trends in microbiology,* vol. 5, no. 9, pp. 372-375.

Kohli, A., Smriti, Mukhopadhyay, K., Rattan, A. & Prasad, R. 2002, "In vitro low-level resistance to azoles in *Candida albicans* is associated with changes in membrane lipid fluidity and asymmetry", *Antimicrobial Agents and Chemotherapy,* vol. 46, no. 4, pp. 1046-1052.

Koike, K., Oleschuk, C.J., Haimeur, A., Olsen, S.L., Deeley, R.G. & Cole, S.P.C. 2002, "Multiple membrane-associated tryptophan residues contribute to the transport activity and substrate specificity of the human multidrug resistance protein, MRP1", *Journal of Biological Chemistry,* vol. 277, no. 51, pp. 49495-49503.

Kolaczkowski, M. & Goffeau, A. 1997, "Active efflux by multidrug transporters as one of the strategies to evade chemotherapy and novel practical implications of yeast pleiotropic drug resistance", *Pharmacology and Therapeutics,* vol. 76, no. 1-3, pp. 219-242.

Krishnamurthy, S., Gupta, V., Snehlata, P. & Prasad, R. 1998, "Characterisation of human steroid hormone transport mediated by Cdr1p, a multidrug transporter of *Candida albicans,* belonging to the ATP binding cassette super family", *FEMS microbiology letters,* vol. 158, no. 1, pp. 69-74.

Krogh, A., Larsson, B., Von Heijne, G. & Sonnhammer, E.L.L. 2001, "Predicting transmembrane protein topology with a hidden Markov model: Application to complete genomes", *Journal of Molecular Biology,* vol. 305, no. 3, pp. 567-580.

Kurtz, M.B., Abruzzo, G., Flattery, A., Bartizal, K., Marrinan, J.A., Li, W., Milligan, J., Nollstadt, K. & Douglas, C.M. 1996, "Characterization of echinocandin-resistant mutants of *Candida albicans*: Genetic, biochemical, and virulence studies", *Infection and immunity,* vol. 64, no. 8, pp. 3244-3251.

Laemmli, U.K. 1970, "Cleavage of structural proteins during the assembly of the head of bacteriophage T4", *Nature,* vol. 227, no. 5259, pp. 680-685.

Lamb, D.C., Kelly, D.E., White, T.C. & Kelly, S.L. 2000, "The R467K amino acid substitution in *Candida albicans* sterol 14α- demethylase causes drug resistance through reduced affinity", *Antimicrobial Agents and Chemotherapy,* vol. 44, no. 1, pp. 63-67.

Lamb, D.C., Maspahy, S., Kelly, D.E., Manning, N.J., Geber, A., Bennett, J.E. & Kelly, S.L. 1999, "Purification, reconstitution, and inhibition of cytochrome P-450 sterol Δ22-desaturase from the pathogenic fungus *Candida glabrata*", *Antimicrobial Agents and Chemotherapy,* vol. 43, no. 7, pp. 1725-1728.

Law, C.J., Maloney, P.C. & Wang, D.N. 2008, "Ins and outs of major facilitator superfamily antiporters", vol. 62, pp. 289-305.

Lemieux, M.J. 2007, "Eukaryotic major facilitator superfamily transporter modeling based on the prokaryotic GlpT crystal structure", *Molecular membrane biology,* vol. 24, no. 5-6, pp. 333-341.

Lemieux, M.J., Huang, Y. & Wang, D.N. 2004, "The structural basis of substrate translocation by the *Escherichia coli* glycerol-3-phosphate transporter: A member of the major facilitator superfamily", *Current opinion in structural biology,* vol. 14, no. 4, pp. 405-412.

Li, L., Shakhnovich, E.I. & Mirny, L.A. 2003, "Amino acids determining enzyme-substrate specificity in prokaryotic and eukaryotic protein kinases", *Proceedings of the National Academy of Sciences of the United States of America,* vol. 100, no. 8, pp. 4463-4468.

Li, X.Z. & Nikaido, H. 2004, "Efflux-Mediated Drug Resistance in Bacteria", *Drugs,* vol. 64, no. 2, pp. 159-204.

Livingstone, C.D. & Barton, G.J. 1993, "Protein sequence alignments: A strategy for the hierarchical analysis of residue conservation", *Computer Applications in the Biosciences,* vol. 9, no. 6, pp. 745-756.

Locher, K.P., Lee, A.T. & Rees, D.C. 2002, "The E. coli BtuCD structure: A framework for ABC transporter architecture and mechanism", *Science,* vol. 296, no. 5570, pp. 1091-1098.

Löffler, J., Einsele, H., Hebart, H., Schumacher, U., Hrastnik, C. & Daum, G. 2000, "Phospholipid and sterol analysis of plasma membranes of azole-resistant *Candida albicans* strains", *FEMS microbiology letters,* vol. 185, no. 1, pp. 59-63.

Loo, T.W. & Clarke, D.M. 1993, "Functional consequences of phenylalanine mutations in the predicted transmembrane domain of P-glycoprotein", *Journal of Biological Chemistry,* vol. 268, no. 27, pp. 19965-19972.

Loo, T.W. & Clarke, D.M. 1994, "Mutations to amino acids located in predicted transmembrane segment 6 (TM6) modulate the activity and substrate specificity of human P-glycoprotein", *Biochemistry,* vol. 33, no. 47, pp. 14049-14057.

Loo, T.W. & Clarke, D.M. 1994, "Reconstitution of drug-stimulated ATPase activity following co-expression of each half of human P-glycoprotein as separate polypeptides", *Journal of Biological Chemistry,* vol. 269, no. 10, pp. 7750-7755.

Loo, T.W. & Clarke, D.M. 2001, "Defining the Drug-binding Site in the Human Multidrug Resistance P-glycoprotein Using a Methanethiosulfonate Analog of

Verapamil, MTS-verapamil", *Journal of Biological Chemistry,* vol. 276, no. 18, pp. 14972-14979.

Loo, T.W. & Clarke, D.M. 2001, "Determining the Dimensions of the Drug-binding Domain of Human P-glycoprotein Using Thiol Cross-linking Compounds as Molecular Rulers", *Journal of Biological Chemistry,* vol. 276, no. 40, pp. 36877-36880.

Lopez-Ribot, J.L., Mcatee, R.K., Lee, L.N., Kirkpatrick, W.R., White, T.C., Sanglard, D. & Patterson, T.F. 1998, "Distinct patterns of gene expression associated with development of fluconazole resistance in serial *Candida albicans* isolates from human immunodeficiency virus-infected patients with oropharyngeal candidiasis", *Antimicrobial Agents and Chemotherapy,* vol. 42, no. 11, pp. 2932-2937.

Lopez-Ribot, J.L., McAtee, R.K., Perea, S., Kirkpatrick, W.R., Rinaldi, M.G. & Patterson, T.F. 1999, "Multiple resistant phenotypes of *Candida albicans* coexist during episodes of oropharyngeal candidiasis in human immunodeficiency virus- infected patients", *Antimicrobial Agents and Chemotherapy,* vol. 43, no. 7, pp. 1621-1630.

Lubelski, J., van Merkerk, R., Konings, W.N., and Driessen, A.J. 2006, "Nucleotide-binding sites of the heterodimeric LmrCD ABC-multidrug transporter of *Lactococcus lactis* are asymmetric", *Biochemistry,* vol 45, pp. 648–656.

Lugo, M.R. & Sharom, F.J. 2005, "Interaction of LDS-751 and rhodamine 123 with P-glycoprotein: Evidence for simultaneous binding of both drugs", *Biochemistry,* vol. 44, no. 42, pp. 14020-14029.

Ma, J.F., Grant, G. & Melera, P.W. 1997, "Mutations in the sixth transmembrane domain of P-glycoprotein that alter the pattern of cross-resistance also alter sensitivity to cyclosporin A reversal", *Molecular pharmacology,* vol. 51, no. 6, pp. 922-930.

Maiden, M.C.J., Davis, E.O. & Baldwin, S.A. 1987, "Mammalian and bacterial sugar transport proteins are homologous", *Nature,* vol. 325, no. 6105, pp. 641-643.

Majumdar, D.S., Smirnova, I., Kasho, V., Nir, E., Kong, X., Weiss, S. & Kaback, H.R. 2007, "Single-molecule FRET reveals sugar-induced conformational dynamics in LacY", *Proceedings of the National Academy of Sciences of the United States of America,* vol. 104, no. 31, pp. 12640-12645.

Maloney, P.C. 1994, "Bacterial transporters", *Current Opinions in Cellular Biology,* vol. 6, pp. 571–582.

Marger, M.D. & Saier Jr., M.H. 1993, "A major superfamily of transmembrane facilitators that catalyse uniport, symport and antiport", *Trends in biochemical sciences,* vol. 18, no. 1, pp. 13-20.

Marichal, P. 1999, "Mechanisms of resistance to azole antifungal compounds", *Current Opinion in Anti-infective Investigational Drugs,* vol. 1, pp. 318-333.

Marichal, P., Koymans, L., Willemsens, S., Bellens, D., Verhasselt, P., Luyten, W., Borgers, M., Ramaekers, F.C.S., Odds, F.C. & Bossche, H.V. 1999,

"Contribution of mutations in the cytochrome P450 14α-demethylase (Erg11p, Cyp51p) to azole resistance in *Candida albicans*", *Microbiology,* vol. 145, no. 10, pp. 2701-2713.

Marichal, P., Vanden Bossche, H., Odds, F.C., Nobels, G., Warnock, D.W., Timmerman, V., Van Broeckhoven, C., Fay, S. & Mose-Larsen, P. 1997, "Molecular biological characterization of an azole-resistant *Candida glabrata* isolate", *Antimicrobial Agents and Chemotherapy,* vol. 41, no. 10, pp. 2229-2237.

Marie C., White T.C. 2009, "Genetic Basis of Antifungal Drug Resistance", *Genomics and pathogenesis,* vol. 3, pp. 163-169.

Martin, C., Berridge, G., Higgins, C.F., Mistry, P., Charlton, P. & Callaghan, R. 2000, "Communication between multiple drug binding sites on P-glycoprotein", *Molecular pharmacology,* vol. 58, no. 3, pp. 624-632.

Martin, C., Berridge, G., Mistry, P., Higgins, C., Charlton, P. & Callaghan, R. 2000, "Drug binding sites on P-glycoprotein are altered by ATP binding prior to nucleotide hydrolysis", *Biochemistry,* vol. 39, no. 39, pp. 11901-11906.

Martin, L.C., Gloor, G.B., Dunn, S.D. & Wahl, L.M. 2005, "Using information theory to search for co-evolving residues in proteins", *Bioinformatics,* vol. 21, no. 22, pp. 4116-4124.

Martins, M.D., Rex, J.H. 1997, "Antifungal drug resistance: a focus on *Candida", Clinical Updates in Fungal Infections* vol. 1, pp. 1-6.

McKenna, E., Hardy, D. & Kaback, H.R. 1992, "Insertional mutagenesis of hydrophilic domains in the lactose permease of *Escherichia coli*", *Proceedings of the National Academy of Sciences of the United States of America,* vol. 89, no. 24, pp. 11954-11958.

Monk, B.C., Kurtz, M.B., Marrinan, J.A. & Perlin, D.S. 1991, "Cloning and characterization of the plasma membrane H+-ATPase from *Candida albicans*", *Journal of Bacteriology,* vol. 173, no. 21, pp. 6826-6836.

Moran, G.P., Sanglard, D., Donnelly, S.M., Shanley, D.B., Sullivan, D.J. & Coleman, D.C. 1998, "Identification and expression of multidrug transporters responsible for fluconazole resistance in *Candida dubliniensis*", *Antimicrobial Agents and Chemotherapy,* vol. 42, no. 7, pp. 1819-1830.

Mosser, J., Douar, A.M., Sarde, C.O., Kioschis, P., Feil, R., Moser, H., Poustka, A.M., Mandel, J.L. & Aubourg, P. 1993, "Putative X-linked adrenoleukodystrophy gene shares unexpected homology with ABC transporters", *Nature,* vol. 361, no. 6414, pp. 726-730.

Mueckler, M. & Makepeace, C. 2006, "Transmembrane segment 12 of the Glut1 glucose transporter is an outer helix and is not directly involved in the transport mechanism", *Journal of Biological Chemistry,* vol. 281, no. 48, pp. 36993-36998.

Mukhopadhyay, K., Kohli, A. & Prasad, R. 2002, "Drug susceptibilities of yeast cells are affected by membrane lipid composition", *Antimicrobial Agents and Chemotherapy,* vol. 46, no. 12, pp. 3695-3705.

Mukhopadhyay, K., Prasad, T., Saini, P., Pucadyil, T.J., Chattopadhyay, A. & Prasad, R. 2004, "Membrane Sphingolipid-Ergosterol Interactions Are Important

Determinants of Multidrug Resistance in *Candida albicans*", *Antimicrobial Agents and Chemotherapy,* vol. 48, no. 5, pp. 1778-1787.

Nakamura, K., Niimi, M., Niimi, K., Holmes, A.R., Yates, J.E., Decottignies, A., Monk, B.C., Goffeau, A. & Cannon, R.D. 2001, "Functional expression of *Candida albicans* drug efflux pump Cdr1p in a *Saccharomyces cerevisiae* strain deficient in membrane transporters", *Antimicrobial Agents and Chemotherapy,* vol. 45, no. 12, pp. 3366-3374.

Nelissen, B., De Wachter, R. & Goffeau, A. 1997, "Classification of all putative permeases and other membrane plurispanners of the major facilitator superfamily encoded by the complete genome of *Saccharomyces cerevisiae*", *FEMS microbiology reviews,* vol. 21, no. 2, pp. 113-134.

Ng, P.C., Henikoff, J.G. & Henikoff, S. 2000, "PHAT: A transmembrane-specific substitution matrix", *Bioinformatics,* vol. 16, no. 9, pp. 760-766.

Nishi, K., Yoshida, M., Nishimura, M., Nishikawa, M., Nishiyama, M., Horinouchi, S. & Beppu, T. 1992, "A leptomycin B resistance gene of *Schizosaccharomyces pombe* encodes a protein similar to the mammalian P-glycoproteins", *Molecular microbiology,* vol. 6, no. 6, pp. 761-769.

Odds, F.C.1988, "*Candida* and Candidosis: A Review and Bibliography", 2 edn. Ballière Tindall, London.

Oldham, M.L., Khare, D., Quiocho, F.A., Davidson, A.L. & Chen, J. 2007, "Crystal structure of a catalytic intermediate of the maltose transporter", *Nature,* vol. 450, no. 7169, pp. 515-521.

Onishi, J., Meinz, M., Thompson, J., Curotto, J., Dreikorn, S., Rosenbach, M., Douglas, C., Abruzzo, G., Flattery, A., Kong, L., Cabello, A., Vicente, F., Pelaez, F., Diez, M.T., Martin, I., Bills, G., Giacobbe, R., Dombrowski, A., Schwartz, R., Morris, S., Harris, G., Tsipouras, A., Wilson, K. & Kurtz, M.B. 2000, "Discovery of novel antifungal (1,3)-β-D-glucan synthase inhibitors", *Antimicrobial Agents and Chemotherapy,* vol. 44, no. 2, pp. 368-377.

Orlowski, S., Mir, L.M., Belehradek Jr., J. & Garrigos, M. 1996, "Effects of steroids and verapamil on P-glycoprotein ATPase activity: Progesterone, desoxycorticosterone, corticosterone and verapamil are mutually non-exclusive modulators", *Biochemical Journal,* vol. 317, no. 2, pp. 515-522.

Pao, S.S., Paulsen, I.T. & Saier Jr., M.H. 1998, "Major facilitator superfamily", *Microbiology and Molecular Biology Reviews,* vol. 62, no. 1, pp. 1-34.

Papon, N., Noël, T., Florent, M., Gibot-Leclerc, S., Jean, D., Chastin, C., Villard, J. & Chapeland-Leclerc, F. 2007, "Molecular mechanism of flucytosine resistance in Candida lusitaniae: Contribution of the *FCY2*, *FCY1*, and *FUR1* genes to 5-fluorouracil and fluconazole cross-resistance", *Antimicrobial Agents and Chemotherapy,* vol. 51, no. 1, pp. 369-371.

Pasrija, R., Banerjee, D. & Prasad, R. 2007, "Structure and function analysis of CaMdr1p, a major facilitator superfamily antifungal efflux transporter protein of *Candida albicans*: Identification of amino acid residues critical for drug/H+ transport", *Eukaryotic Cell,* vol. 6, no. 3, pp. 443-453.

Paulsen, I.T., Brown, M.H. & Skurray, R.A. 1996, "Proton-dependent multidrug efflux systems", *Microbiological reviews,* vol. 60, no. 4, pp. 575-608.

Paulusma, C.C., Bosma, P.J., Zaman, G.J.R., Bakker, C.T.M., Otter, M., Scheffer, G.L., Scheper, R.J., Borst, P. & Oude Elferink, R.P.J. 1996, "Congenital jaundice in rats with a mutation in a multidrug resistance-associated protein gene", *Science,* vol. 271, no. 5252, pp. 1126-1128.

Pawagi, A.B., Wang, J., Silverman, M., Reithmeier, R.A.F. & Deber, C.M. 1994, "Transmembrane aromatic amino acid distribution in P-glycoprotein. A functional role in broad substrate specificity", *Journal of Molecular Biology,* vol. 235, no. 2, pp. 554-564.

Pinkett, H.W., Lee, A.T., Lum, P., Locher, K.P. & Rees, D.C. 2007, "An inward-facing conformation of a putative metal-chelate-type ABC transporter", *Science,* vol. 315, no. 5810, pp. 373-377.

Pirovano, W., Feenstra, K.A. & Heringa, J. 2008, "PRALINE™: A strategy for improved multiple alignment of transmembrane proteins", *Bioinformatics,* vol. 24, no. 4, pp. 492-497.

Prasad, R. & Kapoor, K. 2004, "Multidrug resistance in yeast Candida", *International Rivew of Cytology,* vol. 242, pp. 215-248.

Prasad, R. 1991, "*Candida albicans*: Cellular and Molecular Biology", Springer-Verlag, Berlin.

Prasad, R., De Wergifosse, P., Goffeau, A. & Balzi, E. 1995, "Molecular cloning and characterization of a novel gene of *Candida albicans*, CDR1, conferring multiple resistance to drugs and antifungals", *Current genetics,* vol. 27, no. 4, pp. 320-329.

Prasad, R., Lata Panwar, S. & Smriti 2002, "Drug resistance in yeasts - An emerging scenario", Advances in Microbial Physiology. Vol. 46, pp. 155-201.

Procko, E., Ferrin-O'Connell, I., Ng, S.-. & Gaudet, R. 2006, "Distinct Structural and Functional Properties of the ATPase Sites in an Asymmetric ABC Transporter", *Molecular cell,* vol. 24, no. 1, pp. 51-62.

Procko, E., O'Mara, M.L., Drew Bennett, W.F., Peter Tieleman, D. & Gaudet, R. 2009, "The mechanism of ABC transporters: General lessons from structural and functional studies of an antigenic peptide transporter", *FASEB Journal,* vol. 23, no. 5, pp. 1287-1302.

Puri, N., Gaur, M., Sharma, M., Shukla, S., Ambudkar, S.V. & Prasad, R. 2009, "The amino acid residues of transmembrane helix 5 of multidrug resistance protein CaCdr1p of *Candida albicans* are involved in substrate specificity and drug transport", *Biochimica et Biophysica Acta - Biomembranes,* vol. 1788, no. 9, pp. 1752-1761.

Redding, S., Smith, J., Farinacci, G., Rinaldi, M., Fothergill, A., Rhine-Chalberg, J. & Pfaller, M. 1994, "Resistance of *Candida albicans* to fluconazole during treatment of oropharyngeal candidiasis in a patient with AIDS: Documentation by in vitro susceptibility testing and DNA subtype analysis", *Clinical Infectious Diseases,* vol. 18, no. 2, pp. 240-242.

Reva, B., Antipin, Y. & Sander, C. 2007, "Determinants of protein function revealed by combinatorial entropy optimization", *Genome biology,* vol. 8, no. 11.

Rex, J.H., Pfaller, M.A., Galgiani, J.N., Bartlett, M.S., Espinel-Ingroff, A., Ghannoum, M.A., Lancaster, M., Odds, F.C., Rinaldi, M.G., Walsh, T.J. & Barry, A.L. 1997, "Development of interpretive breakpoints for antifungal susceptibility testing: Conceptual framework and analysis of in vitro-in vivo correlation data for fluconazole, itraconazole, and candida infections", *Clinical Infectious Diseases,* vol. 24, no. 2, pp. 235-249.

Reynolds, T.B. & Fink, G.R. 2001, "Bakers' yeast, a model for fungal biofilm formation", *Science,* vol. 291, no. 5505, pp. 878-881.

Rothnie, A., Storm, J., Campbell, J., Linton, K.J., Kerr, I.D. & Callaghan, R. 2004, "The topography of transmembrane segment six is altered during the catalytic cycle of P-glycoprotein", *Journal of Biological Chemistry,* vol. 279, no. 33, pp. 34913-34921.

Ruetz, S. & Gros, P. 1994, "Phosphatidylcholine translocase: A physiological role for the mdr2 gene", *Cell,* vol. 77, no. 7, pp. 1071-1081.

Sá-Correia, I. & Tenreiro, S. 2002, "The multidrug resistance transporters of the major facilitator superfamily, 6 years after disclosure of *Saccharomyces cerevisiae* genome sequence", *Journal of Biotechnology,* vol. 98, no. 2-3, pp. 215-226.

Sá-Correia, I., dos Santos, S.C., Teixeira, M.C., Cabrito, T.R. & Mira, N.P. 2009, "Drug:H+ antiporters in chemical stress response in yeast", *Trends in microbiology,* vol. 17, no. 1, pp. 22-31.

Saier Jr., M.H. & Paulsen, I.T. 2001, "Phylogeny of multidrug transporters", *Seminars in Cell and Developmental Biology,* vol. 12, no. 3, pp. 205-213.

Saier Jr., M.H. 1999, "A functional-phylogenetic system for the classification of transport proteins", *Journal of cellular biochemistry,* vol. 76, no. SUPPL. 32/33, pp. 84-94.

Saier Jr., M.H. 2003, "Tracing pathways of transport protein evolution", *Molecular microbiology,* vol. 48, no. 5, pp. 1145-1156.

Saier Jr., M.H., Beatty, J.T., Goffeau, A., Harley, K.T., Heijne, W.H.M., Huang, S.C., Jack, D.L., Jahn, P.S., Lew, K., Liu, J., Pao, S.S., Paulsen, I.T., Tseng, T.-. & Virk, P.S. 2000, "The major facilitator superfamily, *Journal of Molecular Microbiology and Biotechnology,* vol. 2, no. 2, pp. 255-279.

Saini, P., Prasad, T., Gaur, N.A., Shukla, S., Jha, S., Komath, S.S., Khan, L.A., Haq, Q.M.R. & Prasad, R. 2005, "Alanine scanning of transmembrane helix 11 of Cdr1p ABC antifungal efflux pump of *Candida albicans*: Identification of amino acid residues critical for drug efflux", *Journal of Antimicrobial Chemotherapy,* vol. 56, no. 1, pp. 77-86.

Sali, A. & Blundell, T.L. 1993, "Comparative protein modelling by satisfaction of spatial restraints", *Journal of Molecular Biology,* vol. 234, no. 3, pp. 779-815.

Samuelson, J., Ayala, P., Orozco, E. & Wirth, D. 1990, "Emetine-resistant mutants of *Entamoeba histolytica* overexpress mRNAs for multidrug resistance", *Molecular and biochemical parasitology,* vol. 38, no. 2, pp. 281-290.

Samuelson, J.C., Burke, A. & Courval, J.M. 1992, "Susceptibility of an emetine-resistant mutant of *Entamoeba histolytica* to multiple drugs and to channel blockers", *Antimicrobial Agents and Chemotherapy,* vol. 36, no. 11, pp. 2392-2397.

Sanglard, D. & Odds, F.C. 2002, "Resistance of *Candida* species to antifungal agents: Molecular mechanisms and clinical consequences", *Lancet Infectious Diseases,* vol. 2, no. 2, pp. 73-85.

Sanglard, D., Ischer, F., Calabrese, D., Majcherczyk, P.A. & Bille, J. 1999, "The ATP binding cassette transporter gene *CgCDR1* from *Candida glabrata* is involved in the resistance of clinical isolates to azole antifungal agents", *Antimicrobial Agents and Chemotherapy,* vol. 43, no. 11, pp. 2753-2765.

Sanglard, D., Ischer, F., Koymans, L. & Bille, J. 1998, "Amino acid substitutions in the cytochrome P-450 lanosterol 14α- demethylase (CYP51A1) from azole-resistant *Candida albicans* clinical isolates contribute to resistance to azole antifungal agents", *Antimicrobial Agents and Chemotherapy,* vol. 42, no. 2, pp. 241-253.

Sanglard, D., Ischer, F., Monod, M. & Bille, J. 1997, "Cloning of *Candida albicans* genes conferring resistance to azole antifungal agents: Characterization of *CDR2,* a new multidrug ABC transporter gene", *Microbiology,* vol. 143, no. 2, pp. 405-416.

Sanglard, D., Ischer, F., Monod, M., Bille, J. 1996, "Susceptibilities of *Candida albicans* multidrug transporter mutants to various antifungal agents and other metabolic inhibitors" *Antimicrobial Agents and Chemotherapy,* vol. 40, pp.2300-2305.

Schiffer, M., Chang, C.H., & Stevens, F.J. 1992, "The functions of tryptophan residues in membrane proteins", *Protein engineering,* vol. 5, no. 3, pp. 213-214.

Senior, A.E., Al-Shawi, M.K. & Urbatsch, I.L. 1995, "The catalytic cycle of P-glycoprotein", *FEBS letters,* vol. 377, no. 3, pp. 285-289.

Seok, Y.J., Sun, J., Kaback, H.R. & Peterkofsky, A. 1997, "Topology of allosteric regulation of lactose permease", *Proceedings of the National Academy of Sciences of the United States of America,* vol. 94, no. 25, pp. 13515-13519.

Shannon, C.E. 1997, "The Mathematical Theory of Communication", *M.D.Computing,* vol. 14, no. 4, pp. 306-317.

Shukla, S., Saini, P., Smriti, Jha, S., Ambudkar, S.V. & Prasad, R. 2003, "Functional Characterization of *Candida albicans* ABC Transporter Cdr1p", *Eukaryotic Cell,* vol. 2, no. 6, pp. 1361-1375.

Skovsgaard, T., Nielsen, D., Maare, C. & Wassermann, K. 1994, "Cellular resistance to cancer chemotherapy", *International review of cytology,* vol. 156, pp. 77-157.

Smirnova, I., Kasho, V., Choe, J.-., Altenbach, C., Hubbell, W.L. & Kaback, H.R. 2007, "Sugar binding induces an outward facing conformation of LacY", *Proceedings of the National Academy of Sciences of the United States of America,* vol. 104, no. 42, pp. 16504-16509.

Smriti, Krishnamurthy, S., Dixit, B.L., Gupta, C.M., Milewski, S. & Prasad, R. 2002, "ABC transporters CdrLp, Cdr2p and Cdr3p of a human pathogen *Candida albicans* are general phospholipid translocators", *Yeast,* vol. 19, no. 4, pp. 303-318.

Sondej, M., Sun, J., Seok, Y.J., Kaback, H.R. & Peterkofsky, A. 1999, "Deduction of consensus binding sequences on proteins that bind IIAGlc of the phosphoenolpyruvate:sugar phosphotransferase system by cysteine scanning mutagenesis of *Escherichia coli* lactose permease", *Proceedings of the National Academy of Sciences of the United States of America,* vol. 96, no. 7, pp. 3525-3530.

Sonne, J., Kandt, C., Peters, G.H., Hansen, F.Y., Jensen, M.O. & Tieleman, D.P. 2007, "Simulation of the coupling between nucleotide binding and transmembrane domains in the ATP binding cassette transporter BtuCD", *Biophysical journal,* vol. 92, no. 8, pp. 2727-2734.

Srivastava, P.K., Desai, D.K., Nandi, S. & Lynn, A.M. 2007, "HMM-ModE - Improved classification using profile hidden Markov models by optimising the discrimination threshold and modifying emission probabilities with negative training sequences", *BMC Bioinformatics,* vol. 8.

Stark, G.R., and Wahl, G.M. 1984, "Gene amplification", *Annual Reiews of Biochemistry,* vol. 53, pp. 447-491.

Storm, J., O'Mara, M.L., Crowley, E.H., Peall, J., Tieleman, D.P., Kerr, I.D. & Callaghan, R. 2007, "Residue G346 in transmembrane segment six is involved in inter-domain communication in P-glycoprotein", *Biochemistry,* vol. 46, no. 35, pp. 9899-9910.

Talibi, D. & Raymond, M. 1999, "Isolation of a putative *Candida albicans* transcriptional regulator involved in pleiotropic drug resistance by functional complementation of a *pdr1 pdr3* mutation in *Saccharomyces cerevisiae*", *Journal of Bacteriology,* vol. 181, no. 1, pp. 231-240.

Tutulan-Cunita, A.C., Mikoshi, M., Mizunuma, M., Hirata, D. & Miyakawa, T. 2005, "Mutational analysis of the yeast multidrug resistance ABC transporter Pdr5p with altered drug specificity", *Genes to Cells,* vol. 10, no. 5, pp. 409-420.

Valdar, W.S.J. 2002, "Scoring residue conservation", *Proteins: Structure, Function and Genetics,* vol. 48, no. 2, pp. 227-241.

Van Den Hazel, H.B., Pichler, H., Do Valle Matta, M.A., Leitner, E., Goffeau, A. & Daum, G. 1999, "*PDR16* and *PDR17*, two homologous genes of *Saccharomyces cerevisiae*, affect lipid biosynthesis and resistance to multiple drugs", *Journal of Biological Chemistry,* vol. 274, no. 4, pp. 1934-1941.

Van Der Bliek, A.M., Baas, F., Van Der Velde-Koerts, T., Biedler, J.L., Meyers, M.B., Ozols, R.F., Hamilton, T.C., Joenje, H. & Borst, P. 1988, "Genes amplified and overexpressed in human multidrug-resistant cell lines", *Cancer research,* vol. 48, no. 21, pp. 5927-5932.

Vanden Bossche, H., Warnock, D.W., Dupont, B., Kerridge, D., Sen Gupta, S., Improvisi, L., Marichal, P., Odds, F.C., Provost, F. & Ronin, O. 1994, "Mechanisms and clinical impact of antifungal drug resistance", *Journal of Medical and Veterinary Mycology, Supplement,* vol. 32, no. 1, pp. 189-202.

Vanden Bossche, H., Willemsens, G. & Marichal, P. 1987, "Anti-Candida drugs--the biochemical basis for their activity", *Critical reviews in microbiology,* vol. 15, no. 1, pp. 57-72.

Wang, K. & Samudrala, R. 2006, "Incorporating background frequency improves entropy-based residue conservation measures", *BMC Bioinformatics,* vol. 7.

Ward, A., Reyes, C.L., Yu, J., Roth, C.B. & Chang, G. 2007, "Flexibility in the ABC transporter MsbA: Alternating access with a twist", *Proceedings of the National Academy of Sciences of the United States of America,* vol. 104, no. 48, pp. 19005-19010.

Weinglass, A.B. & Kaback, H.R. 1999, "Conformational flexibility at the substrate binding site in the lactose permease of *Escherichia coli*", *Proceedings of the National Academy of Sciences of the United States of America,* vol. 96, no. 20, pp. 11178-11182.

Weinglass, A.B. & Kaback, H.R. 2000, "The central cytoplasmic loop of the major facilitator superfamily of transport proteins governs efficient membrane insertion", *Proceedings of the National Academy of Sciences of the United States of America,* vol. 97, no. 16, pp. 8938-8943.

White, T.C. 1997, "Antifungal drug resistance in *Candida albicans*", *ASM News,* vol. 63, pp. 427-433.

White, T.C. 1997, "Increased mRNA levels of ERG16, CDR, and MDR1 correlate, with increases in azole resistance in *Candida albicans* isolates from a patient infected with human immunodeficiency virus", *Antimicrobial Agents and Chemotherapy,* vol. 41, no. 7, pp. 1482-1487.

White, T.C., Marr, K.A. & Bowden, R.A. 1998, "Clinical, cellular, and molecular factors that contribute to antifungal drug resistance", *Clinical microbiology reviews,* vol. 11, no. 2, pp. 382-402.

Wilkinson, C.F., Hetnarski, K. & Hicks, L.J. 1974, "Substituted imidazoles as inhibitors of microsomal oxidation and insecticide synergists", *Pesticide biochemistry and physiology,* vol. 4, no. 3, pp. 299-312.

Wilkinson, C.F., Hetnarski, K. & Yellin, T.O. 1972, "Imidazole derivatives-A new class of microsomal enzyme inhibitors", *Biochemical pharmacology,* vol. 21, no. 23, pp. 3187-3192.

Wilson, R., Ainscough, R., Anderson, K., Baynes, C., Berks, M., Bonfield, J., Burton, J., Connell, M., Copsey, T., Cooper, J., Coulson, A., Craxton, M., Dear, S., Du, Z., Durbin, R., Favello, A., Fraser, A., Fulton, L., Gardner, A., Green, P., Hawkins, T., Hillier, L., Jier, M., Johnston, L., Jones, M., Kershaw, J., Kirsten, J., Laisster, N., Latrellle, P., Lightning, J., Lloyd, C., Mortimore, B., O'Callaghan, M., Parsons, J., Percy, C., Rifken, L., Roopra, A., Saunders, D., Shownkeen, R., Sims, M., Smaldon, N., Smith, A., Smith, M., Sonnhammer, E., Staden, R., Sulston, J., Thierry-Mieg, J., Thomas, K., Vaudin, M., Vaughan, K., Waterston, R., Watson, A., Weinstock, L., Wilkinson-Sproat, J. & Wohldman, P. 1994, "2.2

Mb of contiguous nucleotide sequence from chromosome III of C. elegans", *Nature,* vol. 368, no. 6466, pp. 32-38.

Wolfger, H., Mamnun, Y.M. & Kuchler, K. 2001, "Fungal ABC proteins: Pleiotropic drug resistance, stress response and cellular detoxification", *Research in microbiology,* vol. 152, no. 3-4, pp. 375-389.

Wu, C.T., Budding, M., Griffin, M.S. & Croop, J.M. 1991, "Isolation and characterization of Drosophila multidrug resistance gene homologs", *Molecular and cellular biology,* vol. 11, no. 8, pp. 3940-3948.

Wynn, R.L., Jabra-Rizk, M.A. & Meiller, T.F. 2003, "Fungal drug resistance, biofilms, and new antifungals", *General dentistry,* vol. 51, no. 2, pp. 94-98.

Yang, Q., Wang, X., Ye, L., Mentrikoski, M., Mohammadi, E., Kim, Y.-. & Maloney, P.C. 2005, "Experimental tests of a homology model for OxlT, the oxalate transporter of *Oxalobacter formigenes*", *Proceedings of the National Academy of Sciences of the United States of America,* vol. 102, no. 24, pp. 8513-8518.

Yin, Y., He, X., Szewczyk, P., Nguyen, T. & Chang, G. 2006, "Structure of the multidrug transporter EmrD from *Escherichia coli*", *Science,* vol. 312, no. 5774, pp. 741-744.

Zhou, Y., Gottesman, M.M. & Pastan, I. 1999, "Studies of human MDR1-MDR2 chimeras demonstrate the functional exchangeability of a major transmembrane segment of the multidrug transporter and phosphatidylcholine flippase", *Molecular and cellular biology,* vol. 19, no. 2, pp. 1450-1459.

APPENDICES

APPENDIX I

YEPD (Yeast extract peptone dextrose)

Component	Concentration (gm /100 ml)
Yeast extract	1
Bactopeptone	2
D-glucose	2
Bacto agar (for solid medium)	2.5

YNB (Yeast nitrogen base medium)

Component	Concentration (gm /100 ml)
Yeast nitrogen base (w/o aa)	0.67
lucose	2
Bacto agar (for solid medium)	2.5
Uracil (supplement)	30 µg/ml

Bacterial culture media: Luria Bertini Broth (LB)

Component	Concentration (gm /100 ml)
Tryptone	1
Yeast extract	0.5
Sodium chloride	1
Bacto agar (for solid medium)	1.5

SD-URA$^-$ media

Component Concentration (g/100 ml)

Component	Concentration (gm /100 ml)
Yeast nitrogen base (w/o aa)	0.67
D-glucose	2
Bacto agar (for solid medium)	2.5
Dropout mix	0.2

10 X TBE (pH 8.0)

Component	Concentration (gm /litre)
Tris –Cl	108
Boric Acid	55
EDTA	7.4

APPENDIX II

SD dropout mixture

Component Amount (gm)

Component	Concentration (gm / 100 ml)
Adenine	**2.0**
Uracil	**1.0**
Tryptophan	**2.0**
Histidine	**1.0**
Arginine	**1.0**
Methionine	**1.0**
Tyrosine	**1.5**
Isoleusine	**1.5**
Valine	**7.5**
Lysine	**1.5**
Phenylalanine	**2.5**
Glutamic acid	**5.0**
Aspartic acid	**1.8**
Theronine	**10.0**
Serine	**1.8**
Leucine	**3.0**

Depending upon the auxotropy of the strain DROP OUT the respective amino acid from the mix. (For example, in this study URACIL was the amino acid that was excluded from the MIX of amino acids).

APPENDIX III

Solvents for drugs

Drugs Solvent used

Drug	Solvent
Fluconazole	**Water**
Cycloheximide	**Water**
Anisomycin	**DMSO**
4-Nitrosoquinoline oxide	**DMSO**
Cerulenin A	**DMSO**
Methotrexate	**10 mM Tris-Cl pH 7.5**

APPENDIX IV

8 % POLYACRYLAMIDE GEL (Resolving)

Component	Volume for 50 ml
30 % Polyacrylamide	13 ml
1.5 M TE (pH 8.8)	13 ml
10 % SDS	500 µl
10 % APS	500 µl
TEMED	30 µl
M.Q. water	23 ml

5 % POLYACRYLAMIDE GEL (Stacking)

Component	Volume for 30 ml
30 % Polyacrylamide	5 ml
1 M TE (pH 6.8)	3.8 ml
10 % SDS	300 µl
10 % APS	300 µl
TEMED	30 µl
M.Q. water	21 ml

PUBLICATIONS

PUBLICATIONS

This thesis is based on the following original published / unpublished research article.

1. Multidrug resistance in yeast *Candida*. Rajendra Prasad, **Khyati Kapoor**. *Int. Rev. Cytol.* 2005; 242: 215-48. Review.

2. Rational Mutational Analysis of a Multidrug MFS Transporter CaMdr1p of *Candida albicans* by Employing a Membrane Environment Based Computational Approach. **Khyati Kapoor**, Mohd Rehan, Ajeeta Kaushiki, Ritu Pasrija, Andrew. M. Lynn and Rajendra Prasad. *PLoS Comput Biol.* 2009 Dec; 5(12):e1000624. Epub 2009 Dec 24.

3. Employing Information Theoretic Measures and Mutagenesis to Identify Residues Critical for Drug-proton antiporter function of CaMdr1p. **Khyati Kapoor**, Mohd Rehan, Andrew. M. Lynn and Rajendra Prasad. (Under Revision *PLoS ONE*)

OPEN ACCESS Freely available online

Rational Mutational Analysis of a Multidrug MFS Transporter CaMdr1p of *Candida albicans* by Employing a Membrane Environment Based Computational Approach

Khyati Kapoor[1☯], Mohd Rehan[2☯], Ajeeta Kaushiki[2], Ritu Pasrija[1¤], Andrew M. Lynn[2*], Rajendra Prasad[1*]

1 School of Life Sciences, Jawaharlal Nehru University, New Delhi, India, **2** School of Information Technology, Jawaharlal Nehru University, New Delhi, India

Abstract

CaMdr1p is a multidrug MFS transporter of pathogenic *Candida albicans*. An over-expression of the gene encoding this protein is linked to clinically encountered azole resistance. In-depth knowledge of the structure and function of CaMdr1p is necessary for an effective design of modulators or inhibitors of this efflux transporter. Towards this goal, in this study, we have employed a membrane environment based computational approach to predict the functionally critical residues of CaMdr1p. For this, information theoretic scores which are variants of Relative Entropy (Modified Relative Entropy RE_M) were calculated from Multiple Sequence Alignment (MSA) by separately considering distinct physico-chemical properties of transmembrane (TM) and inter-TM regions. The residues of CaMdr1p with high RE_M which were predicted to be significantly important were subjected to site-directed mutational analysis. Interestingly, heterologous host *Saccharomyces cerevisiae*, over-expressing these mutant variants of CaMdr1p wherein these high RE_M residues were replaced by either alanine or leucine, demonstrated increased susceptibility to tested drugs. The hypersensitivity to drugs was supported by abrogated substrate efflux mediated by mutant variant proteins and was not attributed to their poor expression or surface localization. Additionally, by employing a distance plot from a 3D deduced model of CaMdr1p, we could also predict the role of these functionally critical residues in maintaining apparent inter-helical interactions to provide the desired fold for the proper functioning of CaMdr1p. Residues predicted to be critical for function across the family were also found to be vital from other previously published studies, implying its wider application to other membrane protein families.

Citation: Kapoor K, Rehan M, Kaushiki A, Pasrija R, Lynn AM, et al. (2009) Rational Mutational Analysis of a Multidrug MFS Transporter CaMdr1p of *Candida albicans* by Employing a Membrane Environment Based Computational Approach. PLoS Comput Biol 5(12): e1000624. doi:10.1371/journal.pcbi.1000624

Editor: Roland Dunbrack, Fox Chase Cancer Center, United States of America

Received June 15, 2009; **Accepted** November 20, 2009; **Published** December 24, 2009

Funding: This work was supported in parts by grants to one of us (RP) from the Department of biotechnology (BT/PR9100/Med/29/03/2007, BT/PR9563/BRB/10/567/2009); Council of Scientific and Industrial Research (38 (1122)/06/EMR-II, 22/3/2006) and Department of Science and Technology (SR/SO/BB-12/2004, 5/9/2005). KK acknowledges Council of Scientific and Industrial Research, India, for Senior Research fellowship. The funders had no role in study design, data collection and analysis, decision to publish, or preparation of the manuscript.

Competing Interests: The authors have declared that no competing interests exist.

* E-mail: andrew@mail.jnu.ac.in (AML); rp47@mail.jnu.ac.in (RP)

¤ Current address: Infectious Diseases Department, New Drug Discovery Research, Ranbaxy Laboratories Ltd., Gurgaon, India

☯ These authors contributed equally to this work.

Introduction

In yeasts, including the pathogenic *Candida*, an up-regulation of multidrug transporter genes belonging to either ATP Binding Cassette (ABC) or Major Facilitator Superfamily (MFS) is frequently observed in the cells exposed to the drugs leading to the phenomena of multidrug resistance (MDR) [1]. Among the 28 putative ABC and 95 MFS transporter genes identified in the *C. albicans* genome, only ABC transporters CaCdr1p and CaCdr2p and MFS transporter CaMdr1p, are found to be the major determinants of azole resistance [2,3]. The reversal of the functionality of these multidrug efflux pump proteins represents an attractive strategy to combat azole resistance.

The major ABC transporters such as CaCdr1p, CaCdr2p bear similar topology and exist as two homologous halves. These, like any other member of the ABC superfamily have four distinct modules: two transmembrane domains (TMDs) each consisting of six transmembrane segments (TMSs) and two nucleotide binding domains (NBDs) located on the cytosolic side of the membrane. Though similar in topology and promiscuity towards substrate specificity, these ABC multidrug transporters of *C. albicans* also display selectivity to the range of substrates they can export [4].

The transporters belonging to MFS, consists of membrane proteins from bacteria to higher eukaryotes and these are involved in symport, antiport or uniport of various substrates [5,6]. One of the 17 families of MFS transporters uses the proton motive force to drive drug transport and has been identified in both prokaryotes and eukaryotes [7]. Crystal structures of MFS proteins such as lactose permease (LacY), glycerol-3-phosphate (GlpT), EmrD and oxalate: formate antiporter (OxlT), suggest high structural resemblance among this family of proteins [8]. These consist of 12 TMS, arranged with a similar predicted topology, strongly supporting a common structural architecture or fold across all the MFS transporters [9–12]. The fungal MFS members particularly those involved in drug transport are poorly explored in terms of their structure and function [13]. The multidrug MFS transporter

Author Summary

Membrane proteins belonging to the Major Facilitator Superfamily (MFS) transport molecules, including drugs, across the membrane and are known to be associated with drug resistance. CaMdr1p is one such MFS major multidrug efflux pump whose over-expression is linked to frequently encountered azole resistance in hospital isolates of *C. albicans*. Amino acid residues critical for a protein's function are conserved across members of the protein family. However, the traditional measure of conservation is not a useful parameter in mapping a functionally important residue in membrane proteins e.g., hydrophobically conserved stretches form helical transmembrane regions of the protein and are responsible for membrane localization, which individually have limited effect on binding and transport. We have developed a method that uses information theory to score the conservation of a residue relative to its context within the membrane and hypothesize that these residues would be critical for the protein's function. The relevance of predicted residues in the functioning of MFS is validated on CaMdr1p.

CaMdr1p belongs to DHA1 family which is widely distributed and includes both drug-specific and multidrug efflux pumps [14].

Random and site-directed mutational strategies have been extensively used to understand the structure and function of these MDR efflux proteins. For example, random mutational analysis of an ABC transporter, ScPdr5p of budding yeast identified several amino acid residues that alter its substrate specificity and sensitivity to various inhibitors [15,16]. Tutulan-Cunita *et al.* observed that several point mutations led to significant changes in drug specificity of ScPdr5p which are distributed throughout the length of the protein [17]. Site-directed mutagenesis followed by an elegant screen done by Golin's group has revealed interactions between TMS 2 and the NBD which may help to define at least part of the translocation pathway for coupling ATP hydrolysis to drug transport mediated by ScPdr5p. Recently, Schmitt *et al.* have elucidated the role of H1068 in H-loop of ScPdr5p which couples ATP hydrolysis with drug transport [18].

Site-directed mutational analysis of multidrug ABC multidrug transporter CaCdr1p (a close homologue of ScPdr5p) has revealed insight into its drug binding and efflux properties. These studies have implicated some of the amino acid residues of TMS 5, 6, 11 and 12 as the components of the substrate binding pocket(s) of CaCdr1p [19,20]. Together, these studies suggest that the drug binding sites in CaCdr1p are scattered throughout the protein and probably more than one residue of different helices are involved in binding and extrusion of drugs. However, there is still insufficient information available to predict where and how exactly the most common antifungals such as azoles bind and how are they extruded by CaCdr1p.

Site-directed mutational strategies rely on conservation of residues in a Multiple Sequence Alignment (MSA). The conservation of a residue is calculated from the amino acid frequency distribution in the corresponding column of a MSA. However, the physicochemical conservation is not necessarily responsible for a protein's structure and function but could reflect a more general function such as membrane localization. Thus conservation alone is not sufficient to distinguish between residues responsible for the protein function and membrane localization. Membrane proteins differ from soluble proteins because of their inter-TM hydrophilic and TM hydrophobic propensities, which have allowed the development of efficient membrane protein TM prediction methods [21] and of membrane protein specific substitution matrices [22].

The quantification of residue conservation has evolved over the last few years to the use of information theoretic measures [23]. Relative entropy is a distance measure commonly applied to multiple alignments by comparing the observed frequency distribution with a background distribution. In the present study, we have developed and employed a new method using information theory to rationalize mutation strategies and also applied it to a MFS multidrug transporter CaMdr1p [24]. Relative Entropy (RE) or the Kullback-Liebler divergence is an information theoretic measure of the difference between two probability distributions and has been increasingly applied in bioinformatics to identify functional residues [24,25]. The use of RE with background frequencies [26] can improve the prediction of a protein's functional residues [27–32] as well as detect residues that determine the functional subtype of proteins [28]. Though the basic Kullback-Liebler equation has not changed, its intelligent application in our method calculates Relative Entropy (RE_M) relative to its context within the membrane. The RE_M scoring scheme has been improved by treating TM and inter-TM regions of MFS proteins separately which has drastically increased the credibility over the existing methods [23]. In this manuscript, we have compared traditional treatment of conservation, and standard RE, with our improved method. We validated our predictions by replacing the predicted highest RE_M positions of CaMdr1p with alanine by site-directed mutagenesis. We show that most of these residues when replaced with alanine showed decreased resistance to drugs which was corroborated by abrogated efflux of drugs. Additionally, we could further confirm the functional relevance of each of these high RE_M residues by predicting their location in deduced 3D model of CaMdr1p and their role in maintaining apparent inter-helical interactions. With this approach, our method enabled us to accurately predict MFS-wide function-specific residues, validated by using CaMdr1p.

Results

RE_M considers conservation as well as the background probability of each alignment position of a MSA

A comprehensive non-redundant data set, sourced from all MFS sequences present in the 56.2 release, was generated. This data set was then aligned using a membrane-specific multiple alignment program, which stacked the helices appropriately. A highly conserved residue in a multiple alignment is predicted to have a functional significance. We calculated conservation values using the algorithm from Jalview. Residues shown to be conserved dominate the TM helices, and on closer evaluation are largely hydrophobic residues associated with membrane localization. The traditional relative entropy and our modified treatment of the method (RE_M) were calculated on the same alignment using scripts written in-house. (Fig. 1 shows a representative section of the alignment along with the RE_M, RE and conservation scores; see supplementary Table S1 for the RE_M, RE and conservation scores for the entire MSA). The distribution curve generated on the basis of RE_M from the MSA is shown in Fig. 2A. Notably the dominant signal using a conventional conservation measure lies in the TM helices and traditional RE also issues high scores to these residues which are less frequent in nature. Our treatment using a RE_M dampens the membrane localization signals further increasing the signal from atypically occurring conserved residues (Figure S1). Since RE_M considers conservation as well as the background probability of a residue at a particular alignment position, it is an improved index of the functional significance of a residue. To emphasize this fact, thirty residues with highest values were short-listed each from the conservation list, RE list and RE_M list. On comparison, it was found that there are thirteen residues

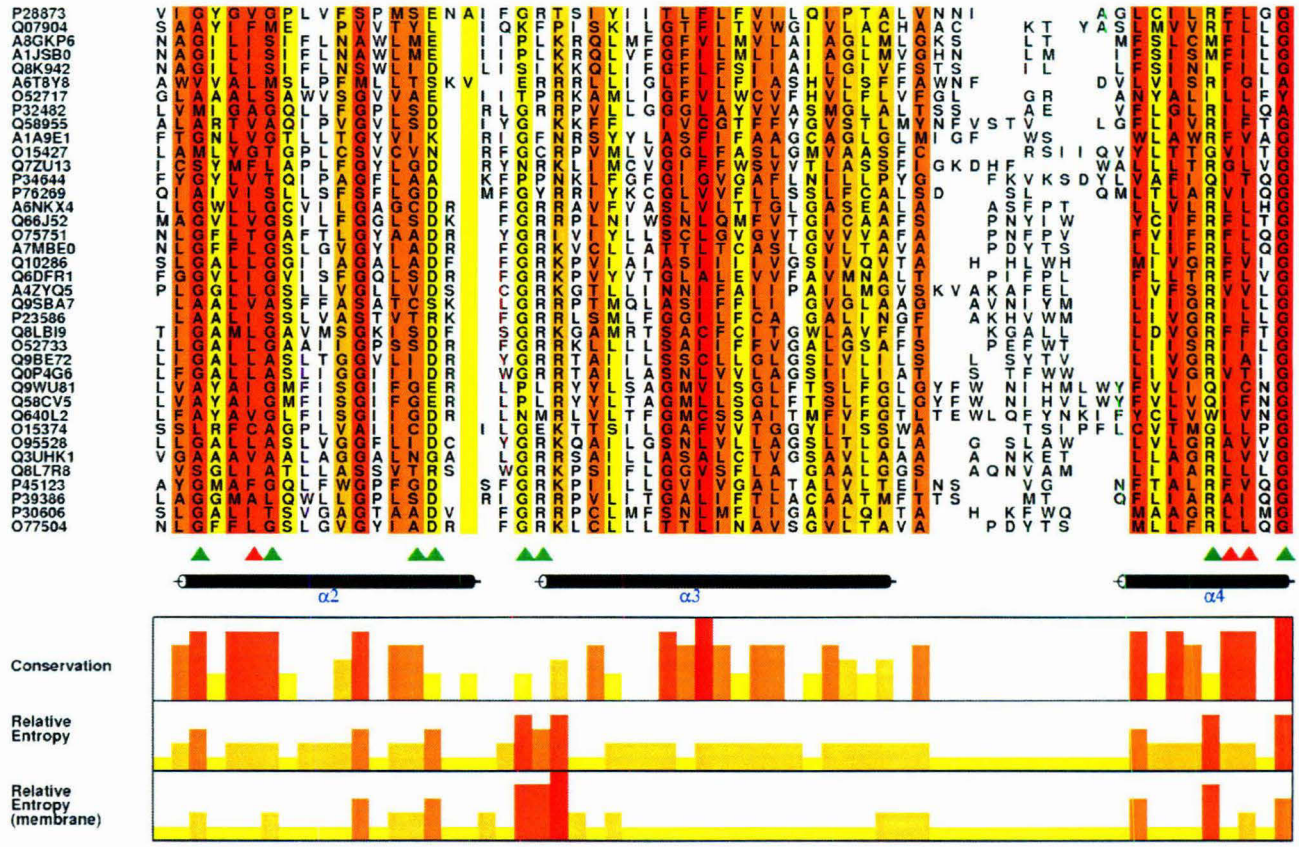

Figure 1. A portion of Multiple Alignment showing conservation and RE_M for each column. Figure showing a representative portion of the alignment of MFS sequences and is generated using Alscript [48]. The alignment is coloured in a gradient from red to yellow on the basis of decreasing conservation score. Conservation was calculated using a method by Livingstone *et al.* [49] and the scores are shown as a histogram. The histogram compares the conservation, RE and the RE_M scores for the alignment columns shows in the figure. Results of selected mutations in CaMdr1p are indicated by triangles, green being sensitive while red are resistant. RE_M scores are better indicators of functional relevance than physicochemical conservation.
doi:10.1371/journal.pcbi.1000624.g001

shortlisted as both conserved and with high RE while it was found that only nine out of these short-listed columns are both conserved and have high RE_M (Supplementary Table S2). The thirty alignment positions with high RE_M were further studied to assess their functional relevance. Expectedly, all residues predicted using RE_M, are not present in every protein in the family. In CaMdr1p, 16 residues were identical with the most frequently occurring residue in the thirty highest scored alignment columns, and were mutated to alanine to directly validate the prediction (Fig. 2B).

Residues with high RE_M are part of the known motifs of Major Facilitator Superfamily

These sixteen out of the top thirty positions, wherein the residue in CaMdr1p matched with the most occurring residue across that alignment position in MSA were analyzed for further studies by site-directed mutagenesis. Interestingly, most of the sixteen residues with high RE_M turned out to be part of the well-known motifs of the MFS. These motifs are identified as Motif A (GxLaDrxGrkxxl), Motif B (lxxxRxxqGxgaa) which are conserved throughout the MFS, Motif C (gxxxGPxxGGxl) only in 12 and 14-TMS family and Motif D2 exclusive to 12-TMS family [7]. Three out of the sixteen residues short-listed for CaMdr1p; E178, G183 and R184 are a part of Motif A; residues L211, R215 and G219 are a part of Motif B and G256 is a part of motif C. In addition to the known motifs mentioned above, two new motifs have been identified by our study. The residues in these stretches ^{273}Wrxxf^{277} and ^{296}Pespr^{300} have high RE_M scores. However, the known motif D2 does not appear to be highly conserved in our alignment and is thus not predicted to be family-wide function-specific.

Site-specific mutagenesis of residues with high RE_M shows that they are functionally critical

All the sixteen residues selected on the basis of high RE_M were mutated by employing site-directed mutagenesis and were replaced with alanine except G165, G183 and G256 which were replaced by leucine. For functional analysis of the mutant variants, a heterologous hyper-expression system, where GFP-tagged CaMdr1p (CaMDR1-GFP) was stably over-expressed from a genomic *PDR5* locus in a *S. cerevisiae* mutant AD1-8u$^-$, was used [33]. The host AD1-8u$^-$ developed by Goffeau's group, was derived from a *Pdr1-3* mutant strain with a gain-of-function mutation in the transcription factor Pdr1p, resulting in constitutive hyper-induction of the *PDR5* promoter [34]. A single-copy integration of each transformant at the *PDR5* locus was confirmed by Southern hybridization (data not shown). Two positive clones of each mutant were selected to rule out clonal variations. These residues with high RE_M score showed increased drug susceptibility and abrogated efflux of substrates such as [^{3}H] MTX and [^{3}H]

A

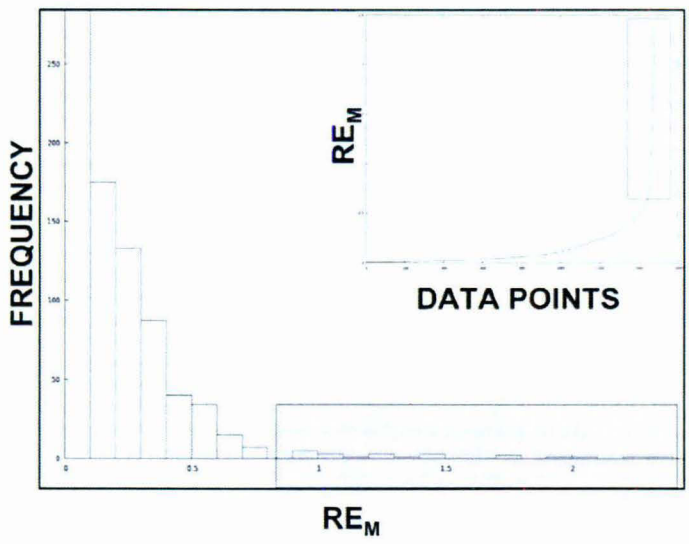

B

RE_M	RESIDUE	LOCATION
2.2	W273	Loop
1.9	R215	TMS 4
1.7	G183	Loop
1.7	D235	TMS 4
1.4	G219	TMS 4
1.4	R184	TMS 3
1.3	P296	Loop
1.2	E178	TMS 2
1.0	R274	Loop
1.0	T160	TMS 2
0.94	F277	TMS 6
0.94	E297	Loop
0.91	G256	TMS 5
0.72	T298	Loop
0.72	L211	TMS 4
0.71	G165	TMS 2

Figure 2. Distribution curve of RE_M values of complete MSA. Panel A: Histogram of the RE_M scores (+ve/background frequency) vs frequency for all positions of MSA of the MFS transporters. The top 30 RE_M positions depicted in the boxed region were selected for further analysis. The inset represents the same data by a line graph. B: The table shows 16 out of the top 30 high RE_M alignment positions where the residue in CaMdr1p matched with the most frequent amino acid at that particular position in a MSA of 342 MFS members. Their predicted location with respect to CaMdr1p is also displayed in the next column.
doi:10.1371/journal.pcbi.1000624.g002

FLU (Fig. 3). Of note, there were few exceptions to the list of residues with high RE_M. For example residues T160, L211, W273 and R274 have high RE_M values but do not appear to be critical for function of CaMdr1p since the drug susceptibility and efflux are not affected upon replacement of these residues with alanine.

All the mutant variants of CaMdr1p are properly surface localized

To confirm that the change in susceptibility observed in the mutant variants was not due to their poor expression or mislocalization, we compared the localization of GFP-tagged version of CaMdr1p (CaMDR1-GFP) and its mutant variants by FACS and confocal imaging. A proper localization of all the mutant variants was confirmed by both these methods which showed proper rimmed appearance of GFP-tagged CaMdr1p. The Western Blot analysis further confirmed that the expression levels of CaMdr1p of all the mutant variants were similar thus corroborating FACS and confocal data (Fig. 4).

Distance plot of CaMdr1p from deduced 3D homology model reveals inter-helical interactions

For evaluating the relevance of high RE_M residues in CaMdr1p, a 3D homology model was constructed using available crystal structures of lac permease of *E. coli* (1pv6), glycerol-3-phophate of *E. coli* (1pw4) and oxalate: formate transporter of *O. formigenes* (1zc7) as described in Materials and Methods. All the top thirty positions of highest RE_M are marked in the model which mostly lie in the N-terminal half of the protein (Fig. 5A). Using the homology model, a symmetric contact map of CaMdr1p was generated as discussed in Materials and Methods (Fig. 5B). We exploited this distance plot to ascertain the role of these residues with high RE_M.

It is apparent that residues L211, R215 and G219 in TMS 4 are within 8 A° distance to many residues of TMS 1, 2 and 3. For example, it can be seen that residue G219 on TMS 4 lie on the same face of the helix and is within 8 A° to the residues G165 and G169 on TMS 2. Indeed, the mutation of predicted G165 and G169 on TMS 2 resulted in abrogated drug susceptibility and transport (data not shown). All the predicted interactions are summarized in Fig. 6A and shown in a pictorial representation of the homology model in Fig. 6B.

Discussion

The multidrug MFS transporter CaMdr1p harbors a conserved antiporter 'motif C' within TMS 5. Our recent study has revealed that the conserved and critical residues of this motif and of TMS 5 are bunched together on the same face of its helical wheel

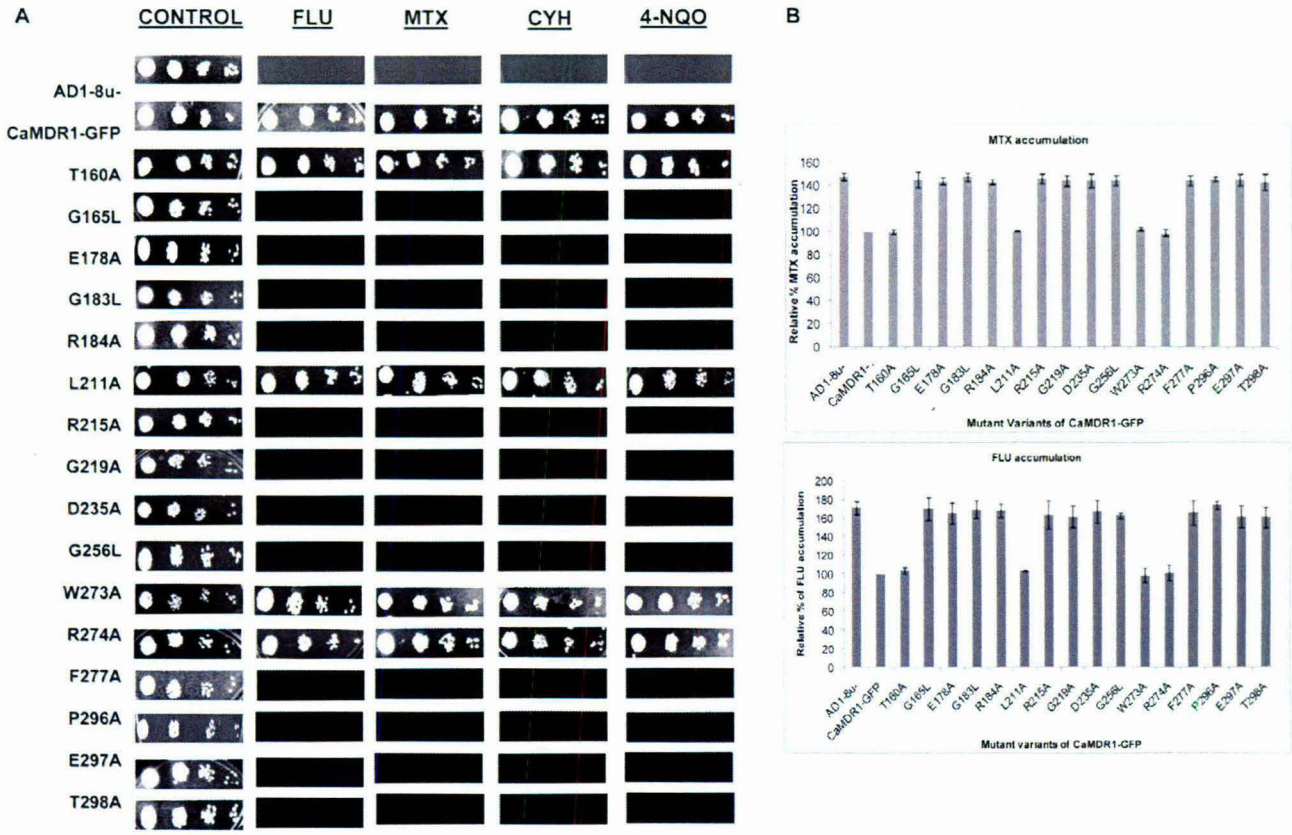

Figure 3. Drug susceptibility and transport assays of mutant variants of CaMDR1-GFP in *S. cerevisiae*. Panel A: Drug resistance profile of wild type and mutant CaMDR1-GFP yeast strains determined by spot assay. For spot assay, cells were freshly streaked, grown overnight and then resuspended in normal saline to an A_{600} of 0.1 (1×10^6 cells) and 5 µl of five-fold serial dilutions, namely 1 (1:5), 2 (1:25), 3 (1:125) and 4 (1:625), of each strain was spotted on to YEPD plates in the absence (control) and presence of the following drugs: FLU (0.20 µg/ml), CYH (0.20 µg/ml), 4-NQO (0.20 µg/ml) and MTX (65 µg/ml). Growth differences were recorded following incubation of the plates for 48 hrs at 30°C. Growth was not affected by the presence of the solvents used for the drugs (data not shown). B: [^{3}H] MTX and [^{3}H] FLU accumulation in the different mutant variants of CaMdr1p-GFP. Controls AD1-8u$^-$ and RPCaMDR1-GFP have also been included for comparison. The results are means±standard deviations for three independent experiments.
doi:10.1371/journal.pcbi.1000624.g003

projection and are critical in drug efflux [35]. However, the structure and function aspects of this major multidrug transporter remain poorly understood. To address some of these questions, in this study, we have rationalized conventional mutational strategy and applied computational approach to predict functionally critical residues of CaMdr1p.

The sequence set described in this manuscript represents a comprehensive non-redundant coverage of annotated MFS sequences from SWISSPROT. Many methods have been developed to improve the MSA of membrane protein families for accurate predictions of residues critical for structure and function [36]. Membrane proteins have fold signals which are easily mapped to the primary sequence as TM and inter-TM stretches. Considering the differences in physico-chemical properties of these two regions, membrane protein specific substitution matrices have been developed [22]. However, we argued that a conservation score on the basis of identity or physico-chemical similarity still remains inadequate as the background frequencies of their immediate environmental milieu are radically different with respect to hydrophilic and hydrophobic propensities. This is also apparent from the conservation scores of the MSA wherein a large proportion of the conserved columns correspond to hydrophobic TM regions. Notably, two CaMdr1p residues (F216 and L217) with high conservation but low RE_M were taken as controls, when replaced with alanine showed no change in the phenotype (data not shown). One of the most basic fold specific signals is the hydrophobic core in globular proteins, and the TM region in membrane proteins. Unlike globular proteins, the hydrophobic TM region is continuous in the membrane protein's primary structure, and indeed this still remains one of the preferred methods to identify membrane proteins, and map their TM regions. While it is intuitive that the synchronous stretch of hydrophobic residues is responsible for membrane localization, the application of a scoring method that can distinguish these residues from family-wide alignment columns associated with other functions has not yet been deployed. In essence, we require a method that can objectively separate the TM signals from other signals. To overcome these limitations, we improved existing method(s) of information theory wherein RE_M was calculated on the basis of MSA of MFS proteins, keeping in mind the differences in the environmental milieus. We thus treated TM and inter-TM regions by different background probabilities for calculation of RE_M. These RE_M scores helped us to predict those sites which have amino acid distributions very different from the respective background distribution thereby statistically predicted to be functionally critical. Not all the residues predicted using RE_M,

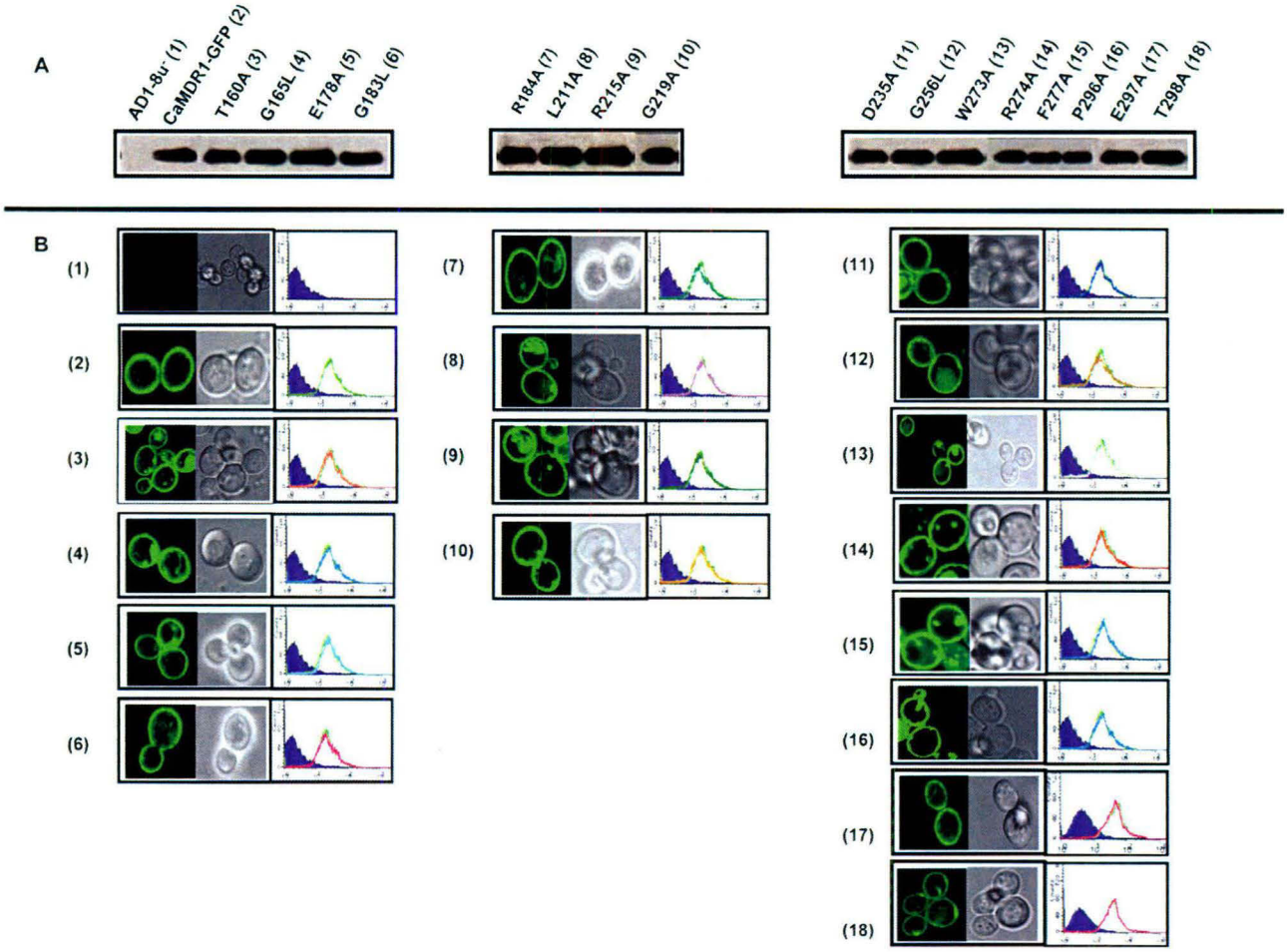

Figure 4. Protein expression profiles of CaMdr1p-GFP and its mutant variants in *S. cerevisiae*. Panel A: Western Blot analysis of the PM fraction of mutant variants with anti-GFP antibody. B: Confocal and FACS analysis of the all the mutant variants to check their expression and localization in comparison with AD1-8u⁻ (negative control) and RPCaMDR1-GFP (positive control) [46].
doi:10.1371/journal.pcbi.1000624.g004

are present in every protein in the family. In CaMdr1p, 16 residues were identical with the most frequently occurring residue in the thirty highest scored alignment columns, and were mutated to directly validate the prediction (Fig. 2B). Our results of drug susceptibility assays revealed that almost all of these matched residues with high RE_M when replaced with alanine displayed sensitivity to the tested drugs and showed abrogated drug transport (Fig. 3). Interestingly, when we mutated residues which had high conservation values but lower RE_M values (negative control); none showed alterations in drug susceptibilities and thus did not retain the functionally critical stringency as was evident from residues with higher RE_M. For example, analysis of a few conserved columns of the MSA, such as F216, L217 and L171 having RE_M values between 0.57-0.44 revealed that their replacement with alanine did not affect the function of CaMdr1p (data not shown). This strengthens the fact that our method takes into account the conservation along with the background frequency and thus lists out residues which affect the function. Also, to check the efficiency of the method, another negative control used was to mutate residues which are having low conservation and low RE_M values but lie in the vicinity of one of the 16 selected high RE_M residues. For example, when C225 which is closer to the critical G219 and D235, was mutated to C225A, the functioning of the protein was not affected (data not shown). Similarly, for critical G256, when residues A248, A253 and V254 which are within its vicinity were mutated as A248G, A253G and V254A, the mutant variants continued to behave as WT-CaMDR1-GFP [35].

To further elucidate the role of predicted residues in the functionality of CaMdr1p, a homology model based on the available crystal structures of lac permease, glycerol-3-phophate and oxalate: formate transporter was deduced [9-11]. The RE_M method predicts the relative importance of a residue purely from sequence analysis and is independent of the protein's structure. However, the role a residue plays in the protein's function is not readily apparent from its sequence. We exploited the protein's 3D model as a guide to reason why a residue is functionally critical. The deduced 3D model suggested that similar to other MFS structures, the 12 TM helices of the CaMdr1p span the membrane in such a way that they form the channel pore particularly aligned by residues of TMS 2, 4, 5, 7, 8, 10 and 11. From the deduced homology model of CaMdr1p, a symmetric contact map was generated to highlight the inter-helical interactions of the protein (Fig. 5B). Based on the predictions from the distance map, we could show that many high RE_M residues are indeed a part of inter-helical interactions (Fig. 6B). It is apparent that more than one residue pair is predicted to be involved in maintaining the interactions between helices (Fig. 6A).

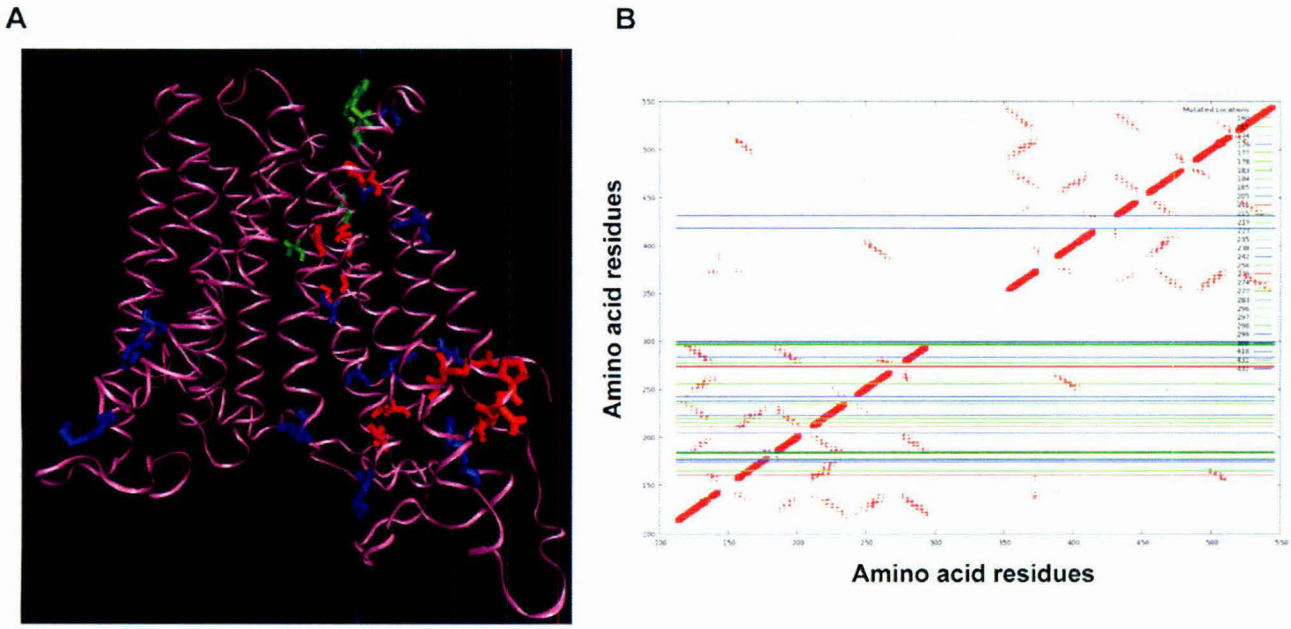

Figure 5. The 3D homology model of CaMdr1p and the contact map derived from it. Panel A: The 3D homology model of CaMdr1p wherein the mutated residues are marked onto the model and are coloured on the basis of the phenotypes exhibited upon mutation. Red denotes sensitive, green shows resistant and blue marks a position predicted to be important but not mutated as the CaMdr1p residues did not match the conserved residue in that alignment position. The structure is viewed using Visual Molecular Dynamic (VMD) software. B: The contact map of CaMdr1p is plotted between all the residues vs all the residues and displays the interactions between the beta carbon of each residue and beta carbon atoms of every other residue within and up to 8 A° of distance (Cα is used for glycine). Each cross points to an interaction between a residue on x-axis and a residue on y-axis. The lines represent the top thirty high RE_M residues and are coloured on the basis of the phenotypes where green represents the residues that are sensitive upon mutation while red are the ones that do not show any phenotype. The blue lines mark the residues in CaMdr1p that did not match with the most frequent residue in that particular column of the MSA.
doi:10.1371/journal.pcbi.1000624.g005

Our aim in developing this method was to identify residues with high specificity which would play a critical role across this entire MFS protein family. Although signals associated with antiporter motifs have been identified using this method, a finer granularity in function such as substrate specificity determining residues is not expected, as these signals would not be family-wide. Since the enlisted residues with high RE_M values which are functionally critical for CaMdr1p are expected to be family-wide function-specific and thus critical for the entire MFS protein data set, we validated their relevance from the earlier published work. It is known that Motif A of the MFS transporters span an eight residue long loop between TMS 2 and 3 and is suggested to be involved in maintaining a β-turn linking the adjacent TM helices [14]. In the present study, G183 and R184 in the loop between TMS 2 and TMS 3 of CaMdr1p were picked up as family-wide function-specific residues thus corroborating that these residues are a part of Motif A (GxLaDrxGrkxxl) which holds importance throughout the MFS transporters. The hypothesized rocking motion in MFS presumably requires conformational changes in the TMS and the β–turns. In this, the transporter inter-converts between C_i (inward facing) and C_o (outward facing) states for translocation of substrates. In glycerol-3-phosphate of *E. coli*, it was seen that D88 was involved in inter-conversion between these C_i and C_o states of the protein [10]. Interestingly, D88 corresponds to E178 of CaMdr1p which also lies in Motif A which upon mutation to alanine turns out to be critical for drug susceptibility and efflux (Table 1).

Motif B (lxxxRxxqGxgaa) of all MFS has a role in energy coupling which spans the N-terminal half of TMS 4 [7]. CaMdr1p contact map reveals that residues in Motif B interface with residues ^{165}GxxxG^{169} on TMS 2. Motifs rich in glycine and proline residues promote formation of special backbone conformation including kinks in TMS, tight interactions between TMS and very flexible β-turns. In human VAchT, Motif B and the adjacent sequences contain a total of nine notch signatures. A notch allows two helical TMS to approach each other unusually closely because small side chains are located at the interface. R124 of PcaK of *Pseudomonas putida* which is equivalent to high RE_M R215 of CaMdr1p of *C. albicans* is shown to be critical for helix packing [37]. Interestingly, G111 of LacY of *E.coli* which also occupies a position in the same alignment column is also critical and earlier shown to be a residue at a kink.

Residues from Motif C (gxxxGPxxGGxl) which is exclusive to 12-TMS family are also picked up by our calculations [7]. G150 of LacY of *E.coli* which is equivalent to high RE_M G256 of CaMdr1p is function-specific for LacY protein [38]. A stretch of conserved residues ^{296}Pespr^{300}, previously unidentified, at the end of TMS 6 were also predicted with high RE_M. We have mutated equivalent residues P296A, E297A and T298A of CaMdr1p that overlap with the consensus residues in the stretch and found that cells expressing these mutated variants displayed increased sensitivity to drugs. However, the functional significance of these residues is yet to be established.

There are a few exceptions which emerged from our method. For example, our method did not pick up any residue of Motif D2. This could be an artifact of the method used for alignments in earlier studies. In this study we have employed a membrane protein specific alignment method whereas earlier reports have used standard multiple alignments substitution matrices with smaller data sets. However, when we repeated the alignment using

A

RESIDUES	LOCATION	PREDICTED INTERHELICAL INTERACTIONS
G165	TMS 2	TMS 4
R184	TMS 3	TMS 6
R215	TMS 4	TMS 1
		TMS 2
		TMS 3
G219	TMS 4	TMS 1
		TMS 2
		TMS 3
G256	TMS 5	TMS 1
		TMS 8
F277	TMS 6	TMS 1
		TMS 3
		TMS 5

B

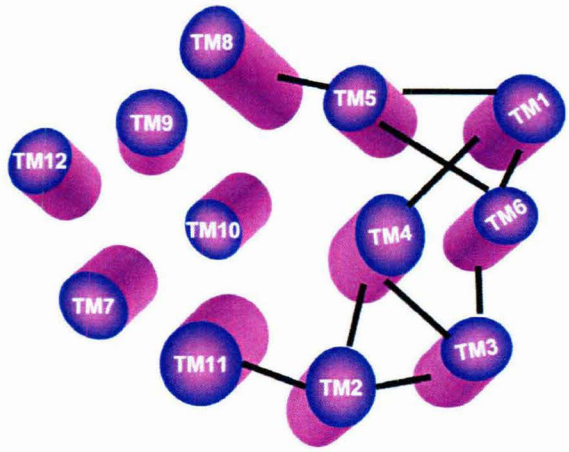

Figure 6. Summary of inter-helical interactions via high RE_M residues. Panel A: The table summarizes predicted inter-helical interactions mediated via selected residues with high RE_M. More than one residue pair is predicted to be involved in maintaining the interactions between the helices. B: Pictorial representation of inter-helical interactions via these high RE_M residues. Figure shows that the residues involved in these interactions are majorly confined to the N-terminal half of the protein.
doi:10.1371/journal.pcbi.1000624.g006

MUSCLE [39] and with the standard substitution matrix (Blosum 62) [40] on the complete data set the motif still did not appear (data not shown). Motif D2 is assumed to have a structural significance as it holds a major kink within TMS 1 but mutations in this motif do not alter the backbone conformation. As an example of the possibly insignificant role of the motif, in human VAchT, the mutation of L49G in this motif completely eliminates propensity for a kink or notch and abolishes activity while normally a glycine itself is expected to be present at this position and is supposed to be involved in maintaining a major kink in this motif [41].

Out of the 16 residues that were mutated, T160A, L211A, W273A and R274A did not lead to any phenotypic changes. It is known that for some of the positions in alignment, the most frequent amino acid does not match with the residue of CaMdr1p at that site. One reason for this could be that some of the

Table 1. High RE_M alignment positions shown to be critical for function in other MFS members.

MFS Transporter	Organism	Critical Residue	Location	Function	References
LacY	*E. coli*	G111 (1.9)	TM4	Residue at kink	[9]
LacY	*E. coli*	G150 (0.91)	TM5	Residue at kink	-do-
PcaK	*Pseudomonas putida*	R124 (1.9)	TM4	Helix Packing	[37]
PcaK	*Pseudomonas putida*	E144 (0.76)	TM4	Helix Packing	-do-
GlpT	*E. coli*	D88 (1.27)	TM2	Involved in the C_i and C_o inter-conversion	[10]
MdfA	*E. coli*	D77 (1.2)	TM2	No activity seen if mutated to alanine	[50]
EmrD	*E. coli*	R118 (0.59)	TM4	Role in defining topology	[14]

The residues with high RE_M positions and their predicted roles in the case of other MFS members are enlisted. The residues of CaMdr1p at the same position in the alignment are shown to be critical in this study.
doi:10.1371/journal.pcbi.1000624.t001

functionally important residues co-evolve i.e., these residues may mutate, with compensatory mutation occurring elsewhere in the protein to regain function [42]. T160 where the most frequent residue is a serine at that position may be one such case. Another reason may be that the alignment used in this study involved prediction of TMS with the possibility of errors in demarcating the edges of TM helices. Residues from columns lining the edges of the helices may be wrongly assigned to TM and inter-TM regions. This probably explains the lack of any effect of mutation on residues T160 of TMS 2 and L211 of TMS 4 which lie at the edge of the respective TMS. Other exceptions to our predictions are the mutation of W273 and R274 which though highly conserved and probably a part of the new motif but do not abrogate function upon mutation. Although a few tryptophans in an ABC transporter MRP1, have been shown to be involved in substrate binding and transport [43], generally, in a membrane protein tryptophan residues located on the surface of the molecule are mainly positioned to form hydrogen bonds with the lipid head groups while their hydrophobic rings are immersed in the lipid part of the bilayer [44]. We predict that W273 and R274 may be associated with membrane helix orientation and this function may not be perturbed by mutating them individually through alanine scanning. Alternatively, the tryptophan-arginine residues could be functionally critical in tandem and compensate each other for the loss of either one of them.

Of note, in our predictions, substrate specific residues with high RE_M are not picked up which predominantly occur in C-terminal of MFS proteins. It should be mentioned that since our alignment considers the entire MFS, residues responsible for substrate specificity would only be selectively conserved within a subfamily and would not have sufficiently strong signals to be visible in this present family-wide study. For this, the same method may be applied to a data set classified on the basis of substrate selectivity to identify residues critical to the functioning of that subfamily.

There are a number of conservation methods known but none has yet achieved both biological and statistical rigor. We have used RE_M to separate conserved residues from the background function of TM localization. The interpretations support the well-known fact that MFS has a conserved N-terminal half which has residues important for maintenance of a specific fold for this class of proteins while C-terminal half has a more specific role in substrate binding and recognition [7]. Taken together, our study provides an insight into the molecular details of MFS transporters in general and CaMdr1p in particular. Our method of scaled RE_M calculations improves its performance over other information theoretic methods. Additionally, this study also provides a method for rational mutational analysis not only for MFS proteins but can be applied to any class of membrane proteins and thus makes it possible to predict and locate family-wide functionally relevant residues.

Materials and Methods

Materials

Anti-GFP monoclonal antibody was purchased from BD Biosciences Clontech, Palo Alto, CA, USA. DNA modifying enzymes were purchased from NEB. The drugs cycloheximide (CYH), 4-Nitroquinoline oxide (4-NQO), Methotrexate (MTX) and Protease inhibitors (Phenylmethylsulfonyl fluoride, Leupeptin, Aprotinin, Pepstatin A, TPCK, TLCK) and other molecular grade chemicals were obtained from Sigma Chemicals Co. (St. Louis, MO, USA) Fluconazole (FLU) was generously provided by Ranbaxy Laboratories, India. [^{3}H] Fluconazole was custom prepared and [^{3}H] Methotrexate (MTX) was purchased from Amersham Biosciences, United Kingdom.

Media and strains

Plasmids were maintained in *Escherichia coli* DH5α. *E.coli* was cultured in Luria-Bertani medium (Difco, BD Biosciences, NJ, USA) to which ampicillin was added (100 μg/ml). The *S. cerevisiae* strain used was AD1-8u$^-$ (*MATa pdr1-3 his1 ura3 Δyor1::hisG Δsnq2::hisG Δpdr5::hisG Δpdr10::hisG Δpdr11::hisG Δycf1::hisG Δpdr3::hisG Δpdr15::hisG*), provided by Richard D. Cannon, University of Otago, Dunedin, New Zealand [33], [34]. The yeast strains used in this study are listed in the Supplementary Table S3. The yeast strains were cultured in YEPD broth (Bio101, Vista, CA, USA) or in SD-ura$^-$ dropout media (0.67% yeast nitrogen base, 0.2% dropout mix, and 2% glucose; Difco). For agar plates, 2.5% (w/v) Bacto agar (Difco, NJ, USA) was added to the medium.

Methods

Multiple sequence alignment. 561 MFS sequences having 12 TMS as predicted by TMHMM [21] were extracted from SWISSPROT release 56.2. Redundancy in the sequences is reduced to 90% on the basis of identity using BLASTclust by setting the identity threshold S to 90 and keeping all other parameters to default values (http://genomes.ucsd.edu/manuals/blast/blastclust.html). The resulting 342 sequences were then aligned by PRALINETM using TMHMM as the method for predicting TM lengths and keeping all other parameters at their default values [36,45] (See Supplementary Dataset S1).

Calculation of conservation score, RE and RE_M. Conservation of an amino acid in an alignment column was calculated using Jalview using available scoring schemes which are restricted to soluble proteins, was modified to accommodate different background probabilities for TM and inter-TM regions.

RE is calculated as the deviation of the amino acid distribution $P_i(a)$ from a background disribution $f(a)$.

$$REM = \sum_{a=1..20} Pi(a) \log \frac{Pi(a)}{f(a)}$$

where $\boldsymbol{P_i(a)}$ is the probability of the occurrence of amino acid $\boldsymbol{a}$ in column $\boldsymbol{i}$ of the MSA $\boldsymbol{f(a)}$ is the background probability of amino acid $\boldsymbol{a}$ and is classically estimated from SWISSPROT as the probability of occurrence of an amino acid in a large data set of proteins.

In our method RE_M, $\boldsymbol{f(a)}$ is the background probability of amino acid $\boldsymbol{a}$ and is classically estimated as the probability of occurrence of an amino acid in a large data set of proteins. $\boldsymbol{f(a)=f(a)_{TM}}$ or $\boldsymbol{f(a)_{iTM}}$ where $\boldsymbol{f(a)_{TM}}$ and $\boldsymbol{f(a)_{iTM}}$ is the background probability calculated separately for TM and inter-TM regions of the alignment. The background probability is thus replaced with this environment specific background frequency. A classical description of entropy also does not take into consideration the absence of data points which are gaps in the case of a multiple alignment column. We used a scaling factor which is equal to number of amino acid positions excluding gaps in column $\boldsymbol{i}$ divided by total number of sequences. The scores were then divided by this scaling factor to give scaled RE_M score.

Site-directed mutagenesis of CaMdr1p. Site-directed mutagenesis was performed by using the Quick-Change Mutagenesis kit (Stratagene, La Jolla, CA, USA) as described previously [46]. The mutations were introduced into the plasmid pRPCaMDR1-GFP according to the manufacturer's instructions, and the desired nucleotide sequence alterations were confirmed by DNA sequencing of the ORF. The primers used for the purpose are listed in Supplementary Table S4. The mutated plasmid, after linearising

with *XbaI*, was used to transform AD1-8u$^-$ cells for uracil prototrophy by lithium acetate transformation protocol [46]. Integration was confirmed by Southern Blot analysis (data not shown).

Preparation of the plasma membranes and immunodetection of CaMdr1p and its mutant variants. The plasma membranes (PM) were prepared from *S. cerevisiae* cells, as described previously [46]. The PM protein concentration was determined by bicinchonic acid assay using bovine serum albumin as the standard. For Western Blot analysis the immunoblot was incubated with anti-GFP monoclonal antibody (1:5000 JL-8 BD Biosciences as described previously. Immunoreactivity of GFP antibody was detected using goat anti-mouse horseradish peroxidase-labelled antibody (1:5,000) and was visualized using the enhanced chemiluminescence assay system (ECL kit, Amersham Biosciences, Arlington Heights, IL, USA) [46].

Drug susceptibility. The susceptibilities of yeast cells, harboring wild type CaMDR1-GFP and its mutant variants, were tested to different drugs by spot assay. For spot assay, 5 µl samples of five-fold serial dilutions of yeast culture each with cells suspended in normal saline to an OD of 0.1 (1×10^6 cells) at A_{600} were spotted onto YEPD plates in the absence (control) or in the presence of the drugs [35]. Growth differences were recorded following incubation of the plates for 48 hrs at 30 C.

Drug transport of mutant variants. The accumulation of [^{3}H] MTX (specific activity, 8.60 Ci/mmol) and [^{3}H] FLU (specific activity, 19 Ci/mmol) was determined by protocol described previously [35]. Cells from mid-log phase were centrifuged at 500×g for 3 min and resuspended in fresh YEPD medium as 5% cell suspension. 100 µl of cell suspension was incubated in shaking water bath at 150 rpm at 30°C and [^{3}H] MTX was added to a final concentration of. The cells were incubated in [^{3}H] MTX (25 µM) or [^{3}H] FLU (100 nM) for 30 min, filtered rapidly and washed twice with 1x PBS, pH 7.4 on Millipore manifold filter assembly using 0.45 µm nitrocellulose filter discs (Millipore, U.S.A). The filter discs were dried and put in cocktail-O and the radioactivity was measured in a liquid scintillation counter (Packard, Beckman, USA). The accumulation was expressed relative to the wild type CaMdr1p-GFP.

Molecular modeling of CaMdr1p. Structures of known MFS proteins [PDB id – 1pv6 [9], 1pw4 [10] and 1zc7 [11]] were retrieved from Protein Data Bank www.rscb.org and aligned using MODELLER9V5 [47]. MFS sequences containing CaMdr1p aligned earlier with PRALINETM were aligned to this structure alignment after removing the sequences which corresponded to known structures. These were aligned using the profile-profile alignment option of ClustalW. The Profile alignment was then manually refined based on helix packing information of known MFS structures. Manual refinement was restricted to incorporating gaps in the loop regions without disturbing either the structural alignment or PRALINE sequence alignment. The homology model for the target sequence CaMdr1p was generated using MODELLER9V5 [47] using 1pv6, 1pw4 and 1zc7 as template sequences. The initial 90 residues from N-terminal of CaMdr1p did not align with any of the templates, and were omitted from further study. The model was evaluated and validated by PROCHECK.

Generating the contact map. The contact map displays the distances between Cβ of one residue and Cβ of every other residue within 8 A° distance (Cα is considered in case of glycine). Using the homology model a symmetric contact map for CaMdr1p was generated using a PERL program written in-house.

Supporting Information

Dataset S1 The PRALINETM alignment of 342 MFS sequences as described in Materials and Methods.
Found at: doi:10.1371/journal.pcbi.1000624.s001 (0.77 MB DOC)

Table S1 RE_M, RE and conservation scores for all the positions of the MSA of 342 MFS sequences.
Found at: doi:10.1371/journal.pcbi.1000624.s002 (2.01 MB DOC)

Table S2 Comparison of RE_M and conservation scores.
Found at: doi:10.1371/journal.pcbi.1000624.s003 (0.26 MB DOC)

Table S3 List of yeast strains used in this study
Found at: doi:10.1371/journal.pcbi.1000624.s004 (0.04 MB DOC)

Table S4 List of oligonucleotides used for site-directed mutagenesis.
Found at: doi:10.1371/journal.pcbi.1000624.s005 (0.05 MB DOC)

Figure S1 Comparative plot of conservation (red), RE (green) and RE_M (blue) across the entire alignment. The conservation scores are scaled for comparison with RE and REM. Positions of the highest scoring alignment columns by each method are shown above the graph, along with the results of mutation of the matching residues. Out of these top scoring positions by three different calculations, the mutated positions showing resistant phenotype are marked in red triangles, those showing sensitive on all drugs are marked in green triangles while those which were not mutated are marked by empty triangles. Locations of the transmembrane regions are marked by black bars on the x-axis.
Found at: doi:10.1371/journal.pcbi.1000624.s006 (0.03 MB PDF)

Acknowledgments

We thank R. D. Cannon for providing us with the plasmid and the strains used in this study. We further thank Ranbaxy Laboratories Limited, India for providing us with Fluconazole. We are thankful to K. Natrajan and Devapriya Choudhury for their valuable comments on our manuscript.

Author Contributions

Conceived and designed the experiments: KK AML RP. Performed the experiments: KK MR AK. Analyzed the data: KK MR RP AML RP. Contributed reagents/materials/analysis tools: AML RP. Wrote the paper: KK AML RP.

References

1. Prasad R, Kapoor K (2005) Multidrug resistance in yeast cells. Int Rev Cytol 242: 215–248.
2. Gaur M, Choudhury D, Prasad R (2005) Complete inventory of ABC proteins in human pathogenic yeast, *Candida albicans*. J Mol Microbiol Biotechnol 9: 3–15.
3. Gaur M, Puri N, Manoharlal R, Rai V, Mukhopadhayay G, et al. (2008) MFS transportome of the human pathogenic yeast *Candida albicans*. BMC Genomics 9: 579.
4. Smriti, Krishnamurthy S, Dixit BL, Gupta CM, Milewski S, et al. (2002) ABC transporters Cdr1p, Cdr2p and Cdr3p of a human pathogen *Candida albicans* are general phospholipid translocators. Yeast 19: 303–318.
5. De RE, Arrigo P, Bellinzoni M, Silva PA, Martin C, et al. (2002) The multidrug transporters belonging to major facilitator superfamily in *Mycobacterium tuberculosis*. Mol Med 8: 714–724.
6. Ginn SL, Brown MH, Skurray RA (2000) The TetA K tetracycline/H(+) antiporter from *Staphylococcus aureus*: mutagenesis and functional analysis of motif C. J Bacteriol 182: 1492–1498.
7. Paulsen IT, Brown MH, Skurray RA (1996) Proton-dependent multidrug efflux systems. Microbiol Rev 60: 575–608.
8. Law CJ, Maloney PC, Wang DN (2008) Ins and outs of major facilitator superfamily antiporters. Annu Rev Microbiol 62: 289–305.

9. Abramson J, Smirnova I, Kasho V, Verner G, Kaback HR, et al. (2003) Structure and mechanism of the lactose permease of *Escherichia coli*. Science 301: 610–615.
10. Huang Y, Lemieux MJ, Song J, Auer M, Wang DN (2003) Structure and mechanism of the glycerol-3-phosphate transporter from *Escherichia coli*. Science 301: 616–620.
11. Yin Y, He .X, Szewczyk P, Nguyen T, Chang G (2006) Structure of the multidrug transporter EmrD from *Escherichia coli*. Science 312: 741–744.
12. Yang Q, Wang X, Ye L, Mentrikoski M, Mohammadi E, et al. (2005) Experimental tests of a homology model for OxlT, the oxalate transporter of *Oxalobacter formigenes*. Proc Natl Acad Sci U S A 102: 8513–8518.
13. Sa-Correia I, dos Santos SC, Teixeira MC, Cabrito TR, Mira NP (2009) Drug:H^+ antiporters in chemical stress response in yeast. Trends Microbiol 17: 22–31.
14. Pao SS, Paulsen IT, Saier MH Jr (1998) Major Facilitator Superfamily. Microbiol Mol Biol Rev 62: 1–34.
15. Egner R, Bauer BE, Kuchler K (2000) The transmembrane domain 10 of the yeast Pdr5p ABC antifungal efflux pump determines both substrate specificity and inhibitor susceptibility. Mol Microbiol 35: 1255–1263.
16. Shukla S, Robey RW, Bates SE, Ambudkar SV (2006) The calcium channel blockers, 1,4-dihydropyridines, are substrates of the multidrug resistance-linked ABC drug transporter, *ABCG2*. Biochemistry 45: 8940–8951.
17. Tutulan-Cunita AC, Mikoshi M, Mizunuma M, Hirata D, Miyakawa T (2005) Mutational analysis of the yeast multidrug resistance ABC transporter Pdr5p with altered drug specificity. Genes Cells 10: 409–420.
18. Ernst R, Kueppers P, Klein CM, Schwarzmueller T, Kuchler K, et al. (2008) A mutation of the H-loop selectively affects rhodamine transport by the yeast multidrug ABC transporter Pdr5. Proc Natl Acad Sci U S A 105: 5069–5074.
19. Saini P, Prasad T, Gaur NA, Shukla S, Jha S, et al. (2005) Alanine scanning of transmembrane helix 11 of Cdr1p ABC antifungal efflux pump of *Candida albicans*: identification of amino acid residues critical for drug efflux. J Antimicrob Chemother 56: 77–86.
20. Puri N, Gaur M, Sharma M, Shukla S, Ambudkar SV, et al. (2009) The amino acid residues of transmembrane helix 5 of multidrug resistance protein CaCdr1p of *Candida albicans* are involved in substrate specificity and drug transport. Biochim Biophys Acta 1788: 1752–1761.
21. Krogh A, Larsson B, von HG, Sonnhammer EL (2001) Predicting transmembrane protein topology with a hidden Markov model: application to complete genomes. J Mol Biol 305: 567–580.
22. Ng PC, Henikoff JG, Henikoff S (2000) PHAT: a transmembrane-specific substitution matrix. Bioinformatics 16: 760–766.
23. Valdar WS (2002) Scoring residue conservation. Proteins 48: 227–241.
24. Cover T, Thomas J (2009) Elements of Information Theory.
25. Shannon CE (1997) The mathematical theory of communication. 1963. MD Comput 14: 306–317.
26. Wang K, Samudrala R (2006) Incorporating background frequency improves entropy-based residue conservation measures. BMC Bioinformatics 7: 385.
27. Hannenhalli SS, Russell RB (2000) Analysis and prediction of functional sub-types from protein sequence alignments. J Mol Biol 303: 61–76.
28. Srivastava PK, Desai DK, Nandi S, Lynn AM (2007) HMM-ModE improved classification using profile hidden Markov models by optimising the discrimination threshold and modifying emission probabilities with negative training sequences. BMC Bioinformatics 8: 104.
29. Reva B, Antipin Y, Sander C (2007) Determinants of protein function revealed by combinatorial entropy optimization. Genome Biol 8: R232.
30. Li L, Shakhnovich EI, Mirny LA (2003) Amino acids determining enzyme-substrate specificity in prokaryotic and eukaryotic protein kinases. Proc Natl Acad Sci U S A 100: 4463–4468.
31. Fischer JD, Mayer CE, Soding J (2008) Prediction of protein functional residues from sequence by probability density estimation. Bioinformatics 24: 613–620.
32. Capra JA, Singh M (2008) Characterization and prediction of residues determining protein functional specificity. Bioinformatics 24: 1473–1480.
33. Decottignies A, Grant AM, Nichols JW, De Wet H, McIntosh DB, et al. (1998) ATPase and multidrug transport activities of the overexpressed yeast ABC protein Yor1p. J Biol Chem 273: 12612–12622.
34. Nakamura K, Niimi M, Niimi K, Holmes AR, Yates JE, et al. (2001) Functional expression of *Candida albicans* drug efflux pump Cdr1p in a *Saccharomyces cerevisiae* strain deficient in membrane transporters. Antimicrob Agents Chemother 45: 3366–3374.
35. Pasrija R, Banerjee D, Prasad R (2007) Structure and function analysis of CaMdr1p, a major facilitator superfamily antifungal efflux transporter protein of *Candida albicans*: identification of amino acid residues critical for drug/H^+ transport. Eukaryot Cell 6: 443–453.
36. Pirovano W, Feenstra KA, Heringa J (2008) PRALINETM: a strategy for improved multiple alignment of transmembrane proteins. Bioinformatics 24: 492–497.
37. Ditty JL, Harwood CS (1999) Conserved cytoplasmic loops are important for both the transport and chemotaxis functions of PcaK, a protein from *Pseudomonas putida* with 12 membrane-spanning regions. J Bacteriol 181: 5068–5074.
38. Guan L, Kaback HR (2006) Lessons from lactose permease. Annu Rev Biophys Biomol Struct 35: 67–91.
39. Edgar RC (2004) MUSCLE: multiple sequence alignment with high accuracy and high throughput. Nucleic Acids Res 32: 1792–1797.
40. Henikoff S, Henikoff JG (1992) Amino acid substitution matrices from protein blocks. Proc Natl Acad Sci U S A 89: 10915–10919.
41. Chandrasekaran A, Ojeda AM, Kolmakova NG, Parsons SM (2006) Mutational and bioinformatics analysis of proline- and glycine-rich motifs in vesicular acetylcholine transporter. J Neurochem 98: 1551–1559.
42. Martin LC, Gloor GB, Dunn SD, Wahl LM (2005) Using information theory to search for co-evolving residues in proteins. Bioinformatics 21: 4116–4124.
43. Koike K, Oleschuk CJ, Haimeur A, Olsen SL, Deeley RG, et al. (2002) Multiple membrane-associated tryptophan residues contribute to the transport activity and substrate specificity of the human multidrug resistance protein, MRP1. J Biol Chem 277: 49495–49503.
44. Schiffer M, Chang CH, Stevens FJ (1992) The functions of tryptophan residues in membrane proteins. Protein Eng 5: 213–214.
45. Chen CP, Kernytsky A, Rost B (2002) Transmembrane helix predictions revisited. Protein Sci 11: 2774–2791.
46. Shukla S, Saini P, Smriti, Jha S, Ambudkar SV, et al. (2003) Functional characterization of *Candida albicans* ABC transporter Cdr1p. Eukaryot Cell 2: 1361–1375.
47. Sali A, Blundell TL (1993) Comparative protein modelling by satisfaction of spatial restraints. J Mol Biol 234: 779–815.
48. Barton GJ (1993) ALSCRIPT: a tool to format multiple sequence alignments. Protein Eng 6: 37–40.
49. Livingstone CD, Barton GJ (1993) Protein sequence alignments: a strategy for the hierarchical analysis of residue conservation. Comput Appl Biosci 9: 745–756.
50. Sigal N, Molshanski-Mor S, Bibi E (2006) No single irreplaceable acidic residues in the *Escherichia coli* secondary multidrug transporter MdfA. J Bacteriol 188: 5635–5639.

Multidrug Resistance in Yeast *Candida*

Rajendra Prasad and Khyati Kapoor
Membrane Biology Laboratory, School of Life Sciences, Jawaharlal Nehru University, New Delhi-110067, India

The opportunistic human pathogens *Candida albicans* and other non-*albicans* species have acquired considerable significance in the recent past due to the enhanced susceptibility of immunocompromised patients. These pathogenic species of *Candida* derive their importance not only from the severity of their infections but also from their ability to develop resistance against antifungals. Widespread and prolonged use of azoles has led to the rapid development of the phenomenon of multidrug resistance (MDR), which poses a major hurdle in antifungal therapy. Various mechanisms that contribute to the development of MDR have been implicated in *Candida* as well as in other human fungal pathogens, and some of these include overexpression of or mutations in the target enzyme of azoles, lanosterol 14α-demethylase, and transcriptional activation of genes encoding drug efflux pump proteins belonging to ATP-binding cassette (ABC) as well as to major facilitator superfamilies (MFS) of transporters. The ABC transporters, *CDR1, CDR2*, and an MFS pump *CaMDR1*, play a key role in azole resistance as deduced from their high level of expression found in several azole-resistant clinical isolates.

KEY WORDS: Multidrug resistance, ABC transporter, MFS transporters, Azoles, Efflux pumps, *Candida*, Ergosterol.

I. Introduction

Due to a sudden spurt in immunocompromised patients, fungal infections have become more common. Among various human fungal pathogens, *Candida albicans* accounts for the majority of systemic infections. But

infections caused by non-*albicans* species, such as *C. glabrata, C. parapsilosis, C. tropicalis*, and *C. krusei*, are also common, particularly in neutropenic patients and neonates (Coleman *et al.*, 1998; Ghannoum and Rice, 1999; Vanden Bossche and Koymans, 1998; Vanden Bossche *et al.*, 1994a; White *et al.*, 1998). Recently, incidences of *C. albicans* cells acquiring resistance to antifungals like azoles have increased considerably, which has posed serious problems in successful chemotherapy (Hitchcock, 1993; Prasad *et al.*, 2000; Scholer and Polak, 1984; Sternberg, 1994; Vanden Bossche, 1995). Unfortunately, the incidence of antifungal resistance is not restricted to *C. albicans* alone since the non-*albicans* species, such as *C. glabrata, C. parapsilosis, C. tropicalis*, and *C. krusei*, also display this phenomenon (Bennett *et al.*, 2004; Coleman *et al.*, 1998; Vanden Bossche and Koymans, 1998). Both *C. albicans* as well as non-*albicans* species have evolved a variety of mechanisms to combat antifungal resistance (Table I). This review focuses on the molecular mechanisms of antifungal resistance with a special emphasis on major drug efflux pump proteins of *Candida*.

II. Resistance to Antifungals

A. Antifungals and Their Targets

The antifungals, which are commonly used to treat *Candida* infections and their mode of actions, are listed in Table II. Most of the antifungals in use or at various stages of development belong to five major classes based on their mode of action: (1) azoles, which represent the most common class in use, inhibit ergosterol synthesis by blocking 14α-lanosterol demethylase (*ERG11*), (2) allylamines block the synthesis of ergosterol (*ERG1*) and result in the accumulation of toxic squalene, (3) polyenes, on the other hand, directly bind to membrane ergosterol resulting in pore formation, which makes the cell membrane leaky and results in cell death, (4) candins constitute a class of antifungals that inhibits fungal cell wall synthesis by inhibiting the synthesis of the major structural polymer β-1,3-glucan, and (5) pyrimidines, like flucytosine, inhibit nucleic acid synthesis by inhibiting thymidylate synthase.

B. Mechanisms of Resistance to Antifungals

Resistance to antifungals can be visualized as a gradually evolving process wherein different mechanisms may appear during the course of chemotherapy. Studies so far suggest that antifungal resistance in *Candida*

is a multifactorial phenomenon (Fig. 1) (Balkis *et al.*, 2002; Morschhauser, 2002). The main mechanisms of antifungal resistance include alterations in the ergosterol biosynthetic pathway by an overexpression of the *ERG11* gene, which encodes the drug target enzyme 14α-demethylase or by an alteration in target enzymes (point mutations), which leads to reduced affinity to fluconazole. Reduced intracellular accumulation of drugs is another prominent mechanism of resistance in *Candida* cells wherein genes encoding drug extrusion pumps belonging to ABC (the ATP-binding cassette) and MFS (major facilitator) superfamilies of proteins are over-expressed. It has been well documented that clinical azole-resistant isolates of *C. albicans* display transcriptional activation of genes encoding ABC (Cdr1p, Cdr2p) or MFS (CaMdr1p) proteins. Invariably, resistant *Candida* cells, which show enhanced expression of efflux pumps encoding genes, also show a simultaneous increase in the efflux of drugs. Rapid efflux of incoming drug prevents cells from accumulating lethal concentration of azoles and enable them to survive (Prasad *et al.*, 1995; Sanglard *et al.*, 1995; White 1997a). Interestingly, drug inactivation, which is a very common mechanism in bacteria, has not been observed in *Candida* cells. Recent gene profiling results already suggest even more complexities, which may affect and control the phenomena of antifungal resistance (De Backer *et al.*, 2001; Kaur *et al.*, 2004; Krishnamurthy *et al.*, 2004; Rogers and Barker, 2002, 2003). Some of the most common mechanisms of azole resistance found in *Candida* cells are discussed next.

1. Lipids in Drug Resistance

a. 14α-Lanosterol Demethylase (ERG11) Azoles resistance in *C. albicans* occurs primarily through *ERG11*, which encodes 14α-lanosterol demethylase (CYP51, also known as P45014DM) involved in sterol biosynthesis. Azoles inhibit this step in the ergosterol biosynthesis in fungi by binding to and inhibiting P45014DM (Vanden Bossche *et al.*, 1989; Wilkinson *et al.*, 1972, 1974). The inhibition of P45014DM leads to high levels of 14-methylated sterols, which causes disruption of membrane structures. The alteration of the target protein P45014DM by point mutation and an overexpression of its gene (*ERG11*) encoding the target protein are the most predominant resistant mechanisms adopted by fungal cells (Ghannoum and Rice, 1999; Marichal, 1999; White 1997b).

i. Alterations in Erg11p Since Erg11p is the target of azole derivatives, it can be expected that amino acid substitution could affect the affinity of the drug. Indeed, many studies have documented point mutations in the P45014DM (*ERG11*) gene, which resulted in changes in the affinity of the azoles to its target protein leading to resistance (Favre *et al.*, 1999; Kakeya *et al.*, 2000; Kelly *et al.*, 1999; Lamb *et al.*, 1997; Loffler *et al.*, 1997; Marichal

TABLE I

Different Mechanisms of Drug Resistance Developed toward Common Antifungals by *albicans* as well as Non-*albicans* Species of *Candida*

Fungi	Antifungals	Target gene	Target	Mechanism of resistance	References
Candida albicans	Azoles	*ERG11*	Cytochrome P450 14α-demethylase	Point mutation in the target enzyme alters the affinity of the enzyme to azoles	Lamb *et al.*, 1997; Sanglard *et al.*, 1995
				Overexpression of target gene	
		CaCDR1, *CaCDR2*	ABC transporters	Overexpression of ABC and MFS family of multidrug transporters	Prasad *et al.*, 1995; Sanglard *et al.*, 1995; White, 1997a
		CaMDR1			
		ERG3	$\Delta^{5,6}$-Desaturase	Alteration of the sterol	Kelly *et al.*, 1997a
	Nonazoles				
	5-Flucytosine		Thymidylate synthase	Not reported	Cuenca-Estrella *et al.*, 2001
	Amphotericin B		Membrane ergosterol	Increased membrane fluidity	Kelly *et al.*, 1997
	Nystatin		Membrane ergosterol	Alterations in membrane sterols	Martin and Dinsdale, 1982
Candida dubliniensis	Azoles	*ERG11*	Cytochrome P450 14α-demethylase	Overexpression of target gene	Pinjon *et al.*, 2003
		CdCDR1, *CdCDR2*	ABC transporters	Overexpression of ABC and MFS family of multidrug transporters	Moran *et al.*, 1998
		CdMDR1			
		ERG3	$\Delta^{5,6}$-Desaturase	Defects in the sterol	Pinjon *et al.*, 2003
Candida krusei	Azoles	*ABC1*	ABC transporters	Overexpression of target gene	Katiyar and Edlind, 2001; Orozco *et al.*, 1998
		ABC2			
			Cytochrome P450 14α-demethylase	Reduced susceptibility of target enzyme to inhibition	Venkateswarlu *et al.*, 1996

				Reduced accumulation of drug	
	Nonazoles				
	Amphotericin B			Decreased membrane ergosterol content	Safe *et al.*, 1977
	Nystatin			Absence of membrane ergosterol	Mas and Pina, 1980
	5-Flucytosine				Pfaller *et al.*, 2002
Candida glabrata	Azoles	*ERG11*		Overexpression of target gene	Hitchcock *et al.*, 1993; Miyazaki *et al.*, 1998; Redding *et al.*, 2003; Sanglard *et al.*, 2001
		CgCDR1, *CgCDR2*	ABC transporters	Overexpression of efflux pumps	
		CgMDR1			
		PDH1		Overexpression of target gene	
				Mitochondrial loss	
				Decreased membrane permeability	
	Nonazoles				
	Amphotericin B			Decreased membrane ergosterol component	Sterling *et al.*, 1996
	5-Flucytosine			Not reported	Cuenca-Estrella *et al.*, 2001
Candida tropicalis	Azoles	*CtCDR1*	ABC transporters	Overexpression of efflux pumps	Barchiesi *et al.*, 2000; Jandourek *et al.*, 1999

TABLE II

Structure of Representative Antifungals of Each Class along with Its Target and Mode of Action in a Yeast Cell

Class	Drug and structure	Site of action	Target	Mode of action	Resistant organisms
Polyenes	Amphotericin B 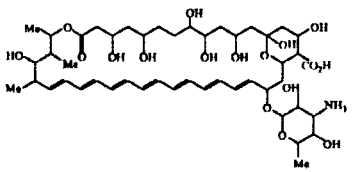 Nystatin 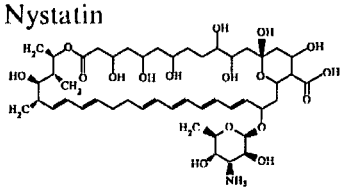	Membrane	Membrane ergosterol	Binds to sterols, mainly ergosterol, in cell membrane resulting in change in permeability of the membrane and cell death	*Fusarium* spp., *Aspergillus nidulans*, *Candida* spp., *Trichosporon* spp.
Pyrimidines	5-Flucytosine 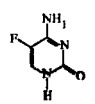	Nucleic acid function and synthesis	Cytosine permease, cytosine deaminase, uracil:phosphoribosyltransferase	It enters cells via cytosine permease and is deaminated to active form 5-FU by cytosine deaminase. 5-FU is then converted to FUMP by uracil: phosphoribosyltransferase. FUMP can be converted into FUTP or FdUMP, which inhibits protein synthesis or DNA synthesis, respectively	*Candida* spp., *Cryptococcus neoformans*, *Aspergillus*

Azoles	Ketoconazole 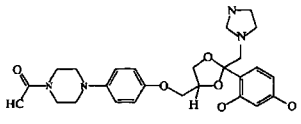			Inhibition of cytochrome P450 14α-demethylase; accumulation of lanosterol leading to perturbation of fungal cell membrane	*Candida* spp., *Cryptococcus* spp.
	Fluconazole 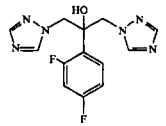	Ergosterol synthesis	Cytochrome P450 14α-demethylase	More selective inhibition of P450 14α-demethylase	*Candida* spp., *Cryptococcus* spp., *Histoplasma capsulatum*
	Itraconazole 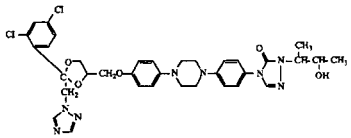			Inhibition of cytochrome P450 14α-demethylase	*Candida* spp., *Aspergillus*
	Miconazole 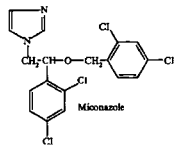				*Candida* spp.
	Voriconazole 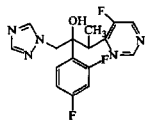			More selective inhibition of cytochrome P450 14α-demethylase	*Candida* spp., *Mucor, Rhizomucor*

(*continued*)

TABLE II (*continued*)

Class	Drug and structure	Site of action	Target	Mode of action	Resistant organisms
Candins	Echinocandins 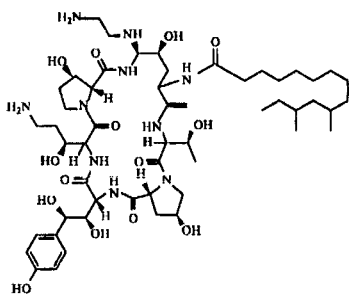	Cell wall synthesis	β-1,3-Glucan synthase	Inhibition of cell-wall glucan synthesis leading to susceptibility of fungal cell to osmotic lysis	*Candida* spp., *Aspergillus* spp., *Cryptococcus* spp.
Allylamines	Terbinafine 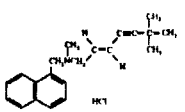	Ergosterol synthesis	Squalene epoxidase	Inhibition of squalene epoxidase; fungicidal effect may be due to accumulation of toxic squalene rather than deficiency of ergosterol	*Saccharomyces cerevisiae*, *Ustilago maydis*, *Candida glabrata*

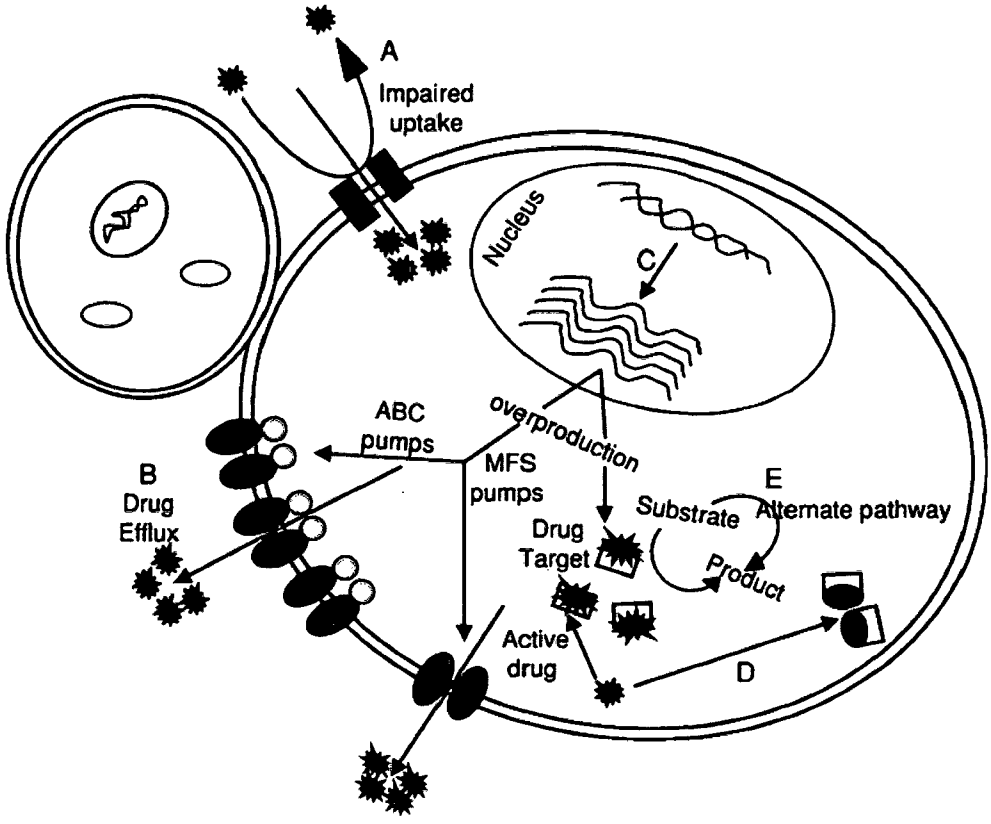

FIG. 1 Predominant drug resistance mechanisms of *Candida*. (A) Reduced drug uptake (import) due to compositional changes in the cell wall or plasma membrane. (B) Rapid efflux of drugs mediated by the ABC or MFS transporters. (C) Overexpression of the genes encoding drug target *ERG11* and/or of efflux pumps, e.g., *CDR1, CDR2*, and *CaMDR1*. (D) Mutation in drug target Erg11p (P45014DM) leads to reduction or loss in drug binding. (E) Activation of alternate ergosterol pathways such as $\Delta^{5,6}$-desaturase.

et al., 1999; Perea *et al.*, 2001; Sanglard *et al.*, 1998a; White *et al.*, 2002; Xiao *et al.*, 2004). White's group who analyzed a series of *C. albicans* strains isolated earlier by Redding *et al.* (1994) from a single HIV patient over a period of 2 years and identified a single amino acid substitution, viz. R467K in Erg11p. Since this mutation is close to amino acid cysteine, which participates in the coordination of the iron atom in the heme cofactor of enzyme, it has been proposed that the mutation causes structural changes associated with the heme. It has been further reported that R467K alone can confer azole resistance by reducing the affinity of the enzyme for fluconazole (Lamb *et al.*, 2000). Based on the architecture of the active site of the enzyme, Lamb *et al.* (1997) introduced a point mutation T315A in Erg11p and observed that the mutant variant protein had higher MIC values for fluconazole and ketoconazole. The purified mutated protein exhibited reduced enzyme activity and affinity for azoles, thus providing an example of a single amino acid change in the target protein leading to azole resistance. There are several

reports wherein in response to azoles, many point mutations in Erg11p have been identified (Marichal *et al.*, 1999). The known point mutations in *C. albicans* have been compiled in a graphic representation by Marichal *et al.* (1999) to show the frequency and position of each substitution. It is observed that four mutations, D116E, K128T, E266D, and G464S, occurred with highest frequency, whereas G464S was the only substitution exclusively seen in azole-resistant isolates. The exact placement of these mutations in a three-dimensional model of the protein shows that these mutations are not randomly distributed but rather clustered in three hot spot regions between amino acid residues 105–165, 266–287, and 405–488 (Marichal *et al.*, 1999).

ii. Up-regulation of ERG11 Resistance to fluconazole in many clinical isolates has often been associated with the transcriptional activation of *ERG11* (the gene-encoding target protein P45014DM) (Harry *et al.*, 2002). However, it has been difficult to correlate the up-regulation of the gene with the observed fluconazole resistance mainly due to the simultaneous occurrence of mutations in *ERG11* or to the overexpression of the efflux pumps encoding genes. Gene amplification is one of the common mechanisms of resistance in eukaryotic cells (Stark and Wahl, 1984; Van der Bleik *et al.*, 1988). However, overexpression of *ERG11* in *C. albicans* has not been linked to gene amplification (Vanden Bossche *et al.*, 1992, 1994b; Marichal *et al.*, 1997). In a clinical isolate of *C. glabrata*, an increased level of P45014DM was shown to be associated with the amplification of the *ERG11* gene (Vanden Bossche *et al.*, 1992, 1994b; Marichal *et al.*, 1997). The amplification of the *ERG11* gene in this isolate was linked to chromosomal duplication, which in turn resulted in high levels of the P45014DM protein (Marichal *et al.*, 1997). That gene conversion or mitotic recombination could also play a role in fluconazole resistance in *C. albicans* was apparent from a study done by White's group in which additional genetic variations in a clinical isolate of *C. albicans* with R467K substitution have been reported (White, 1997c). It was shown that all allelic differences present in sensitive isolates of *C. albicans* were eliminated in the resistant isolates from the *ERG11* by gene conversion or mitotic recombination (White, 1997c). The resulting strain had an R467K mutation in both copies of *ERG11* and was more resistant to azoles as compared to a strain with single allelic substitution.

b. $\Delta^{5,6}$-Desaturase (ERG3) Another enzyme of the ergosterol biosynthesis pathway, $\Delta^{5,6}$-desaturase (*ERG3*), has been shown to contribute to azole's resistance. A defect in *ERG3* leads to the accumulation of 14α-methylfecosterol instead of 14α-methylergosta-8,24(28)-dien-3β,6α-diol. Accumulation of sufficient amounts of 14α-methylfecosterol compensates for ergosterol in the membranes and thus contributes to azole resistance in *C. albicans* (Ghannoum and Rice, 1999; Vanden Bossche and Koymans, 1998; White *et al.*, 1998). The lethality of the *S. cerevisiae* disruptant of *ERG11* can be

suppressed by $\Delta^{5,6}$-desaturase (Kelly *et al.*, 1997a). The decrease in ergosterol content due to a defect in $\Delta^{5,6}$-desaturase in fluconazole-resistant clinical isolates of *C. albicans* also results in cross-resistance to amphotericin B (Kelly *et al.*, 1997a).

c. Δ^{22}-Desaturase (ERG5) Another cytochrome P450, Δ^{22}-desaturase (CYP61 and also *ERG5*) has been purified from an *ERG11* (P45014DM)-disrupted strain of *C. glabrata* (Lamb *et al.*, 1999). The purified enzyme showed desaturase activity in a reconstituted system. Δ^{22}-Desaturase and its homologues have also been identified in *C. albicans* and *Schizosaccharomyces pombe*. The spectral analyses obtained with azole antifungal compounds, viz. ketoconazole, fluconazole, and itraconazole in reconstituted Δ^{22}-desaturase, suggest that these drugs directly interact with the cytochrome heme (Lamb *et al.*, 1999).

d. Membrane Lipid Composition In addition to membrane ergosterol, which mainly provides rigidity, stability, and resistance to physical stresses, there are other membrane lipid components, which also affect drug susceptibilities of *Candida* cells (Loffler *et al.*, 2000; Mukhopadhyay *et al.*, 2002). It is well documented that clinical as well as adopted azole-resistant isolates of *C. albicans* exhibit altered membrane phospholipids as well as sterol composition (Loffler *et al.*, 2000; Mukhopadhyay *et al.*, 2002). Additionally, recent reports suggest that the interactions between membrane ergosterol and sphingolipid are important determinants of drug susceptibilities of *C. albicans* cells (Mukhopadhyay *et al.*, 2002). In a recent study, close interactions between ergosterol and sphingolipid, which appeared to be disrupted in *erg* mutants, were found to be critical for drug sensitivity of *C. albicans* cells. It is observed that *Candida* cells, when grown in the presence of fumonisin B1 (specific inhibitor of sphingolipid synthesis), had a lower sphingolipid content and, similar to *erg* mutant cells, became hypersensitive to drugs (Mukhopadhyay *et al.*, 2004).

The existence of discrete membrane microdomains, known as lipid rafts, within a lipid bilayer, predominantly composed of sphingolipid and sterol, is well documented in several systems. Interestingly, the acquisition of the MDR phenotype is also accompanied by the up-regulation of lipids and proteins that constitute lipid rafts (Lavie and Liscovitch, 2001; Lavie *et al.*, 1998). Luker *et al.* (2000) and others (Demeule *et al.*, 2000) recently observed that human P-gp (ABC transporter) is predominantly localized in cholesterol-enriched membrane domains and depletion of cholesterol impairs human Pgp-mediated drug transport. Liscovitch and Lavie (2000) hypothesize that raft-dependent cholesterol efflux pathways may play a role in delivering drugs from various intracellular membranes to the plasma membrane, from which drugs can be extruded from the cells by drug efflux

pumps. The existence of ergosterol and sphingolipid-rich microdomains (membrane raft) in *C. albicans* has recently been established (Martin and Konopka, 2004). Whether drug efflux proteins of *Candida* are also localized within these domains remains to be established.

The alteration in the physical state of plasma membrane lipid is another factor that seems to affect drug susceptibility of yeast cells. By employing isogenic *erg2, erg3, erg4,* and *erg6* mutants of *S. cerevisiae* strains, it was observed that due to defective ergosterol biosynthesis and accumulation of various intermediates therein, these mutants possessed high membrane fluidity. These mutants became sensitive to several tested drugs and elicited enhanced level of passive diffusion. This suggested that passive diffusion of drugs could contribute to hypersensitivity of *erg* mutants. However, when a membrane fluidizer benzyl alcohol enhanced membrane fluidity, it was observed that the increment in fluidity alone did not affect the susceptibility of the tested drugs in *S. cerevisiae* cells. Thus, it appears that the change in membrane fluidity and increased diffusion therein alone are not sufficient to result in the observed higher susceptibility of *erg* mutants. In conclusion, the hypersensitivity of *erg* mutants of *S. cerevisiae* could be attributed to membrane permeability changes, which may involve changes in passive diffusion across the membrane or in active transport of these drugs. In support of the former, Van Den Hazel *et al.* (1999) have shown that *S. cerevisiae* cells lacking *PDR16* and *PDR17* (encoding homologues of Sec14p) result in altered phospholipid and sterol composition and render cells hypersensitive to many drugs due to their increased passive diffusion. In support of the later possibility, ABC transporter Pdr5p of *S. cerevisiae* has been shown to function less efficiently in *erg6*-deleted cells (Emter *et al.*, 2002; Kaur and Bachhawat, 1999). Taken together, it is becoming apparent that the membrane lipid composition, with changes in membrane fluidity and interactions between membrane ergosterol and sphingolipid, particularly affects drug susceptibilities of *Candida* cells.

2. Drug Efflux and Import

a. Efflux of Drugs The permeability constraints imposed by the pathogen to drugs (mainly by way of increased efflux) represent one of the important molecular mechanisms of antifungal resistance. Several azole-resistant clinical isolates of *C. albicans* as well as of other fungal pathogens like *Aspergillus fumigatus* and *Cryptococcus neoformans* display transcriptional activation of efflux pump-encoding genes and often show reduced intracellular accumulation of drugs (Nascimento *et al.*, 2003; Posteraro *et al.*, 2003; Semighini *et al.*, 2002; Slaven *et al.*, 2002; Thornewell *et al.*, 1997; Tobin *et al.*, 1997). The azole-resistant isolates mainly overexpress genes encoding multidrug efflux transporters proteins (MET) belonging to two superfamilies: the ABC transporters and MFS (Fig. 2).

i. ABC Efflux Proteins Cdr1p was the first ABC transporter identified as a drug efflux pump of *C. albicans* (Prasad *et al.*, 1995). The gene encoding *CDR1* was cloned by complementation of the *S. cerevisiae pdr5* mutant exhibiting hypersensitivity to cycloheximide and other drugs. Cdr1p is a close homologue of the ABC transporter human MDR1/P-gp. To date, Cdr1p and Cdr2p, which are very close homologues, represent two major drug extrusion pumps of *C. albicans*. These pump proteins not only efflux azoles and its derivatives but also extrude a variety of structurally unrelated compounds. Despite a high level of structural similarities, Cdr1p and Cdr2p display major functional differences particularly with regard to substrate specificity (Table III). Other homologues of *CDR1* and *CDR2*, namely *CDR3* and *CDR4* (75% similarity), have also been identified, but neither an overexpression nor a deletion of *CDR3* or *CDR4* genes affects drug susceptibilities of *C. albicans* (Balan *et al.*, 1997; Franz *et al.*, 1998; Sanglard *et al.*, 1998b) (Table IV). Cannon's group has recently found that there is allelic variation in a number of genes involved in fungal drug resistance (Cannon *et al.*, 2004). There are two *CDR1* alleles designated A and B, for example, in *C. albicans* ATCC 10261. Sequencing of both alleles revealed 37 synonymous single nucleotide polymorphisms (SNPs) and 6 nonsynonymous SNPs. When hyperexpressed in *S. cerevisiae*, allele A conferred slightly less resistance to fluconazole (FLU) (MIC 200 μg/ml) than allele B (MIC 300 μg/ml) (Cannon *et al.*, 2004). Considering the widely observed polymorphism of human P-gp/MDR1 (Brinkmann and Eichelbaum, 2001; Cascorbi *et al.*, 2001; Hoffmeyer *et al.*, 2000; Woodahl and Ho, 2004) the characterization of an allelic variation of drug extrusion proteins of *Candida* represents an interesting possibility, which may also contribute to azole resistance. This definitely needs to be examined to assess if allelic variations in MDR genes of *Candida* have any clinical relevance. The reported glucose-induced phosphorylation of CgCdr1p and Pdh1p, drug efflux proteins of *C. glabrata*, suggests that posttranslational modification of efflux proteins could represent yet another novel mechanism of drug resistance (Wada *et al.*, 2002).

Structure and Function of ABC Proteins. The molecular mechanisms that govern the function of Cdr1p or Cdr2p as efflux pumps for azoles are not well known, and information is needed to (1) understand how the protein can bind a structurally diverse range of compounds including different azoles, (2) define drug-substrate binding, and (3) determine how ATP binding and hydrolysis are linked to drug transport (Fig. 3). The analysis of the molecular mechanism of azole transport by efflux pump proteins is expected to provide the basis for rational designing of a modulator/inhibitor for the proteins.

Similar to mammalian homologues, ABC transporters of *Candida* and of other yeasts like *S. cerevisiae* possess specific domains for membrane association, ATP binding, and hydrolysis. A typical Cdr1p, like most of the fungal ABC drug transporter, is composed of two homologous halves, each made

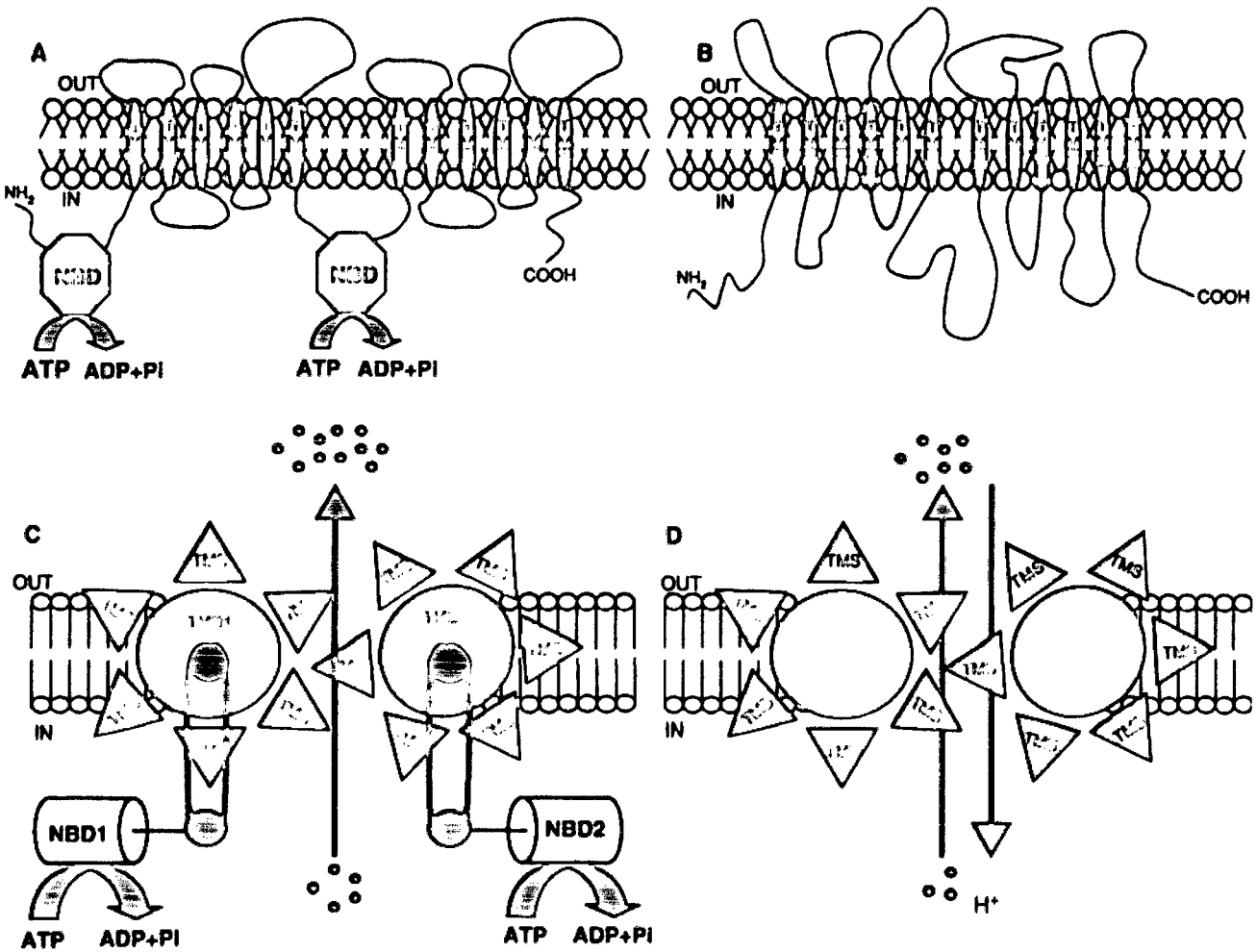
A
OUT
IN
NH2
NBD
NBD
COOH
ATP ADP+Pi
ATP ADP+Pi
B
OUT
IN
NH2
COOH
C
OUT
IN
NBD1
NBD2
ATP ADP+Pi
ATP ADP+Pi
D
OUT
IN
TMS
TMS
TMS
H+

up of a hydrophilic, cytoplasmic nucleotide-binding domain (NBD) and a transmembrane domain (TMD) represented by six transmembrane segments (TMS) (Fig. 2). *Candida* Dbase predicts several ABC transporters, which show NBD conserved sequences upon multiple alignments (http://genolist.pasteur.fr/CandidaDB). Although many transporters are predicted to have an $(NBD\text{-}TMD)_2$ topology, there are also some putative ORFs that have only $(NBD\text{-}TMD)_1$ and thus appear to be half proteins. Among all the putative ABC proteins, only *CDR1* and *CDR2* are experimentally implicated in azole resistance. The structural and functional analysis of human P-gp/MDR1 and its other homologues in mouse has demonstrated the importance of NBDs and TMDs in drug extrusion (Loo and Clarke, 1993, 1994a,b, 1995a,b). In comparison, studies pertaining to the identification of the molecular determinants of yeast ABC drug transporters have only been recently initiated (Egner *et al.*, 1998, 2000).

In an effort to develop an understanding of the molecular details of drug binding and efflux, in a recent study Cdr1p was overexpressed as a GFP-tagged fusion protein in a heterologous hyperexpression system (Shukla *et al.*, 2003) and was characterized for drugs and nucleotide binding (Shukla *et al.*, 2003). Iodoarylazidoprazosin (IAAP, a photoaffinity analogue of the P-gp substrate prazosine) and azidopine (a dihydropyridine photoaffinity analogue of the P-gp modulator verapamil) were shown specifically to bind with Cdr1p-GFP. Interestingly, IAAP binding with Cdr1p-GFP was competed out by nystatin, while azidopine binding could be competed out only by miconazole, thus demonstrating the possibility of different drug-binding sites for the two analogues (Shukla *et al.*, 2003). For detailed structural and functional analysis, point mutations were also introduced in Cdr1p. Several point mutations yielded interesting phenotypes (Table V and Fig. 4). The studies conducted so far with Cdr1p suggest that in spite of topological differences with human P-gp, there is a conserved functional homology between the two multidrug transporters (Shukla *et al.*, 2003). Gauthier *et al.* (2003) have recently shown that membranes prepared form Cdr1p and Cdr2p expressing cells are able to bind the photoaffinity analogue of rhodamine 123

FIG. 2 ABC and MFS drug transporters of *Candida*. Putative topology of multidrug transporters. (A) Diagrammatic representation of an ABC transporter. The structural organization is characterized by two homologous halves $(NBD\text{-}TMD)_2$, each comprising a hydrophilic nucleotide-binding domain (NBD) followed by a hydrophobic region transmembrane domain (TMD) containing six transmembrane segments (TMS). (B) Diagrammatic representation of an MFS transporter. The MFS transporter depicted here has two structural units each of six transmembrane spanning α-helical segments, linked by cytoplasmic loops. (C) The NBDs of the ABC transporters hydrolyze ATP thus facilitating the transport of drugs out of the cell. ABC protein functions as a pump. (D) MFS protein utilizes a proton gradient to expel the drug.

TABLE III
Substrate Specificity of Major ABC and MFS Transporters

Class of transporter	Efflux pump	Substrates	References
ABC transporter	*CDR1*	Fluconazole, itraconazole, ketoconazole, cycloheximide, amorolfine, fluphenazine, rhodamine 6G, cerulenin, brefeldin, miconazole, chloramphenicol, sulfomethuron methyl, rhodamine 123, β-estradiol, 4-nitrosoquinoline, *O*-phenanthroline, erythromycin, oligomycin, nystatin, dinitrophenol, corticosterone, FK-520, anisomycin, azidopine, IAAP	Krishnamurthy *et al.*, 1998; Prasad *et al.*, 1995; Sanglard *et al.*, 1997; Schuetzer-Muehlbauer *et al.*, 2003b; Shukla *et al.*, 2003
	CDR2	Fluconazole, itraconazole, ketoconazole, cycloheximide, amorolfine, fluphenazine, rhodamine 6G, cerulenin, brefeldin, caspofungin, crystal violet	
MFS transporter	*CaMDR1*	Benomyl, methotrexate, cycloheximide, 4-nitrosoquinolone, benzimidazole-2-yl-carbamatel-(2′-furoyl)-5-trifluoromethyl benztriazole, 1-benzoylbenztriazole	Ben-Yaacov *et al.*, 1994; Fling *et al.*, 1991; Gupta *et al.*, 1998
	FLU1	Fluconazole, itraconazole, ketoconazole, mycophenolic acid	Calabrese *et al.*, 2000

TABLE IV
ABC Transporters of *Candida*

Organism	Subfamily of transporter[a]	Gene	Size[b]	Topology[c]	Functions	References
Candida albicans	PDR	*CaCDR1*	1501	$(NBD\text{-}TMS_6)_2$	Drug efflux, phospholipid translocation	Dogra *et al.*, 1999; Prasad *et al.*, 1995; Sanglard *et al.*, 1995
		CaCDR2	1499	$(NBD\text{-}TMS_6)_2$	Drug efflux, phospholipid translocation	Dogra *et al.*, 1999; Sanglard *et al.*, 1997
		CaCDR3	1501	$(NBD\text{-}TMS_6)_2$	Phospholipid translocation, opaque-phase specific	Balan *et al.*, 1997; Smriti *et al.*, 2002
		CaCDR4	1490	$(NBD\text{-}TMS_6)_2$	Phospholipid translocation?	Franz *et al.*, 1998
	MDR	*HST6*	1323	$(TMS_6\text{-}NBD)_2$	Transport of drugs and a-factor	Raymond *et al.*, 1998
	MRP/CFTR	*CaYOR1*		?	Drug efflux	Ogawa *et al.*, 1998
		CaYCF1	1606	?	Drug efflux	Theiss *et al.*, 1999
Candida glabrata	PDR	*CgCDR1*	1499	$(NBD\text{-}TMS_6)_2$	Drug efflux	Sanglard *et al.*, 1998b, 1999
		CgCDR2	?	$(NBD\text{-}TMS_6)_2$	Drug efflux	
		PDH1	1542	$(NBD\text{-}TMS_6)_2$	Drug efflux	Miyazaki *et al.*, 1998
Candida dubliniensis	PDR	*CdCDR1*	?	$(NBD\text{-}TMS_6)_2$	Drug efflux	Moran *et al.*, 1998
		CdCDR2	?	$(NBD\text{-}TMS_6)_2$	Drug efflux	
Candida krusei	PDR	*ABC1*	?	?	Drug efflux	Katiyar and Edlind, 2001
		ABC2	?	?	Drug efflux	

[a]Subfamily based on sequence similarity with human ABC transporters ALDP, MRP/CFTR, MDR, and yeast (PDR, YEF3).
[b]Number of amino acid residues.
[c]NBD, nucleotide-binding domains; TMS, transmembrane segment.

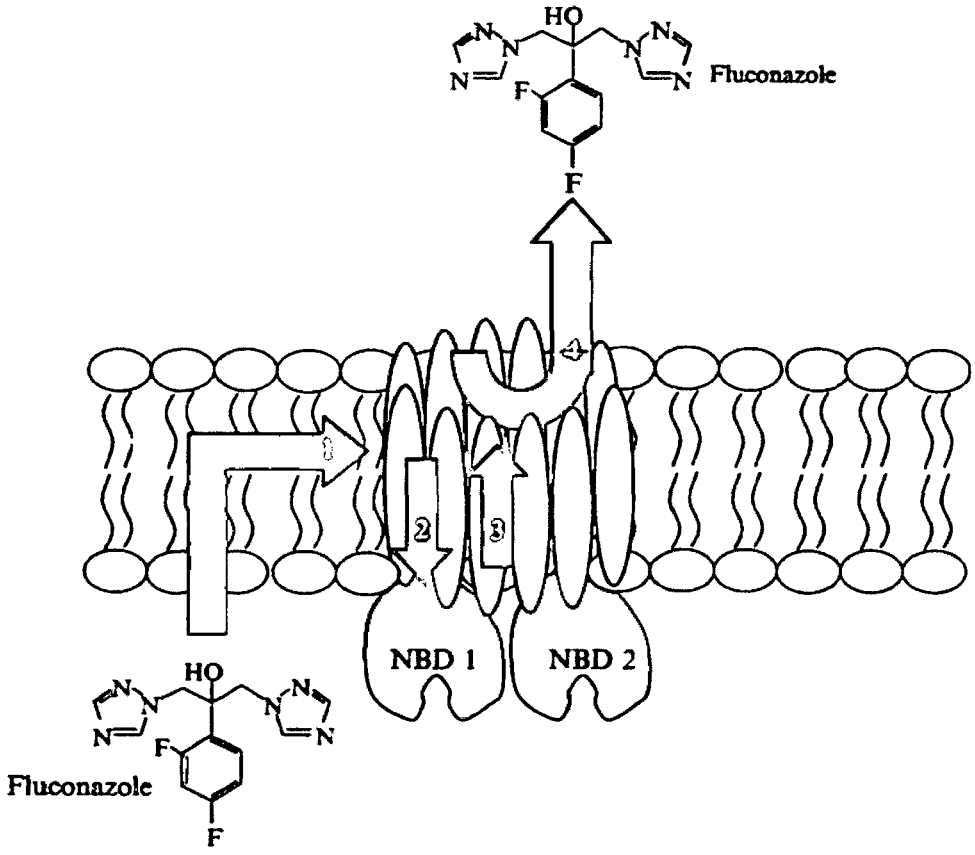

FIG. 3 Sequence of probable steps involved in the expulsion of fluconazole or any other drug from yeast cell. (1) Interaction of drug with drug-binding site (DBS) present in TMS. (2) Drug binding may stimulate ATP hydrolysis in the nucleotide-binding domain (NBD). (3) ATP hydrolysis in NBDs initiates conformational changes in TMDs. (4) The conformational changes result in release and efflux of drugs. None of these steps (1–4) has been proven experimentally for azole efflux. These steps are only predictions based upon observations from human MDR1/MRPs (Pajeva *et al.*, 2004).

([^{123}I]iodo-arylazido-rhodamine123, IAARh123), and that both N-terminal and C-terminal halves of Cdr2p contribute to rhodamine binding.

NBDs in ATP Binding and Hydrolysis. An important characteristic feature of ABC drug transporters is that they use the energy of nucleotide (ATP) hydrolysis to transport drugs across the membrane, against the concentration gradient. The conserved NBDs located at the cytoplasmic periphery are the hub of such an activity. In an attempt to understand the molecular basis of ATP hydrolysis of Cdr1p, recently the active N-terminal nucleotide-binding domain (NBD1) of Cdr1p was purified and characterized. It is demonstrated that this purified domain elicits a cation-dependent general ribonucleotide triphosphatase activity (Jha *et al.*, 2003a). Jha *et al.* (2003a) found an evolutionary divergence in this domain wherein a conserved variation exists within the catalytically crucial Walker A motif of NBD1. The

Cdr1p Walker A motif contains an atypical but conserved cysteine-193, which appears to be a common feature of fungal ABC transporters. It was found to be critical for ATP hydrolysis. Reports from nonfungal transporters suggest that the Walker A motifs of NBDs have a well-conserved lysine residue at an equivalent position, which is indispensable for ATP hydrolysis (Azzaria *et al.*, 1989). In a recent *in vivo* study, the relative contribution of both the N- and C-terminal NBDs in ATP binding, hydrolysis, and transporter activity of native Cdr1p (full protein) was examined wherein an atypical Cys-193 of Walker A of NBD1 (C193K) and a conserved Lys-901 (K901C) of Walker A of NBD2 were replaced (Jha *et al.*, 2004). The drug resistance profile of Cdr1p mutant variant cells harboring C193K or K901C provided interesting insight into the functioning of the two NBDs. The cells expressing K901C were hypersensitive to drugs as compared to the C193K variant or to native Cdr1p. This clearly establishes that the two NBDs respond asymmetrically to the substitution of conserved residues of their respective Walker A motifs. The divergence in functioning of two NBDs was further evident when the efflux ability of these mutant proteins was compared. An in-depth analysis of the catalytic cycle, namely nucleotide binding, hydrolysis, and substrate binding/efflux, is required to determine the reasons behind the dichotomy in functioning of the NBDs. This study, however, demonstrated that a diverse N-terminal NBD (GxxGxGCS/T) of Cdr1p is functional where uncommon C193 is critical. Considering that all other fungal ABC transporters, including the well-studied Pdr5p of *S. cerevisiae*, have uncommon cysteine in Walker A of NBD1 (with the exception of Ste6p of *S. cerevisiae*), it is expected that this residue will have an indispensable role in the catalytic cycle (Jha *et al.*, 2003b).

ii. MFS Efflux Proteins The MFS was originally defined as a superfamily of permeases characterized by two structural units of six TMS-α-helical segments, linked by a cytoplasmic loop. Out of several MFS proteins listed in the *Candida* database (http://genolist.pasteur.fr/CandidaDB), *CaMDR1*, its alleles, and *FLU1* are the only drug transporters. *CaMDR1* was initially identified as a gene, which conferred resistance to the tubulin-binding agent benomyl and the tetrahydrofolate reductase inhibitor methotrexate (Ben-Yaacov *et al.*, 1994; Fling *et al.*, 1991). *CaMDR1* expression in *S. cerevisiae* confers resistance to several unrelated drugs and its overexpression has been linked to azole resistance in *C. albicans*. The expression of *CaMDR1* in *C. albicans* cells is enhanced by benomyl, methotrexate, and several other unrelated drugs, and is found to be more pronounced in some of the azole-resistant clinical isolates (Becker *et al.*, 1995; Gupta *et al.*, 1998). Morschhäuser and his group employed a proteomic approach to understand the molecular basis of drug resistance in *C. albicans*. By comparing the protein expression pattern of matched pairs of fluconazole-resistant

TABLE V
Location and Phenotype of Mutant Variant Cdr1p of *Candida albicans*[a,b]

Domains	Location	Mutation	Phenotype[c]
NBD1	Walker A	C193A	95% loss in ATPase activity
		C193K	78% loss in ATPase activity
	Signature C	G305A	Similar to wild type
		G305V	
		R308S	
		K309E	
	Stretch between Walker A and Signature C	D232E	Similar to wild type
		D232K	Hypersensitive to all the drugs tested[d]
		G296D	
NBD2	Walker A	K901A	~88% loss in ATPase activity
		K901C	
	Stretch between Walker A and Signature C	G995S	Hypersensitive to Cyh and Flu
		G998S	Similar to wild type
		G1000C	Sensitive to Mic
Transmembrane domain 1	TMS 6	V773A	Similar to wild type
		V773I	
		F774A	Sensitive to Cyh, Flu, and Nys
		ΔF774	Improper localization of protein, hypersensitive to all drugs tested[d]
Transmembrane domain 2	TMS11	N1348A	Similar to wild type
		T1351F	Hypersensitive to all drugs tested[d]
		L1353A	Similar to wild type
		T1355F	Hypersensitive to all drugs tested[d]
		T1355S	Similar to wild type
		N1359A	
		F1360A	Hypersensitive to all drugs tested[d]
		C1361A	Similar to wild type
	Extracellular loop 6	C1418Y	Sensitive to Mic
		T1449I	
		V1456I	

and susceptible clinical isolates, they identified several proteins whose expression was up-regulated specifically when only the *CaMDR1* gene was overexpressed. These proteins, mostly belonging to the putative aldo-keto reductase family, were not up-regulated in a fluconazole-resistant strain that overexpressed only *CDR1/CDR2* and not *CaMDR1*. This implied that the expression of efflux pump-encoding genes is controlled by a different regulatory network (Kusch *et al.*, 2004).

Recently *FLU1*, another gene encoding the MFS protein of *C. albicans*, was cloned by a complementing strain of *S. cerevisiae*, which was hypersensitive to fluconazole. However, *FLU1* is not involved in the development of fluconazole resistance in clinical isolates of *C. albicans*. Interestingly, studies revealed that the preferred substrate of Flu1p is mycophenolic acid rather than fluconazole. Although more than two dozen putative MFS genes have been identified in the *Candida* genome, except for CaMdr1p none of the other proteins of this superfamily of MFS is reported to have any direct role in clinical fluconazole resistance.

In contrast to the ABC drug transporter, the structure–function relationship of MFS has not been generalized in detail due to the diversity in their nucleotide and amino acid sequences. There are, however, some reports that suggest that the N-terminal halves of different major facilitator families share greater similarities than their C-terminal halves, which suggests that C-terminal regions are involved in substrate recognition and N-terminal regions are involved in proton translocation (Paulsen *et al.*, 1996; Saier and Reizer, 1991).

b. Import of Drugs The hydrophobic nature of drugs permits their easy import by passive diffusion. However, the contribution of drug import to the overall scenario of MDR is not well established since technically it has not been possible to separate efflux of drugs from their import. Nonetheless, there are a few studies particularly with mammalian cells in which passive diffusion of drugs through a lipid bilayer has been shown to be an important determinant of MDR (Ferte, 2000). The variations in membrane fluidity are expected to affect passive diffusion of drugs and, in turn, their sensitivity.

The enhanced fluidity has been linked to enhanced diffusion of drugs (Mukhopadhyay *et al.*, 2002). There are factors, other than membrane

---

[a]Data taken from Shukla *et al.* (2003).

[b]Location of each mutation is marked in the two-dimensional representation of Cdr1p in Fig. 5.

[c]Aniso, anisomycin; Cyh, cycloheximide; Flu, fluconazole; Mic, miconazole; Nys, nystatin.

[d]Phenotype was checked in the presence of Flu, Cyh, Aniso, Mic, and Nys.

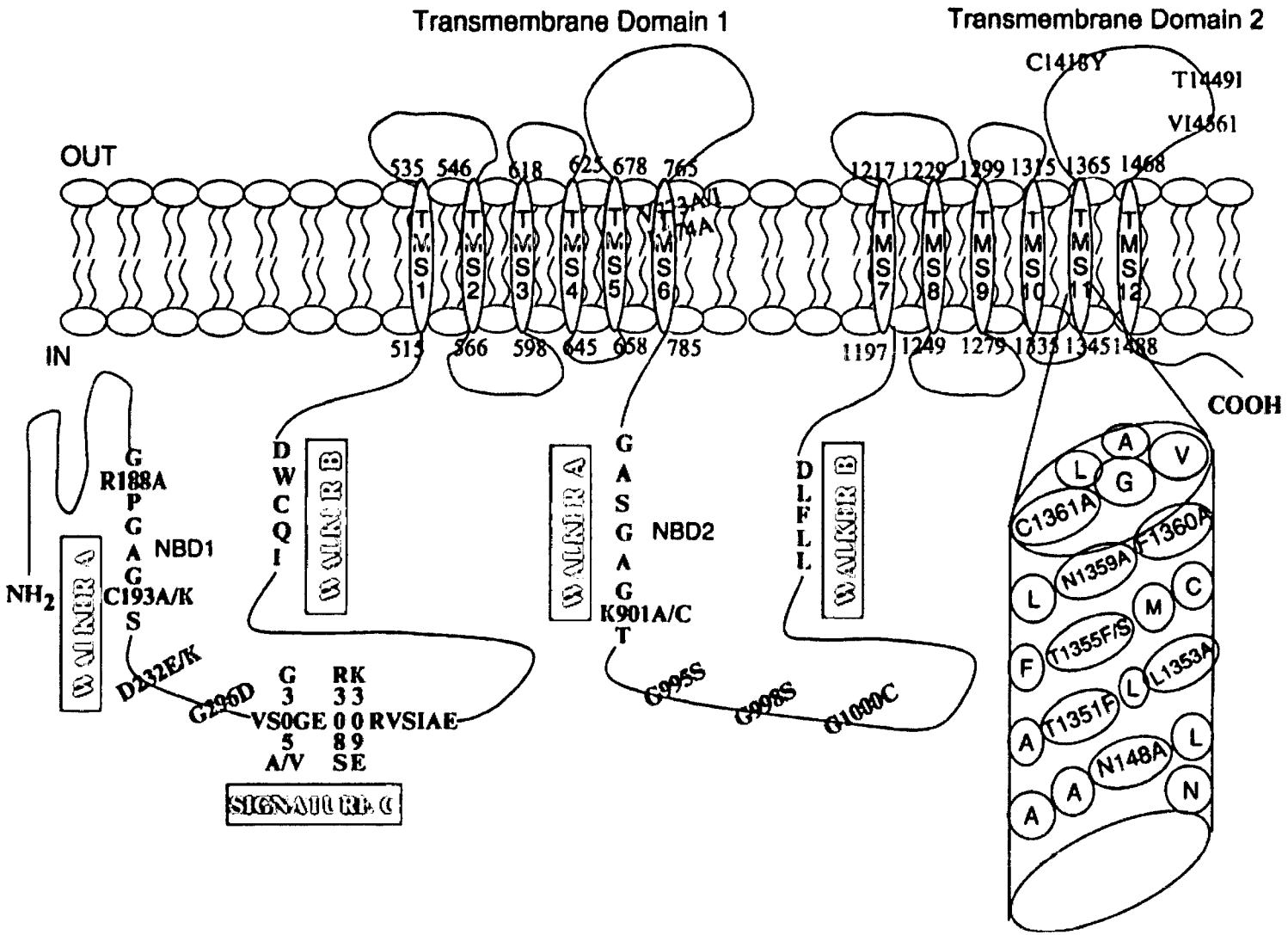
Transmembrane Domain 1
Transmembrane Domain 2
OUT
IN
NH2
COOH
NBD1
NBD2
WALKER A
WALKER B
SIGNATURE C
C1418Y
T1449I
V1456I
535 546 618 625 678 765
1217 1229 1299 1375 1365 1468
515 566 598 645 658 785
1197 1249 1279 1335 1345 1488
TMS1
TMS2
TMS3
TMS4
TMS5
TMS6
TMS7
TMS8
TMS9
TMS10
TMS11
TMS12
R188A
C193A/K
D232E/K
G290D
K901A/C
G995S
G998S
Q1000C
C1361A
T1360A
N1359A
T1355F/S
L1353A
T1351F
N148A

fluidity, that can also influence passive diffusion of drugs across the membrane bilayer and thus can affect drug susceptibilities (Van Den Hazel *et al.*, 1999). The import of drugs and its impact on drug resistance need to be analyzed more carefully. It is expected that with better experimental designs, the contribution of import of drugs in MDR can be established.

3. Other Mechanisms of Drug Resistance

In addition to the mechanisms of drug resistance commonly found in *Candida* (discussed above), other mechanisms may also be important contributors to antifungal resistance.

a. Mitochondrial Respiration The petite mutants (which lack mitochondrial DNA) of *S. cerevisiae* display resistance to fluconazole due to an uncoupling of oxidative phosphorylation. Interestingly, petite mutants that also have an *erg3* mutation were found to be sensitive to fluconazole. It has been suggested by Kontoyiannis and his group that an *erg3* mutant lacking mitochondria could accumulate toxic steroid intermediates that arrest growth (Kontoyiannis, 2000). A relationship between mitochondrial function and azole resistance is also observed in pathogenic *C. glabrata* wherein blockage of respiration by inhibitors or by mutation leads to decreased susceptibility to azoles (Kaur *et al.*, 2004). The resistance to azoles accompanied with the loss of mitochondria was also linked to the up-regulation of *CgCDR1* and *CgCDR2*, genes encoding ABC pumps of *C. glabrata* (Brun *et al.*, 2003, 2004). Petite mutants of *C. albicans* are known to exist but so far a relationship between mitochondrial function and azole resistance has not been demonstrated (Aoki *et al.*, 1990; Arie *et al.*, 1998; Roth-Ben *et al.*, 1998). However, given the similarities between *Candida* species, such as association is expected. Genome-wide expression profile analysis revealed coordinately regulated genes associated with azole resistance in clinical isolates of *C. albicans*. Many genes that are involved in the oxidative stress response are also regulated, which may contribute to azole resistance (Rogers and Barker, 2002, 2003). Taken together, mitochondrial respiratory status

FIG. 4 Two-dimensional depiction of Cdr1p topology that displays the site of point mutations introduced in this protein. The NH_2 and COOH mark the N-terminal and C-terminals, respectively. The conserved Walker and signature regions are indicated in a gray background. The two transmembrane domains and individual transmembrane segments are marked. Numbers indicate the beginning and end of transmembrane segments. The mutated residues are indicated at respective positions. The mutations in TMS11 are depicted in an enlarged helix (Shukla *et al.*, 2003).

affecting azole resistance could represent another mechanism of drug resistance in yeasts.

b. Calcium Homeostasis Azoles are fungistatic rather than fungicidal to *Candida* cells and this tolerance to azoles contributes to the development of resistance encountered in clinical isolates from immunocompromised patients (St-Gremain *et al.*, 2001; White *et al.*, 1998, 2002). Recently, it was observed that the protein phosphatase calcineurin allows survival of *C. albicans* during membrane stress exerted by azoles (Cruz *et al.*, 2002). The calcineurin inhibitors cyclosporine A (CsA) and tacrolimus (FK506) exhibit fungicidal synergism with azoles in *C. albicans, C. glabrata, C. krusei*, and *S. cerevisiae* (Edlind *et al.*, 2002; Kaur *et al.*, 2004; Onyewu *et al.*, 2003). Recently, Shukla *et al.* (2004) observed that the T1351F mutant variant of Cdr1p exhibited abrogated synergism of FK520 (a structural analogue of FK506) with fluconazole, ketoconazole, and cycloheximide. The fact that the other mutant variants of Cdr1p, which have been substituted in different domains spanning the entire protein molecule, remained synergistically susceptible to FK520 suggests that T1351 of the predicted TMS11 specifically contributes to this synergism. Since antifungal agents of varied structures including azoles derivatives are substrates of Cdr1p, it is very likely that the immunosuppressants or their analogues might increase intracellular levels of drugs by competition and thus by blocking pump activity directly (Maesaki *et al.*, 1998; Marchetti *et al.*, 2001, 2003). The inhibition of fluconazole efflux by FK520 suggests the possibility of a direct interaction of FK520 with Cdr1p. That FK520 synergism is mediated at least in part by its interaction with Cdr1p is supported by a set of observations: (1) T1351 replacement abrogates synergism, (2) FK520 is ineffective in cells not expressing Cdr1p, (3) FK520 shows synergism with other substrates of Cdr1p, and (4) FK520 competes with fluconazole efflux. Recently Raymond's group has also shown that Cdr1p can affect cell tolerance to FK520 and suggested a possible involvement of these transporters in the synergism between azoles and FK520 in *C. albicans* (Gauthier *et al.*, 2003). However, Marchetti *et al.* (2003) in a simultaneously appearing report suggested that the fungicidal synergism of fluconazole with cyclosporine may not be dependent on the MDR transporters of *C. albicans*. Since azoles are actively exported by ABC transporters such as Cdr1p and Cdr2p, a direct inhibitory effect of the immunosuppressants on these transporters is likely. Egner *et al.* (1998, 2000) also observed that the replacement of S1360 (equivalent to T1351 of Cdr1p) of Pdr5p to phenylalanine resulted in the loss of synergism of FK506 with fluconazole. Further, if serine was changed to alanine, it resulted in hypersensitivity to FK506. Their observations suggested a direct role of S1360 in mediating the synergy of fluconazole activity with FK506 in Pdr5p. The sequence alignment of TMD11 of various ABC transporters of *C. albicans* and their

comparison with Pdr5p reveals that instead of a serine residue, which is present in Pdr5p, the major drug transporters of *C. albicans* (Cdr1p and Cdr2p) instead possess threonine. When TMD11 of Cdr1p was looked at in a helical wheel projection, an amphipathic structure with a hydrophilic and a hydrophobic side was revealed, where T1351 lies near the boundary of the two faces of the putative helix. The importance of T1351 in drug as well as in inhibitor susceptibility is well evident from its placement in a helical wheel projection wherein probably the hydrophilic face of the helix plays a crucial role in the recognition/transport of Cdr1p substrates. Thus it is likely that the hydrophobic face of TMD11 could interact with the lipid layer while the hydrophilic face may interact with other TM helices or could have direct contact with the substrate molecule. The interactivity of the other residues of TMD11 positioned at the hydrophilic face remains to be examined.

c. An Alkane Inducible Cytochrome P450 (CaALK8) The modification of drugs to their nontoxic forms mediated by cytochrome P450 represents an important mechanism by which a cell could confer resistance to different drugs. The role of cytochrome P450 as the detoxifying enzymes in prokaryotes as well as in eukaryotes is well established (Graham-Lorence and Peterson, 1996; Nebert and Gonzalez, 1987). Although, in yeast, the existence of two different classes of cytochrome P450, viz. P45014DM and P450alk (alkane-inducible), has been shown, neither has been linked to xenobiotics metabolism (Kappeli, 1986; Vanden Bossche and Koymans, 1998). Recently, an alkane-inducible cytochrome P450 gene of *C. albicans* has been identified and it has been shown that it is involved in multidrug resistance (Panwar *et al.*, 2001). This gene, designated *CaALK8*, shows sequence homology to a family of alkane-inducible cytochrome P450 genes involved in hydrocarbon assimilation. Interestingly, when *CaALK8* is expressed in *S. cerevisiae* or in *C. albicans*, it confers resistance to fluconazole, cycloheximide, *o*-phenanthroline and nitrosoquinoline oxide, miconazole, and itraconazole. Eight members of P450alk genes have already been identified in *C. maltosa* and *C. tropicalis* and the availability of sequences in the *Candida* database (http://alces.med.umn.edu/Candida.html) suggests the existence of a multigene family of *ALK* genes in *C. albicans* (Ohkuma *et al.*, 1995; Seghezzi *et al.*, 1992). The involvement of all *CaALK* genes in conferring multidrug resistance and the mechanism by which they render the drug nontoxic are two important aspects that require attention. An interesting possibility could be that the incoming drug is modified by *CaALK8* like the alkanes. However, so far the metabolic conversion of drugs has not been shown to be part of the drug resistance mechanism in *Candida*. Kelly *et al.* (1997b) observed that CYP61 (Δ^{22}-desaturase), which is involved in 22-desaturation in ergosterol biosynthesis in *S. cerevisiae*, can metabolize xenobiotics.

III. Concluding Remarks

The involvement of various mechanisms of antifungal resistance suggests that it is a multifactorial phenomenon. Among different mechanisms, drug efflux represents one of the predominant determinants of antifungal susceptibility. Given the promiscuity of efflux pumps with regard to substrate specificity, it is necessary to determine if the new antifungals under development are not potential substrates of efflux pump proteins, otherwise the resistance to new compounds could eventually develop. Alternatively, inhibitors or modulators of efflux pump proteins could be developed and exploited to block pump activity and thus increase efficacy. There are certain efflux protein inhibitors that increase the susceptibility of *Candida* cells to azoles (Chamberland *et al.*, 1999; Schuetzer-Muehlbauer *et al.*, 2003a). Recently Shukla *et al.* (2004) observed that the drug disulfiram, used for treatment of alcoholism, reverses Cdr1p-mediated drug resistance in *C. albicans* by inhibiting both ATP and substrate binding to the transporter. They speculate that this drug may be useful as a modulator of Cdr1p in antifungal therapy to overcome drug resistance in certain strains. Notwithstanding the need for further research in this area, the possibility of an inhibitor or a modulator of efflux pump protein is very promising. It is worth mentioning a recent report in which Niimi *et al.* (2004), by using a D-octapeptide combinatorial library, identified a Pdr5p ATPase inhibitor that chemosensitized clinical isolates of *C. albicans* probably by inhibiting ATPase activity of Cdr1p and Cdr2p.

References

Aoki, S., Ito-Kuwo, S., Nakamura, Y., and Masuhara, T. (1990). Comparative pathogenicity of a wild-type strain and respiratory mutants of *Candida albicans* in mice. *Zentralbl. Bakteriol.* **273,** 332–343.

Arie, Z. R., Altboum, Z., Sandovsky-Losica, H., and Segal, E. (1998). Adhesion of *Candida albicans* mutant strains to host tissue. *FEMS Microbiol. Lett.* **163,** 121–127.

Azzaria, M., Schurr, E., and Gros, P. (1989). Discrete mutations introduced in the predicted nucleotide-binding site of the mdr1 gene abolish its ability to confer multidrug resistance. *Mol. Cell. Biol.* **9,** 5289–5297.

Balan, I., Alarco, A. M., and Raymond, M. (1997). The *Candida albicans CDR3* gene codes for an opaque-phase ABC transporter. *J. Bacteriol.* **179,** 7210–7218.

Balkis, M. M., Leidich, S. D., Mukherjee, P. K., and Ghannoum, M. A. (2002). Mechanism of fungal resistance. *Drugs* **62,** 1025–1040.

Barchiesi, F., Calabrese, D., Sanglard, D., Falconi Di Francesco, L., Caselli, F., Giannini, D., Giacometti, A., Gavaudan, S., and Scalise, D. (2000). Experimental induction of fluconazole resistance in *Candida tropicalis* ATCC 750. *Antimicrob. Agents Chemother.* **44,** 1578–1584.

Becker, J. M., Henry, L. K., Jiang, W., and Koltin, Y. (1995). Reduced virulence of *Candida albicans* mutants affected in drug resistance. *Infect. Immun.* **63,** 4515–4518.

Bennett, J. E., Izumikawa, K., and Marr, K. A. (2004). Mechanism of increased fluconazole resistance in *Candida glabrata* during prophylaxis. *Antimicrob. Agents Chemother.* **48,** 1773–1777.

Ben-Yaacov, R., Knoller, S., Caldwell, G. A., Becker, J. M., and Koltin, Y. (1994). *Candida albicans* gene encoding resistance to benomyl and methotrexate is a multidrug resistance gene. *Antimicrob. Agents Chemother.* **38,** 648–652.

Brinkmann, U., and Eichelbaum, M. (2001). Polymorphisms in the ABC drug transporter gene *MDR1*. *Pharmacogenom. J.* **1,** 59–64.

Brun, S., Aubry, C., Lima, O., Filmon, R., Berges, T., Chabasse, D., and Bouchara, J. P. (2003). Relationships between respiration and susceptibility to azole antifungals in *Candida glabrata*. *Antimicrob. Agents Chemother.* **47,** 847–853.

Brun, S., Berges, T., Poupard, P., Vauzelle-Moreau, C., Renier, G., Chabasse, D., and Bouchara, J. P. (2004). Mechanisms of azole resistance in petite mutants of *Candida glabrata*. *Antimicrob. Agents Chemother.* **48,** 1788–1796.

Calabrese, D., Bille, J., and Sanglard, D. (2000). A novel multidrug efflux transporter gene of the major facilitator superfamily from *Candida albicans (FLU1)* conferring resistance to fluconazole. *Microbiology* **146,** 2743–2754.

Cannon, R. D., Tsao, S., Ong, S., Niimi, K., Lamping, E., Monk, B. C., and Holmes, A. R. (2004). Allelic variation affecting drug pump function in *Candida albicans*. ASM Conference on Candida and Candidiasis, abstract no. 147(C). March 18–22, Austin, TX.

Cascorbi, I., Gerloff, T., Johne, A., Christian, M., Hoffmeyer, S., Schwab, M., Schaeffeler, E., Eichelbaum, M., and Brinkmann, U. (2001). Frequency of single nucleotide polymorphisms in the P-glycoprotein drug transporter *MDR1* gene in white subjects. *Clin. Pharmacol. Ther.* **69,** 169–174.

Chamberland, S., Blais, J., and Cotter, D. P. (1999). Impact of MC510,027, a fungal efflux pump inhibitor, on the susceptibility of clinical isolates of Candida spp. to antifungal agents. Proceedings of Interscience Conference on Antimicrobial Agents and Chemotherapy, abstract no. 1270. September 26–29, 1999, San Francisco, CA.

Coleman, D. C., Rinaldi, M. G., Haynes, K. A., Rex, J. H., Summerbell, R. C., Anaissie, E., Li, A., and Sullivan, D. J. (1998). Importance of *Candida* species other than *Candida albicans* as opportunistic pathogens. *Med. Mycol.* **36,** 156–165.

Cruz, M. C., Goldstein, A. L., Blankenship, J. R., Poeta, M. D., Davis, D., Cardenas, M. E., Perfect, J. R., McCusker, J. H., and Heitman, J. (2002). Calcineurin is essential for survival during membrane stress in *Candida albicans*. *EMBO J.* **21,** 546–559.

Cuenca-Estrella, M., Diaz-Guerra, T. M., Mellado, E., and Rodriguez-Tudela, J. L. (2001). Flucytosine primary resistance in *Candida* species and *Cryptococcus neoformans*. *Eur. J. Clin. Microbiol. Infect. Dis.* **20,** 276–279.

De Backer, M. D., Ilyina, T., Ma, X-J., Vandoninck, S., Luyten, W. H., and Vanden Bossche, H. (2001). Genomic profiling of the response of *Candida albicans* to itraconazole treatment using a DNA microarray. *Antimicrob. Agents Chemother.* **45,** 1660–1670.

Demeule, M., Jodoin, J., Gingras, D., and Beliveau, R. (2000). P-glycoprotein is localized in caveolae in resistant cells and in brain capillaries. *FEBS Lett.* **466,** 219–224.

Dogra, S., Krishnamurthy, S., Gupta, V., Dixit, B. L., Gupta, C. M., Sanglard, D., and Prasad, R. (1999). Asymmetric distribution of phosphatidylethanolamine in *C. albicans*: Possible mediation by *CDR1*, a multidrug transporter belonging to ATP binding cassette (ABC) superfamily. *Yeast* **15,** 111–121.

Edlind, T. D., Smith, L., and Henry, K. (2002). Antifungal activity in *Saccharomyces cerevisiae* is modulated by calcium signaling. *Mol. Microbiol.* **46,** 257–268.

Egner, R., Rosenthal, F. E., Kralli, A., Sanglard, D., and Kuchler, K. (1998). Genetic separation of FK506 susceptibility and drug transport in the yeast Pdr5 ATP-binding cassette multidrug resistance transporter. *Mol. Biol. Cell.* **9,** 523–543.

Egner, R., Bauer, B. E., and Kuchler, K. (2000). The transmembrane domain 10 of the yeast Pdr5p ABC antifungal efflux pump determines both substrate specificity and inhibitor susceptibility. *Mol. Microbiol.* **35,** 1255–1263.

Emter, R., Hesse-Peck, A., and Kralli, A. (2002). *ERG6* and *PDR5* regulate small lipophilic drug accumulation in yeast cells via distinct mechanisms. *FEBS Lett.* **521,** 57–61.

Favre, B., Didmon, M., and Ryder, N. S. (1999). Multiple amino acid substitutions in lanosterol 14α-demethylase contribute to azole resistance in *Candida albicans*. *Microbiology* **145,** 2715–2725.

Ferte, J. (2000). Analysis of the tangled relationships between P-glycoprotein-mediated multidrug resistance and the lipid phase of the cell membrane. *Eur. J. Biochem.* **267,** 277–294.

Fling, M. E., Kopf, J., Tamarkin, A., Gorman, J. A., Smith, H. A., and Koltin, Y. (1991). Analysis of a *Candida albicans* gene that encodes a novel mechanism for resistance to benomyl and methotrexate. *Mol. Gen. Genet.* **227,** 318–329.

Franz, R., Michel, S., and Morschhauser, J. (1998). A fourth gene from the *Candida albicans* *CDR* family of ABC transporters. *Gene* **220,** 91–98.

Gauthier, C., Weber, S., Alarco, A-M., Alqawi, O., Daoud, R., Georges, E., and Raymond, M. (2003). Functional similarities and differences between *Candida albicans* Cdr1p and Cdr2p transporters. *Antimicrob. Agents Chemother.* **47,** 1543–1554.

Ghannoum, M., and Rice, L. B. (1999). Antifungal agents, mode of action, mechanism of resistance, and correlation of these mechanisms with bacterial resistance. *Clin. Microbiol. Rev.* **12,** 501–512.

Graham-Lorence, S., and Peterson, J. A. (1996). P450s, structural similarities and functional differences. *FASEB J.* **10,** 206–214.

Gupta, V., Kohli, A. K., Krishnamurthy, S., Puri, N., Aalamgeer, S. A., Panwar, S. L., and Prasad, R. (1998). Identification of mutant alleles of *CaMDR1*, a major facilitator of *Candida albicans* which confers multidrug resistance and its *in vitro* transcriptional activation. *Curr. Genet.* **34,** 192–199.

Harry, J. B., Song, J. L., Lyons, C. N., and White, T. C. (2002). Transcription initiation of genes associated with azole resistance in *Candida albicans*. *Med. Mycol.* **40,** 73–81.

Hitchcock, C. A. (1993). Resistance of *Candida albicans* to azole antifungal agents. *Biochem. Soc. Trans.* **21,** 1039–1047.

Hitchcock, C. A., Pye, G. W., Troke, P. F., *et al.* (1993). Fluconazole resistance in *Candida glabrata*. *Antimicrob. Agents Chemother.* **37,** 1962–1965.

Hoffmeyer, S., Burk, O., Von Richter, H. P., Arnold, H. P., Brockmoller, J., Johne, A., Cascorbi, I., Gerloff, T., Roots, I., Eichelbaum, M., and Brinkmann, U. (2000). Functional polymorphisms of the human multidrug-resistance gene, multiple sequence variations and correlation of one allele with P-glycoprotein expression and activity *in vivo*. *Proc. Natl. Acad. Sci. USA* **97,** 3473–3478.

Jandourek, A., Brown, P., and Vazquez, J. A. (1999). Community-acquired fungemia due to a multiple-azole-resistant strain of *Candida tropicalis*. *Clin. Infec. Dis.* **29,** 1583–1584.

Jha, S., Karnani, N., Dhar, S. K., Mukhopadhayay, K., Shukla, S., Saini, P., Mukhopadhayay, G., and Prasad, R. (2003a). Purification and characterization of N-terminal nucleotide binding domain of an ABC drug transporter of *Candida albicans*, uncommon cysteine 193 of Walker A is critical for ATP hydrolysis. *Biochemistry* **42,** 10822–10832.

Jha, S., Karnani, N., Lynn, A. M., and Prasad, R. (2003b). Covalent modification of cysteine 193 impairs ATPase function of nucleotide-binding domain of *Candida* drug efflux pump. *Biochem. Biophys. Res. Commun.* **310,** 869–875.

Jha, S., Dabas, N., Karnani, N., Saini, P., and Prasad, R. (2004). ABC multidrug transporter Cdr1p of *Candida albicans* has divergent nucleotide binding domains which display functional asymmetry. *FEMS Yeast Res.* **5,** 63–72.

Kakeya, H., Miyazaki, Y., Miyazaki, H., Nyswaner, K., Grimberg, B., and Bennett, J. E. (2000). Genetic analysis of azole resistance in the Darlington strain of *Candida albicans*. *Antimicrob. Agents Chemother.* **44,** 2985–2990.

Kappeli, O. (1986). Cytochromes P-450 of yeasts. *Microbiol. Rev.* **50,** 244–258.

Katiyar, S. K., and Edlind, T. D. (2001). Identification and expression of multidrug resistance-related ABC transporter genes in *Candida krusei*. *Med. Mycol.* **39,** 109–116.

Kaur, R., and Bachhawat, A. K. (1999). The yeast multidrug resistance pump, Pdr5p, confers reduced drug resistance in *erg* mutants of *Saccharomyces cerevisiae*. *Microbiology* **145,** 809–818.

Kaur, R., Castano, I., and Cormack, B. P. (2004). Functional genomic analysis of fluconazole susceptibility in the pathogenic yeast *Candida glabrata*, roles of calcium signaling and mitochondria. *Antimicrob. Agents Chemother.* **48,** 1600–1613.

Kelly, S. L., Lamb, D. C., Kelly, D. E., Manning, N. J., Loeffler, J., Hebart, H., Schumacher, U., and Einsele, H. (1997a). Resistance to fluconazole and cross-resistance to amphotericin B in *Candida albicans* from AIDS patients caused by defective sterol $\Delta^{5,6}$-desaturation. *FEBS Lett.* **400,** 80–82.

Kelly, S. L., Lamb, D. C., Baldwin, B. C., Corran, A. J., and Kelly, D. E. (1997b). Characterization of *Saccharomyces cerevisiae CYP61*, sterol Δ^{22}-desaturase, and inhibition by azole antifungal agents. *J. Biol. Chem.* **272,** 9986–9988.

Kelly, S. L., Lamb, D. C., Juergen, L., Einsele, H., and Kelly, D. E. (1999). The G464S amino acid substitution in *Candida albicans* sterol 14α-demethylase causes fluconazole resistance in the clinic through reduced affinity. *Biochem. Biophys. Res. Commun.* **262,** 174–179.

Kontoyiannis, D. P. (2000). Modulation of fluconazole sensitivity by the interaction of mitochondria and Erg3p in *Saccharomyces cerevisiae*. *J. Antimicrob. Chemother.* **46,** 191–197.

Krishnamurthy, S., Chatterjee, U., Gupta, V., Prasad, R., Das, P., Snehlata, P., Hasnain, S. E., and Prasad, R. (1998). Deletion of transmembrane domain 12 of *CDR1*, a multidrug transporter from *Candida albicans*, leads to altered drug specificity: Expression of a yeast multidrug transporter in baculovirus expression system. *Yeast* **14,** 535–550.

Krishnamurthy, S., Plaine, A., Albert, J., Prasad, T., Prasad, R., and Ernst, J. F. (2004). Dosage-dependent functions of fatty acid desaturase Ole1p in growth and morphogenesis of *Candida albicans*. *Microbiology* **150,** 1991–2003.

Kusch, H., Biswas, K., Schwanfelder, S., Engelmann, S., Rogers, P. D., Hecker, M., and Morschhauser, J. (2004). A proteomic approach to understanding the development of multidrug-resistant *Candida albicans* strains. *Mol. Genet. Genom.* **271,** 554–565.

Lamb, D. C., Kelly, D. E., Schunck, W-H., Shyadehi, A. Z., Akhtar, M., Lowe, D. J., Baldwin, B. C., and Kelly, S. L. (1997). The mutation T315A in *Candida albicans* sterol 14α-demethylase causes reduced enzyme activity and fluconazole resistance through reduced affinity. *J. Biol. Chem.* **272,** 5682–5688.

Lamb, D. C., Maspahy, S., Kelly, D. E., Manning, N. J., Geber, A., Bennett, J. E., and Kelly, S. L. (1999). Purification, reconstitution, and inhibition of cytochrome P-450 sterol delta^{22}-desaturase from the pathogenic fungus *Candida glabrata*. *Antimicrob. Agents Chemother.* **43,** 1725–1728.

Lamb, D. C., Kelly, D. E., White, T. C., and Kelly, S. L. (2000). The R467K amino acid substitution in *Candida albicans* sterol 14α-demethylase causes drug resistance through reduced affinity. *Antimicrob. Agents Chemother.* **44,** 63–67.

Lavie, Y., and Liscovitch, M. (2001). Changes in lipid and protein constituents of rafts and caveolae in multidrug resistance cancer cells and their functional consequences. *Glycoconj. J.* **17,** 253–259.

Lavie, Y., Fiucci, G., and Liscovitch, M. (1998). Up-regulation of caveolae and caveolar constituents in multi-drug-resistant cancer cells. *J. Biol. Chem.* **273,** 32380–32383.

Liscovitch, M., and Lavie, Y. (2000). Multidrug resistance, a role for cholesterol efflux pathways? *Trends. Biochem. Sci.* **25,** 530–537.

Loffler, J., Kelly, S. L., Hebart, H., Schumacher, U., Lass-Florl, C., and Einsele, H. (1997). Molecular analysis of cyp51 from fluconazole-resistant *Candida albicans* strains. *FEMS Microbiol. Lett.* **151,** 263–268.

Loffler, J., Einsele, H., Hebart, H., Schumacher, U., Hrastnik, C. and Daum, G. (2000). Phospholipid and sterol analysis of plasma membranes of azole-resistant *Candida albicans* strains. *FEMS Microbiol. Lett.* **185,** 59–63.

Loo, T. W., and Clarke, D. M. (1993). Functional consequences of phenylalanine mutations in the predicted transmembrane domain of P-glycoprotein. *J. Biol. Chem.* **268,** 19965–19972.

Loo, T. W., and Clarke, D. M. (1994a). Functional consequences of glycine mutations in the predicted cytoplasmic loops of P-glycoprotein. *J. Biol. Chem.* **269,** 7243–7248.

Loo, T. W., and Clarke, D. M. (1994b). Functional consequences of proline mutations in the predicted transmembrane domain of P-glycoprotein. *J. Biol. Chem.* **268,** 3143–3149.

Loo, T. W., and Clark, D. M. (1995a). Covalent modification of human P-glycoprotein mutants containing a single cysteine in either nucleotide-binding fold abolishes drug-stimulated ATPase activity. *J. Biol. Chem.* **270,** 22957–22961.

Loo, T. W., and Clark, D. M. (1995b). Rapid purification of human P-glycoprotein mutants expressed transiently in HEK 293 cells by nickel-chelate chromatography and characterization of their drug-stimulated ATPase activities. *J. Biol. Chem.* **270,** 21449–21452.

Luker, G. D., Pica, C. M., Kumar, A. S., Covey, D. F., and Piwnica-Worms, D. (2000). Effects of cholesterol and enantiomeric cholesterol on P-glycoprotein localization and function in low-density membrane domains. *Biochemistry* **39,** 7051–7661.

Maesaki, S., Marichal, P., Hossain, M. A., Sanglard, D., Bossche, H. V., and Kohno, S. (1998). Synergic effects of tacrolimus and azole antifungal agents against azole-resistant *Candida albicans* strains. *J. Antimicrob. Chemother.* **42,** 747–753.

Marchetti, O., Moreillon, P., Glauser, M. P., Bille, J., and Sanglard, D. (2001). Potent synergism of the combination of fluconazole and cyclosporine in *Candida albicans*. *Antimicrob. Agents Chemother.* **44,** 2373–2381.

Marchetti, O., Moreillon, P., Entenza, J. M., Vouillamoz, J., Glauser, M. P., Bille, J., and Sanglard, D. (2003). Fungicidal synergism of fluconazole and cyclosporine in *Candida albicans* is not dependent on multidrug efflux transporters encoded by the *CDR1, CDR2, CaMDR1,* and *FLU1* genes. *Antimicrob. Agents Chemother.* **47,** 1565–1570.

Marichal, P. (1999). Mechanisms of resistance to azole antifungal compounds. *Curr. Opin. Antiinfect. Invest. Drugs* **1,** 318–333.

Marichal, P., Vanden Bossche, H., Odds, F. C., Nobels, G., Warnock, D. W., Timmerman, V., Van Broeckhoven, C., Fay, S., and Mose-Larsen, P. (1997). Molecular biological characterization of an azole-resistant *Candida glabrata* isolate. *Antimicrob. Agents Chemother.* **41,** 2229–2237.

Marichal, P., Koymans, L., Willemsens, S., Bellens, D., Verhasselt, P., Luyten, W., Borgers, M., Ramaekers, F. C. S., Odds, F. C., and Vanden Bossche, H. (1999). Contribution of mutations in the cytochrome P450 14alpha-demethylase (Erg11p, Cyp51p) to azole resistance in *Candida albicans*. *Microbiology* **145,** 2701–2713.

Martin, M. V., and Dinsdale, R. C. (1982). Nystatin-resistance of *Candida albicans* isolates from two cases of oral candidiasis. *Br. J. Oral Surg.* **20,** 294–298.

Martin, S. W., and Konopka, J. B. (2004). Lipid rafts polarization contributes to hyphal growth in *Candida albicans*. *Eukaryot. Cell* **3,** 675–684.

Mas, J., and Pina, E. (1980). Disappearance of nystatin resistance in Candida mediated by ergosterol. *J. Gen. Microbiol.* **117,** 249–252.

Miyazaki, H., Miyazaki, Y., Geber, A., Parkinson, T., Hitchcock, C., Falconer, D. J., Ward, D. J., Marsden, K., and Bennett, J. E. (1998). Fluconazole resistance associated with drug efflux and increased transcription of a drug transporter gene, *PDH1*, in *Candida glabrata*. *Antimicrob. Agents Chemother.* **42,** 1695–1701.

Moran, G. P., Sanglard, D., Donnelly, S. M., Shanley, D. B., Sullivan, D. J., and Coleman, D. C. (1998). Identification and expression of multidrug transporters responsible for fluconazole resistance in *Candida dubliniensis*. *Antimicrob. Agents Chemother.* **42,** 1819–1830.

Morschhauser, J. (2002). The genetic basis of fluconazole resistance development in *Candida albicans*. *Biochim. Biophys. Acta* **1587,** 240–248.

Mukhopadhyay, K., Kohli, A. K., and Prasad, R. (2002). Drug susceptibilities of yeast cells are affected by membrane lipid composition. *Antimicrob. Agents Chemother.* **46,** 3695–3705.

Mukhopadhyay, K., Prasad, T., Saini, P., Pucadyil, T. J., Chattopadhyay, A., and Prasad, R. (2004). Membrane sphingolipid-ergosterol interactions are important determinants of multidrug resistance in *Candida albicans*. *Antimicrob. Agents Chemother.* **48,** 1778–1787.

Nascimento, A. M., Goldman, G. H., Park, S., Marras, S. A. E., Delmas, G., Oza, U., Lolans, K., Dudley, M. N., Mann, P. A., and Perlin, D. S. (2003). Multiple resistance mechanisms among *Aspergillus fumigatus* mutants with high-level resistance to itraconazole. *Antimicrob. Agents Chemother.* **47,** 1719–1726.

Nebert, D. W., and Gonzalez, F. J. (1987). P450 genes, structure, evolution, and regulation. *Annu. Rev. Biochem.* **56,** 945–993.

Niimi, K., Harding, D. R., Parshot, R., King, A., Lun, D. J., Decottignies, A., Niimi, M., Lin, S., Cannon, R. D., Goffeau, A., and Monk, B. C. (2004). Chemosensitization of fluconazole resistance in *Saccharomyces cerevisiae* and pathogenic fungi by a D-octapeptide derivative. *Antimicrob. Agents Chemother.* **48,** 1256–1271.

Ogawa, A., Hashida-Okado, T., Endo, M., Yoshioka, H., Tsuruo, T., Takesako, K., and Kato, I. (1998). Role of ABC transporters in aureobasidin A resistance. *Antimicrob. Agents Chemother.* **42,** 755–761.

Ohkuma, M., Muraoka, S-I., Tanimoto, T., Fujii, M., Ohta, A., and Takagi, M. (1995). *CYP52* (cytochrome P450alk) multigene family in *Candida maltosa* Identification and characterization of eight members. *DNA Cell Biol.* **14,** 163–173.

Onyewu, C., Blankenship, J. R., Poeta, M. D., and Heitman, J. (2003). Ergosterol biosynthesis inhibitors become fungicigal when combined with calcineurin inhibitors against *Candida albicans, Candida glabrata* and *Candida krusei*. *Antimicrob. Agents Chemother.* **47,** 956–964.

Orozco, A. S., Higginbotham, L. M., Hitchcock, C. A., Parkinson, T., Falconer, D., Ibrahim, A. S., Ghannoum, M. A., and Filler, S. G. (1998). Mechanism of fluconazole resistance in *Candida krusei*. *Antimicrob. Agents Chemother.* **42,** 2645–2649.

Pajeva, I. K., Globisch, C., and Weise, M. (2004). Structure-function relationships of multidrug resistance P-glycoprotein. *J. Med. Chem.* **47,** 2523–2533.

Panwar, S. L., Krishnamurthy, S., Gupta, V., Alarco, A. M., Raymond, M., Sanglard, D., and Prasad, R. (2001). *CaALK8*, an alkane assimilating cytochrome P450, confers multidrug resistance when expressed in a hypersensitive strain of *Candida albicans*. *Yeast* **18,** 1117–1129.

Paulsen, I. T., Brown, M. H., and Skurray, R. A. (1996). Proton-dependent multidrug efflux systems. *Microbiol. Rev.* **60,** 575–608.

Perea, S., Lopez-Ribot, J. L., Kirkpatrick, W. R., McAtee, R. K., Santillan, R. A., Martinez, M., Calabrese, D., Sanglard, D., and Patterson, T. F. (2001). Prevalence of molecular mechanisms of resistance to azole antifungal agents in *Candida albicans* strains displaying high-level fluconazole resistance isolated from human immunodeficiency virus-infected patients. *Antimicrob. Agents Chemother.* **45,** 2676–2684.

Pfaller, M. A., Messer, S. A., Boyken, L., Huynh, H., Hollis, R. J., and Diekema, D. J. (2002). *In vitro* activities of 5-fluorocytosine against 8,803 clinical isolates of Candida spp.: Global assessment of primary resistance using National Committee for Clinical Laboratory Standards susceptibility testing methods. *Antimicrob. Agents Chemother.* **46,** 3518–3521.

Pinjon, E., Moran, G. P., Jackson, C. J., Kelly, S. L., Sanglard, D., Coleman, D. C., and Sullivan, D. J. (2003). Molecular mechanisms of itraconazole resistance in *Candida dubliniensis*. *Antimicrob. Agents Chemother.* **47,** 2424–2437.

Posteraro, B., Sanguinetti, M., Sanglard, D., La Sorda, M., Boccia, S., Romano, L., Morace, G., and Fadda, G. (2003). Identification and characterization of a *Cryptococcus neoformans* ATP binding cassette (ABC) transporter-encoding gene, *CnAFR1*, involved in the resistance to fluconazole. *Mol. Microbiol.* **47,** 357–371.

Prasad, R., Worgifosse, P. D., Goffeau, A., and Balzi, E. (1995). Molecular cloning and characterization of a novel gene of *C. albicans, CDR1*, conferring multiple resistance to drugs and antifungals. *Curr. Genet.* **27,** 320–329.

Prasad, R., Panwar, S. L., and Krishnamurthy, S. (2000). Drug resistance mechanisms of human pathogenic fungi. *In* "Fungal Pathogenesis: Principles and Clinical Applications" (R. A. Calderone and R. L. Cihlar, Eds.), pp. 601–631. Marcel Dekker, New York.

Raymond, M., Dignard, D., Alarco, A. M., Mainville, N., Magee, B. B., and Thomas, D. Y. (1998). A Ste6p/P-glycoprotein homologue from the asexual yeast *Candida albicans* transports the a-factor mating pheromone in *Saccharomyces cerevisiae. Mol. Microbiol.* **27,** 587–598.

Redding, S. J., Smith, J., Farinacci, G., Rinaldi, M., Fothergill, A., Rhine-Chalberg, J., and Pfaller, M. (1994). Resistance of *Candida albicans* to fluconazole during treatment of oropharyngeal candidiasis in a patient with AIDS, documentation by *in vitro* susceptibility testing and DNA subtype analysis. *Clin. Infect. Dis.* **18,** 240–242.

Redding, S. W., Kirkpatrick, W. R., Saville, S., Coco, B. J., White, W., Fothergill, A., Rinaldi, M., Eng, T., Patterson, T. F., and Lopez-Ribot, J. (2003). Multiple patterns of resistance to fluconazole in *Candida glabrata* isolates from a patient with oropharyngeal candidiasis receiving head and neck radiation. *J. Clin. Microbiol.* **41,** 619–622.

Rogers, P. D., and Barker, K. S. (2002). Evaluation of differential gene expression in fluconazole-susceptible and -resistant isolates of *Candida albicans* by cDNA analysis. *Antimicrob. Agents Chemother.* **46,** 3412–3417.

Rogers, P. D., and Barker, K. S. (2003). Genome-wide expression profile analysis reveals coordinately regulated genes associated with stepwise acquisition of azole resistance in *Candida albicans* clinical isolates. *Antimicrob. Agents Chemother.* **47,** 1220–1227.

Roth-Ben, A. Z., Altboum, Z., Berdicevsky, I., and Segal, E. (1998). Isolation of a petite mutant from a histidine auxotroph of *Candida albicans* and its characterization. *Mycopathologia* **141,** 127–135.

Safe, L. M., Safe, S. H., Subden, R. E., and Morris, D. C. (1977). Sterol content and polyene antibiotic resistance in isolates of *Candida krusei, Candida parakrusei,* and *Candida tropicalis. Can. J. Microbiol.* **23,** 398–401.

Saier, M. H., Jr., and Reizer, J. (1991). Families and super families of transport proteins common to prokaryotes and eukaryotes. *Curr. Opinion Struct. Biol.* **1,** 362–368.

Sanglard, D., Kuchler, K., Ischer, F., Pagani, J. L., Monod, M., and Bille, J. (1995). Mechanisms of resistance to azole antifungal agents in *Candida albicans* isolates from AIDS patients involve specific multidrug transporters. *Antimicrob. Agents Chemother.* **39,** 2378–2386.

Sanglard, D., Ischer, F., Monod, M., and Bille, J. (1997). Cloning of *Candida albicans* genes conferring resistance to azole antifungal agents, Characterization of *CDR2*, a new multidrug ABC transporter gene. *Microbiology* **143,** 405–416.

Sanglard, D., Ischer, F., and Koymans, L. (1998a). Amino acid substitutions in the cytochrome P-450 lanosterol 14α-demethylase (CYP51A1) from azole-resistant *Candida albicans* clinical isolates contribute to resistance to azole antifungal agents. *Antimicrob. Agents Chemother.* **42,** 241–255.

Sanglard, D., Ischer, F., Calabrese, D., de Micheli, M., and Bille, J. (1998b). Multiple resistance mechanism to azole antifungals in yeast clinical isolates. *Drug Resist. Updates* **1,** 255–265.

Sanglard, D., Ischer, F., and Bille, J. (1999). The role of the ATP binding cassette (ABC)-transporter genes *CgCDR1* and *CgCDR2* in the resistance of *Candida glabrata* to azole antifungals. ASM Conference on Candida and Candidiasis, abstract no. C25. March 1–4, 1999, Charleston, SC.

Sanglard, D., Ischer, F., and Bille, J. (2001). Role of ATP-binding-cassette transporter genes in high-frequency acquisition of resistance to azole antifungals in *Candida glabrata. Antimicrob. Agents Chemother.* **45,** 1174–1183.

Scholer, H. J., and Polak, A. (1984). Resistance to systemic antifungal agents in antimicrobial drug resistance. *In* "Antimicrobial Drug Resistance" (L. Bryan, Ed.), pp. 393–460. Academic Press, Orlando, FL.

Schuetzer-Muehlbauer, M., Willinger, B., Egner, R., Ecker, G., and Kuchler, K. (2003a). Reversal of antifungal resistance mediated by ABC efflux pumps from *Candida albicans* functionally expressed in yeast. *Int. J. Antimicrob. Agents* **22,** 291–300.

Schuetzer-Muehlbauer, M., Willinger, B., Krapf, G., Enzinger, S., Presterl, E., and Kuchler, K. (2003b). The *Candida albicans* Cdr2p ATP-binding cassette (ABC) transporter confers resistance to caspofungin. *Mol. Microbiol.* **48,** 225–235.

Seghezzi, W., Meili, C., Ruffiner, R., Kuenzi, R., Sanglard, D., and Fiechter, A. (1992). Identification and characterization of additional members of the cytochrome P450 multigene family *CYP52* of *Candida tropicalis*. *DNA Cell Biol.* **11,** 767–780.

Semighini, C. P., Marins, M., Goldman, M. H., and Goldman, G. H. (2002). Quantitative analysis of the relative transcript levels of ABC transporter *Atr* genes in *Aspergillus nidulans* by real-time reverse transcription-PCR assay. *Appl. Environ. Microbiol.* **68,** 1351–1357.

Shukla, S., Saini, P., Smriti, Jha, S., Ambudkar, S. V., and Prasad, R. (2003). Functional characterization of *Candida albicans* ABC transporter Cdr1p. *Eukaryot. Cell* **2,** 1361–1375.

Shukla, S., Ambudkar, S. V., and Prasad, R. (2004). Substitution of threonine-1351 in the multidrug transporter Cdr1p of *Candida albicans* results in hypersusceptibility to antifungal agents and threonine-1351 is essential for synergic effects of calcineurin inhibitor FK520. *J. Antimicrob. Chemother.* **54,** 38–45.

Shukla, S., Sauna, Z. E., Prasad, R., and Ambudkar, S. V. (2004). Disulfiram is a potent modulator of multidrug transporter Cdr1p of *Candida albicans*. *Biochem. Biophys. Res. Commun.* **322,** 520–525.

Slaven, J. W., Anderson, M. J., Sanglard, D., Dixon, G. K., Bille, J., Roberts, I. S., and Denning, D. W. (2002). Increased expression of a novel *Aspergillus fumigatus* ABC transporter gene, *atrF*, in the presence of itraconazole in an itraconazole resistant clinical isolate. *Fungal Genet. Biol.* **36,** 199–206.

Smriti, Krishnamurthy, S., Dixit, B. L., Gupta, C. M., Milewski, S., and Prasad, R. (2002). ABC transporters Cdr1p, Cdr2p and Cdr3p of a human pathogen *Candida albicans* are general phospholipid translocators. *Yeast* **19,** 303–318.

Stark, G. R., and Wahl, G. M. (1984). Gene amplification. *Annu. Rev. Biochem.* **53,** 447–491.

Sterling, T. R., Gasser, R. A. J., and Ziegler, A. (1996). Emergence of resistance to amphotericin B during therapy for *Candida glabrata* infection in an immunocompetent host. *Clin. Infect. Dis.* **23,** 187–188.

Sternberg, S. (1994). The emerging fungal threat. *Science* **266,** 1632–1634.

St-Gremain, G., Laverdiere, M., Pelletier, R., Bourgault, A. M., Libman, M., Lemieux, C., and Noel, G. (2001). Prevalence and antifungal susceptibility of 442 *Candida* isolates from blood and other normally sterile sites, results of a 2-year (1996 to 1998) multicenter survillance study in Quebec, Canada. *J. Clin. Microbiol.* **39,** 949–953.

Theiss, S., Agabian, N., and Kohler, G. (1999). Molecular characterization of a new ATP-dependent transporter in *Candida albicans*. ASM Conference on Candida and Candidiasis, abstract no. C29. March 1–4, 1999, Charleston, SCASM Conference on Candida and Candidiasis, abstract no. C25. March 1–4, 1999, Charleston, SC.

Thornewell, S. J., Peery, R. B., and Skatrud, P. L. (1997). Cloning and characterization of *CneMDR1*, a *Cryptococcus neoformans* gene encoding a protein related to multidrug resistance proteins. *Gene* **201,** 21–29.

Tobin, M. B., Peery, R. B., and Skatrud, P. L. (1997). Genes encoding multiple drug resistance-like proteins in *Aspergillus fumigatus* and *Aspergillus flavus*. *Gene* **200,** 11–23.

Vanden Bossche, H. (1995). Chemotherapy of human fungal infections.. *In* "Modern Selective Fungicides: Properties, Applications, Mechanisms of Action" (H. Lyr, Ed.), pp. 431–484. Gustav Fisher Verlag, Jena, Germany.

Vanden Bossche, H., and Koymans, L. (1998). Cytochromes P450 in fungi. *Mycoses* **41**, 32–38.

Vanden Bossche, H., Marichal, P., Gorrens, J., Coene, M. C., Willemsens, G., Bellens, D., Roels, I., Moereels, H., and Janssen, P. A. J. (1989). Biochemical approaches to selective antifungal activity, focus on azole antifungals. *Mycoses* **32**, 35–52.

Vanden Bossche, H., Marichal, P., Odds, F. C., Le Jeune, L., and Coene, M. C. (1992). Characterization of an azole resistant *Candida glabrata* isolate. *Antimicrob. Agents Chemother.* **36**, 2602 2610.

Vanden Bossche, H., Marichal, P., and Odds, F. C. (1994a). Molecular mechanisms of drug resistance in fungi. *Trends Microbiol.* **2**, 393–400.

Vanden Bossche, H., Warnock, D. G., Dupont, B., Kerridge, D., Sengupta, S., Improvisi, L., Marichal, P., Odds, F. C., Provost, F., and Ronin, O. (1994b). Mechanisms and clinical impact of antifungal drug resistance. *J. Med. Vet. Mycol.* **32**, 189–202.

Van Den Hazel, H. B., Pichler, H., Do Valle Matta, M. A., Leitner, E., Goffeau, A., and Daum, G. (1999). *PDR16* and *PDR17*, two homologous genes of *Saccharomyces cerevisiae*, affect lipid biosynthesis and resistance to multiple drugs. *J. Biol. Chem.* **274**, 1934–1941.

Van der Bleik, A. M., Baas, F., Van der Velde-Koerts, T., Biedler, J. L., Meyers, M. B., Ozols, R. F., Hamilton, T. C., Joenje, H., and Borst, P. (1988). Genes amplified and overexpressed in human multidrug-resistant cell lines. *Cancer Res.* **48**, 5927–5932.

Venkateswarlu, K., Denning, D. W., Manning, N. J., and Kelly, S. L. (1996). Reduced accumulation of drug in *Candida krusei* accounts for itraconazole resistance. *Antimicrob. Agents Chemother.* **40**, 2443–2446.

Wada, S., Niimi, M., Niimi, K., Holmes, A. R., Monk, B. C., Cannon, R. D., and Uehara, Y. (2002). *Candida glabrata* ATP-binding cassette transporter Cdr1p and Pdh1p expressed in a *Saccharomyces cerevisiae* strain deficient in membrane transporters show phosphorylation dependent pumping properties. *J. Biol. Chem.* **277**, 46809 46821.

White, T. C. (1997a). Increased mRNA levels of *ERG16*, *CDR*, and *MDR1* correlate with increased azole resistance in *Candida albicans* isolates from a patient infected with human immunodeficiency virus. *Antimicrob. Agents Chemother.* **41**, 1482 1487.

White, T. C. (1997b). Antifungal drug resistance in *Candida albicans*. *ASM News* **63**, 427–433.

White, T. C. (1997c). The presence of an R467K amino acid substitution and loss of allelic variation correlate with an azole-resistant lanosterol 14α-demethylase in *Candida albicans*. *Antimicrob. Agents Chemother.* **41**, 1488–1494.

White, T. C., Marr, K. A., and Bowden, R. A. (1998). Clinical, cellular, and molecular factors that contribute to antifungal drug resistance. *Clin. Microbiol. Rev.* **11**, 382 402.

White, T. C., Holleman, S., Dy, F., Mirels, L. F., and Stevens, D. A. (2002). Resistance mechanisms in clinical isolates of *Candida albicans*. *Antimicrob. Agents Chemother.* **46**, 1704–1713.

Wilkinson, C. F., Hetnarski, K., and Yellin, T. O. (1972). Imidazole derivatives – a new class of microsomal enzyme inhibitors. *Biochem. Phamacol.* **21**, 3187-3192.

Wilkinson, C. F., Hetnarski, K., and Hicks, L. J. (1974). Substituted imidazoles as inhibitors of microsomal oxidation and insecticide synergists. *Pestic. Biochem. Physiol.* **4**, 299–312.

Woodahl, E. L., and Ho, R. J. (2004). The role of MDR1 genetic polymorphisms in interindividual variability in P-glycoprotein expression and function. *Curr. Drug Metab.* **5**, 11–19.

Xiao, L., Madison, V., Chau, A. S., Loebenberg, D., Palermo, R. E., and McNicholas, P. M. (2004). Three-dimensional models of wild-type and mutated forms of cytochrome P450 14alpha-sterol demethylases from *Aspergillus fumigatus* and *Candida albicans* provide insights into posaconazole binding. *Antimicrob. Agents Chemother.* **48**, 568 574.